

Characterization of the Ubiquitin N-end Rule Pathway in *Arabidopsis*

Kevin Goslin BSc MSc



Thesis submitted to the
National University of Ireland
for the degree of
Doctor of Philosophy

2019

Supervisor:
Dr. Emmanuelle Graciet,
Plant Biochemistry Lab,
Department of Biology,
National University of
Ireland Maynooth
Co. Kildare

Head of department:
Prof. Paul Moynagh

Declaration of Authorship

This thesis has not been submitted in whole or in part to this or any other university for any degree, and is original work of the author except where otherwise stated.

Signed: _____

Date: _____

Acknowledgements

I would like to express a huge thanks to my supervisor Dr. Emmanuelle Graciet. Throughout this PhD you've provided endless support and guidance and I really appreciate all of the time that you've given towards helping me and answering my vast amount of questions. Your positivity and enthusiasm in all situations made a big difference to me!

To all the members of the PBL crew – Maud, Brian, Alexandra, Rémi and Tara, and everyone next door in the ARM lab, you guys have been amazing and I can honestly say I enjoyed going to the lab every day and seeing friends. You've helped me so much with everything, and were always able to cheer me up whenever my experiments flopped - I'm really going to miss being in the lab with you.

I want to say a big thanks to everyone in the biology department for all of your help over the last few years. To Paul and Jackie for all of their time spent carrying out annual reports and for giving me advice, the guys in the the Prep lab and Patricia for being extremely helpful, to Nick and Noel for keeping everything running smoothly, to Alan, Michelle and Aine for supplying the lab and to Ilona for all of her help with the microscopy, thanks!

To my friends, who have been extremely understanding of my long hours in the lab and showing up to everything late, you have been very supportive and were always able to keep me motivated, and sane!

To Emma and Eóin, thank you for always being there to ask about how I'm getting on and for listening to me complain about things going wrong in and outside of the lab. I really appreciate it a lot!

Finally, I wish to thank my parents who have given me an incredible amount of support throughout my life. Thanks to you I'm able to spend my time doing something that I truly enjoy. I know it must have been difficult putting up with me when I was stressed about experiments! Thank you both so much.

Publications and Presentations

Research publications:

Goslin, K.,[†] Eschen-Lippold, L.,[†] Christin Naumann, C., Linster, E., Sorel, M., Klecker, M., de Marchi, R., Kind, A., Wirtz, M., Lee, J., Dissmeyer, N., Graciet, E. Differential N-end rule degradation of RIN4/NOI fragments generated by the AvrRpt2 effector protease. **(Manuscript in preparation)**. [†]Equal contribution

Serrano-Mislata, A., **Goslin, K.**, Zheng, B., Rae, L., Wellmer, F., Graciet, E., and Madueno, F. (2017) Regulatory interplay between *LEAFY*, *APETALA1/CAULIFLOWER* and *TERMINAL FLOWER1*: New insights into an old relationship. *Plant Signaling and Behaviour*. e1370164. DOI: 10.1080/15592324.2017.1370164.

Goslin, K.[†], Zheng, B.[†], Serrano-Mislata, A., Rae, L., Ryan, P., Kwasniewska, K., Thomson, B., O'Maoileidigh, D., Madueno, F., Wellmer, F., Graciet, E. (2017) Transcription factor Interplay between *LEAFY* and *APETALA1/CAULIFLOWER* during Floral Initiation. *Plant Physiology*, pp.17.00098v1-pp.00098.2017. DOI: <https://doi.org/10.1104/pp.17.00098>. [†]Equal contribution

de Marchi, R.,[†] Sorel, M.,[†] Mooney, B., Fudal, I., **Goslin, K.**, Kwaśniewska, K., Ryan, P.T., Pfalz, M., Kroymann, J., Pollmann, S., Feechan, A., Wellmer, F., Rivas, S. & Graciet, E. (2016) The N-end rule positively regulates pathogen responses in plants. *Scientific Reports*, **6**. DOI: 10.1038/srep26020. [†]Equal contribution

Review publications:

Miricescu, A[¶], **Goslin, K[¶]** and Graciet, E. (2018) Ubiquitylation in plants: signaling hub for the integration of environmental signals. ***Journal of Experimental Botany***. DOI: 10.1093/jxb/ery165. [Epub ahead of print]. [¶]Equal contribution

Conference Presentations:

- Dec 2017 Selected poster presentation at the SEB Cell Symposium: 'From Proteome to Phenotype: role of post-translational modifications' Edinburgh, Scotland. 'Investigating the degradation of Arabidopsis RIN4 fragments after cleavage by the Pseudomonas syringae effector AvrRpt2'.
- May 2015 Selected oral presentation at Irish Plant Scientist's Association Meeting Maynooth, Ireland. 'Analysis of LEAFY function during Floral Initiation'.

Table of Contents

Chapter 1. Characterization of the Ubiquitin N-end Rule Pathway in <i>Arabidopsis</i>: An Overview	1
1.1 Introduction	1
1.1.1. The Ub-proteasome system	2
1.1.2 Components of the plant Ub system	4
1.1.2.1 Ub genes	4
1.1.2.2 E1 Ub-activating enzymes	4
1.1.2.3 E2 Ub-conjugating enzymes	5
1.1.2.4 E3 Ub ligases	5
1.1.2.5 E4 Ub ligases	6
1.1.2.6 The 26S proteasome	7
1.2. The N-end rule pathway	7
1.2.1 The arginine N-end rule pathway	8
1.2.2 The proline N-end rule pathway	10
1.2.3 The acetylation N-end rule pathway	10
1.2.4 Components of the N-end rule pathway in plants	12
1.2.4.1 Overview of the plant N-end rule pathway	12
1.2.4.2 The N-recognins PRT1 and PRT6	13
1.2.5 Functions of the N-end rule pathway in plants	14
1.3 Methods for the identification of plant N-end rule substrates	18
1.3.1 Proteomic methods to identify N-end rule substrates in plants	18
1.3.2 Biochemical methods to identify plant N-end rule substrates	22
1.3.3 Candidate approaches to identify plant N-end rule substrates	23
1.4 Overview of projects	23
1.4.1 Investigating the Degradation of Arabidopsis Protein Fragments Following Cleavage by the <i>Pseudomonas syringae</i> Effector Protease AvrRpt224	
1.4.2 Developing a molecular tagging tool to identify N-end rule substrates	24
1.4.3 Characterization of Arabidopsis PRT6 in yeast	25
Chapter 2. Materials and Methods	26
2.1 Materials	26
2.1.1 Bacterial strains	26

2.1.2 Yeast Strains	26
2.1.3 Plant Lines	27
2.1.4 Oligonucleotides	27
2.2 Methods	30
2.2.1 Microbiology methods	30
2.2.1.1 Bacterial growth media	30
2.2.1.2 Yeast growth media	30
2.2.1.3 Preparation of chemically competent <i>E. coli</i> stbl2 and XL1 blue cells	31
2.2.1.4 Preparation of chemically competent <i>E. coli</i> Rosetta-GamiB (DE3) cells	31
2.2.1.5 Preparation of competent <i>Agrobacterium tumefaciens</i> cells	32
2.2.1.6 <i>E. coli</i> transformation	32
2.2.1.7 <i>A. tumefaciens</i> transformation	32
2.2.1.8 <i>S. cerevisiae</i> transformation	33
2.2.1.9 Dipeptide treatment of <i>S. cerevisiae</i> cells	34
2.2.1.10 Colony lift assay for <i>S. cerevisiae</i> β -gal activity	34
2.2.2 Plant-related methods	35
2.2.2.1 Plant growth conditions	35
2.2.2.2 Seed sterilization	35
2.2.2.3 Transient gene expression in <i>N. benthamiana</i>	35
2.2.2.4 Transient gene expression in <i>N. benthamiana</i> followed by inoculation	
of <i>P. syringae</i>	36
2.2.2.5 Treatment of plants with dexamethasone	36
2.2.3 Molecular biology methods	36
2.2.3.1 Plasmid preparation from <i>E. coli</i>	36
2.2.3.2 Plant genomic DNA extraction	36
2.2.3.3 Plant RNA extraction	37
2.2.3.4 Plasmid preparation from yeast	37
2.2.3.5 RNA preparation from yeast	38
2.2.3.6 cDNA synthesis	38
2.2.3.7 PCR-based methods	39
2.2.3.8 Plant Genotyping Assays	40
2.2.4 Biochemical methods	40

2.2.4.1 Protein expression in <i>E. coli</i>	40
2.2.4.2 Protein extraction from plants	41
2.2.4.3 Immunoprecipitation of proteins from tobacco leaf extracts.....	41
2.2.4.4 Protein extraction from yeast	42
2.2.4.5 Pull-down of His-tagged proteins from yeast	42
2.2.4.6 Measurement of protein concentration using amido black.....	43
2.2.4.7 Measurement of protein concentration using Bradford assay	44
2.2.4.8 Measurement of luciferase activity in tobacco leaf extracts	44
2.2.4.9 Protein separation by SDS-PAGE electrophoresis.....	45
2.2.4.10 Immunoblot analysis	45
2.2.5 Confocal imaging	46
2.2.6 Plasmids generated in this study	46
Chapter 3. Investigating the Degradation of Arabidopsis Protein Fragments Following Cleavage by the <i>Pseudomonas syringae</i> Effector Protease AvrRpt253	
3.1 Introduction	53
3.1.1 Overview of the plant immune system	53
3.1.2 Arabidopsis RIN4 is a plant immune regulator that is targeted by multiple bacterial effectors.....	55
3.1.3 RIN4 cleavage by the <i>P. syringae</i> effector AvrRpt2.....	55
3.1.4 Arabidopsis encodes multiple AvrRpt2 cleavage targets	58
3.1.5 Experimental aims.....	59
3.2 Results	60
3.2.1 Characterization of available antibodies for RIN4 stability assays	60
3.2.2 Cleavage of RIN4 by AvrRpt2 in Arabidopsis seedlings	62
3.2.3 Cleavage of mutant RIN4 by AvrRpt2 in tobacco.....	68
3.2.4 Cleavage of epitope-tagged mutant RIN4 in tobacco	70
3.2.5 Generation of RIN4 fragment tandem fluorescent timers	74
3.2.6 AvrRpt2 cleavage of NOI domain proteins	75
3.2.7 Localization of GFP-NOI-HA proteins in tobacco	79
3.3 Discussion	80
3.3.1 Investigating the N-end rule-mediated degradation of RIN4 proteolytic fragments	80

3.3.2 Investigating the N-end rule-dependent degradation of NOI protein fragments	83
3.4 Future work.....	86
3.4.1 Towards characterizing RIN4 fragment degradation.....	86
3.4.2 Understanding the role of NOI protein degradation by the N-end rule pathway	87
Chapter 4. Developing a molecular tagging tool to identify N-end rule substrates.....	89
4.1 Introduction	89
4.1.1 NEDD8 conjugation in plants	89
4.1.2 Proximity labeling of E3 Ub ligase substrates by a NEDDylator	91
4.1.4 The N-recognin PRT6 contains a conserved substrate-binding domain.....	93
4.1.5 Experimental Aims	93
4.2 Results.....	94
4.2.1 Design and generation of a NEDDylator ^{PRT6}	94
4.2.2 Testing <i>in vivo</i> transient neddylation in tobacco	94
4.2.3 Testing self-neddylation of NEDDylator ^{PRT6} in tobacco	96
4.2.4 Testing for the NEDDylator ^{PRT6} -mediated neddylation of physiological PRT6 substrates	100
4.2.4.1 Experiments conducted with an HRE1-FLAG fusion protein.....	101
4.2.4.2 Experiments conducted with HRE2-FLAG fusion proteins.....	104
4.2.5 NEDDylation assays in tobacco using an artificial N-end rule reporter substrate.....	108
4.2.6 Additional strategies to design and test different versions of a NEDDylator ^{PRT6}	114
4.2.6.1. Designing longer versions of NEDDylator ^{PRT6}	114
4.2.6.2. Generation of a NEDDylator ^{PRT6} in yeast	115
4.2.7 Generation of an Arabidopsis N-end rule mutant line expressing tagged NEDD8	120
4.3 Discussion	122
4.3.1 Developing a functional NEDDylator ^{PRT6} in plants	122
4.3.2 Using a yeast-based system to develop a functional NEDDylator ^{PRT6} ..	124
4.3.3 Future Work	125
4.3.3.1 Identification of necessary PRT6 domains for neddylation	125

4.3.3.2 Considerations for novel approaches to design a functional PRT6-specific NEDDylator	127
4.3.3.3 Future experiments to develop a yeast-based assay to test PRT6-specific NEDDylators	127
Chapter 5. Characterization of Arabidopsis PRT6 in yeast	128
5.1 Introduction	128
5.1.1 CUP9 is recognized by yeast UBR1 through an internal degradation signal.....	129
5.1.2 PRT6 contains a conserved wHTH domain of unknown function.....	130
5.1.3 Experimental aims.....	134
5.2 Results.....	134
5.2.1 Assaying CUP9 stability using <i>PTR2</i> expression.....	134
5.2.2 Generation of a PRT6 Δ wHTH yeast expression construct.....	140
5.3 Discussion and future work.....	144
5.3.1 PRT6 may not target CUP9 for degradation.....	144
5.3.2 Characterizing the PRT6 wHTH domain	145
Chapter 6. References	148
Appendix 1	167

Abstract

The control of intracellular protein homeostasis is essential for the ability of plants to grow under different physiological conditions, as well as respond to various biotic or abiotic stresses. One of the ways that cells achieve this equilibrium is through the targeted proteolysis of proteins by the ubiquitin-proteasome system. A subset of this system, termed the N-end rule pathway, relates the *in vivo* longevity of a substrate protein to the nature of its N-terminal amino acid. Although the N-end rule pathway is known to regulate numerous physiological processes in plants relatively few substrates of the pathway have been identified to date. In this study experiments were conducted aimed at identifying N-end rule substrates in the model plant *Arabidopsis thaliana*. One group of candidate substrates is generated after their proteolytic cleavage by a bacterial effector protein. The transient expression of these candidate N-end rule substrates in tobacco coupled with pathogen inoculation and biochemical methods led to the identification of a group of protein fragments that are likely novel N-end rule substrates. Experiments were also conducted towards developing a molecular tagging tool with the aim of conducting a proteome-wide screen for N-end rule substrates. Additionally, experiments were carried out to characterize a component of the Arabidopsis N-end rule pathway by expressing this enzyme in the yeast *S. cerevisiae* under different conditions. This study will allow for a further understanding of the involvement of the N-end rule pathway in plant-pathogen interactions and provides several novel N-end rule substrates for future experiments aimed at dissecting the diverse functions of this pathway in plants.

Chapter 1. Characterization of the Ubiquitin N-end Rule Pathway in *Arabidopsis*: An Overview

1.1 Introduction

Metabolism, from the Greek word *metabolē* for “change”, refers to the collection of chemical reactions necessary to sustain life within the cells of an organism. These changes comprise the constant chemical renewal of each cellular element, as well as their breakdown and conversion into reusable components (Schoenheimer, 1942). A fundamental process by which cells achieve this equilibrium is through the control of protein turnover. Research conducted over the last four decades has made it apparent that this turnover is controlled largely through the stability of proteins and their targeted destruction.

The first main pathway involved in the breakdown of molecules in the cell was discovered in the laboratory of Christian DeDuve. This work identified a group of ‘lytic bodies’ in liver tissue cells, which they termed the ‘lysosome’ (DeDuve *et al.*, 1955). This fraction of the cell, where a number of hydrolytic enzymes localized, was then shown *via* electron microscopy to be enclosed by a membrane (Novikoff *et al.*, 1956). The lysosome was subsequently found to play a role in the degradation of a large range of extracellular particles derived from endocytosis and intracellular particles *via* autophagy (reviewed in: Xu and Ren., 2015). Following the discovery of the lysosome, a number of independent experiments suggested that another lysosome-independent protein degradation pathway existed. When the weak bases chloroquine and ammonium chloride, which act as lysosomal inhibitors, were used to treat macrophage cells, extracellular - but not intracellular - protein degradation was inhibited (Poole *et al.*, 1977). In addition, experiments conducted using purified rabbit reticulocyte cells, which lack lysosomes, indicated that intracellular proteolysis was still present, with different proteins displaying varying rates of degradation. This degradation also appeared to be ATP-dependent, unlike the process of lysosomal degradation (Etlinger and Goldberg, 1977). Subsequent research carried out by Avram Hershko, Aaron Ciechanover, Irwin Rose, as well as Alexander Varshavsky, showed that this degradation process required the presence of the small 8.5 kDa protein ubiquitin

(Ub) (Ciechanover *et al.*, 1978; Hershko *et al.*, 1980) and that Ub conjugation was achieved through the action of E1, E2 and E3 enzymes (Ciechanover *et al.*, 1982; Hershko *et al.*, 1983). The discovery of Ub-dependent proteolysis and a specific mechanism for targeting molecules for destruction revolutionized the field of protein degradation, and a vast amount of research has since been conducted towards understanding its role in eukaryotic organisms.

In the paragraphs that follow, I will provide an overview of the Ub-proteasome system (UPS) and detail components of this system in plants. This section is partly based on portions of a review I co-authored (Miricescu *et al.*, 2018). The focus of this Ph.D. thesis is the characterization of a subset of the UPS, known as the N-end rule pathway, in the model angiosperm *Arabidopsis thaliana*. I will outline this pathway and its discovery, the enzymatic components that have been identified in plants and the current state of the field, including the role of the N-end rule pathway in plants and methods that have been used to identify substrates of this pathway.

1.1.1. The Ub-proteasome system

The Ub system typically involves the covalent attachment of the 76-amino acid polypeptide Ub to the ϵ -amino group of a lysine (Lys) residue of a substrate protein. Ub is conserved across eukaryotic organisms (Zuin *et al.*, 2014) with the yeast and human Ub sequences differing by only 3 amino acid residues (Ozkaynak *et al.*, 1984). In eukaryotic cells, Ub is redundantly coded by at least three different loci: (i) as contiguous repeats of Ub units (poly-Ub) (Sharp and Li, 1987); or (ii) as a single Ub moiety translationally fused to another protein such as ribosomal proteins (Finley *et al.*, 1989). In order for these fusion proteins to be attached to substrate proteins, Ub must first be processed. This is achieved through the action of a family of hydrolase enzymes termed deubiquitinases (DUBs). Free Ub can then be conjugated to a substrate protein via the successive activity of three groups of enzymes: an E1, or Ub activating enzyme (UBA); an E2 Ub-conjugating enzyme (UBC); and an E3 Ub ligase. E1 enzymes 'activate' Ub by first catalyzing the adenylation of Ub's C-terminus and then forming a thioester bond between the E1's active site cysteine and Ub's C-terminal carboxylate group (Haas *et al.*, 1982). Activated Ub can then be transferred to a cysteine residue of an E2 enzyme (again

through a thioester bond) before the Ub is covalently attached to the substrate protein, typically through the activity of a substrate-specific E3 ligase together with an E2 enzyme. After the activity of the E1, E2 and E3, a fourth enzyme, known as an E4 ligase, may also be involved in the elongation of poly-Ub chains (Koegl et al., 1999). Conjugation of a chain of four or more Ub molecules to a substrate protein, particularly using the Lys48 residue of Ub, may direct the substrate to the 26S proteasome for proteolysis (Thrower et al., 2000). This large (~2.5 MDa) ATP-dependent multi-subunit protease complex contains various sites that facilitate the unfolding, release of free Ub and subsequent degradation of substrates into peptides (Yang et al., 2004; also reviewed in (Bedford et al., 2010)). Ubiquitination of a substrate is a dynamic process and Ub can be removed through the hydrolysis activity of a deubiquitinase enzyme, adding another layer of regulation to the system.

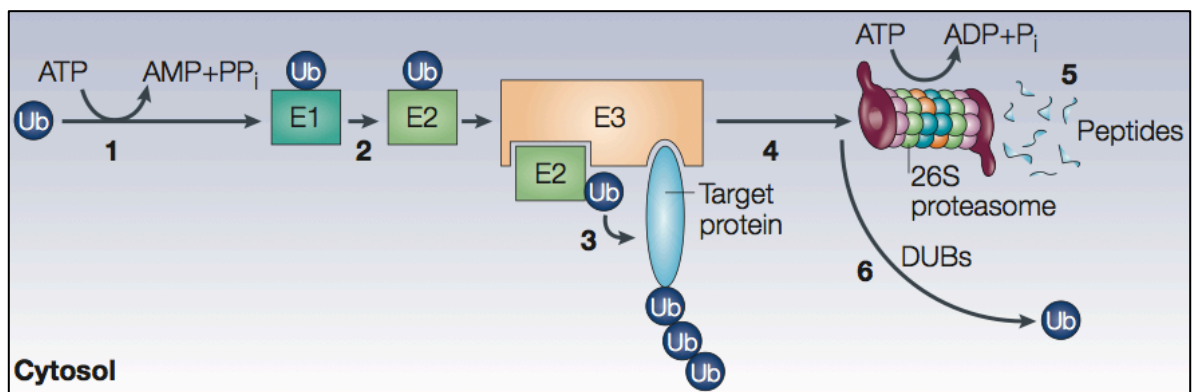


Fig 1.1 The Ub-proteasome system. (1) Free Ub is 'activated' in an ATP-dependent manner and forms an E1~Ub complex ('~' denotes a thioester bond between a Cys residue of the E1 and the last Gly residue of Ub). (2) Ub is transferred to a cysteine residue of an E2-conjugating enzyme and is bound *via* a thioester bond. (3) Ub is covalently attached to a target protein through the activity of an E3 ligase together with the E2 enzyme. (4) Successive addition of Ub to previously conjugated Ub moieties generates a poly-Ub chain on a lysine residue of the target protein. (5) The poly-Ub conjugated protein is targeted to the 26S proteasome which leads to its degradation (6) Free Ub is released by DUBs. Figure from (Welchman *et al.*, 2005).

The list of UPS substrates is now extensive and the UPS has been identified as playing a role in a wide range of cellular processes including protein quality control, cell cycle control, programmed cell death, inflammation, transcription, signal transduction and many others (reviewed in Finley, 2009). Interestingly, apart from its role in the UPS as a degradation signal, the conjugation of Ub to

substrate proteins also has non-proteasomal functions. In recent years, a 'Ub code' has been identified wherein either the type of poly-Ub chain conjugated to a target (i.e. depending on which internal Lys residue of Ub is used to form the poly-Ub chain) or its monoubiquitination can result in changes of the target's activity, interaction partners, or sub-cellular localization, but not its degradation by the proteasome (reviewed in Komander and Rape, 2012).

1.1.2 Components of the plant Ub system

1.1.2.1 Ub genes

As mentioned above, in eukaryotes, Ub is redundantly coded as poly-Ub or as a translational fusion to a ribosomal protein. In plants, but not yeast or animals, Ub genes are also expressed as translational head-to-tail fusions with the small Ub-like protein RELATED TO UBIQUITIN (RUB) (Callis et al., 1995). In Arabidopsis, 12 genes that express functional Ub have been identified. Five of these genes encode Ub-ribosomal fusion proteins, five encode poly-Ub and two encode Ub-RUB fusion proteins (reviewed in (Callis, 2014)). To produce free Ub, these precursors are processed by DUBs, of which there are approximately 50 in Arabidopsis (Isono and Nagel, 2014).

1.1.2.2 E1 Ub-activating enzymes

The E1 Ub-activating enzyme initiates the Ub conjugation cascade by 'activating' Ub and then directing it towards the next enzyme of the pathway (Fig 1.1). The enzyme contains two conserved domains: an adenylation domain, which catalyzes the adenylation of Ub's C-terminal glycine; and a catalytic domain, which contains a conserved cysteine residue that can form a thioester bond with the resulting Ub-adenylate (reviewed in Streich and Lima, 2015). Typically, eukaryotes encode a small number of E1 UBAs. In Arabidopsis, two enzymes have been identified that carry out E1 function, UBA1 and UBA2 (Hatfield et al., 1997). A mutation in both of these enzymes is lethal, which implies that they share some redundant functions (Goritschnig *et al.*, 2007). However, in a *suppressor of npr1-1 constitutive 1 (snc1)* mutant background, which displays constitutive activation of defence responses, a mutation in *UBA1*, but not in *UBA2*, was found to suppress the *snc1* mutant phenotype. This suggests that the two E1 enzymes may have some differing

functions, and that UBA1 plays a role in plant defence responses (Goritschnig *et al.*, 2007).

1.1.2.3 E2 Ub-conjugating enzymes

After forming a thioester bond with an E1 UBA, Ub is transferred to an active site cysteine residue on an E2 Ub-conjugating enzyme (Fig 1.1). This cysteine residue is located on a highly conserved Ub-conjugating catalytic (UBC) domain. Many E2 enzymes also contain short N or C-terminal extensions that create specific E2 functionality (reviewed in Stewart *et al.*, 2016). E2 enzymes can be broadly classified based on these extensions: Class I, which contain only the catalytic UBC domain; Class II that also contain a C-terminal extension; Class III, which have an additional N-terminal extension; and Class IV that contain both N and C-terminal extensions. Approximately 37 Ub-conjugating E2 enzymes are predicted to be encoded in the Arabidopsis genome (Kraft *et al.*, 2005). These enzymes have been shown to be involved in a diverse range of processes including flowering time, phosphate sensing, endoplasmic reticulum associated degradation, histone monoubiquitination and many others (reviewed in Callis *et al.*, 2014).

1.1.2.4 E3 Ub ligases

The transfer of Ub from an E2-Ub complex typically involves an E3 ligase that binds to both the target protein and the E2~Ub complex and mediates the transfer of Ub to the target protein. Strikingly, around ~1,500 genes coding for components of E3 ligases have been identified so far in Arabidopsis, in agreement with the idea that these enzymes provide the bulk of substrate specificity for the Ub system at large (Lee and Kim, 2011). The abundance of E3 ligase components encoded by the Arabidopsis genome is also indicative of the particular importance of the Ub system in plants in comparison with other eukaryotes, such as humans or yeast, which encode approximately 600 and 100 E3 Ub ligases, respectively (Finley *et al.*, 2012; Li *et al.*, 2008). The E3 ligases identified in plants can be divided into three groups, depending on the domains that mediate interaction with the E2 enzyme: (i) HECT (Homology to E6-AP C-Terminus) domain E3 ligases, (ii) RING (Really Interesting New Gene) domain ligases, or (iii) RING finger-like U-box domain Ub

ligases (reviewed in (Chen and Hellmann, 2013)).

HECT domain containing E3 ligases are relatively large (>100 kDa) proteins that form a thioester bond between a conserved cysteine residue located in the HECT domain and a Ub moiety before transfer of the Ub to the substrate (Scheffner et al., 1995; Schwarz et al., 1998). In Arabidopsis, seven HECT-containing Ub-protein ligases (noted UPLs) have been identified, UPL1-UPL7, which can be further divided into four subfamilies (Downes et al., 2003; Marin, 2013). The RING domain is a conserved protein-protein interaction domain of 40-60 amino acids that can interact with an E2 UBC (Deshaies and Joazeiro, 2009; Freemont et al., 1991; Lorick et al., 1999). RING domain E3 ligases can be (i) monomeric, whereby the E3 ligases can interact with the substrate and the E2 without additional binding partners; or (ii) multimeric, in which case they act as part of an E3 ligase complex. Multimeric RING-domain E3 ligases include CULLIN-RING ligase (CRL) complexes (Hua and Vierstra, 2011). The Arabidopsis genome encodes over 460 RING-type proteins, many of which have not yet been characterized (Stone *et al.*, 2005). The U-box domain is made up of a sequence of approximately 70 amino acid residues. It has a similar fold to RING finger domains but lacks conserved cysteine and histidine residues (Ohi et al., 2003). Arabidopsis is predicted to encode 64 U-box genes (Azevedo *et al.*, 2001). E3 ligases containing RING-finger domain and plant U-box (PUB) domains have been implicated in a vast number of processes in plants, including stress responses (reviewed in Trujillo, 2018).

1.1.2.5 E4 Ub ligases

In some cases, the elongation of a Ub chain is dependent on the activity of an E4 Ub ligase. These ligases can recognize Ub substrates that are conjugated with only a few Ub molecules and catalyze multi-Ub chain assembly (reviewed in Hoppe, 2005). To date, one E4 ligase called MUTANT, SNC1-ENHANCING3 (MUSE3), homologous to the yeast E4 ligase UBIQUITIN FUSION DEGRADATION PROTEIN2 (UFD2), has been identified in Arabidopsis (Huang et al., 2014). One identified function of this E4 ligase is to catalyze the elongation of poly-Ub chains targeting

plant nucleotide-binding leucine rich repeat immune receptors for degradation (Huang et al., 2014).

1.1.2.6 The 26S proteasome

After a substrate protein has been polyubiquitinated it may be directed to the 26S proteasome to undergo proteolysis. This large protease complex is composed of 2 sub-complexes, the 20S core particle and the 19S regulatory particle. The 20S particle is a 700 kDa cylinder-like structure that degrades proteins using 6 proteolytic sites that exhibit different protease activities. In contrast, the 19S particle, which is approximately 700 kDa, acts as a proteasome activator that binds to one or both ends of the 20S particle and is involved in the recognition of ubiquitinated substrates, as well as unfolding these proteins so that they may enter the narrow entrance to the 20S particle (reviewed in Tanaka, 2009). In *Arabidopsis*, 23 genes encode for subunits of the 20S particle, and 31 genes encode subunits of the 19S particle (Fu *et al.*, 1998; reviewed in Vierstra, 2003). As substrate proteins are degraded, they are deubiquitinated by a subunit of the 19S particle, the metalloprotease DUB RPN11, and this free Ub can be recycled by the cell (Yao and Cohen, 2002; Verma *et al.*, 2002).

1.2. The N-end rule pathway

Considering the central functions of the UPS, the Ub system at large must be able to integrate and convey large amounts of specific information. One source of selectivity for the system is a substrate's N-terminal residue, which may act as a degradation signal or 'degron' (Varshavsky, 1991). This particular degradation signal (also termed N-degron) was discovered in the laboratory of Alexander Varshavsky when investigators cloned variants of the yeast enzyme β -galactosidase (β gal) as a translational fusion with an N-terminal Ub moiety. These authors also replaced the first methionine (Met) of β gal with 15 other amino acid residues, thus yielding a protein fusion noted Ub-X- β gal, in which X can be any amino acid. They then expressed these constructs in the yeast *S. cerevisiae*, where the N-terminal Ub is cleaved by yeast DUBs, resulting in a β -gal enzyme with

different N-terminal residues X (i.e. X-βgal). The investigators found that the stability of the resulting X-βgal enzyme varied greatly depending on the nature of the N-terminal residue X, with the protein's *in vivo* half-life ranging from less than 3 minutes to ~20 hours or more (Bachmair *et al.*, 1986). They termed this phenomenon the '*N-end rule*' with nascent N-terminal residues that resulted in a stabilized protein being described as '*stabilizing residues*' and those conferring a short half-life as '*destabilizing residues*' (Bachmair *et al.*, 1986). The N-end rule pathway has since been the focus of a large amount of research in eukaryotes and has been shown to comprise at least two main branches, one which recognizes unacetylated N-termini and another branch which detects acetylated N-termini.

1.2.1 The arginine N-end rule pathway

The first branch of the N-end rule pathway to be discovered is now known as the '*classical N-end rule pathway*' or the '*arginine N-end rule pathway*' (simply termed '*N-end rule pathway*' below for simplicity). This pathway is conserved among eukaryotic organisms, with components of the pathway being highly similar in both plants and animals (reviewed in Graciet and Wellmer, 2010; Varshavsky, 2011; Tasaki *et al.*, 2012; Gibbs *et al.*, 2014). The N-end rule pathway has a hierarchical structure with primary, secondary and tertiary destabilizing residues (Gonda *et al.*, 1989)(Fig 1.2). Primary destabilizing residues include (i) type 1 destabilizing residues which are Arg, Lys, His; and (ii) type 2 destabilizing residues such as Trp, Try, Phe, Leu, Ile. In addition, unacetylated N-terminal Met if it is followed by a bulky hydrophobic residue (Mϕ) has recently been shown to also act as an N-degron (Gonda *et al.*, 1989; Kim *et al.*, 2014). Primary destabilizing residues are so-called because they can be directly recognized by E3 Ub ligases termed N-recognins, resulting in polyubiquitination of the substrate protein and its degradation *via* the 26S proteasome. Secondary destabilizing residues of the pathway (Asp, Glu and oxidized Cys) must first be conjugated to Arg - or arginylated - through the action of arginyl transferases, before being recognized by an N-recognin. These enzymes transfer Arg from Arg-tRNA to the N-terminal amino group of acceptor substrates (Soffer and Hoeyinshi, 1969; Balzi *et al.*, 1990).

Tertiary destabilizing residues require further modifications in order to be recognized by downstream arginyl transferases. These modifications include N-terminal Met excision followed by oxidation in the case of Cys, or deamidation *via* deamidase enzymes that are specific for N-terminal Asn and Gln (Reviewed in Varshavsky, 2011)(Fig 1.2).

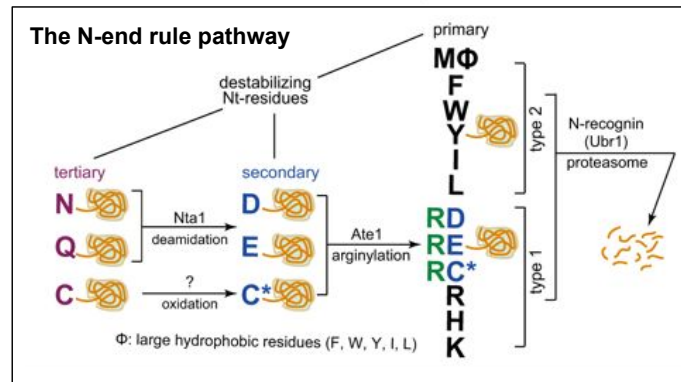


Fig 1.2. The N-end rule pathway in yeast. Tertiary residues Asn and Gln are deamidated by the N-terminal amidase Nta1 into secondary destabilizing residues Asp and Glu. The arginyl transferase Ate1 attaches Arg to the N-terminus of Asp or Glu. The N-recognin UBR1 can recognize the arginylated N-terminus of these substrates and other primary destabilizing residues and polyubiquitinate them, targeting them to the proteasome for degradation. The mechanism for cysteine oxidation has not yet been identified in yeast. Figure adapted from (Nguyen *et al.*, 2018).

In yeast and animals, the N-recognins that mediate the polyubiquitination of N-end rule substrates are characterized by a substrate recognition domain called the UBR domain (Tasaki *et al.*, 2009). The first N-recognin to be identified was the yeast N-recognin UBR1 (Bartel *et al.*, 1990). In this recognin, the UBR domain binds the basic N-terminal residues Arg, Lys and His (type 1 destabilizing residues), while a ClpS-like domain is responsible for the binding of bulky hydrophobic N-terminal residues Trp, Phe, Tyr and Leu (type 2 destabilizing residues) (Varshavsky, 1996). In addition to its function in the recognition of N-end rule substrates, yeast UBR1 also binds substrates through internal degrons (Xia *et al.*, 2008). A classic example of a substrate that is recognized by UBR1 through an internal degron is the transcription factor (TF) CUP9, which is involved in repressing the transcription of the di and tri-peptide transporter *PTR2* (Byrd *et al.*, 1998). In this case, CUP9 is bound by a third substrate-recognition domain of UBR1, which becomes allosterically 'activated' when pairs of di-peptides bind to

the type 1 and 2 substrate binding domains of UBR1 and disrupt UBR1's autoinhibitory C-terminal domain (Du *et al.*, 2002).

Interestingly, a mammalian N-recognin has recently been identified that does not act as a Ub E3 ligase. The mammalian autophagy receptor SQSTM1 (SEQUESTOME1/p62) was demonstrated to bind to substrates with N-terminal Arg and lead to substrate degradation *via* autophagy (Cha-Molstad *et al.*, 2015; Cha-Molstad *et al.*, 2017).

1.2.2 The proline N-end rule pathway

Recently, another branch of the unacetylated N-end rule pathway was described, the '*Proline N-end rule pathway*' in yeast (Chen *et al.*, 2017)(Fig 1.3). This pathway targets substrates that have a Pro at their N-terminus at either the first or second position after N-terminal Met excision. Recognition of these substrates is mediated by a subunit of the GLUCOSE INDUCED DEGRADATION DEFICIENT (Gid) Ub ligase complex, an N-recognin called Gid4, that targets enzymes involved in gluconeogenesis (Santt *et al.*, 2008; Chen *et al.*, 2017). This pathway has so far only been characterized in yeast.

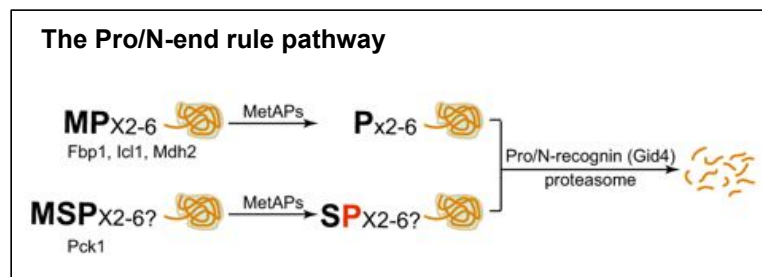


Fig 1.3. The Pro/N-end rule pathway in yeast. The N-recognin Gid4 in the GID E3 ligase complex can recognize N-terminal Pro or N-terminal Ser with Pro at position 2. This leads to the substrates polyubiquitination and destruction *via* the proteasome. Figure adapted from (Nguyen *et al.*, 2018).

1.2.3 The acetylation N-end rule pathway

In eukaryotes, approximately 50-80% of proteins are co-translationally acetylated at their N-terminus, making it a highly abundant protein modification. Acetylation of N-terminal residues can also occur post-translationally and the modification appears to be an irreversible process (reviewed in (Aksnes *et al.*, 2016; Nguyen *et*

al., 2018)). Upon translation of a nascent protein, a retained N-terminal Met is usually acetylated if it is followed by 'permissive' amino acids (Moerschell *et al.*, 1990). Specifically, if the amino acid at position 2 of this nascent protein has a small enough side chain, such as Ala, Val, Ser, Thr, Cys, Gly and Pro, the initial Met residue will be cleaved off by Met-aminopeptidases (MetAPs) and the resulting N-terminal residue will usually also be acetylated (Moerschell *et al.*, 1990). Complexes termed N-acetyltransferases (NATs) catalyze the transfer of acetyl groups to the N-terminus of substrates. Seven of these complexes have been identified to date, grouped by their substrate specificity, with the yeast *S. cerevisiae* possessing five (NatA - NatE) complexes (Polevoda *et al.*, 2009), multicellular eukaryotes possessing six NAT complexes (NatA - NatF) (Van Damme *et al.*, 2011), and plants encoding an additional seventh (NatG), which is located in the chloroplast (Dinh *et al.*, 2015).

In a set of experiments carried out by Hwang *et al.*, investigators observed that when they expressed reporter constructs with N-termini that are typically acetylated in mutant yeast cells lacking a functional Doa10 E3 ligase, the reporter constructs were stabilized in the mutant compared to a wild type strain (Hwang *et al.*, 2010b). These results led to the identification of the 'acetylation N-end rule', and to the discovery of an N-recognin, Doa10, specific for acetylated N-terminal residues (Fig. 1.4). Subsequent experiments revealed another Ub E3 ligase, Not4, that acts as an N-recognin by targeting the acetylated N-terminus of Cog1, a subunit of the conserved oligomeric golgi (COG) complex (Shemorry *et al.*, 2013).

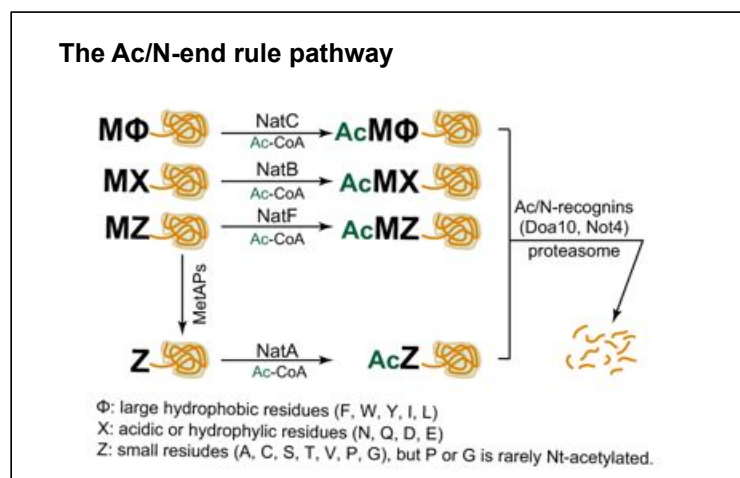


Fig 1.4. The acetylation N-end rule pathway in yeast. If the residue following the initiator Met are smaller than Val, the initial Met can be removed by MetAPs. Depending on the first two N-terminal residues the substrate is then acetylated by NatA, NatB or NatC. The N-recognins Doa10

and Not4 can recognize the N-terminal acetyl group of these substrates, resulting in their polyubiquitination and degradation *via* the proteasome. Figure adapted from (Nguyen *et al.*, 2018).

As most proteins are co-translationally N-terminal acetylated, the acetylation N-end rule greatly expands the N-termini of proteins that may act as N-degrons. This recognition however is conditional on the N-terminus of the protein being available or 'unshielded' for N-recognin binding. In this way the acetylation N-end rule may target 'overproduced' or free proteins that do not have their N-terminus shielded, perhaps by correct folding of the protein or by forming complexes with binding partners (Hwang *et al.*, 2010b; Shemorry *et al.*, 2013). For example, when the short lived Not4 substrate Cog1 has its N-terminus sterically shielded or the protein is co-expressed in yeast with binding partner Cog2-4 the protein becomes long-lived (Shemorry *et al.*, 2013).

As the focus of this thesis is the characterization of the arginine branch of the N-end rule pathway I will discuss the components of this pathway in plants in more detail and refer to this branch as the N-end rule hereafter.

1.2.4 Components of the N-end rule pathway in plants

1.2.4.1 Overview of the plant N-end rule pathway

As mentioned above, components of the N-end rule pathway are highly conserved across eukaryotic organisms. In Arabidopsis, deamidation of tertiary destabilizing residues Asn and Gln is carried out by two separate deamidases, NTAN1 and NTAQ1, respectively (Graciet *et al.*, 2010). N-terminal Cys oxidation is mediated by a class of PLANT CYSTEINE OXIDASE (PCO) enzymes, of which *PCO1* and *PCO2* are the most highly expressed (Weits *et al.*, 2014; White *et al.*, 2017). Secondary destabilizing residues are then arginylated by a set of arginyl transferases, ATE1 and ATE2, which share some redundant functions (Yoshida *et al.*, 2002; Graciet *et al.*, 2009). In Arabidopsis, two E3 Ub ligases that function as N-recognins have been identified to date. PROTEOLYSIS1 (PRT1) binds the bulky hydrophobic N-terminal residues Trp, Phe and Tyr (Potuschak *et al.*, 1998; Stary *et al.*, 2003), while PROTEOLYSIS6 (PRT6) recognizes the basic N-terminal residues Arg, Lys and His (Garzon *et al.*, 2007). Arabidopsis plants encoding mutant *PRT1* or *PRT6*

are defective in targeting reporter substrates with bulky hydrophobic or basic side chains, respectively (Potuschak *et al.*, 1998; Garzon *et al.*, 2007). In these mutant plants, the stability of reporter substrates with N-terminal Ile or Leu are not affected however, indicating that at least one other (unknown) N-recognin exists in Arabidopsis. One candidate gene encoding this E3 ligase is the putative mammalian UBR4 homolog BIG (Tasaki *et al.*, 2005).

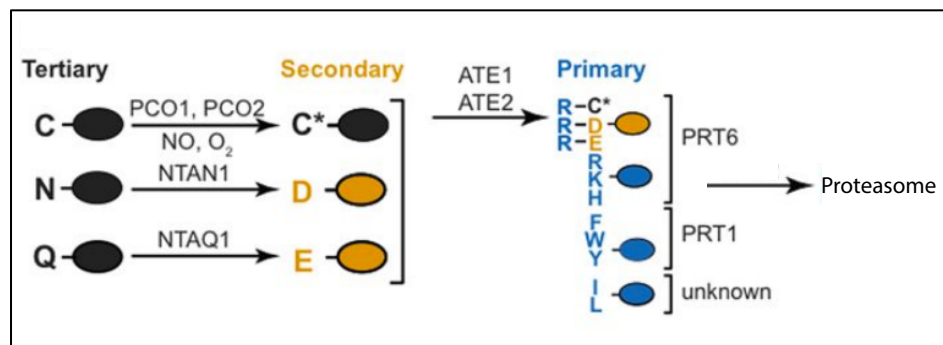


Fig 1.5. The N-end rule pathway in Arabidopsis. Tertiary destabilizing residues Asn and Gln are deamidated by NTAN1 and NTAQ1, respectively. N-terminal Cys residues are oxidized by the plant cysteine oxidases PCO1 and PCO2. Secondary destabilizing residues are arginylated by the set of functionally redundant arginyl transferases ATE1 and ATE2. Primary destabilizing residues are recognized by N-recognins PRT6, PRT1 and an as yet unidentified N-recognin. These substrates are polyubiquitinated and targeted to the proteasome for degradation. Figure adapted from (de Marchi *et al.*, 2016).

1.2.4.2 The N-recognins PRT1 and PRT6

As noted above, two N-recognins have been identified so far in Arabidopsis. *PRT1* encodes a 46 kDa E3 Ub ligase that does not bear sequence similarity to previously identified N-recognins. This ligase contains two RING finger domains and a single ZZ domain, a zinc-binding domain similar to the RING domain that can mediate protein-protein interactions (Fig. 1.6)(Potuschak *et al.*, 1998; Stary *et al.*, 2003; reviewed in Gamsjaeger *et al.*, 2007). Although the exact substrate-binding domains/residues of PRT1 have yet to be identified it has been shown to bind artificial reporter substrates with bulky hydrophobic N-terminal residues *in vitro*

and mediate both mono and polyubiquitination of these substrates (Mot *et al.*, 2018).

PRT6 encodes a 224 kDa E3 ligase that has sequence similarities to yeast UBR1. This ligase contains a winged helix-turn-helix (wHTH) domain, an E2 UBC-interacting RING domain (discussed in Section 1.1.2.4), a UBR substrate-binding domain, through which the ligase recognizes basic N-terminal residues and a C-terminal domain (noted Ct) similar to that of yeast UBR1 (Fig. 1.6). *PRT6* substrate specificity has so far been determined through genetic experiments and the use of reporter constructs, but its E3 ligase activity has yet to be fully characterized biochemically (Garzon *et al.*, 2007).

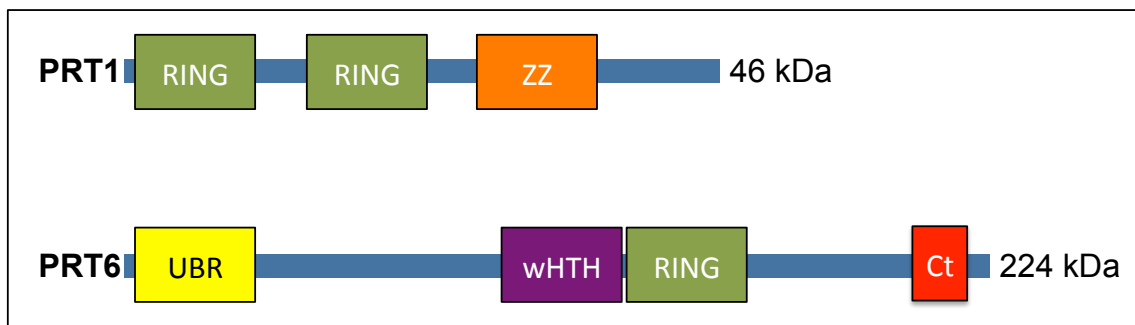


Fig 1.6. Conserved domains of identified Arabidopsis-encoded N-recognins. PRT1 contains two RING type domains and a ZZ domain. PRT6 encompasses a substrate-binding UBR domain, a wHTH domain, a RING domain and a C-terminal domain (noted Ct) similar to that of the yeast UBR1 (Garzon *et al.*, 2007). Based on figure from (Tasaki *et al.*, 2012).

1.2.5 Functions of the N-end rule pathway in plants

The N-end rule pathway has been implicated in a number of biological processes in plants. Early studies showed that an Arabidopsis mutant with a delayed leaf senescence phenotype carried a mutation in the arginyl transferase *ATE1* gene (Yoshida *et al.*, 2002). Plants mutant for the *PRT6* N-recognin, or double mutant plants for the arginyl transferases (mutant noted *ate1 ate2*) display hypersensitivity of germination to the phytohormone abscisic acid (ABA), indicating a role of the N-end rule pathway in the promotion of seed germination through removal of ABA sensitivity (Holman *et al.*, 2009). In addition, the N-end rule pathway was shown to play a role in shoot and leaf development. Mutant *ate1*

ate2 or *prt6* plants exhibit changes in leaf morphology, loss of apical dominance, as well as stem and internode elongation defects (Graciet *et al.*, 2009). When *ate1 ate2* double mutant plants were further characterized, it was revealed that a positive regulator of meristem identity - *BREVIPEDICELLUS (BP)* - is mis-regulated in this double mutant (Graciet *et al.*, 2009).

The N-end rule has also been shown to act as an oxygen (O₂) and nitric oxide (NO) sensor in plants, much like some of its functions in mammals (Hu *et al.*, 2005). In plants, this function is mediated through the proteolysis of a family of hypoxia-sensitive TFs. The five members of the ethylene response factor (ERF) group VII are TFs that positively regulate plant responses to hypoxia or anoxia. These ERF VII TFs include HYPOXIA RESPONSIVE (HRE) 1 and 2 (Licausi *et al.*, 2010), RELATED TO AP2 (RAP)2.2, RAP2.3 and RAP2.12 (Hinz *et al.*, 2010; Papdi *et al.*, 2008; Bui *et al.*, 2015). These TFs are encoded with the pro N-degron Met-Cys, with the initiator Met excised by MetAPs. Under normoxic conditions, the N-terminal Cys residue is oxidized *via* PCOs (White *et al.*, 2017), before its arginylation and recognition by the N-recognin PRT6. Under hypoxic conditions however, such as in water-logged soils (Abbas *et al.*, 2015), the N-terminal Cys may not be oxidized, allowing the stabilized TFs to then activate downstream core hypoxia signaling genes (Gibbs *et al.*, 2011; Licausi *et al.*, 2011; Bui *et al.*, 2015; Gasch *et al.*, 2016)(Fig. 1.7). As well as their role in hypoxia response, the ERF VII TFs also act as sensors for NO, with NO playing a major role in the oxidation of the ERF VIIs N-terminal Cys (Gibbs *et al.*, 2014). NO signaling is known to regulate a variety of processes in plants, including seed germination (reviewed in Arc *et al.*, 2013). As plants with mutant N-end rule components were previously shown to be hypersensitive to ABA (see above), Gibbs *et al.* (Gibbs *et al.*, 2014) investigated if this might be due to the stabilization of the ERF VII TFs. Interestingly, the quadruple mutant *prt6 rap2.2 rap2.3 rap2.12* showed a reduced hypersensitivity to ABA and a highly reduced dormancy compared to single mutant *prt6* plants, indicating that at least some of the ERF VII TFs do play a role in this response (Gibbs *et al.*, 2014).

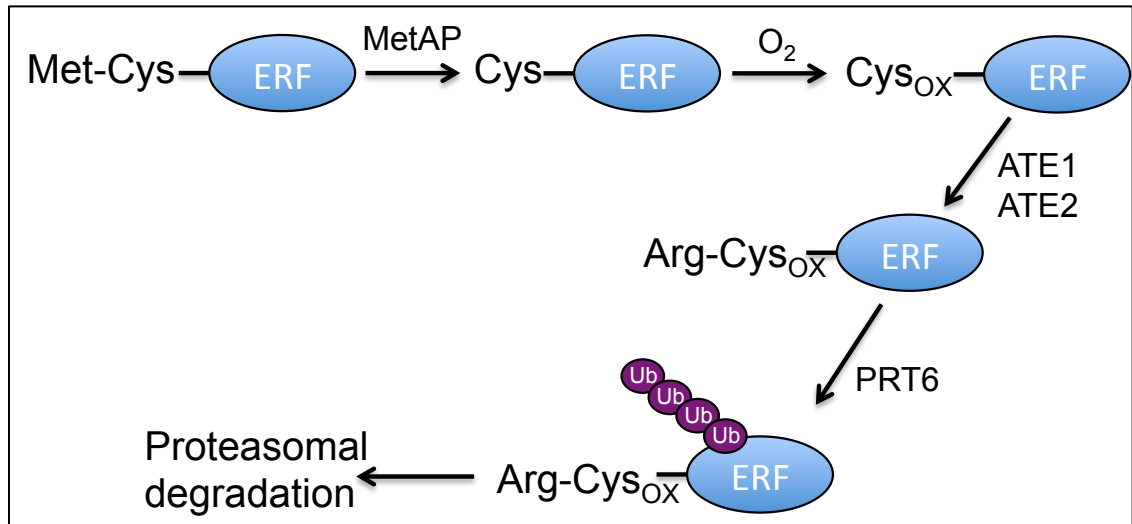


Fig 1.7. ERF VII TFs are oxidized and degraded by the N-end rule pathway under normoxia.

ERF VII TFs initiator Met is excised *via* MetAP activity. This N-terminal Cys residue can then be oxidized, before being arginylated by the arginyl transferases ATE1 and ATE2. The N-recognin PRT6 can then recognize the modified N-terminus of the ERF VII substrate and mediate its polyubiquitination, resulting in its degradation by the 26S proteasome. Figure based on image from (Licausi *et al.*, 2011).

The N-end rule has recently also been implicated in other abiotic stress signaling pathways. Vicente *et al.* found that both Arabidopsis and barley plants with a defective *PRT6* function displayed enhanced survival under a number of different abiotic stresses, including high salinity, drought and heat, although the molecular mechanisms underlying these functions are not fully understood (Vicente *et al.*, 2017). In addition to these functions, the N-end rule pathway has been shown to play numerous roles in plant defence responses against pathogens. Arabidopsis *ate1 ate2* and *prt6* mutant plants were found to be more susceptible to infection by the protist *Plasmodiophora brassicae* (Gravot *et al.*, 2016). Disease symptoms were reduced in quintuple *rap2.12 rap2.2 rap2.3 hre1 hre2* mutant plants (mutant noted *erfvII*), as well as in the *prt6 ervvII* sextuple mutant (Abbas *et al.*, 2015), indicating that the stabilization of these TFs may play a role in plant immunity, in addition to their known roles in hypoxia response. In a series of experiments conducted by de Marchi *et al.* (de Marchi *et al.*, 2016), plants mutant for N-end rule pathway components (e.g. *ate1 ate2*, *prt6* and *prt1*) were shown to be more sensitive to pathogens with a variety of lifestyles, including fungi and bacteria. These experiments revealed that *ate1 ate2* and *prt6* mutants exhibit a

dampened transcriptional response to *Pseudomonas syringae* pathovar tomato DC3000 expressing the effector protein AvrRpm1 (*P. syringae* AvrRpm1) (deMarchi *et al.*, 2016). These authors also observed that *ate1 ate2* mutants have reduced levels of the phytohormone jasmonic acid (JA) and exhibit a reduction in the expression of JA-response genes (de Marchi *et al.*, 2016). The levels of secondary metabolites belonging to the family of glucosinolates, which play important roles in plant defences against pathogens, were also found to be reduced in *ate1 ate2* mutant seedlings (de Marchi *et al.*, 2016), thus again providing a potential link with the increased susceptibility of this mutant. Interestingly, in another set of experiments conducted by Vicente *et al.* (Vicente *et al.*, 2018), N-end rule mutant plants with defective *NTAQ1* or *PRT6* displayed a higher level of resistance to both virulent (*P. syringae* DC3000) and avirulent (*P. syringae* AvrRpm1) bacterial strains. *prt6* and *ntaq1* mutants were also found to express a higher level of transcripts related to the synthesis of the phytoalexin camalexin, an alkaloid involved in the plant defence response (Ferrari *et al.*, 2003), as well as containing higher levels of camalexin (Vicente *et al.*, 2018). Barley plants (*Hordeum vulgare*) encoding an RNAi construct that represses expression of the barley *PRT6* orthologue (Mendiondo *et al.*, 2016) were also demonstrated to have increased resistance towards *P. japonica*, a *Pseudomonas* strain with known pathogenicity to barley (Dey *et al.*, 2014), but were more susceptible to the fungal hemi-biotrophs *Fusarium graminearum* and *Fusarium culmorum* (Vicente *et al.*, 2018). These experiments with barley indicate that the N-end rule's role in plant defence responses are conserved among both monocots and dicots (Vicente *et al.*, 2018).

Although the N-end rule pathway has been shown to play a role in a variety of processes, there have still only been a handful of *bona fide* substrates identified to date (reviewed in Dissmeyer *et al.*, 2018). This is due to a number of technical challenges in identifying substrates, which will be further discussed in the next section.

1.3 Methods for the identification of plant N-end rule substrates

The recognition of a potential substrate by components of the N-end rule pathway is reliant on various factors in addition to the nature of an individual N-terminal residue. In order for a tertiary or secondary destabilizing residue to be modified to form a primary N-degron there must be sufficient activity of the enzymes involved, including oxidases, N-terminal deamidases, arginyl transferases and N-recognins. The presence or rate of enzymatic activity required for modification may only occur under specific conditions (e.g. environmental parameters such as temperature, light, or upon stress), or in a given tissue or cell type. The N-terminal region of a substrate must also be flexible enough to allow for the substrate to be modified by the appropriate enzymes and finally the substrate's conformation must allow for the N-terminus to be accessible for recognition. Importantly, the substrate also requires an accessible Lys residue that can be ubiquitinated (reviewed in Varshavsky, 2011).

A number of N-end rule substrates identified so far in mammals are generated as the result of a proteolytic cleavage event, which lead to protein fragments with new N-terminal residues (Rao *et al.*, 2001; Ditzel *et al.*, 2003; Piatkov *et al.*, 2012; Brower *et al.*, 2013). The latter may act as N-degrons that are sufficient to target a protein fragment for degradation by the N-end rule pathway. As endopeptidases that function in plants are not well characterized, the use of bioinformatic methods is currently limited in identifying potential substrates of the pathway. To date a number of strategies have been used to try and identify plant N-end rule substrates including proteomics, biochemical methods and candidate approaches.

1.3.1 Proteomic methods to identify N-end rule substrates in plants

Proteomic approaches with the aim of identifying potential N-end rule substrates in plants have been implemented in different forms. In order to circumvent typical sensitivity limitations associated with a shotgun proteomic approach, Majovsky *et al.* used a targeted proteomics approach termed parallel reaction monitoring

(PRM). PRM involves the use of a high-resolution hybrid mass spectrometer such as quadrupole-Orbitrap (qOT). It is termed a targeted approach because a predefined precursor ion is selected in the quadrupole and used to generate fragment ions, which are analyzed in an Orbitrap mass analyzer (reviewed in Rauniyar *et al.*, 2015). This approach reduces biological complexity of samples and allows for a higher detection rate of peptides, as well as a higher reproducibility rate compared to a classical shotgun approach (Rauniyar *et al.*, 2015). When this method was used to analyze peptide abundance in wild-type *Arabidopsis* plants compared to N-end rule mutant plants such as *ate1 ate2*, *prt1*, or *prt6*, a small number of enriched substrates were identified (Majovsky *et al.*, 2015). In *ate1 ate2* and *prt6* mutants these enriched proteins include some that start with the Met-Cys sequence, such as a component of the JA signaling pathway METHYLESTERASE 10 (MES10) (Majovsky *et al.*, 2015). These are potentially of relevance to N-end rule-mediated degradation because the initial Met residue may be cleaved by MetAPs, thus exposing an N-terminal Cys, which may be oxidized and act as N-degron (Hu *et al.*, 2005). A limitation of this approach in characterizing N-end rule substrates is that the N-terminus of the protein for which enriched peptides are detected is not experimentally known (i.e. the N-terminal residue of the protein can only be presumed based on the genome sequence). Hence this method is not sufficient to identify with confidence potential N-end rule substrates, and it is also inappropriate to uncover substrates that may be generated following endoproteolytic cleavage. In addition, no information is collected concerning N-terminal post-translational modifications, which is also essential to determine whether a protein may be an N-end rule substrate or not.

In order to identify N-termini generated by endoproteolytic events and their post-translational modifications, a number of proteomic approaches termed N-terminomics have recently been developed. These proteomic methods are based on the chemical labeling of a peptide's N-terminal α -amine group prior to the protein extract being enzymatically digested for tandem mass spectrometry (MS/MS) analysis. Using this chemical label, original N-termini can be differentiated from N-termini generated by the enzymatic digestion applied for MS/MS analysis, allowing for enrichment and subsequent identification of true original N-terminal residues in the sample (reviewed in Huesgen and Overall,

2012). Different N-terminomic approaches utilize different enrichment strategies for N-terminal peptides prior to MS/MS analysis. Combined FRActional Diagonal Chromatography (COFRADIC) (Gevaert *et al.*, 2002) and Charge-based FRActional Diagonal Chromatography (ChaFRADIC) (Venne *et al.*, 2013) both make use of chromatography-based techniques to first enrich for N-terminal peptides. When a ChaFRADIC enrichment approach coupled with liquid-chromatography (LC)-MS/MS was applied towards investigating proteolytic cleavage events in Arabidopsis, Venne *et al.* found that N-terminal residues termed as stabilizing by the N-end rule were over represented, while destabilizing residues were under represented, reflective of a functional N-end rule pathway in plants (Venne *et al.*, 2015).

Another N-terminomics approach, Terminal Amine Isotopic Labeling of Substrates (TAILS) (Kleifeld *et al.*, 2010) involves the dimethyl labeling of free α -amine groups located on lysine amines or N-terminal residues. After labeling, the samples are enzymatically digested and free amine groups representing N-termini generated by enzymatic digestion (e.g. trypsin digest) are cleared from the sample, resulting in an enrichment of peptides bearing the original N-terminal residues, including acetylated ones. This sample can then be analyzed using MS/MS (Kleifeld *et al.*, 2010). In a study conducted by Rowland *et al.*, TAILS coupled with LC-MS/MS was used to investigate the N-terminome of Arabidopsis stromal proteins (Rowland *et al.*, 2015). The majority of proteins found in plastids are encoded in the nucleus and then targeted to the plastid *via* an N-terminal chloroplast transit peptide, which is then cleaved by a stromal processing peptidase (Richter and Lamppa, 1998). Interestingly, N-terminal residues that are termed destabilizing as *per* the prokaryotic N-end rule pathway were under-represented in the N-terminome dataset (Rowland *et al.*, 2015). These results, together with the fact that a chloroplast orthologue of the bacterial ClpS N-recognin was recently identified in Arabidopsis (Nishimura *et al.*, 2013), suggests that a prokaryotic-like N-end rule pathway may exist in plastids, whereby destabilizing N-termini could be generated upon cleavage of the substrate's chloroplast transit peptide (Rowland *et al.*, 2015).

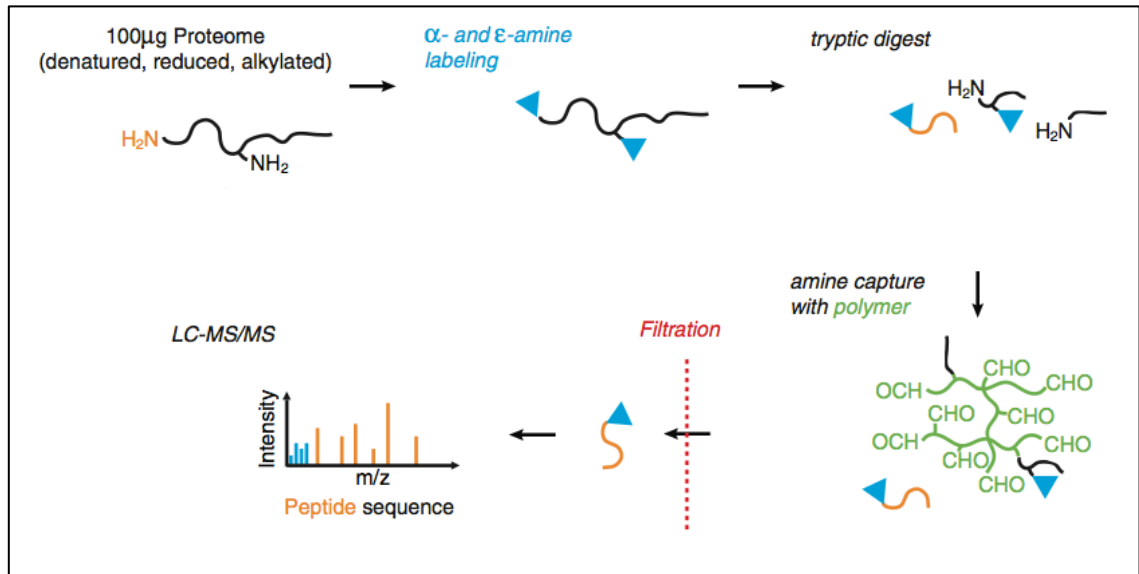


Fig. 1.8. Overview of TAILS enrichment of N-termini coupled with LC-MS/MS. Following denaturation, reduction and alkylation, primary amines are labeled with different stable isotope variants of formaldehyde. Peptides are then enzymatically digested, in this case with trypsin. A dendritic polyglycerol aldehyde polymer is used to covalently bind internal and C-terminal peptides containing free α-amine groups generated by enzymatic digestion. Filtration with a spin filter removes this polymer and enriches N-terminal peptides in the flow-through fraction. This fraction is analyzed using LC-MS/MS. Figure adapted from (Huesgen and Overall, 2012).

In another set of experiments, Zhang *et al.* used TAILS coupled to LC-MS/MS to investigate N-terminal peptide abundance in root cells of wild-type and N-end rule mutant plants (Zhang *et al.*, 2015). Among the proteins identified as being upregulated in the N-end rule mutants were several targets of the ERF VII TFs (see Section 1.2.5), although relatively few enriched proteins were identified, possibly indicating that the N-end rule may not have a significant impact on the proteome of roots under the physiological conditions tested (Zhang *et al.*, 2015). Alternatively, it is also possible that N-end rule substrates accumulate at low levels or in restricted cell types, so that the sensitivity of these proteomics approaches may not be sufficient at this stage to detect N-end rule substrates and their N-termini. Zhang *et al.* also carried out TAILS with LC-MS/MS to analyze the proteome of wild-type and *prt6* mutant Arabidopsis etiolated seedlings (Zhang *et al.*, 2017). These experiments revealed that *prt6* mutant seedlings contain a higher abundance of various N-terminal peptides that include a number of cruciferins, proteins that are involved in seed storage, and that this abundance is regulated by the ERF VII TFs (Zhang *et al.*, 2017). The abundance of the N-termini of several

proteases however was lower in *prt6* mutants, such as RESPONSIVE TO DEHYDRATION 21 (RD21), a protease that plays a role in plant immunity, cell death and senescence (Shindo *et al.*, 2012; Lampl *et al.*, 2013; Rustgi *et al.*, 2017). These experiments indicate that *via* the degradation of the ERF VII TFs, the N-end rule is involved in regulating seed storage, as well as controlling protease activities in etiolated seedlings (Zhang *et al.*, 2017).

In sum, as N-terminomic methods become more sensitive they are likely to be a powerful approach in the characterization of N-terminomes under different physiological conditions, with the potential to identify novel substrates of the N-end rule pathway.

1.3.2 Biochemical methods to identify plant N-end rule substrates

In order to identify interacting partners and substrates of the arginyl transferase ATE in the moss *Physcomitrella patens* (*P. patens*), Hoernstein *et al.* employed two different immune-affinity strategies (Hoernstein *et al.*, 2016). The first strategy involved stably expressing ATE-GUS (Schuessele *et al.*, 2016) in *P. patens* followed by immunoprecipitation (IP) with anti-GUS antibodies and analysis of the IP-ed fraction using LC-MS/MS. One protein identified as an ATE interaction partner with this approach was a class I chaperone termed HSP20 (Hoernstein *et al.*, 2016). To identify arginylated proteins, these investigators carried out another IP on *P. patens* ATE-GUS protein extracts using antibodies that were generated against N-terminal Arg residues (Wong *et al.*, 2007) followed by analysis *via* LC-MS/MS. This approach yielded four high-confidence arginylated proteins, including a putative AAA-type ATPase PpATAD3.1. This ATPase bore an N-terminal Gln residue that was deamidated to Glu prior to its arginylation, reflective of processing *via* at least two different enzymatic components of the N-end rule pathway (Hoernstein *et al.*, 2016).

1.3.3 Candidate approaches to identify plant N-end rule substrates

The analysis of previously published studies coupled with bioinformatics can also be used to identify candidate N-end rule substrates, which can then be experimentally verified. A recent study using this approach was conducted by Dong *et al.* in which they investigated the interaction between an organ-size regulator termed BIG BROTHER (BB) and the Ub receptor DA1, which had been shown to interact genetically (Li *et al.*, 2008; Dong *et al.*, 2017). This study revealed that Ub-activated DA1 mediates the cleavage of BB, resulting in a BB C-terminal fragment that appears to be targeted for degradation by PRT1 (Dong *et al.*, 2017).

Another putative N-end rule substrate generated by proteolysis is the Arabidopsis immune regulator RPM1-INTERACTING PROTEIN 4 (RIN4). Upon cleavage by the *P. syringae* protease effector AvrRpt2, RIN4 is cleaved into three fragments, two of which bear N-terminal destabilizing residues (Chisholm *et al.*, 2005). Preliminary research studying the stability of these fragments indicated that they may be N-end rule substrates (Takemoto and Jones, 2005). Interestingly a number of other Arabidopsis AvrRpt2 targets also bear destabilizing residues indicating that they may be N-end rule substrates (discussed further below in Section 3.1.4).

As mentioned above the ERF VII TF group start with the N-terminal Met-Cys sequence, whereby the Met is cleaved by MetAPs resulting in N-terminal Cys, which can then be processed by N-end rule components (Section 1.2.5). Screening plant genomes for proteins encoded with an N-terminal Met-Cys sequence, of which there are ~230 in Arabidopsis, may therefore allow for the identification of candidate N-end rule substrates in the future (reviewed in Dissmeyer *et al.*, 2018).

1.4 Overview of projects

The projects described in this work are aimed at obtaining insights into the Ub-dependent N-end rule pathway in Arabidopsis. Although this pathway has been shown to be involved in a large number of physiological processes relatively few *bona fide* substrates have been identified to date due to lack of information on

protease cleavage sites and to technical limitations. Therefore, new experimental strategies are necessary to dissect at the molecular level the roles of this pathway in plants. In addition, most enzymatic components of the pathway have yet to be biochemically characterized. The work carried out in this study is aimed at (i) identifying novel substrates of the N-end rule pathway in Arabidopsis using both candidate and unbiased approaches; and (ii) characterizing at the biochemical level one particular E3 ligase or N-recognin of the N-end rule pathway in plants.

1.4.1 Investigating the Degradation of Arabidopsis Protein Fragments Following Cleavage by the *Pseudomonas syringae* Effector Protease AvrRpt2

As mentioned above, one method for the identification of N-end rule substrates is a candidate approach. Previous experiments have shown that the *P. syringae* protease effector AvrRpt2 cleaves a number of Arabidopsis proteins. These include the Arabidopsis immune regulator RIN4, as well as a group of other proteins that share some sequence similarities with RIN4. Cleavage of these Arabidopsis proteins by AvrRpt2 results in the generation of protein fragments that are predicted to be N-end rule substrates. The aim of this project was to experimentally determine if these AvrRpt2 substrates are *bona fide* N-end rule substrates using biochemical methods. Establishing whether or not the fragments released after AvrRpt2 cleavage are processed by the N-end rule pathway is significant towards understanding what biological role the N-end rule plays in Arabidopsis in the context of plant immunity and plant-pathogen interactions. This study may also contribute to our understanding of how a pathogen effector such as AvrRpt2 manipulates the host defence responses to increase its virulence.

1.4.2 Developing a molecular tagging tool to identify N-end rule substrates

E3 Ub ligases termed N-recognins are responsible for targeting N-end rule substrates for degradation through the recognition of the substrate's N-terminal residue. Identifying the substrates of an N-recognin can be used to gain understanding of the molecular mechanisms that underlie roles of the N-end rule

pathway in plants. The interaction between an E3 Ub ligase and a substrate is typically a weak and transient one, making it difficult to isolate proteins that interact with the E3 Ub ligase. A recently developed approach towards identifying substrates of an E3 Ub ligase involves the expression of a molecular tagging tool that can (irreversibly) label substrates of the ligase, so that they can be isolated from a complex mixture and identified.

During my PhD, I aimed at generating a molecular tagging tool that has specific activity towards PRT6 substrates and that can be used for identifying the substrates of this N-recognin in Arabidopsis. These tagged substrates can then be affinity purified and identified using a proteomic approach. As discussed above a number of N-end rule substrates identified to date are only generated under specific physiological conditions. The development of a PRT6 substrate-tagging enzyme that could be expressed in plant tissues would be a powerful approach towards identifying substrates as the enzyme could be expressed in plants that were grown in different conditions or treated with different biotic/abiotic stresses.

1.4.3 Characterization of Arabidopsis PRT6 in yeast

The Arabidopsis N-recognin PRT6 has not yet been biochemically characterized, despite the central roles it plays in the regulation of a wide range of physiological and developmental processes. This may be due to the fact that the *PRT6* coding sequence is not stable in bacteria, making it difficult to express and purify the enzyme in bacteria or to generate transgenic plants with mutant PRT6 enzymes. Previous experiments conducted in the lab have shown that PRT6 is functional in the yeast *S. cerevisiae* and targets reporter substrate proteins with a basic N-terminal residue for degradation, so that a yeast *ubr1* Δ mutant strain can be rescued by expressing PRT6.

This project is aimed at characterizing PRT6 by expressing this N-recognin in yeast cells and monitoring the enzyme's activity towards different reporter substrates. This characterization of PRT6 will allow for an understanding of the contribution of different domains of the enzyme towards its function as an N-recognin and may facilitate the identification of PRT6 substrates in the future.

Chapter 2. Materials and Methods

2.1 Materials

2.1.1 Bacterial strains

The bacterial strains used in this study were:

***Escherichia coli* strain BL21 Rosetta-GamiB (DE3)** - F⁻ *ompT hsdSB (rB⁻ mB⁻) gal dcm lacY1 ahpC (DE3) gor522::Tn10 trxB* pRARE (CamR, KanR, TetR)

***Escherichia coli* strain XL1-Blue** – Genotype *recA1 endA1 gyrA96 thi-1 hsdR17 supE44 relA1 lac* [F' *proAB lacIZΔM15 Tn10* (Tet)] (Agilent Technologies)

***Escherichia coli* strain STBL2** – Genotype F⁻ *endA1 glnV44 thi-1 recA1 gyrA96 relA1 Δ(lac-proAB) mcrA Δ(mcrBC-hsdRMS-mrr) λ⁻* (Thermo Fisher)

***Agrobacterium tumefaciens* strain C58 pGV2260** (McBride and Summerfelt, 1990)

2.1.2 Yeast Strains

The strains of *S. cerevisiae* used in this study were:

JD52 – Genotype *MATa ura3-52 his3-Δ200 leu2-3, 112 trp1- Δ63 lys2-801*

JD52 *ubr1* Δ – Genotype *MATa ura3-52 his3-Δ200 leu2-3, 112 trp1-Δ63 lys2-801 ubr1::HIS3*

Sc 295 - Genotype *MATa ura3-52 leu2-3,112 reg1-501 gal1 pep4-3*

2.1.3 Plant Lines

For all experiments, *A. thaliana* accession Columbia-0 (Col-0) and *N. benthamiana* were used.

Plant lines used for this work are listed in Table 2.1.

Table 2.1: List of lines used in this work

Line (Col-0 accession)	Reference
AvrRpt2 ^{DEX}	McNellis <i>et al.</i> , 1998
AvrRpt2 ^{DEX} RIN4 ^{N11G}	This study
HSN ^{DEX}	Hakenjos <i>et al.</i> , 2011
<i>prt6-5</i>	Graciet <i>et al.</i> , 2009
<i>prt6-5</i> HSN ^{DEX}	This study
<i>rps2 rin4</i>	Mackey <i>et al.</i> , 2003

2.1.4 Oligonucleotides

The oligonucleotides used for cloning of DNA constructs are described in Table 2.2, while oligonucleotides used for qPCR analysis are described in Table 2.3.

Table 2.2: List of oligonucleotides used in this study for cloning and genotyping.

Primer stock ref.	Sequence 5' to 3'
At93	CACTCACTGGCAAGACTATCACT
At121	CAACATAAGAATCTGCGGGAG
At452	TATCCATACGATGTTCCAGATTATGCT
At453	ACCACCCCTAAGGGCAAGAAC
KG4	ATGGAGCAAAAGCTCATTCTGAAGAGGACTTGGCTGCCGCA
KG5	TGCGGCAGCCAAGTCCTCTTCAGAAATGAGCTTTTGCTCCAT
KG6	ACTTGGCTGCCGCAATGATTGGGTTGTTTAAAGTAAAG
KG7	AAAAGGTACCTGATCCTCCGATACAACGCGGGAAAAAGG
KG9	GCTGCCGCAATGGAGCAAAAGCTCATTCTGAAGAGGACTTGTAG
KG10	CTACAAGTCCTCTTCAGAAATGAGCTTTTGCTCCATTGCCGCAGC
KG11	GCTCCATTGCCGCAGCGATACAACGCGGGAAAAAGG
KG12	AAAAAAGCTTGGAGGATCAGGCATGATTGGGTTGTTTAAAGTAAA
KG17	AAAAGGTACCGGTGTTTGTGGCTCTGTCT
KG18	AAAATCTAGACTATTTATGATTTGAACAGAAACCATCAG
KG19	AAAACCTGAGATGGGTGTTTGTGGCTCTGTCT
KG20	AAAAAAGCTTTTTATGATTTGAACAGAAACCATCAGG

KG21	CAGCTCCTCCGCATCGACCACCTCTTAACCTGAGAAC
KG22	CGATGCGGAGGAGCTGTAATTTCCGATTACATAGCGCC
KG23	CCTTATAGTCTGCGGCAGCGGACCATAGACCCATGTCAT
KG24	TTTTGGATCCTCATTGTGTCGTCATCATCCTTATAGTCTGCGGCAGC
KG31	AAAAGAATTCATGTGTGGGGGAGCTATCATT
KG33	CCTTATAGTCTGCGGCAGCATTGGAGTCTTGATAGCTCCAT
KG34	AAAAAAGCTTTTCATTTGTCGTCATCATCCTTATAGTCTGCGGCAGC
KG35	AAAAGAATTCATGTGCGGAGGAGCTGTAATTTTC
KG36	AAAAAAGCTTTTCATTTGTCGTCATCATCCTTATAGTC
KG46	AAAAAAGCTTCAGATCTGCAGGTGCGACG
KG47	AAAATCTAGAATTACACGGCGATCTTTC
KG50	AAAACCCGGGATGGCACGTTTCAATGTACC
KG51	AAAAAAGCTTTTTTCTCCAAAGCCAAAGCA
KG52	AAAAAAGCTTCACTGTGACTTTTTTCAGGACTTTCA
KG60	AAAACCCGGGATGGAAATCTTCGTGAAAACACT
KG61	CCTTATAGTCACCTGATCCTCCACGGCGATCTTTCCGC
KG62	AAAAAAGCTTTTCATTTGTCGTCATCATCCTTATAGTCACCTGATCCT CC
KG63	AAAAACTAGTGGAGGATCAGGCATGATTGG
KG64	AAAAAAGCTTTCAGTGATGGTGGTGGTGGAGATCCCAAGTCCT CTTCAGAAATGAGC
KG82	TCAACTCCAAGCTGGCCGCTCTAGAAGTAGACCATGGGTGTTTGTG GCTCTGTCT
KG83	ACAACCCAATCATGCCTGATCCTCCACTAGCACCTTTATGATTTGAA CAGAAACCA
KG84	ACAACCCAATCATGCCTGATCCTCCACTAGCTGTAGCCTGTAGCAA ACCATC
KG112	TTAATCCGGATATAACAAATGAGTATGAA
KG113	AACGCAGACACTCCACAATAAGCAGTAGAAAGACCACAAAATC
KG116	GATTTTGTGGTCTTTCTACTGCTTATTGTGGAGTGTCTGCGT
KG119	AGCCACATCAGTGATGAAAA
KG122	GACCCACGCATGTATCTATCTCA
KG144	CGA GCT TAA GGG AAT CGA TTT CAA G
KG145	CATTCACATCCCATGCCCGAAT
KG146	ATTCGGGGCATGGGATGTGAATG
KG147	CGAACCCGGGTACGCAT
KG155	GTCGATTTGGGCTCTCAAGCTATCTTCACTTAATCCGGATATAAC AAATGAGTATGAA
KG156	CGTGAGAAAAGGAAAAGGAAGACAAAAGAGAGCCACATCAGT GATGAAAA
KG160	TCAACTCCAAGCTGGCCGCTCTAGAAGTAGACCATGGAGACCAA CTCTTCTTTTTG
KG161	CGAATTCCTGCAGCCCGGGGATCCACTAGTTAAGCGTAATCTG GAACGTCATATG
KG165	ACATCCCATGCCCAAACCT

KG166	AAGTTTGGGGCATGGGATGT
KG167	TCACGTCCCATGCTCCAAATTT
KG168	AAATTTGGAGCATGGGACGTGA
KG169	GCATCCCATGCCCAAATTTTG
KG170	CAAAATTTGGGGCATGGGATGC
KG171	TTTTTGATCCCAAGCTCCAACTGT
KG172	ACAGTTTGGAGCTTGGGATCAAAAA
KG173	TTGTTCCAGGCCCAAACCTC
KG174	GAAGTTTGGGGCCTGGAACAA
KG183	AAAACCCGGGATGTCCGTTGCTGATGATGATT
KG184	AAAACCTCGAGTTAAGCGTAATCTGGAA
KG185	AAAACCCGGGATGGAAATCTTCG
KG186	TCTCCTCAGCTTCCCAGTTACCACCTCTTAACCTGAGAAC
KG187	AACTGGGAAGCTGAGGAGAA
KG188	AAAACCCGGGGAACCGAATTTAGGCACCACTG
KG189	CCTCAGCTTCCCAGGCACCACCTCTTAACCTGAGAAC
KG190	GCCTGGGAAGCTGAGGAGAATG
KG191	GGTTGTTCTCGTCCCAGTCACCACCTCTTAACCTGAGAAC
KG192	GACTGGGACGAGAACAACC
KG193	AAAACCCGGGGATTTTCTCCAAAGCCAAAGC
KG194	TTGTTCTCGTCCCAGGCACCACCTCTTAACCTGAGAAC
KG195	GCCTGGGACGAGAACAACCC
KG198	AAAAGGATCCGATGGCACGTTTCAATGTACC
KG199	AAAAAAGCTTTTCATTTTCTCCAAAGCCAAAG
KG200	AAAAGGATCCGAACCTGGGAAGCTGAGGAGA
KG201	AAAAAAGCTTTCAACCGAATTTAGGCACCACT
KG202	AAAAGGATCCGGACTGGGACGAGAACAACC
KG203	AAAAAAGCTTTTCATTTTCTCCAAAGCCAAAG
KG219	AAAACCCGGGTGATTTTCTCCAAAGCCAAAGC
KG220	AAAACCCGGGGACACCGAATTTAGGCACCACTG
LB2	CCAACTGGAACAACACTCAACCCTATCTC

Table 2.3: Oligonucleotides used for qPCR analysis. Oligonucleotides are specific for cDNA sequences from *Arabidopsis* (At) or *S. cerevisiae* (Sc).

Gene Name	Primer stock ref.	Sequence 5' to 3'
AtNEDD8 (RUB1)	qKG43	GATCGGATTAAGGAACGTGTTGAGGAGA
	qKG44	GAACCAGATGAAGAACAGAGCCTCC
ScPTR2	qKG49	TGGTTCTGCAATCGGTTGTGCA
	qKG50	GTCTTCTTCTTCGTAGTCCATAGCGTTC
AtPRT6	qKG75	GTGGTCCGCCGTATCAGAAGAA
	KG110	ACGTTGCGTCAACTGCACC
AtPRT6 (UBR domain)	qKG55	CCAACTTGTGCAATCTGCGTGC
	qKG56	CCACAATCACAACAACCACCACCT

AtRCE1	qKG53	ACTCTTCCATCTGTTCACGGAACC
	qKG54	ATGGTGAGATCCCAAGTCCTCTTC
AtREF1	DM242	AAGCGGTTGTGGAGAACATGATACG
	DM243	TGGAGAGCTTGATTTGCGAAATACCG
ScTAF10	qKG61	ATATTCCAGGATCAGGTCTTCCGTAGC
	qKG62	GTAGTCTTCTCATTCTGTTGATGTTGTTGTTG
ScUBR1	qKG73	CATTTGGCGCCTTCCTGATGC
	qKG74	GGCATTCTACCAACTTCACCATGCG

2.2 Methods

2.2.1 Microbiology methods

2.2.1.1 Bacterial growth media

LB (Luria-Bertani medium) was used to grow *E. coli* and *A. tumefaciens*. The LB medium used had the following composition: 10 g/L bacto-tryptone, 5 g/L bacto-yeast extract, 10 g/L NaCl. For LB agar, 15 g/L agar was added.

To prepare competent cells, SOB medium was used. The composition was as follows: 2% (w/v) tryptone, 0.5% (w/v) yeast extract, 0.05% (w/v) NaCl, 10 mM MgSO₄, 10 mM MgCl₂

2.2.1.2 Yeast growth media

YPD was used to grow yeast under non-selective conditions. The YPD medium used had the following composition: 10g/L yeast extract, 20 g/L peptone. In addition, 2% glucose (w/v) from a 40% sterile filtered stock solution was added after autoclaving. For YPD agar plants, 15g/L agar was added.

SD (Synthetic Defined) media were used to select for specific yeast strains or plasmids. The composition was as follows: 6.7g/L yeast nitrogen base without amino acids (Sigma). Appropriate amino acids were added to the following concen-

tration: Leu (60 µg/mL), Lys (30 µg/mL), His (20 µg/mL), Trp (40 µg/mL). When needed uracil was added to a final concentration of 20 µg/mL.

2.2.1.3 Preparation of chemically competent *E. coli* stbl2 and XL1 blue cells

Highly competent *E. coli* cells were prepared as described in (Inoue, et al. 1990). stbl2 cells were streaked on a LB plate and incubated overnight at 37°C. Then a 2 mL starter culture in LB was inoculated and grown overnight at 37°C with shaking. The following day, 200 µL of the starter culture were used to inoculate 250 mL SOB medium (Section 2.2.1.1). The culture was grown with shaking (200-250 rpm) at 18-20°C until an OD₆₀₀ of 0.7 was reached. The cell culture was then cooled on ice for 10 min. After cooling, the cells were spun at 4,000xg for 10 min at 4°C and the supernatant was discarded. The cell pellet was resuspended in 80 mL ice-cold TB buffer (Appendix 1). The cells were centrifuged again at 4,000xg for 10 min at 4°C and the supernatant was discarded. The bacterial pellet was resuspended in 20 mL ice-cold TB. DMSO was added slowly until a final concentration of 7% (v/v) was reached. Cells were incubated on ice for 10 min and aliquoted. Aliquots were frozen in liquid nitrogen and stored at - 80°C.

2.2.1.4 Preparation of chemically competent *E. coli* Rosetta-GamiB (DE3) cells

The strain was streaked on an LB plate supplemented with chloramphenicol (35 µg/mL) and incubated at 37°C overnight. A single colony was used to inoculate 4 mL LB supplemented with chloramphenicol (35 µg/mL) and grown overnight at 37°C. 100 mL LB supplemented with 10 mM MgSO₄ and chloramphenicol (35 µg/mL) was inoculated with 200 µL of the overnight culture and grown at 37°C until the OD₆₀₀ was ~0.5 – 0.7. Cells were cooled on ice for 10 min before being centrifuged at 4°C for 10 min. The supernatant was removed and cells were resuspended in 20mL TfbI buffer (Appendix I) and incubated for 30 min on ice. Cells were then spun at 4°C for 10 min and resuspended in 2 mL TfbII buffer (Appendix

l) and kept on ice for 30 min. Cells were aliquoted and frozen in liquid nitrogen for storage at -80°C.

2.2.1.5 Preparation of competent *Agrobacterium tumefaciens* cells

Agrobacterium tumefaciens cells from the C58 pGV2260 strain were streaked on an LB plate supplemented with 100 µg/mL rifampicin and 100 µg/mL ampicillin and incubated for 2 d at 28°C. A single colony was then used to inoculate a 5 mL LB pre-culture with appropriate antibiotics and grown overnight at 28°C. Then 250 mL of LB with appropriate antibiotics and supplemented with 0.2 g/L MgSO₄ was inoculated with 0.5 mL of the pre-culture and grown at 250 rpm at 28°C until an OD₆₀₀ of about 1.0 was reached. The culture was then chilled on ice and spun at 4°C for 10 min at 4500xg. The pellet was resuspended in 20 mL ice-cold sterile 10 mM CaCl₂, spun again at 4°C for 10 min at 4500xg. The pellet was resuspended in 4 mL ice-cold sterile 10 mM CaCl₂. Aliquots of 200 µL were frozen in liquid nitrogen and stored at -80°C.

2.2.1.6 *E. coli* transformation

For each transformation reaction, 100 µL of competent cells were thawed on ice. Plasmid DNA or an aliquot of a ligation reaction was added while keeping the cells on ice. The cells were then transferred to 42°C for 40 sec and then back to ice for 5 min. After the heat shock, 1 mL LB was added to each transformation and incubated at 37°C for 1 hr. An aliquot of each reaction was plated on LB agar plates with appropriate selection.

2.2.1.7 *A. tumefaciens* transformation

Competent cells were thawed at room temperature in aliquots of 100 µL for each transformation and 2-5 µL of purified plasmid was added. The cells were frozen and kept in liquid nitrogen for 5 min, then thawed at room temperature. Subsequently, 1 mL of LB was added and incubated at 28°C for 4 hrs. Cultures were spun

for 5 min at 5,000 rpm at room temperature, 500 μ L of supernatant was discarded and cells were resuspended. 100 μ L of this cell suspension was plated on LB plates with the appropriate antibiotics.

2.2.1.8 *S. cerevisiae* transformation

S. cerevisiae cells were transformed with DNA using a protocol based on the lithium acetate method, first developed by Ito *et al.* (Ito *et al.*, 1983). Yeast strains were streaked out on YPD media plates and incubated for 2-3 d at 30°C. A single colony was used to inoculate 5 mL of YPD liquid media and grown with shaking at 250 rpm at 30°C overnight. 50 mL of YPD liquid media was inoculated with the overnight culture to a final OD₆₀₀ of 0.2 and incubated with shaking at 250 rpm at 30°C until OD₆₀₀ was 0.7 – 1. Cells were transferred to a sterile 50 mL tube and collected by centrifugation at room temperature for 5 min at 3,000 rpm (Sorvall RT7 Plus). Cells were then resuspended in 20 mL of sterile H₂O. Cells were collected by centrifugation at room temperature for 5 min at 3,000 rpm (Sorvall RT7 Plus) and resuspended in 20 mL LiAc buffer (Appendix 1). Cells were collected by centrifugation at room temperature for 5 min at 3,000 rpm and resuspended in 0.5 mL LiAc buffer before being incubated at 30°C for 15 min. Cells were used to prepare yeast transformation mixes where a single transformation mix was made up of 300 μ L PEG/LiAc buffer (Appendix 1), 15 μ L of boiled single-stranded DNA (10 mg/mL)(salmon testes DNA, Sigma) and 50 μ L of yeast cells. This transformation mix was added to 1.5 mL tubes containing 10 μ L of DNA to be transformed into the yeast cells. Cells were incubated in this mixture for 2 hrs with shaking at 1,200 rpm at 30°C. Cells were then incubated at 42°C for 20 min. Cells were pelleted by centrifugation at 5,000 rpm (Hettich Mikro120) for 5 min and supernatant was discarded. Cells were resuspended in 1 mL of sterile H₂O before being pelleted by centrifugation at 5,000 rpm (Hettich Mikro120) for 5 min. Cells were resuspended in 500 μ L and 100 μ L was streaked out on to appropriate media to select for transformants. Plates for incubated for 2-4 d at 30°C.

To carry out cloning using homologous recombination in *S. cerevisiae* cells the 10 μ L of DNA used to transform the yeast cells was made up of 4 μ L of re-

striction enzyme digested linear vector (~300 ng/ μ L) and 6 μ L of purified PCR product (~300ng/ μ L) containing 30 bp of homology to the linearized vector.

2.2.1.9 Dipeptide treatment of *S. cerevisiae* cells

S. cerevisiae cells were grown on either YPD or SD selective media plates containing glucose or galactose (as indicated in the Results sections). A colony from these plates was then used to inoculate YPD or SD liquid selective media containing glucose or galactose (as indicated in the Results sections) and grown overnight with shaking at 250 rpm at 30°C. The following morning cells were treated with a mock solution made up of H₂O or dipeptide Arg-Ala to a final concentration of either 5 mM or 10 mM and incubated for an appropriate amount of time with shaking at 250 rpm at 30°C (as indicated in the Results sections). Cells were collected by centrifugation at room temperature for 5 min at 3,000 rpm (Sorvall RT7 Plus) and pellets were frozen at -80°C for subsequent analysis.

2.2.1.10 Colony lift assay for *S. cerevisiae* β -gal activity

S. cerevisiae strains were streaked onto selective SD medium plates with 2% galactose and grown for 1-2 d at 30°C. Sterile Whatman paper (3MM) was cut into discs and placed on top of the colonies, that were roughly equivalent, so that it was in contact with all colonies. The Whatman paper was then removed and placed colony side-up in liquid nitrogen for 10 – 15 secs. The Whatman paper discs was then thawed at room temperature. Another Whatman paper disc was soaked in Z buffer (Appendix 1) containing 0.5 mg/mL X-gal and placed in a Petri dish. The Whatman paper containing the colonies was placed colony side-up on top of the disc that had been soaked in Z buffer supplemented with X-gal (0.5 mg/mL). The Petri dish was closed and sealed using parafilm. The discs were then incubated at 37°C and imaged when blue colour was visible.

2.2.2 Plant-related methods

2.2.2.1 Plant growth conditions

Plants were grown on a medium consisting of compost, perlite and vermiculite in a ratio of 5:2:3. The plants were grown under constant illumination at 20°C after being incubated at 4°C in the dark for 5 d.

0.5x MS (Murashige and Skoog medium) had the following composition: 2.2 g/L MS salts, pH 5.7. For 0.5x MS agar plates 6 g/L agar included.

2.2.2.2 Seed sterilization

Seeds were sterilized before being grown in liquid 0.5x MS or 0.5x MS agar. Seeds were sterilized using hypochlorous acid generated by mixing 100 mL bleach (Domestos) with 3 mL concentrated hydrochloric acid (37%). Sterilization was performed for 3-4 hrs in a sealed container under a chemical fume hood.

2.2.2.3 Transient gene expression in *N. benthamiana*

A. tumefaciens cells transformed with plasmid DNA or from a glycerol stock were plated or streaked on an LB plate supplemented with appropriate antibiotics for 2-3 d at 28° C. A colony from this plate was used to inoculate LB medium supplemented with appropriate antibiotics and grown overnight at 28°C with shaking (~225 rpm). *A. tumefaciens* cells were centrifuged at 3,000 rpm (Sorvall RT7 Plus) for 10 min and resuspended at an OD₆₀₀ of 0.75 in Infiltration Medium (Appendix 1). Approximately 4-5 week old *N. benthamiana* leaves were infiltrated with this solution using a blunt 1 mL syringe and tissue was viewed under a microscope or frozen in liquid nitrogen after 2-3 d, depending on the experiment being carried out.

2.2.2.4 Transient gene expression in *N. benthamiana* followed by inoculation of *P. syringae*

N. benthamiana leaves were infiltrated with *A. tumefaciens* as described in section 2.2.2.3 above. *Pseudomonas syringae* pathovar tomato DC3000 carrying a plasmid encoding AvrRpt2, or AvrRpt2^{C122A} or an empty plasmid was streaked onto an LB agar plate with 25 mg/L kanamycin, 5 mg/L tetracycline, 100 mg/L rifampicin and grown for 2 d at 28°C. Cells from these plates were then resuspended in 10 mM MgCl₂ to an OD₆₀₀ of either 0.5 or 0.7 before being infiltrated into previously agroinfiltrated *N. benthamiana* leaves using a 1 mL syringe. Depending on the experiment, tissue was collected at different time points after infiltration (as indicated in the Results sections) and frozen in liquid nitrogen.

2.2.2.5 Treatment of plants with dexamethasone

Arabidopsis seeds were grown in 3 mL liquid 0.5x MS medium for 7 or 8 d with shaking at ~130 rpm in continuous light. Dexamethasone (Sigma), prepared as a stock solution of 10 mM in ethanol, was added to a final concentration of 10 µM and tissue was collected after appropriate amount of time, as indicated in the Results sections.

2.2.3 Molecular biology methods

2.2.3.1 Plasmid preparation from *E. coli*

Plasmids were extracted from *E. coli* cells using the EZNA plasmid mini spin kit (Omega Bio-Tek) as per manufacturer's instructions.

2.2.3.2 Plant genomic DNA extraction

Plant genomic DNA was prepared using a protocol described in (Edwards et al., 1991). Briefly, a small amount of leaf tissue, such as a single leaf, was ground using a pestle in 400 µL Edward's extraction buffer (Appendix 1) and spun at 14,000

rpm (Hettich Mikro120) for 3 min. 300 μ L of the supernatant was transferred to a new 1.5 mL tube and 300 μ L isopropanol was added. This solution was vortex and then centrifuged at 14,000 rpm (Hettich Mikro120) for 5 min. pellets were rinsed with 500 μ L 70% ethanol and spun at maximum speed for 3 min. The supernatants were discarded and the DNA pellets were air-dried. Finally, the genomic DNA was resuspended in 75 μ L H₂O.

2.2.3.3 Plant RNA extraction

Plant tissue was ground in liquid nitrogen using a pestle. RNA was extracted using the Spectrum Plant Total RNA kit (Sigma) as per manufacturer's instructions.

2.2.3.4 Plasmid preparation from yeast

To extract DNA plasmids from *S. cerevisiae* cells, the Qiaprep Spin Miniprep Kit (Qiagen) was used. Cells were grown for 16- 24 hrs in 5 mL of appropriate selection medium with shaking at 250 rpm at 30°C. Cells were collected by centrifugation at 3,000 rpm (Sorvall RT7 Plus) for 5 min and resuspended in 250 μ L P1 Buffer (Appendix 1) before being transferred to a 1.5 mL tube. 50 to 100 μ L of acid-washed glass beads (Sigma) were added and cells were vortexed for 5 min. Tubes were let stand to allow beads to settle and supernatant was transferred to a fresh 1.5 mL tube. 250 μ L P2 Buffer (Appendix 1) was added and the tube was inverted a number of times before being incubated for 5 min at room temperature. 350 μ L of N3 Buffer (Appendix 1) was added and the tube was inverted a number of times. The tube was centrifuged for 10 min at 14,000 rpm (Sorvall RT7 Plus) and the cleared lysate was added to a QIAprep Spin Column. This was centrifuged for 1 min at 14,000 rpm. Flow through was discarded and 750 μ L PE Buffer (Appendix 1) added to the column before centrifugation at 14,000 rpm for 1 min. Flow-through was discarded and the column was spun at 14,000 rpm for 1 min. DNA was eluted from the column by adding 25 μ L EB buffer (Appendix 1) to the column and centrifuging for 1 min. Centrifugation steps above at 14,000 rpm were carried out in a Hettich Mikro120 centrifuge.

2.2.3.5 RNA preparation from yeast

RNA was isolated from *S. cerevisiae* using the protocol described by (Hannah and Xiao, 2006) based on the protocol by (Carlson and Botstein, 1982). Cells were grown overnight in 5 mL of appropriate selection medium with shaking at 250 rpm at 30°C. Cells were collected by centrifugation for 5 min at 3,000 rpm (Sorvall RT7 Plus) and washed in sterile H₂O. They were then centrifuged for 5 min at 3,000 rpm. Cells were resuspended in 350 µL Yeast RNA Lysis buffer (Appendix 1) and transferred to a 2 mL Safe-Lock tube. 350 µL of phenol:chloroform:isoamyl alcohol and 0.4 g of acid-washed glass beads (Sigma) was added to the cells and vortexed at top speed in a Hettich Mikro120 centrifuge for ~2.5 min. Tubes were centrifuged at 16,000xg for 4 min at room temperature and the aqueous phase was transferred to a new 2 mL tube. 2.3 volume of 95% ethanol (~0.8 mL) was added and tubes were vortexed immediately. Tubes were centrifuged at 16,000xg for 4 min. RNA pellet was washed with 70% ethanol and then dried briefly under vacuum. RNA pellet was dissolved using 30 µL RNA elution buffer from the Spectrum Plant Total RNA kit (Sigma).

2.2.3.6 cDNA synthesis

Total RNA was isolated from plants (see Section 2.2.3.3) or yeast (see Section 2.2.3.5). RNA was first treated with Ambion DNase I to remove DNA contaminants. RNA (1 µg) was then reverse transcribed using oligo (dT)₁₈ primers and RevertAid reverse transcriptase (Thermo Fisher) according to manufacturer's instructions. cDNA was then used for molecular cloning purposes or for quantitative/semi-quantitative PCR reactions.

2.2.3.7 PCR-based methods

- **Quantitative PCR (qPCR)**

For qPCR reactions, primers were designed to have melting temperatures of $60 \pm 1^\circ\text{C}$ and to be located at an exon-intron boundary of the target sequence if possible. Primers were also designed as close to the 3' end of the template as possible. Melting temperature and primer dimerization information were checked using the online tool Oligo Analyzer available at the Integrated DNA Technologies (IDT) website (<https://eu.idtdna.com/calc/analyzer>). The Lightcycler 480 (Roche) with SYBR green master 1 (Roche) was used to quantify relative enrichments of DNA. One reaction mix contained 5 μL of 2x SYBR green master 1 (Roche), 1 μL cDNA, 1 μL of 20 μM primers (i.e. 2 μM each final concentration) and 3 μL of molecular biology grade water. An equivalent time of 60 sec per 1 kb of DNA was given to generate the amplicons (i.e. elongation time). Relative expression of a gene was determined using the cycle threshold (Ct) value of the gene and a reference gene to calculate ΔCt ('gene Ct' minus 'reference gene Ct'). Using an efficiency value of 2, relative expression was calculated as $2^{\Delta\text{Ct}}$. For qPCR analysis of cDNA generated from Arabidopsis tissue the reference gene *PP2AA3* was used (denoted 'REF1')(Wang *et al.*, 2014). For qPCR analysis of cDNA generated from *S. cerevisiae* the reference gene *TAF10* was used (Teste *et al.*, 2009). Primer sequences used in qPCR reactions are detailed in Table 2.3.

- ***E. coli* colony PCR**

To check the presence of relevant inserts following *E. coli* transformation with a ligation reaction, colonies on a plate were tested by PCR. Single colonies were picked from the plate and resuspended in 40 μL H₂O. This was placed at 95°C for 10 min. After a brief centrifugation to pellet cell debris 2.5 μL of this mix was used as PCR template in a 15 μL reaction mix.

- ***S. cerevisiae* colony PCR**

To check that plasmids contained the relevant inserts following transformation of *S. cerevisiae*, colonies on a plate were tested by PCR. Single colonies were picked

from the plate and resuspended in 10 μ L 20 mM NaOH and then placed at 95°C for 10 min. After a brief centrifugation to pellet cell debris 2.5 μ L of this mix was used as PCR template in a 15 μ L reaction mix.

2.2.3.8 Plant Genotyping Assays

To isolate Arabidopsis lines that were homozygous for the *prt6-5* and HSN T-DNA insertions I extracted plant genomic DNA (see Section 2.2.3.2 above) and used this DNA in PCR genotyping reactions. To test for the presence of the *prt6-5* T-DNA insertion I used the primer pair At121 and LB2 that amplify a region of DNA between the T-DNA left border and *PRT6* coding sequence.

To test for the presence of the HSN T-DNA insertion I used the primer pair At452 and At453 that amplify a region of DNA between the HA tag of pXCS-HAStrep used to clone the HSN construct (Hakenjos *et al.*, 2011) and *NEDD8* coding sequence. See Table 2.2 for primer sequences.

2.2.4 Biochemical methods

2.2.4.1 Protein expression in *E. coli*

E. coli Rosetta-GamiB (DE3) (see Section 2.1.1) cells were transformed with pET28b plasmids encoding different RIN4 fragments (see Table 2.4) and cells were grown overnight at 37°C on LB plates supplemented with 50 μ g/mL kanamycin . The next day, colonies were used to inoculate liquid LB medium supplemented with 50 μ g/mL kanamycin and grown at 37°C with shaking until OD₆₀₀ reached ~0.5. Cells were then chilled on ice for 30 min. To induce expression of recombinant proteins, isopropyl β -D-1-thiogalactopyranoside (IPTG) was added to a final concentration of 0.5 mM and cells were grown for 5 hrs at 30°C with shaking at 225 rpm. Cells were collected by centrifugation at 3,000 rpm (Sorvall RT7 Plus) for 10 min at 4°C and then stored at -80°C. To extract proteins from these pellets, cells were resuspended in 2x SDS loading dye (Appendix 1) and placed at 95°C for 5

min. These samples were spun at 14,000 rpm (Hettich Mikro120) for 10 min at room temperature and the supernatant was used for subsequent analysis.

2.2.4.2 Protein extraction from plants

To prepare total protein extracts from plant tissue for immunoblotting, plant tissue was ground to a fine powder in liquid nitrogen using a pestle. This powder was then resuspended in 2X SDS loading dye (Appendix 1). Samples were spun at 14,000 rpm for 10 min and supernatant was transferred to a new 1.5 mL tube. This step was repeated before samples were placed at 95°C for 5 min. Samples were centrifuged at 14,000 rpm for 10 min and supernatant was used for subsequent analysis. All centrifugation steps were carried out in a Hettich Mikro120 centrifuge.

2.2.4.3 Immunoprecipitation of proteins from tobacco leaf extracts

Leaf tissue prepared as described in Section 2.2.2.3 was ground in liquid nitrogen using a pestle. A small amount of tissue powder was taken at this stage and resuspended in 2x SDS loading dye (Appendix 1) and used as an 'input' sample. The remaining powder was resuspended in IP buffer (Appendix 1). This solution was vortexed before being centrifuged at 16,000xg at 4°C. The supernatant was moved to a fresh 1.5 mL tube. This step was repeated. For experiments described in Section 4.2.2, a sample was taken from this solution and used as an 'input' sample.

For immunoprecipitation of Myc-tagged proteins, 30 µL of EZ-view anti-Myc agarose beads (Sigma) was added to protein extracts and incubated on a rotating wheel at 4°C for 45 min. Beads were then washed 3 x 5 min using IP buffer (Appendix 1). Protein was eluted from the beads by adding 2 x SDS loading dye to the beads and incubating them at 95°C for 5 min. Beads were briefly spun and the supernatant was used for immunoblotting analysis.

For immunoprecipitation of FLAG-tagged proteins, 30 µL of EZ-view anti-FLAG agarose beads (Sigma) was added to protein extracts and incubated on a rotating wheel at 4°C for 1 hr. Beads were then washed 3 x 5 min using IP buffer (Appendix 1). Protein was eluted from beads by adding 30 µL of FLAG peptide

(Sigma) at 100 µg/mL prepared in TBS buffer (Appendix 1) and incubating with shaking (~1,500 rpm) for 10 min at 4°C. This step was then repeated twice more. All centrifugation steps were carried out in a Hettich Mikro120 centrifuge.

2.2.4.4 Protein extraction from yeast

Total protein for immunoblots analysis was extracted from *S. cerevisiae* cells using a method described in (Kushnirov, 2000). Yeast cells that had been growing in SD selective media were collected by centrifugation at 3,000 rpm (Sorvall RT7 Plus) for 10 min. Cells were then washed and resuspended with ice-cold H₂O before being transferred to a 1.5 mL tube and centrifuged again at 3,000 rpm for 10 min. Cells were resuspended in 300 µL of 0.1M NaOH and incubated for 10 min at room temperature. Cells were centrifuged at 3,000 rpm (Sorvall RT7 Plus) for 5 min before being resuspended in 2x SDS loading dye and placed at 95°C for 5 min. Samples were spun at 14,000 rpm (Hettich Mikro120) for 10 min and the supernatant was used for subsequent analysis.

2.2.4.5 Pull-down of His-tagged proteins from yeast

The protocol used to pull-down His-tagged proteins from *S. cerevisiae* cells is based on a protocol described in (Hovsepian *et al.*, 2016). Cells were streaked onto appropriate selective SD medium plates and grown for 2-3 d at 30°C. A colony from these plates was used to inoculate liquid SD medium with appropriate selection in the morning and grown at 30°C with shaking at 250 rpm. In the evening the OD₆₀₀ of these cells was measured and used to inoculate 100 mL of liquid SD medium with appropriate selection to an OD₆₀₀ of 0.001. Cells were grown overnight at 30°C with shaking at 250 rpm. When the cells reached an OD₆₀₀ of 0.3 – 0.5 they were collected using centrifugation at 3,000 rpm (Sorvall RT7 Plus) for 5 min. Supernatant was removed and pelleted cells were placed on ice. 500 µL of 10% (v/v) trichloroacetic acid (TCA) was used to resuspend the cells before the mixture was transferred to a 1.5 mL tube. Samples were left on ice for 10 min. Cells were pelleted by centrifugation at 13,000xg at room temperature. Cells were then resuspended in 100 µL 10% (v/v) TCA by pipetting. Acid-washed glass beads (Sigma) were added to the tubes up to 1 -2 mm below the tube meniscus. Tubes were placed on a

vortex and shaken at high speed for 10 min. Lysate was separated from beads by centrifugation into a fresh tube. Lysate was then centrifuged at 13,000xg at 4°C for 10 min and supernatant was removed. The residual TCA in the pellet was neutralized using 30 μ L of non-buffered 1M Tris-base solution. 200 μ L of HisA buffer (Appendix 1) was used to resuspend the pellet with vortexing. 800 μ L of HisA buffer (Appendix 1) was added to this and the sample was rotated for 10 min at room temperature to solubilize the pellets further. This solution was centrifuged at 13,000xg at room temperature for 5 min. The supernatant containing the solubilized lysate was transferred to a new tube. 25 μ L was taken and used for the 'input' fraction. HIS-Select nickel affinity resin (Sigma) was prepared by washing 200 μ L of the slurry twice with 1.8 mL HisA buffer with collection of the resin carried out by centrifugation at 5,000xg for 30 sec. Solubilized lysate was added to the tube containing the resin and rotated for 2 hrs at room temperature. The tube was centrifuged for 30 sec at 5,000xg and supernatant was removed. The resin was then washed three times using 1.8 mL HisA buffer with the resin collected using centrifugation for 30 sec at 5,000xg. The resin was then washed three times with HisWB1 buffer (Appendix 1) and three times with HisWB2 buffer (Appendix 1), with the resin collected using centrifugation for 30 sec at 5,000xg. Bound proteins were eluted from the resin by adding 100 μ L of HisElution buffer (Appendix 1) and incubating with light shaking for 5 min at room temperature. Resin was spun at 1,000xg for 1 min at room temperature and eluate was transferred to a new tube for subsequent analysis.

To prepare the input sample that was set aside for analysis, the 25 μ L sample was diluted with 1.35 mL of H₂O. 150 μ L of 10% TCA was added to precipitate protein and the sample was kept on ice for 10 min before being centrifuged at 13,000xg for 10 min at 4°C. Supernatant was discarded and the pellet was resuspended in 2x SDS loading dye before being placed at 95°C for 5 min. This sample was centrifuged briefly and used for subsequent analysis.

2.2.4.6 Measurement of protein concentration using amido black

Protein concentrations of extracts solubilized using SDS loading dye were assayed for protein concentration using the amido black concentration assay. 5 μ L of protein extract was added to 195 μ L of H₂O. 800 μ L of amido black staining solution

(Appendix 1) was added and mixed by pipetting. Samples were centrifuged for 20 min at 10,000xg at room temperature. Supernatant was discarded and 1 mL of amido black wash solution (Appendix 1) was added to the tube before centrifugation for 20 min at 10,000xg at room temperature. This step was repeated once more. The pellet was dried under vacuum and then resuspended in 0.2M NaOH. Absorbance was measured at OD₆₀₀ and protein concentration was calculated by interpolation of this value onto a standard curve plot. This standard curve plot was generated using a range of bovine serum albumin (BSA) concentrations, ranging from 0.5 mg/mL to 15 mg/mL.

2.2.4.7 Measurement of protein concentration using Bradford assay

Protein concentrations of extracts solubilized using Luciferase Extraction buffer (Appendix 1) were assayed for protein concentration using the Bradford reagent (Thermo Fisher). Absorbance was measured at OD₆₀₀ and protein concentration was calculated by interpolation of this value on to a standard curve plot. This standard curve plot was generated using a range of bovine serum albumin (BSA) concentrations, ranging from 0.5 mg/mL to 15 mg/mL.

2.2.4.8 Measurement of luciferase activity in tobacco leaf extracts

Measurement of luciferase enzyme activity in tobacco leaf protein extracts was carried out based on methods described in (Luehrsen *et al.*, 1992). Tobacco leaf tissue was frozen in liquid nitrogen and ground to a powder using a pestle. Tissue was resuspended in 150 µL Luciferase Extraction buffer (Appendix 1) and centrifuged at 14,000 rpm at 4°C for 10 min (Hettich Mikro 200R). Supernatant was transferred to a new tube and protein concentration was measured using Bradford reagent (Section 2.2.4.6). 100 µL of LAR buffer (Appendix 1) was added to a well of a white flat bottom 96-well plate. 1 µL of cell lysate was added to the well and mixed by pipetting. Luciferase activity was measured using a POLARstar Omega microplate reader (BMG Labtech) twice for 10 sec intervals each time. This assay was also carried out using protein extracts that did not have any luciferase activity. The background signal from these samples was subtracted from measured sam-

ples and luciferase activity was calculated in relative light units/min/mg protein using the protein concentration determined by Bradford assay.

2.2.4.9 Protein separation by SDS-PAGE electrophoresis

Proteins were denatured by adding 2X SDS loading buffer (Appendix 1), followed by incubation at 95°C for 5 min. After a brief centrifugation at maximum speed at room temperature supernatants were loaded on SDS-PAGE gels with the appropriate acrylamide concentration. The stacking and separating gels were prepared using stacking buffer (Appendix 1) and separating buffer (Appendix 1), respectively.

2.2.4.10 Immunoblot analysis

Protein extracts were separated using SDS-PAGE acrylamide gels, which were run in Tris-glycine buffer (Appendix 1) at 50 V until proteins reached the separating gel and then at 120 V. PVDF membranes were activated by soaking in 100% ethanol for 5 min and then incubated in Transfer buffer (Appendix 1) for 5 min with shaking. Protein extracts were transferred to the PVDF membrane in transfer buffer (Appendix 1) at 60 mA for 1 hr 40 min. After transfer, equal protein loading was checked by Ponceau staining. To this aim, the PVDF membrane was soaked in 7.5% (v/v) acetic acid for 5 min, followed by incubation in Ponceau solution (Appendix 1) for 5 min with shaking. The excess of dye was washed with 7.5% acetic acid. The protein-bound dye was washed away by performing a wash in 0.1 M Tris pH8.8. The PVDF membrane was then rinsed with several washes in PBS-T (Appendix 1) with 0.05% Tween 20 (v/v) and 5% non-fat milk powder (w/v). The primary antibody solution was prepared in PBS-T with 5% milk and was added to the membrane. Incubation with the primary antibody was carried out overnight at 4°C with mild shaking. The next day, the membrane was washed 3 times 5 min with 1x PBS-T. The secondary antibody (anti-rabbit, anti-mouse or anti-goat conjugated to horse radish peroxidase (HRP)) was then added and incubated for at least 2 hrs at room temperature with mild shaking. The excess of secondary antibody was rinsed 3 times for 5 min with 1x PBS-T. Proteins were detected using the WesternBright ECL HRP substrate (Advansta) by chemiluminescence reading carried out with the G:BOX XT4 gel documentation system (SynGene).

Primary antibodies used in this study for immunoblotting were anti-GFP (Ab 290, Abcam), anti-HA (H3663, Sigma), anti-Myc (M5546, Sigma), anti-FLAG (F7425, Sigma), anti-RIN4 (Dangl lab, Gitta Coaker lab or Santa Cruz catalog number Sc-27369)

Secondary antibodies used were anti-rabbit HRP (A0545, Sigma), anti-mouse HRP (A9044, Sigma).

2.2.5 Confocal imaging

In order to visualize GFP-tagged proteins expressed in tobacco leaves an Olympus FluoView1000 laser scanning confocal microscope was used. Tobacco leaf tissue was placed on a slide with H₂O to prevent excessive drying and covered with a coverslip. Protein localization was visualized from the abaxial leaf side. A 488 nm excitation wavelength was used. GFP signal was collected at 500 – 550 nm and auto fluorescence was collected at 600 – 700 nm.

2.2.6 Plasmids generated in this study

The list of plasmids described and generated in this study including a brief description of cloning method used is summarized in table 2.4.

Table 2.4. Plasmids generated in this study and the method by which they were generated.

Plasmid stock ref.	Plasmid description	Cloning strategy
pKG9	pMLBART 35S: UBR ^{PRT6} -RCE1-Myc (noted NEDDylator ^{PRT6} -Myc)	Arabidopsis <i>RCE1</i> was PCR amplified using cDNA as a template with primers KG11 + KG12. The Myc-tag sequence was added using KG9 + KG10 and the two DNA fragments were fused by overlapping PCR and inserted into the pBJ36 35S plasmid using <i>XhoI</i> and <i>Acc65I</i> . This resulted in a plasmid noted pBJ36 35S: RCE1-Myc (pKG5). The UBR domain sequence of <i>PRT6</i> was then amplified by PCR from cDNA using KG19 + KG20 and inserted into pKG5 using <i>Acc65I</i> and <i>XbaI</i> digestion. The resulting construct - noted pBJ36 35S: UBR ^{PRT6} -RCE1-Myc (pKG7) - was then digested out with <i>NotI</i> and inserted into the plant transformation plasmid pMLBART that had been digested with <i>NotI</i> and

		dephosphorylated.
pKG10	pMLBART 35S: Myc- UBR ^{PRT6} - RCE1 (noted Myc- NEDDylator ^{PRT6})	<p>Arabidopsis <i>RCE1</i> was PCR amplified using cDNA with primers KG6 + KG7; the 5' Myc-tag sequence was added using KG4 + KG5 and overlapping PCR. The resulting product was inserted in to a pBJ36 vector containing the 35S promoter sequence (pBJ36 35S) using <i>XhoI</i> and <i>Acc65I</i>. The resulting plasmid is noted pBJ36 35S:Myc-RCE1 (pKG6).</p> <p>The UBR domain sequence of <i>PRT6</i> was amplified using KG17 + KG18 and inserted into pKG6 using <i>Acc65I</i> and <i>XbaI</i> digestion to generate pBJ36 35S: Myc-UBR^{PRT6}-RCE1 (pKG8). The construct was then digested out with <i>NotI</i> and inserted into pMLBART that had been digested with <i>NotI</i> and dephosphorylated.</p>
pKG11	pGreen UBQ3: Ub- Arg-HRE1-FLAG	The coding sequence of Ub was PCR amplified using primers At93 + KG21 and plasmid pEG368 as a template. <i>HRE1</i> cDNA was amplified and fused to a FLAG-tag sequence using KG22, KG23 and KG24. These fragments were fused using overlapping PCR and inserted into a pUC19 plasmid containing the <i>UBQ3</i> promoter sequence using <i>BamHI</i> and <i>XhoI</i> . The construct was transferred to a pGreen vector using <i>HindIII</i> and <i>XbaI</i> .
pKG12	pMLBART 35S: Met-Cys-HRE1- FLAG	HRE1-FLAG sequence was PCR amplified from pKG11 using primers KG35 + KG36. The resulting product was inserted into pBJ36 35S using <i>EcoRI</i> and <i>HindIII</i> . The resulting plasmid was then digested using <i>NotI</i> and the 35S:HRE1-FLAG fragment was ligated into pMLBART that had been <i>NotI</i> digested and dephosphorylated.
pKG13	pMLBART 35S: Met-Cys-HRE2- FLAG	<i>HRE2</i> sequence was PCR amplified from Arabidopsis cDNA and fused to the FLAG-tag sequence using primers KG31, KG33 and KG34. This PCR product was cloned in to pBJ36 35S using <i>EcoRI</i> and <i>HindIII</i> . The resulting construct (pKG14) was then digested out using <i>NotI</i> and the 35S:HRE2-FLAG fragment was inserted into pMLBART that had been digested with <i>NotI</i> and dephosphorylated.
pKG18	pMLBART 35S:GFP-LUC	The luciferase coding sequence was PCR amplified using a plasmid encoding Ub-Arg-Luc available in the lab (pEG368) with the primers KG46 +KG47. This sequence was inserted in to a pBJ36 35S plasmid containing GFP available in the lab (PMU14) using <i>HindIII</i> and <i>XbaI</i> to generate pBJ36 35S: GFP-LUC (pKG15). The 35S:GFP-LUC fragment was then digested out of pKG15 using <i>NotI</i> and inserted in to pMLBART that had been digested with <i>NotI</i> and dephosphorylated.

pKG25	pMLBART 35S: GFP-RIN4- LUC	The <i>RIN4</i> coding sequence was PCR amplified from a plasmid containing the RIN4 sequence available in the lab (pEG349) using primers KG50 + KG51. This sequence was inserted into pBJ36 35S:GFP-LUC (pKG15) using <i>SmaI</i> and <i>HindIII</i> , resulting in pKG21. This plasmid was then digested using <i>NotI</i> and the 35S:GFP-RIN4-LUC fragment was inserted into pMLBART that had been digested with <i>NotI</i> and dephosphorylated.
pKG26	pMLBART 35S:GFP – RIN4 ^{D153G} -LUC	The <i>RIN4</i> sequence with the D153G mutation was PCR amplified from a plasmid containing the mutant RIN4 sequence available in the lab (pEG351) using KG50 + KG51. This sequence was inserted into pBJ36 35S:GFP-LUC (pKG15) using <i>SmaI</i> and <i>HindIII</i> , resulting in pKG22. The 35S:GFP –RIN4 ^{D153G} -LUC fragment was excised using <i>NotI</i> and inserted into pMLBART that had been digested with <i>NotI</i> and dephosphorylated.
pKG27	pMLBART 35S:GFP- RIN4 ^{ΔCt} - LUC	The <i>RIN4</i> ^{ΔCt} sequence was PCR amplified from a plasmid containing the RIN4 sequence available in the lab (pEG349) using primers KG50 + KG52. This sequence was inserted in to pBJ36 35S:GFP-LUC (pKG15) using <i>SmaI</i> and <i>HindIII</i> digestion, resulting in pKG23. The 35S:GFP- RIN4 ^{ΔCt} -LUC fragment was then digested out of pBJ36 using <i>NotI</i> and inserted into pMLBART that had been digested with <i>NotI</i> and dephosphorylated.
pKG28	pMLBART 35S:GFP- RIN4 ^{ΔCtN11G} -LUC	The <i>RIN4</i> ^{ΔCtN11G} sequence was PCR amplified from pEG349 using primers KG50 + KG52. The product was inserted into pBJ36 35S: GFP-LUC (pKG15) using <i>SmaI</i> and <i>HindIII</i> , resulting in pKG24. The 35S:GFP- RIN4 ^{ΔCtN11G} -LUC fragment was then digested out of pKG24 using <i>NotI</i> and inserted into pMLBART that had been digested with <i>NotI</i> and dephosphorylated.
pKG30	pMLBART 35S: Ub-Arg-Luc-FLAG	The Ub-Arg-LUC sequence was PCR amplified from pEG368 using primers KG60, KG61 and KG62. This sequence was inserted into pBJ36 35S using <i>SmaI</i> and <i>HindIII</i> digestion, resulting in pKG29. The 35S: Ub-Arg-Luc-FLAG fragment was then digested out of pKG29 using <i>NotI</i> and inserted in to pMLBART that had been digested with <i>NotI</i> and dephosphorylated.
pKG32	p426 ADH1: RCE1-Myc-6His	The <i>RCE1</i> sequence was PCR amplified from pKG9 using primers KG63 and KG64 that added the 6xHis sequence. This product was cloned in p426 ADH1 yeast expression vector using <i>SpeI</i> and <i>HindIII</i> digestion.
pKG37	p426 ADH1:UBR- RCE1-Myc-6His	The <i>PRT6</i> sequence was PCR amplified from pFrWa4 using primers KG82 + KG83. These primers also added homologous sequences to pKG32. pKG32 was line-

	(noted NEDDylator ^{119 - 188})	arized with <i>SpeI</i> digestion. Linearized pKG32 and the PCR product were co-transformed into <i>S. cerevisiae</i> and the PCR product was introduced into pKG32 by homologous recombination in these cells.
pKG38	p426 ADH1:PRT6 Thr392 RCE1-Myc-6HIS (noted NEDDylator ^{119 - 392})	The <i>PRT6</i> sequence was PCR amplified from pFrWa4 using primers KG82 + KG84. These primers also added homologous sequences to pKG32, which was linearized with <i>SpeI</i> digestion. Linearized pKG32 and the PCR product were co-transformed into <i>S. cerevisiae</i> and the PCR product was introduced into pKG32 by homologous recombination in these cells.
pKG61	pMLBART 35S:GFP-NOI3 ^{E15A} -HA	A plasmid encoding pBJ36 35S:GFP-NOI3-HA available in the lab (pAK7) was used as a template for PCR reactions to mutagenize E15A using primers KG144 + KG145 and KG146 + KG147. The 2 PCR products were then fused by overlapping PCR using KG144 + KG147. This product was digested using <i>AflIII</i> and <i>XmaI</i> and inserted into pBJ36 35S:GFP-NOI3-HA (pAK7) that had been digested with the same enzymes. The resulting construct (pKG56) was digested using <i>NotI</i> and the fragment of interest was inserted into pMLBART that had been digested with <i>NotI</i> and dephosphorylated.
pKG62	p426 ADH1:PRT6-6HA	The <i>PRT6</i> sequence was PCR amplified using primers KG160 + KG161 and pFrWa4 as a template. These primers added homologous sequences to <i>SpeI</i> -linearized p426 ADH1. Linearized plasmid and the PCR product were co-transformed into <i>S. cerevisiae</i> and the PCR product was introduced into p426 ADH1 by homologous recombination in these cells.
pKG63	p415 GALL:PRT6 Δ wHT H-6HA	<i>PRT6</i> sequences flanking the wHTH domain were PCR amplified using primers KG112 + KG113 and KG116 + KG119 (pFrWa4 was used as a template). These two PCR products were then fused using overlapping PCR with KG122 + KG119 to generate a <i>PRT6</i> sequence lacking the wHTH domain. This sequence was inserted into a pJET vector using the pJET cloning kit (Thermo Fisher). This sequence was then used as a template for PCR amplification using KG155 + KG156. These primers added 30 homologous bases to the 5' and 3' end of the sequence to the vector p415 GALL PRT6-6HA (pFrWa4). p415 GALL PRT6-HA was digested with <i>Kpn2I</i> and <i>OliI</i> to remove the wHTH domain. The PCR amplicon generated using KG155 + KG156 was co-transformed into yeast cells with this linearized pFrWa4 plasmid and inserted into the plasmid by homologous recombination in yeast cells.
pKG71	pET28b 6xHis-RIN4	The full-length cDNA sequence of <i>RIN4</i> was PCR amplified with primers KG198 + KG199 using Arabidop-

		sis cDNA as a template. This sequence was digested with <i>Bam</i> HI and <i>Hind</i> III and inserted into pET28b plasmid that had been digested with the same enzymes.
pKG72	pET28b 6xHis-RIN4-II	The cDNA sequence coding for the RIN4-II fragment was PCR amplified with primers KG200 + KG201 using Arabidopsis cDNA as a template. This PCR product was digested with <i>Bam</i> HI and <i>Hind</i> III and inserted into pET28b that had been digested with the same enzymes.
pKG73	pET28b 6xHis-RIN4-III	The cDNA sequence coding for the RIN4-III fragment was PCR amplified with primers KG202 + KG203 using Arabidopsis cDNA as a template. This sequence was digested with <i>Bam</i> HI and <i>Hind</i> III and inserted into pET28b that had been digested with the same enzymes.
pKG74	pMLBART 35S:GFP-NOI2 ^{E20A} -HA	A plasmid encoding pBJ36 35S:GFP-NOI2-HA available in the lab (pAK9) was used as a template for PCR reactions to introduce the E20A mutation using primers KG144 + KG167 and KG168 + KG147. The two PCR products were then fused by overlapping PCR using KG144 + KG147. This product was digested using <i>Afl</i> II and <i>Xma</i> I and inserted into pBJ36 35S:GFP-NOI2-HA (pAK9) that had been digested with the same enzymes. The resulting construct (pKG67) was digested with <i>Not</i> I and the fragment of interest inserted into pMLBART that had been digested with <i>Not</i> I and dephosphorylated.
pKG75	pMLBART 35S:GFP-NOI5 ^{E15A} -HA	A plasmid encoding pBJ36 35S:GFP-NOI5-HA available in the lab (pAK8) was used as a template for PCR reactions to introduce the E15A mutation using primers KG144 + KG169 and KG170 + KG147. The two PCR fragments were then fused by overlapping PCR using KG144 + KG147. The two PCR products were then fused by overlapping PCR using KG144 + KG147. This product was digested using <i>Afl</i> II and <i>Xma</i> I and inserted into pBJ36 35S:GFP-NOI5-HA that had been digested with the same enzymes. The resulting construct (pKG68) was digested with <i>Not</i> I and the fragment of interest inserted into pMLBART that had been digested with <i>Not</i> I and dephosphorylated.
pKG76	pMLBART 35S:GFP-NOI6 ^{D20A} -HA	A plasmid encoding pBJ36 35S:GFP-NOI6-HA available in the lab (pAK6) was used as a template for PCR reactions to introduce the D20A mutation using primers KG144 + KG171 and KG172 + KG147. The two PCR fragments were then fused by overlapping PCR using KG144 + KG147. This product was digested using <i>Afl</i> II and <i>Xma</i> I and inserted into pBJ36 35S:GFP-NOI6-HA that had been digested with the same en-

		zymes. The resulting construct (pKG69) was digested with <i>NotI</i> and the fragment of interest inserted into pMLBART that had been digested with <i>NotI</i> and dephosphorylated.
pKG77	pMLBART 35S: GFP-NOI11 ^{D12A} -HA	A plasmid encoding pBJ36 35S:GFP-NOI11-HA available in the lab (pAK4) was used as a template for PCR reactions to introduce the D12A mutation using primers KG144 + KG173 and KG174 + KG147. The two PCR fragments were then fused by overlapping PCR using KG144 + KG147. This product was digested using <i>AflIII</i> and <i>XmaI</i> and inserted into pBJ36 35S:GFP-NOI11-HA that had been digested with the same enzymes. The resulting construct (pKG70) was digested with <i>NotI</i> and the fragment of interest inserted into pMLBART that had been digested with <i>NotI</i> and dephosphorylated.
pKG78	pMLBART 35S: GFP-NOI1 ^{E14A} -HA	A plasmid encoding pBJ36 35S:GFP-NOI1-HA available in the lab (pAK5) was used as a template for PCR reactions to introduce the E14A mutation using primers KG144 + KG165 and KG166 + KG147 that were then fused by overlapping PCR using KG144 + KG147. This product was digested using <i>AflIII</i> and <i>XmaI</i> and inserted into pBJ36 35S:GFP-NOI1-HA (pAK5) that had been digested with the same enzymes. The resulting construct (pKG78) was digested with <i>NotI</i> and the fragment of interest inserted into pMLBART that had been digested with <i>NotI</i> and dephosphorylated.
pKG79	pBin 35S: Ub-RIN4-II-mCherry-GFP	The Ub-coding sequence was amplified using pKG30 as a template for PCR with primers KG185 + KG186. RIN4-II was PCR amplified using Arabidopsis cDNA with primers KG187 + KG188. These two PCR products were fused using overlapping PCR with primers KG185 and KG188 and cloned into a pJET plasmid using the pJET cloning kit (Thermo Fisher), resulting in pKG83. The pKG83 plasmid was then used as a template for a PCR reaction using primers KG185 + KG220. The resulting amplicon was digested with <i>SmaI</i> and cloned into pBin 35S:mCherry-GFP (Dr. Markus Wirtz; University of Heidelberg; unpublished) that had been digested with <i>KpnI</i> and <i>XhoI</i> before being blunt-ended with T4 polymerase and dephosphorylated.
pKG80	pBin 35S: Ub-RIN4-II ^{N11A} - mCherry-GFP	The Ub coding sequence was amplified using pKG30 as a template for PCR using primers KG185 + KG189. RIN4-II ^{N11A} was PCR amplified using pEG349 with primers KG190 + KG188. These two PCR products were fused using overlapping PCR with primers KG185 and KG188 and cloned into a pJET using the

		pJET cloning kit (Thermo Fisher). The resulting plasmid (pKG84) was used as a template for a PCR reaction using primers KG185 + KG220. The resulting amplicon was digested with <i>SmaI</i> and cloned into pBin 35S:mCherry-GFP (Dr. Markus Wirtz; University of Heidelberg; unpublished) that had been digested with <i>KpnI</i> and <i>XhoI</i> before being blunt-ended with T4 polymerase and dephosphorylated.
pKG81	pBin 35S: Ub-RIN4-III - mCherry-GFP	The Ub coding sequence was amplified using pKG30 as a template for PCR using primers KG185 + KG191. RIN4-III was PCR amplified using pEG349 with primers KG192 + KG193. These two PCR products were fused by overlapping PCR with primers KG185 and KG193 and cloned into a pJET plasmid using the pJET cloning kit (Thermo Fisher). The resulting pJET derivative (pKG85) was used as a template for a PCR reaction using primers KG185 + KG219. The resulting amplicon was digested with <i>SmaI</i> and cloned into pBin 35S:mCherry-GFP (Dr. Markus Wirtz; University of Heidelberg; unpublished) that had been digested with <i>KpnI</i> and <i>XhoI</i> before being blunt-ended with T4 polymerase and dephosphorylated.
pKG82	pBin 35S: Ub-RIN4-III ^{D153A} - mCherry-GFP	The Ub sequence was amplified using pKG30 as a template for PCR using primers KG185 + KG194. RIN4-III ^{D153A} was PCR amplified using pEG349 with primers KG193 + KG195. These two PCR products were fused using overlapping PCR with primers KG185 and KG193 and cloned into a pJET plasmid using the pJET cloning kit (Thermo Fisher). The resulting pJET derivative (pKG86) was used as a template for a PCR reaction using primers KG185 + KG219. The resulting amplicon was digested with <i>SmaI</i> and cloned into pBin 35S:mCherry-GFP (Dr. Markus Wirtz; University of Heidelberg; unpublished) that had been digested with <i>KpnI</i> and <i>XhoI</i> before being blunt-ended with T4 polymerase and dephosphorylated.
pKG83	P426 ADH1: UBR1-6HA	The UBR1-6HA sequence was amplified from a plasmid encoding pGALL: UBR1-6HA available in the lab (pFrWa3) using primers KG183 + KG184. This product was digested using <i>SmaI</i> and <i>XhoI</i> and inserted in to the p426 ADH1 vector that had been digested using the same enzymes.

Chapter 3. Investigating the Degradation of Arabidopsis Protein Fragments Following Cleavage by the *Pseudomonas syringae* Effector Protease AvrRpt2

3.1 Introduction

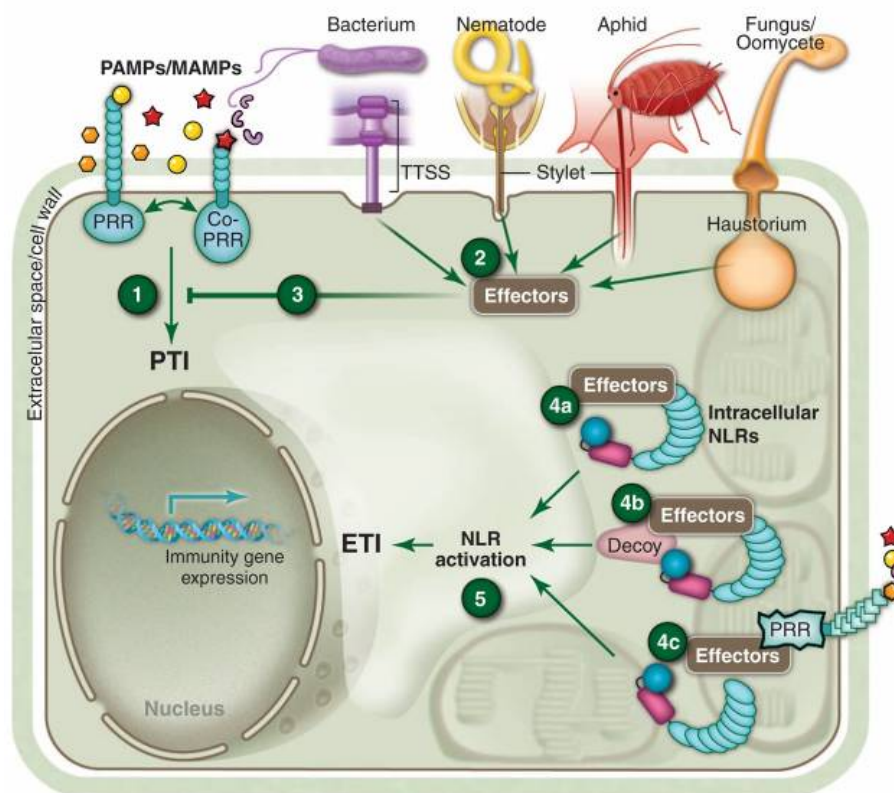
One method for the identification of *bona fide* N-end rule substrates is a candidate approach, whereby knowledge of previously published protease activity and cleavage sites can be used to identify substrates of the pathway (discussed in Section 1.3.3). A group of candidate N-end rule substrates identified in this manner include protein fragments produced following cleavage of host proteins by the *P. syringae* protease effector AvrRpt2. In this chapter, I will give an overview of the plant immune system, as well as discuss AvrRpt2 and its putative Arabidopsis targets. I will then present experiments I have conducted to determine if these protein fragments are unstable and if they are degraded by the N-end rule pathway.

3.1.1 Overview of the plant immune system

Unlike mammals, plants do not have mobile specialized defence cells. Instead, individual cells are capable of mounting an immune response following detection of pathogens by specific receptors with different sub-cellular localizations. Extracellular transmembrane receptors called pattern recognition receptors (PRRs) recognize conserved pathogen elements termed pathogen-associated molecular patterns (PAMPs). This recognition triggers a set of immune responses including a Ca²⁺ burst, callose deposition, stomatal closure, generation of reactive oxygen species, the production of anti-microbial compounds and large changes in gene expression, which are collectively termed pattern triggered immunity (PTI) (reviewed in Jones and Dangl, 2006; Bigeard *et al.*, 2015). Many pathogens have evolved mechanisms to suppress or avoid this PTI response. In particular, pathogens secrete into host cells or the extracellular matrix effector proteins or molecules that manipulate host-signaling pathways and boost pathogen virulence (Bigeard *et al.*, 2015). However, plants have evolved specialized ‘resistance’ (R) genes, which encode intracellular nucleotide-binding/leucine-rich repeat (NLR) receptors (R proteins) that recognize, directly or indirectly, effector proteins or their activity.

This recognition event results in the activation of an effector-triggered immune (ETI) response. This ETI response shares many of the same signaling components of the PTI program, but also typically elicits the activation of a localized programmed cell death termed hypersensitive response (HR) (reviewed in Cui *et al.*, 2015). The onset of ETI triggered by the recognition of pathogen effectors by R proteins relies on different molecular mechanisms, such as (i) the direct recognition of pathogenic effectors by R proteins; (ii) effector detection mediated through the modification of a host-protein; or (iii) recognition of effector-mediated changes of a host decoy protein that structurally mimics the endogenous effector target, but has no other function other than allowing the recognition of the effector's activity (reviewed in Dangl *et al.*, 2013).

Fig 3.1. Overview of plant-pathogen recognition and response pathways. (1) As pathogens



attempt to colonize plants, conserved PAMPs are detected by plant-encoded, membrane-localized PRRs, triggering a PTI response. (2) and (3) Pathogens also secrete effector proteins to modulate plant-signaling pathways. As indicated on the figure, other organisms that interact with plants, such as insects or nematodes, also secrete effectors. NLR receptors can recognize pathogen effectors directly (4a), by sensing modification of a host decoy protein and forming a complex with the effector protein (4b), or through sensing modification of a host virulence target, such as the cytosolic do-

main of a PRR (4c). (5) Effector detection results in the activation of the NLR and to the onset of ETI. Image from (Dangl *et al.*, 2013).

3.1.2 Arabidopsis RIN4 is a plant immune regulator that is targeted by multiple bacterial effectors

The Arabidopsis encoded RPM1-INTERACTING PROTEIN4 (RIN4) is a membrane-localized protein that acts as a negative regulator of both PTI and ETI responses (Kim *et al.*, 2005b; Afzal *et al.*, 2011). This membrane-localization is mediated through C-terminal cysteine residues that are likely palmitoylated or prenylated (Kim *et al.*, 2005a; Takemoto and Jones, 2005). RIN4 is involved in mediating stomatal re-opening after bacterial infection *via* interaction with plasma-membrane H⁺-ATPase proton pumps and also regulates the membrane localization of a subunit of the exocyst complex, EXO70B1, which is involved in protein trafficking (Liu *et al.*, 2009; Sabol *et al.*, 2017). Likely as a result of its central role in immune signaling, RIN4 is targeted for modification by a number of bacterial effectors. Four *P. syringae* effector proteins targeting RIN4 have been identified to date: (i) AvrRpt2, a cysteine protease that cleaves RIN4 (see below for details); (ii) AvrB and AvrRpm1, which trigger phosphorylation of RIN4 by the plant receptor-like kinase RIPK (Liu *et al.*, 2011); and (iii) HopF2, an ADP-ribosylase that can ribosylate RIN4 *in vitro* (Mackey *et al.*, 2003; Axtell *et al.*, 2003; Mackey *et al.*, 2002; Wang *et al.*, 2010). The Arabidopsis genome encodes at least two NLR proteins that detect different effector-triggered modifications of RIN4. One of these NLR proteins, RESISTANCE TO *P. SYRINGAE* PV MACULICOLA1 (RPM1), triggers an ETI response following phosphorylation of RIN4 in the presence of AvrB or AvrRpm1, while the NLR protein RESISTANT TO *P. SYRINGAE*2 (RPS2) activates ETI upon cleavage of RIN4 by AvrRpt2 (Mackey *et al.*, 2002; Mackey *et al.*, 2003).

3.1.3 RIN4 cleavage by the *P. syringae* effector AvrRpt2

The *P. syringae* protease effector AvrRpt2 is introduced as an inactive protease into plant cells *via* a type III secretion system. Once inside the cell it is activated by one or more host cyclophilins before undergoing self-cleavage at its N-terminus

and localizing to the host plasma membrane (Coaker *et al.*, 2005; Axtell *et al.*, 2003; Axtell and Staskawicz, 2003). At the plasma membrane, AvrRpt2 cleaves RIN4 at two sites, noted RCS1 and RCS2, located in the N- and C-terminal plant-specific nitrate-induced (NOI) domains of the RIN4 protein, respectively (Fig 3.2)(Chisholm *et al.*, 2005). Two of the RIN4 fragments generated by this cleavage (noted RIN4-II and RIN4-III; see Fig 3.2) are not detected in immunoblot experiments using antibodies specific to RIN4 following inoculation of wild-type or *rps2* Arabidopsis plants with *P. syringae* encoding AvrRpt2 (strain noted Pst AvrRpt2)(Mackey *et al.*, 2003; Axtell and Staskawicz, 2003). These results suggest that the RIN4-II and RIN4-III fragments may be targeted for degradation upon inoculation with Pst AvrRpt2. Similar results are obtained when Arabidopsis lines encoding a transgene that allows the dexamethasone (DEX)-inducible expression of AvrRpt2 (line noted AvrRpt2^{DEX} hereafter) are treated with a DEX-containing solution (Mackey *et al.*, 2003). The use of AvrRpt2^{DEX} lines allows for a more targeted approach to study the effects of RIN4 cleavage by AvrRpt2 compared to inoculation with Pst AvrRpt2, and hence further supports the idea that the RIN4-II and RIN4-III fragments are unstable *in planta*. It is thought that the potential degradation of these fragments could play an important role in the activation of RPS2-mediated ETI (Mackey *et al.*, 2003, Axtell and Staskawicz, 2003, Axtell *et al.*, 2003), as it would disrupt the interaction of RIN4 and RPS2, thus abolishing the repression of RPS2 activity by RIN4. Importantly, the protein degradation pathway(s) responsible for the degradation of the proteolytic RIN4 fragments in a physiological context have remained largely elusive.

2016). Additionally, RIN4 and its cleavage by AvrRpt2 may disrupt its role in the regulation of the exocyst subunit EXO70B1 (Sabol *et al.*, 2017).

One possible pathway that may be responsible for the processing of RIN4 fragments after cleavage by AvrRpt2 is the N-end rule pathway. RIN4-II and RIN4-III both bear N-terminal destabilizing residues, Asn11 and Asp153, respectively (Fig 3.2). The destabilizing residues following the AvrRpt2 cleavage motifs in RIN4 are also evolutionarily conserved across a number of plant species (Fig 3.2), with a few exceptions including in *Amborella trichopoda* and in monocots, which appear to code for at least two different RIN4 orthologs, some of which bear the stabilizing residue Ser at the N-terminus of the RIN4-II fragment (Fig. 3.2). Experiments with a short fragment of RIN4, composed of the first 30 amino acid residues of RIN4, fused to the GFP reporter protein suggest that cleavage of this RIN4 fragment at RCS1 results in the degradation of the fused GFP reporter (Takemoto and Jones, 2005). Mutation of the newly exposed N-terminal residue (Asn 11 in the full-length RIN4 sequence) into Gly led to a stabilization of the fragment fused to GFP, suggesting that this short RIN4 fragment (i.e. residues 11 to 30) released after AvrRpt2 cleavage may be degraded through the N-end rule pathway when expressed as a fusion protein with GFP.

3.1.4 Arabidopsis encodes multiple AvrRpt2 cleavage targets

Another mechanism through which AvrRpt2 might enhance *P. syringae* virulence is by proteolytically targeting a number of other plant host proteins. Chisholm *et al.*, identified various proteins in Arabidopsis that contain the AvrRpt2 consensus cleavage site motif (i.e. the sequence VPxFGxW, where x is any amino acid residue) (Chisholm *et al.*, 2005). These putative targets include a group of proteins that contain an NOI domain and several C-terminal cysteine residues similarly to RIN4. However, besides these two shared features, these other AvrRpt2 putative targets have no apparent homology to RIN4 (Afzal *et al.*, 2013). More recently, several of these NOI domain proteins were shown to be cleaved by AvrRpt2 (Eschen Lippold *et al.*, 2016). Although the function of these NOI domain proteins is largely unknown, they are hypothesized to play a role in plant defence responses (Afzal *et al.*, 2013). For example, similarly to RIN4, NOI6 was identified in yeast two hybrid screens as interacting with a subunit of the exocyst complex, in this case EXO70A1,

suggesting that perhaps the NOI domains of these proteins facilitate interaction with exocyst complex subunits (Afzal *et al.*, 2013; Sabol *et al.*, 2017). NOI6 also interacts with a protein belonging to the cysteine/histidine rich family, while NOI3 interacts with a heat shock protein in yeast, HSP81-3 (Afzal *et al.*, 2013).

Importantly, cleavage of various NOI domain proteins by AvrRpt2 is predicted to generate C-terminal fragments that bear destabilizing N-terminal residues according to the N-end rule (Chisholm *et al.*, 2005; see also Table 3.1 below). Although it is not known whether these new proteolytic fragments are unstable, we hypothesized that the plant N-end rule pathway could target them for degradation after AvrRpt2 cleavage.

Table 3.1. List of Arabidopsis putative NOI-domain AvrRpt2 targets. The Arabidopsis Gene Identifier (AGI), the protein name and the predicted N-terminal residue after AvrRpt2 cleavage are indicated.

AGI	Protein Name	N-terminal Residue of AvrRpt2 Cleavage Product
At3g25070	RIN4 (RIN4-II fragment)	Asn (N)
At3g25070 At5g64850 At5g09960 At5g48657 At3G07195	RIN4 (RIN4-III fragment) NOI6 NOI7 NOI10 NOI11	Asp (D)
At5g63270 At5g40645 At2g17660 At5g55850 At3g48450 At5g18310	NOI1 NOI2 NOI3 NOI4 NOI5 NOI8	Glu (E)

3.1.5 Experimental aims

As mentioned above numerous lines of evidence suggest that AvrRpt2-generated RIN4 fragments might be substrates of the N-end rule pathway. With the aim of investigating this possibility in a physiological context (as opposed to using short N-terminal fragments (Takemoto and Jones, 2005)), I carried out assays using different variants of RIN4 that were expressed in Arabidopsis AvrRpt2^{DEX} lines. After

AvrRpt2 induction *via* treatment with a DEX-containing solution in different conditions, the stability of the RIN4-II and RIN4-III fragments was assessed by immunoblotting using antibodies raised against Arabidopsis RIN4. I used similar approaches to test the stability of these RIN4 fragments using transient expression of wild-type and mutant RIN4 proteins in tobacco plants, which were also inoculated with Pst AvrRpt2. I also generated fluorescent timer constructs to determine more accurately RIN4 protein fragment stability in Arabidopsis wild-type and N-end rule mutant plants.

Finally, to determine if a subset of the Arabidopsis NOI-domain proteins that are targeted by AvrRpt2 are degraded by the N-end rule pathway, I generated epitope-tagged versions of these constructs with various mutations and assayed their stability after AvrRpt2 cleavage in tobacco plants.

3.2 Results

3.2.1 Characterization of available antibodies for RIN4 stability assays

In order to assay the stability of RIN4-II and III after AvrRpt2 cleavage, I used immunoblotting with different antibodies that had been raised against RIN4 or some RIN4-specific peptides. These antibodies were either commercially available or were kindly shared by other research groups. The generation method of these antibodies, as well as their origin, is summarized in Table 3.2. Antibodies that were generated by the lab of Jeffrey Dangl are denoted 'anti-RIN4 Dangl', while antibodies raised in the lab of Gitta Coaker are denoted 'anti-RIN4 Coaker'. Finally, the RIN4-specific antibodies commercialized by Santa Cruz are abbreviated 'anti-RIN4 Sc' (Santa Cruz catalog number Sc-27369).

Table 3.2. Summary of RIN4 antibodies used and generation methods.

Name	Antibody Generation	RIN4 Antigen	Reference
Anti-RIN4 Dangl	Rabbit polyclonal antibody	Amino acids 77-211	Mackey <i>et al.</i> , 2002
Anti-RIN4 Coaker	Affinity purified rabbit polyclonal antibody	Full-length RIN4	Liu <i>et al.</i> , 2009
Anti-RIN4 Sc	Affinity purified goat polyclonal antibody	N-terminal RIN4 peptide	https://datasheets.scbt.com/sc-27369.pdf

To check the specificity of these antibodies towards full-length RIN4 (noted RIN4^{FL}), as well as RIN4-II and III, I cloned the gene fragments coding for these sequences into the *E. coli* expression vector pET28b (Merck Millipore) (see Section 2.2.6 and Table 2.4 for list of plasmids generated). The resulting plasmids allow for the expression of proteins translationally fused to an N-terminal hexa-histidine (6xHis) tag under the control of the T7lac promoter (i.e. a T7 promoter combined with lac operator sequences), which may be activated in the presence of isopropyl β -D-1-thiogalactopyranoside (IPTG) in BL21 (DE3) *E. coli* cells that also code for the T7 polymerase under the control of the IPTG-inducible lac promoter. After the induced expression of these recombinant RIN4 variants in *E. coli*, crude lysates were analyzed using SDS-PAGE and immunoblotting with the three different RIN4 antibodies mentioned above. As a control, similar immunoblots were carried out using an antibody specific to the 6xHis tag (Fig. 3.3).

The anti-RIN4 antibodies from the Dangl lab and from the Coaker lab were both able to detect full-length RIN4, as well as the RIN4-II and III fragments. In contrast, the Santa Cruz antibody could detect only the full-length protein and RIN4-II, which was in agreement with the use of an N-terminal peptide for antibody generation. Using the His tag-specific antibody, all three proteins could be detected. Because the RIN4-specific antibodies from the Dangl and Coaker labs were able to detect both RIN4-II and III, they were used in subsequent experiments aimed at determining if RIN4-II and III could be N-end rule substrates.

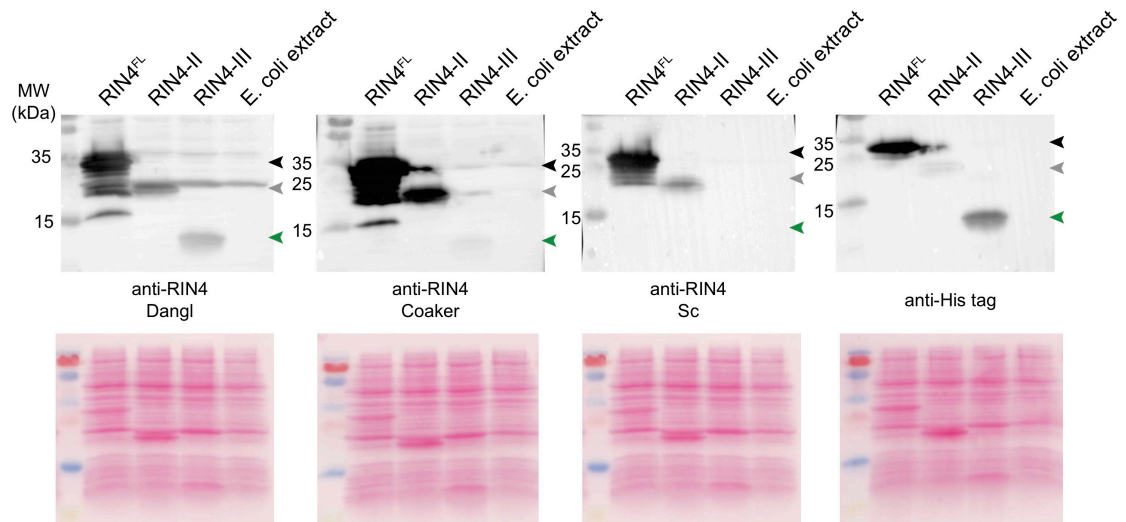


Fig 3.3. Specificity of different antibodies towards RIN4 fragments and the full-length protein. Crude lysates of *E. coli* BL21(DE3) pLysS RARE expressing 6xHis-RIN4^{FL} (~27 kDa; black arrowhead), 6xHis-RIN4-II (~19.5 kDa; grey arrowhead), or 6xHis-RIN4-III (~9.9 kDa; green arrowhead) were prepared in 2X SDS loading buffer (Appendix 1). Protein concentration was measured using an amido black assay. Proteins were then separated using 14% SDS-PAGE electrophoresis and then analyzed using immunoblotting with different RIN4-specific antibodies. An *E. coli* lysate generated from untransformed BL21(DE3) pLysS RARE was also analyzed to determine possible *E. coli* cross-reacting proteins for each of the antibodies tested. Figure from (Goslin *et al.*, manuscript under preparation).

3.2.2 Cleavage of RIN4 by AvrRpt2 in Arabidopsis seedlings

To investigate the degradation of the RIN4-II and III fragments released after AvrRpt2 cleavage, I used a previously published wild-type Arabidopsis AvrRpt2^{DEX} line (Col-0 accession), which allows the inducible expression of AvrRpt2 using a DEX-containing solution (McNellis *et al.*, 1998; see above) (Fig. 3.4A). In addition, I used plants isolated after transformation of the above-mentioned Col-0 AvrRpt2^{DEX} line with a T-DNA coding for a mutated full-length RIN4 in which Asn 11 was changed into Gly (mutant protein noted RIN4^{N11G}; unpublished line generated by E. Graciet) (Fig. 3.4B). The expression of the RIN4^{N11G} mutant sequence was under the control of the constitutive 35S promoter to allow for its ectopic expression. Cleavage of RIN4^{N11G} by AvrRpt2 is predicted to generate a RIN4-II fragment (~15.9 kDa) that has an N-terminal Gly residue, which is a stabilizing residue based on the plant N-end rule (Graciet *et al.*, 2010). Therefore, if the N-end rule

were responsible for the degradation of wild-type RIN4-II, AvrRpt2 cleavage of the mutated RIN4^{N11G} protein would be expected to yield a Gly-RIN4-II fragment that should accumulate in cells. For these experiments, seedlings were grown in liquid 0.5x MS medium for 7 d before addition of 10 μ M DEX (final concentration) for 5 hrs, followed by tissue collection (see Materials and Methods, Section 2.2.2.5). A 5-hr time point was chosen because previous experiments using this Col-0 AvrRpt2^{DEX} line showed a decrease in RIN4 abundance beginning 4 hrs post DEX treatment, with RIN4 levels significantly decreased at 6 hrs post treatment (Elmore *et al.*, 2012). In addition, *rps2 rin4* null mutant plants (Mackey *et al.*, 2003) were subjected to the same treatments in order to identify cross-reacting proteins that may be recognized by the anti-RIN4 Coaker antibody (Fig. 3.4A). These double mutants were used because a *rin4* single mutation is lethal, as RPS2 is constitutively activated (Mackey *et al.*, 2003). Although RIN4 is \sim 23 kDa, it has been previously observed that the fragment migrates slightly higher than this on SDS-PAGE gels at \sim 25 kDa (Hurley *et al.*, 2014).

I also carried out preliminary RIN4 cleavage experiments using a line generated by crossing the *ate1-2 ate2-1* mutant (abbreviated *ate1 ate2*) with the above-mentioned AvrRpt2^{DEX} line (noted *ate1 ate2* AvrRpt2^{DEX}; isolated by E. Graciet). This line was relevant for these experiments because the N-end rule-dependent degradation of the RIN4-II and III fragments would require the activity of the Arg-transferases ATE1 and ATE2 (see Fig. 1.5 and Section 1.2.4.1). It has been previously shown that the *ate1 ate2* mutant has no detectable Arg-transferase activity (Graciet *et al.*, 2009), so that the RIN4-II and III fragments should accumulate in these plants after induction of AvrRpt2 expression. Unfortunately, the AvrRpt2^{DEX} transgene was silenced in the resulting lines, perhaps due to the presence of multiple T-DNA insertions encoding the 35S promoter (data not shown). Such silencing effects in this line have been observed repeatedly with different T-DNAs coding for genes under the control of the 35S promoter.

In AvrRpt2^{DEX} lines expressing endogenous RIN4 or expressing mutant RIN4^{N11G}, DEX treatment induced the disappearance of the endogenous full-length RIN4 and of the full-length mutant RIN4^{N11G} protein (Fig 3.4 A and B), as would be expected following cleavage of these proteins by AvrRpt2 (Elmore *et al.*, 2012). However, treatment with DEX of AvrRpt2^{DEX} 35S_{pro}: RIN4^{N11G} seedlings did not

lead to the accumulation (i.e. stabilization) of the Gly-RIN4-II fragment (~16 kDa) (Fig 3.4B). In sum, the results of these experiments suggest that the RIN4-II fragment is likely targeted for degradation by a different pathway than the N-end rule. It is worth noting that when *AvrRpt2*^{DEX} plants, which only express the endogenous RIN4, were mock treated a protein with a size similar to that of RIN4-II could be detected (Fig 3.4C, indicated by black arrow). This protein was detected reproducibly in the different biological replicates I carried out (data not shown). At this stage, though, it is not known whether this protein corresponds to the RIN4-II fragment, which could have been released due to leaky expression of *AvrRpt2* in the absence of DEX in the medium.

I also attempted similar experiments with *AvrRpt2*^{DEX} lines expressing another mutant version of RIN4, in which Asp 153 was replaced by a Gly (lines noted *AvrRpt2*^{DEX} 35S_{pro}:RIN4^{D153G}; generated by E. Graciet). The latter mutation should result in a RIN4-III fragment with N-terminal Gly, which should be stable if it is an N-end rule substrate. Unfortunately, the lines that had been isolated did not germinate, likely because of the age of the seeds, and hence I could not complete these experiments.

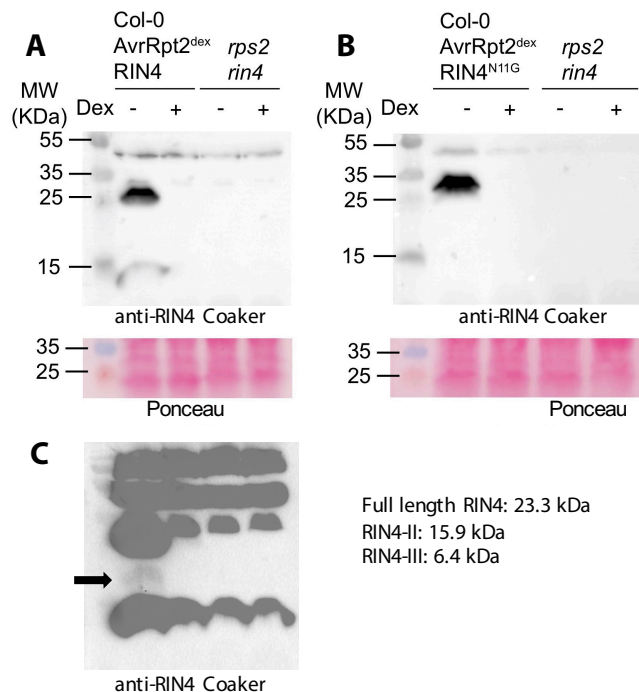


Fig 3.4. Cleavage of RIN4 by *AvrRpt2* in Arabidopsis seedlings. (A) Treatment with a DEX-containing solution induces the disappearance of the endogenous full-length RIN4 (~23 kDa) in Col-0 *AvrRpt2*^{DEX} seedlings, as a result of its cleavage by *AvrRpt2*. (B) Induction of *AvrRpt2* expres-

sion also triggers the disappearance of full-length RIN4^{N11G} in AvrRpt2^{DEX} 35S_{pro}: RIN4^{N11G} seedlings. The Gly-RIN4-II fragment (15 kDa) is not detected despite the presence of a stabilizing N-terminal residue. (C) Overexposure of the immunoblot presented in panel A reveals a band that migrates roughly at the expected molecular weight of RIN4-II in the mock treated Col-0 AvrRpt2^{DEX} seedlings (indicated by black arrow). This is likely due to leaky expression of AvrRpt2 in mock-treated seedlings. For both experiments seedlings were grown in liquid 0.5x MS medium for 7 d before addition of 10 μ M DEX for 5 hrs, followed by tissue collection in liquid nitrogen. Tissue was ground in liquid nitrogen before proteins were solubilized in 2x SDS loading buffer and total protein extracts were separated using SDS-PAGE and analyzed using immunoblotting with anti-RIN4 antibodies.

Next, I investigated whether DEX-mediated induction of AvrRpt2 expression in the presence of different chemical inhibitors could stabilize RIN4 cleavage products. To try and determine if the inhibition of different degradation pathways might have an effect on RIN4 fragment stability, I used three different chemicals: (i) MG132, a proteasome inhibitor; (ii) bafilomycin A1, a vacuole inhibitor which would affect autophagy-mediated degradation; and (iii) MLN4924, a NEDD8-conjugation inhibitor, which would block the action of Cullin-RING E3 ubiquitin ligases (see Section 1.1.2.4). For these experiments, Col-0 AvrRpt2^{DEX} seedlings were grown in liquid 0.5x MS for 7 d, and AvrRpt2 was induced using 10 μ M DEX. In addition, the seedlings were treated with 100 μ M MG132 (concomitantly and sequentially as described below), 1 μ M bafilomycin A1 or 100 μ M MLN4924 (both added at the same time as DEX). Proteins were then extracted in 2x SDS loading buffer and the protein extracts were separated using SDS-PAGE and analyzed *via* immunoblotting with the anti-RIN4 Coaker antibody (Fig. 3.5)

Apart from MG132, the co-treatment of these chemicals with DEX did not have any detectable effect on (i) the activity of AvrRpt2; or (ii) the stability of RIN4-II and III. The stabilization of full-length RIN4 when AvrRpt2^{DEX} lines were co-treated with DEX and MG132 (Fig 3.5A) is likely due to the protease activity of AvrRpt2 being inhibited by MG132, as this chemical is known to inhibit certain cysteine proteases (reviewed in Lee and Goldberg, 1998). To try and circumvent AvrRpt2 inhibition prior to proteasome inhibition, AvrRpt2^{DEX} seedlings were

treated with DEX and then after 3 hrs were treated with MG132, with the tissue being collected 5 hrs after the addition of DEX to the medium. This sequential treatment resulted in the disappearance of full-length RIN4, but no RIN4-II and III fragments were detected (Fig 3.5B), suggesting that they were still unstable. Similarly, for treatments with bafilomycin A1 and MLN4924, no RIN4 fragments were detected (Fig 3.5C and D) despite cleavage of the full-length protein by AvrRpt2. Therefore, it is unclear at this stage whether RIN4 fragments are cleared via the ubiquitin/proteasome system or by another pathway such as autophagy. Unfortunately, the absence of stabilization in these experiments could not be investigated further due to time limitations.

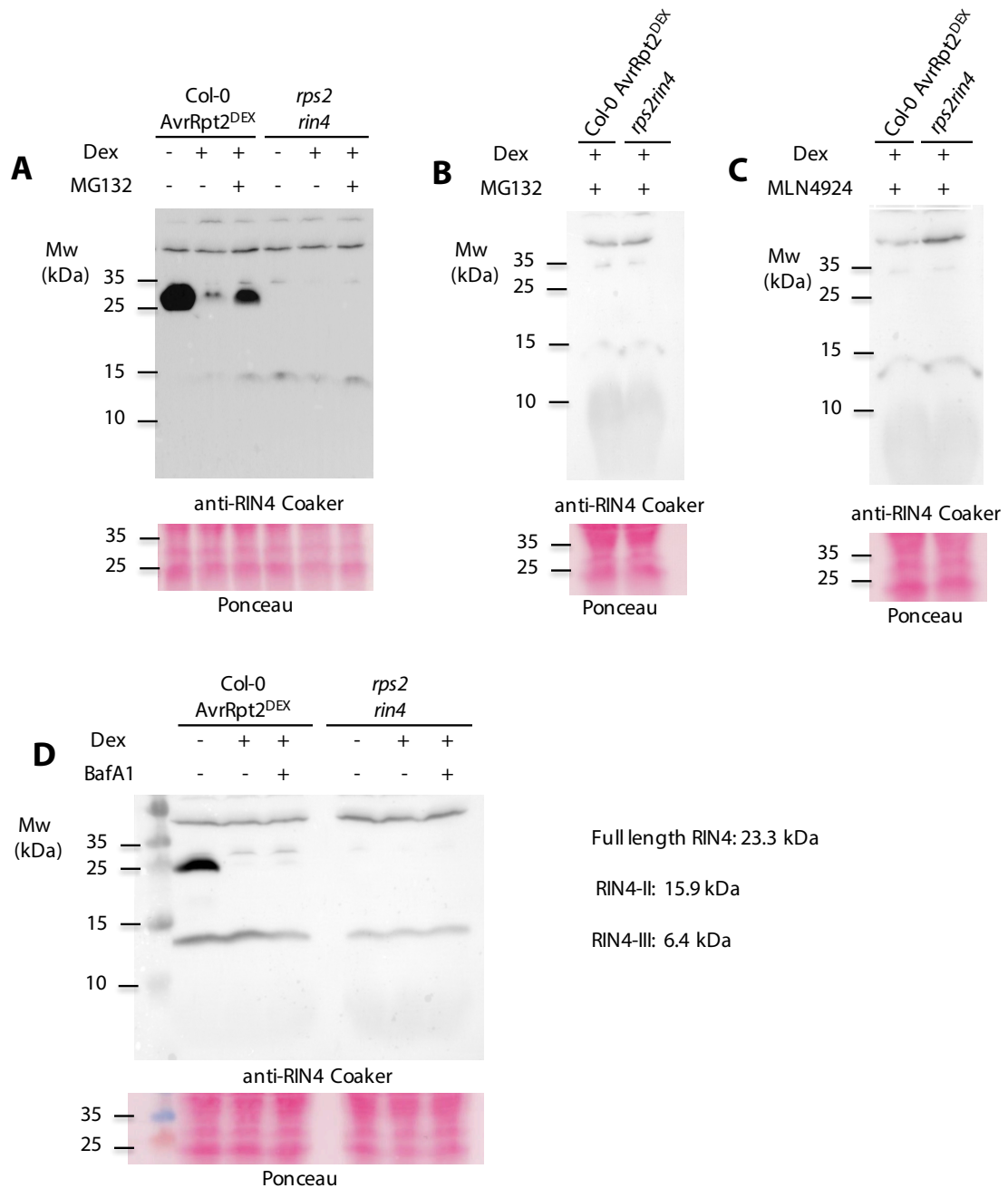


Fig 3.5. Effect of different chemical inhibitors on RIN4 fragment stability. (A) Co-treatment with DEX and the proteasome inhibitor MG132 (100 μ M) appears to inhibit AvrRpt2 cleavage of RIN4. (B) When MG132 is introduced 3 hrs after the beginning of the DEX induction, AvrRpt2 expression correlates with the disappearance of the full-length endogenous RIN4 protein. However, neither RIN4-II nor RIN4-III are detected, suggesting that MG132 treatment does not stabilize the fragments in the current experimental conditions. (C and D) Co-treatment of AvrRpt2^{DEX} seedlings with DEX and either 100 μ M MLN4924 or 1 μ M bafilomycin A1 for 5 hrs does not stabilize the RIN4-II and RIN4-III fragments, despite cleavage of the full-length protein by AvrRpt2.

3.2.3 Cleavage of mutant RIN4 by AvrRpt2 in tobacco

In order to determine if AvrRpt2-generated RIN4 fragments are degraded by the N-end rule pathway, I also made use of a transient expression system using tobacco plants (*Nicotiana benthamiana*) and plasmid constructs previously generated by Dr. Stephen Chisholm (Brian Staskawicz lab). These plasmids encode, under the control of the constitutive 35S promoter, wild-type RIN4 or the RIN4^{N11G} and RIN4^{D153G} mutant proteins that would be expected to generate stable RIN4 fragments according to the N-end rule after AvrRpt2 cleavage (note: these plasmids were used to generate the different Arabidopsis AvrRpt2^{DEX} lines described in Section 3.2.2). To investigate whether the RIN4-II and III fragments were N-end rule substrates in tobacco, *A. tumefaciens* strains carrying these plasmids were infiltrated into tobacco leaves. Two days after agroinfiltration, the same leaves were infiltrated with *P. syringae* expressing either the active AvrRpt2 or the proteolytically inactive mutant AvrRpt2^{C122A}. As a control, agroinfiltrated leaves were also inoculated with *P. syringae* DC3000, which does not code for AvrRpt2. Six hours after the *P. syringae* inoculations, tobacco leaf tissue was collected and protein extracts were analyzed using SDS-PAGE and immunoblotting with the anti-RIN4 Dangl antibody. These results are presented in Fig. 3.6.

Inoculation with Pst AvrRpt2 resulted in a decrease in the abundance of full-length RIN4, as would be expected upon cleavage of this protein by AvrRpt2. In addition, a number of smaller proteins were detected (Fig 3.6), including one slightly lower than 25 kDa, and another one that migrated at ~10 kDa. The apparent molecular weight of these proteins is within the range of those expected for the RIN4-II and III fragments, respectively, but their identity could not be unambiguously established. Importantly though, no further stabilization of the ~10 kDa fragment (which is the closest in molecular weight to RIN4-III) was observed in the samples containing RIN4^{D153G}, and in which we would have expected a stronger accumulation of the Gly-RIN4-III fragment if it were an N-end rule substrate. For the samples containing RIN4^{N11G}, the protein that migrates just below 25 kDa was present, similarly to what was observed with wild-type RIN4 and RIN4^{D153G}, suggesting that if this protein corresponds to RIN4-II, then it is not stabilized by the presence of a stabilizing residue. In addition, when RIN4^{N11G} was expressed, an additional protein migrating around 20 kDa accumulated. This protein or fragment,

which has a molecular weight similar to that observed for the RIN4-II fragment expressed in *E. coli* (Fig. 3.3), was not present in the other samples. It is possible that this particular fragment might correspond to a stabilized Gly-RIN4-II (~16 kDa) fragment. Although the same result was obtained in another independent replicate (data not shown), the exact identity of this fragment remains to be unambiguously determined. To confirm that it corresponded to a stabilized Gly-RIN4-II fragment, I attempted to repeat these experiments using the anti-RIN4 Coaker for the immunoblots, because it has fewer cross-reacting proteins. Unfortunately, I could not complete these experiments on time due to multiple technical problems with the plant growth facilities.

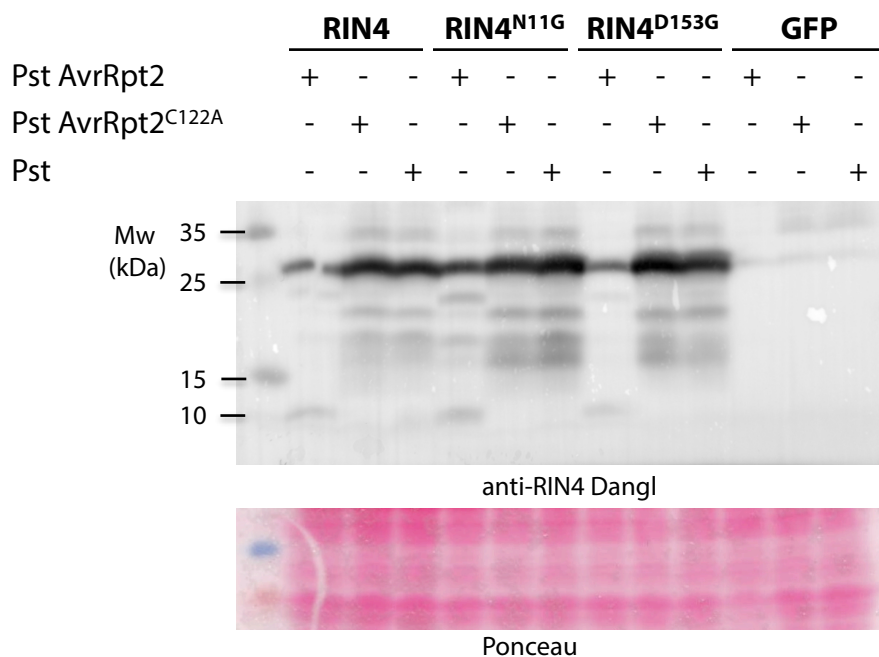


Fig 3.6. Stability of RIN4 mutant fragments in tobacco. Wild-type or mutant RIN4 encoding constructs were expressed in tobacco leaves. As a control for cross-reacting proteins, leaves were also infiltrated with an *A. tumefaciens* strain transformed with a plasmid coding for GFP under the control of the 35S promoter. Subsequently, the same tobacco leaves were inoculated with Pst AvrRpt2, Pst AvrRpt2^{C122A} (an inactive version of AvrRpt2), or a *P. syringae* DC3000 strain. Tissue was collected 6 hrs after *P. syringae* inoculation. Proteins were extracted in 2x SDS loading buffer and total protein extracts were separated using SDS-PAGE and analyzed using immunoblotting with anti-RIN4 antibodies. Expected protein sizes: full-length RIN4 is ~23 kDa; RIN4-II is ~16 kDa; and RIN4-III is ~6.4 kDa.

In summary, the experiments I conducted using transient expression in tobacco strongly suggest that RIN4-III is indeed not an N-end rule substrate. However, the presence of a protein or a fragment with a size similar to that of RIN4-II in samples expressing RIN4^{N11G} in the presence of AvrRpt2 could suggest that this particular fragment could be targeted for degradation by the N-end rule pathway in tobacco. Unfortunately, because it is unclear at this stage whether this fragment indeed corresponds to RIN4-II, it is difficult to draw a clear conclusion.

3.2.4 Cleavage of epitope-tagged mutant RIN4 in tobacco

In order to overcome the problems associated with the cross-reactivity of the anti-RIN4 antibodies (Fig. 3.6) and track the N- and C-terminal fragment of RIN4 with higher confidence, I generated RIN4 constructs with N- and C-terminal epitope tags, GFP and firefly luciferase (LUC), respectively. To compare the stability of wild-type and mutant RIN4-II and III, the constructs used contained either wild-type or mutant stabilizing residues (Gly) after the RCS2 (i.e. D153G mutation) or RCS1 (N11G mutant) cleavage sites, respectively. In order to tag the RIN4-III and RIN4-II fragments, one construct pair contained full-length RIN4, while another pair only contained the N-terminal RCS1 cleavage site and lacked the C-terminal domain beginning at the RCS2 cleavage site (denoted Δ Ct). All fusions were expressed under the control of the constitutive 35S promoter. The design of these constructs is described in Fig. 3.7.

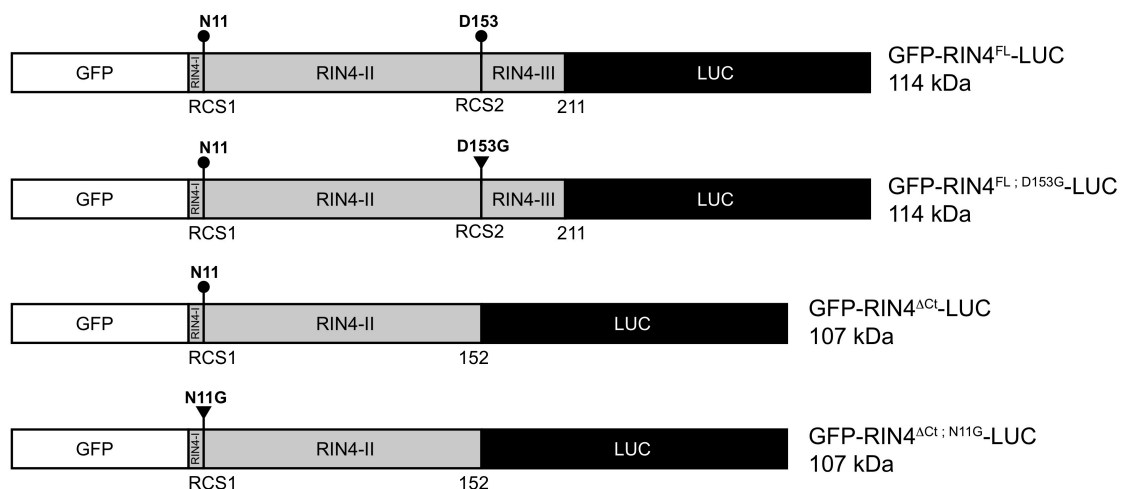


Fig 3.7. Epitope tagged mutant RIN4 design. RIN4^{FL} and RIN4^{ΔCt} were generated as translational fusions with N-terminal GFP and C-terminal luciferase (LUC). These constructs contained either

wild-type or mutant stabilizing residues after AvrRpt2 cleavage sites RCS2 or RCS1, respectively. The 2 upper constructs can be used to test the stability of RIN4-III with destabilizing or stabilizing N-terminal residues. The bottom constructs were generated to test the stability of the RIN4-II fragment with N-terminal destabilizing or stabilizing residues.

To test the cleavage of these proteins by AvrRpt2 and compare RIN4 fragment stability, the constructs were transiently expressed in tobacco leaves using *Agrobacterium*-mediated transformation. After 3 d, the leaves were subsequently inoculated with Pst AvrRpt2 or Pst AvrRpt2^{C122A}, and tissue was collected 6 hrs after this second inoculation. Following protein extraction in 2x SDS loading buffer, these samples were separated by SDS-PAGE and analyzed by immunoblotting with commercial antibodies raised against GFP or against LUC (Fig. 3.8A). In addition, the abundance of the RIN4 fragments translationally fused to LUC was also quantified using LUC enzymatic assays in protein extracts (Fig. 3.8 B-D). A GFP-LUC construct with no RIN4 insert was included as a positive control (also under the control of the 35S promoter).

Western blot analysis indicated that the GFP-RIN4^{ΔCt}-LUC was present at low levels in samples with no *Pseudomonas* or with the inactive AvrRpt2^{C122A} variant (Fig 3.8 A; upper panels). In addition, in the same conditions (i.e. in the absence of active AvrRpt2), the mutant GFP-RIN4^{ΔCt;N11G}-LUC fusion protein was not detectable (Fig 3.8 A; upper panels). The protein does appear to be expressed though, because both the N-terminal GFP tagged RIN4-I and the LUC-tagged RIN4-II fragments are detectable when the tobacco leaves were inoculated with Pst AvrRpt2 (Fig 3.8 A upper panels). These results are in marked contrast with those carried out using tobacco transient expression with untagged versions of RIN4 (Fig. 3.6), as in the absence of epitope tags, the full-length RIN4, RIN4^{N11G} and RIN4^{D153G} proteins accumulated at high levels in the absence of active AvrRpt2. Similar observations were made when the GFP-RIN4^{FL}-LUC and GFP-RIN4^{FL;D153G}-LUC fusion proteins were expressed, wherein the full-length fusion proteins seemed to accumulate to low levels in the absence of AvrRpt2. However, in the presence of active AvrRpt2, the cleaved GFP-RIN4-I and RIN4-III-LUC fragments were detectable (Fig 3.8 A lower panels), indicating that the fusion proteins should have been expressed.

These results, which were reproducibly repeated with 4 different constructs, may therefore suggest that the GFP-RIN4^{ΔCt}-LUC, GFP-RIN4^{ΔCt;N11G}-LUC, GFP-RIN4^{FL}-LUC and GFP-RIN4^{FL;D153G}-LUC fusion proteins are not stable, presumably because of the N- and/or C-terminal tags. Although it would be necessary to determine the transcription level of the fusions using methods that allow joint mRNA and protein extraction from the same sample, the data obtained suggest that tagging RIN4 with N- and C-terminal GFP and LUC, has detrimental effects on the structure of the protein, its sub-cellular localization, or its interaction with other proteins. These negative effects make it very difficult to draw any meaningful conclusions from these experiments, as it is unclear whether the tags could artificially expose or hide a putative N-degron or any other internal degron that may be present in RIN4. Importantly, though, the presence of a stabilizing or destabilizing residue did not appear to have a significant effect on the stability of the RIN4-II-LUC and RIN4-III-LUC fusion proteins (Fig 3.8 C and D; for comparison, the signal obtained for GFP-RIN4-I was used to correct the differences for RIN4-II-LUC). Another important observation made from these experiments, is that the GFP-LUC control protein appears to be cleaved in the presence of AvrRpt2. This could indicate that AvrRpt2 may have some non-specific cleavage effects in these experiments, at least when the GFP-LUC fusion is used as a control.

Despite the potential negative effects of the GFP and/or LUC tags on the stability of the different fusion proteins in the absence of AvrRpt2, I carried out two additional (independent) experiments. This time, however, protein extracts were generated using the CCLR buffer (see Section 2.2.4.8 and Appendix 1), in order to measure LUC activity using quantitative enzymatic assays (Fig. 3.8B-D). Overall, the results of these experiments suggest that the presence of a destabilizing or of a stabilizing residue at the N-terminus of RIN4-II or RIN4-III does not affect the stability of the fragments generated in the presence of AvrRpt2. However, additional replicates would need to be carried out, considering the large error bars obtained in Fig. 3.8C.

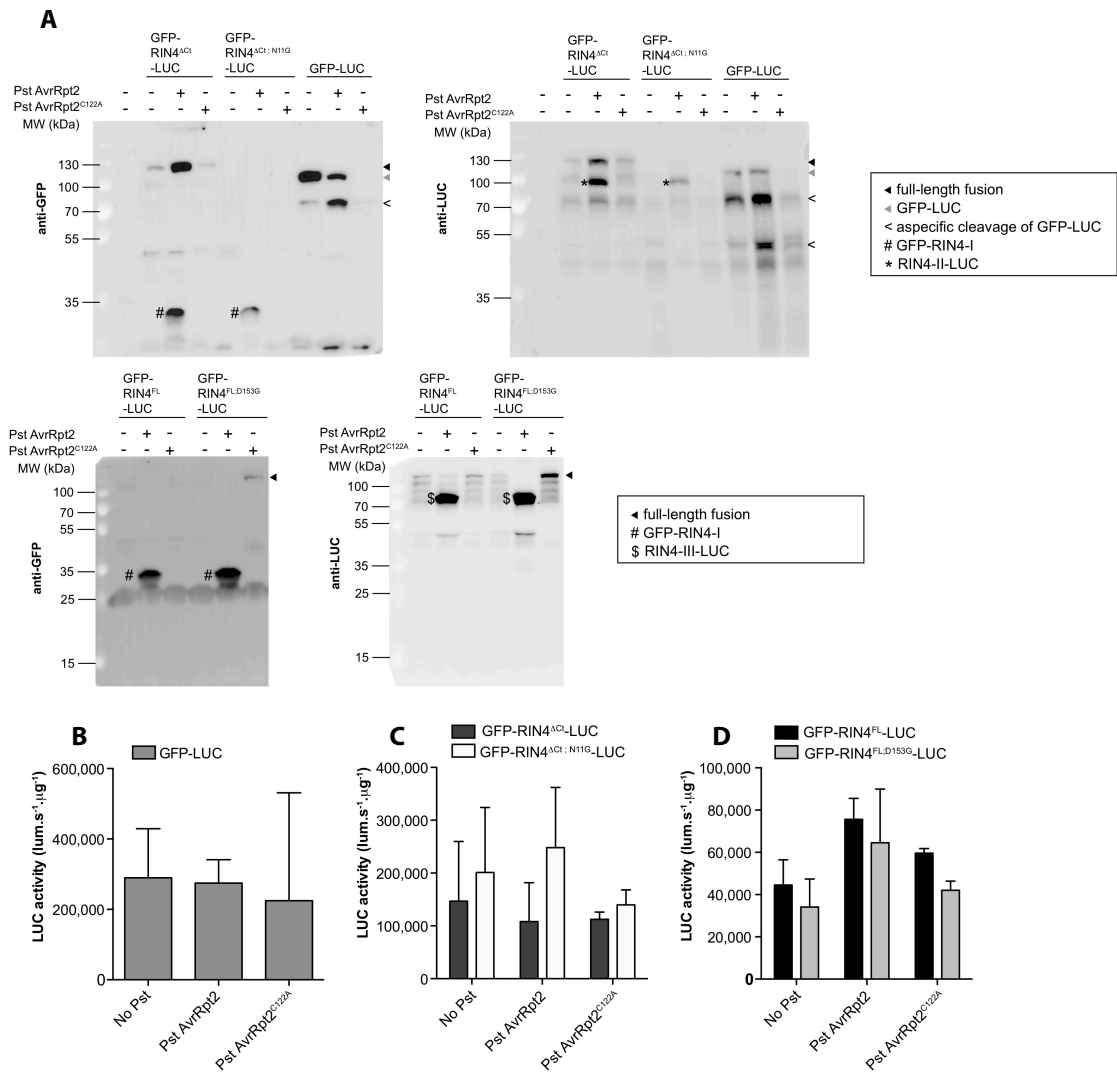


Fig 3.8. Stability of epitope tagged RIN4 fragments following AvrRpt2 cleavage. (A) Inoculation of tobacco leaves expressing GFP-RIN4^{FL}-LUC and GFP-RIN4^{ΔCt}-LUC encoding either wild-type or stabilizing Gly residues followed by Pst AvrRpt2 inoculation generates cleavage products which are detectable using GFP and LUC-specific antibodies. The two upper immunoblots correspond to experiments carried out with the GFP-RIN4^{ΔCt}-LUC fusion, while the two lower immunoblots present the results of experiments conducted with the GFP-RIN4^{FL}-LUC fusion proteins. Antibodies used for the detection of the fragments are indicated next to each immunoblot. (B-D) LUC activity assays using protein extracts containing wild-type and mutant tobacco-expressed RIN4 fragments fused to LUC, in the presence of Pst AvrRpt2, AvrRpt2^{C122A} or in the absence of *P. syringae* as a control. LUC activity is expressed as luminescence.sec⁻¹.μg⁻¹ (lum.s⁻¹. μg⁻¹). For B, C and D error bars correspond to a standard deviation (N=2).

In summary, tagging RIN4 with an N-terminal GFP and with a C-terminal LUC tag affects the stability of the different proteins, which makes it difficult to

draw conclusions reliably. Nevertheless, both immunoblots and LUC enzymatic assays suggest that the RIN4-II and III fragments are not N-end rule substrates, which is in agreement with the results obtained with untagged RIN4 and antibodies raised against this protein.

3.2.5 Generation of RIN4 fragment tandem fluorescent timers

To examine the effects of N-terminal mutations on RIN4-II and III stability more carefully, I generated tandem fluorescent timer (tFT) constructs encoding the RIN4 fragments with and without stabilizing N-terminal residues in the pBin binary plant expression vector (Fig 3.9). These constructs are based on the translational fusion of a protein of interest to two different fluorophores, mCherry and superfolder GFP (sfGFP). These fluorophores have different maturation kinetics such that sfGFP matures in a matter of minutes, while mCherry is slower to mature (Khmelinskii *et al.*, 2012). By comparing the ratio of green fluorescence (sfGFP) to red fluorescence (mCherry) captured at different wavelengths the longevity of the protein of interest within cells can be estimated (Khmelinskii *et al.*, 2012). Hence this technique could allow us to evaluate more carefully the half-life of the different RIN4 fragments, in contrast to estimating the global levels of the protein at a specific time point after the expression of AvrRpt2.

These constructs were designed as N-terminal Ub fusions, so that the constructs could bear N-terminal destabilizing residues after co-translational deubiquitination (Fig 3.9)(discussed in Section 1.1 and 1.2). This part of the project is in collaboration with the lab of Dr. Markus Wirtz (University of Heidelberg). To compare tFTs encoding RIN4 fragments with and without destabilizing residues, Arabidopsis seedlings (wild type and N-end rule mutants) will be transiently transformed with the different tFT constructs. These experiments are currently ongoing in the lab of Dr. Markus Wirtz, and the results are not yet available.



pBin binary vector

Fig 3.9. RIN4-tFT constructs generated to determine the half-life of the different RIN4 fragments. Schematic representation of the tFT constructs generated to compare the half-life of RIN4 fragments with either destabilizing or stabilizing residues. N-terminal Ub is co-translationally processed resulting in N-terminal RIN4-II or III, with either wild-type Asn or Asp, respectively, or mutant Ala residue (denoted 'X'), translationally fused to mCherry and sfGFP, which have slow and fast maturation rates, respectively.

3.2.6 AvrRpt2 cleavage of NOI domain proteins

As discussed in Section 3.1.4, AvrRpt2 has been suggested to cleave several NOI domain-containing proteins encoded in the Arabidopsis genome (Chisholm *et al.*, 2005). More recently, it has been shown that some of these NOI domain proteins are indeed substrates of AvrRpt2 (Elmore *et al.*, 2012; Eschenlippold *et al.*, 2016). A former student in the lab, Anne Kind, had previously cloned the cDNA sequences coding for 6 of these NOI domain proteins as translational fusions with an N-terminal GFP tag and a C-terminal HA tag (fusions noted GFP-NOI-HA and depicted in Fig. 3.10A; see Table 2.4 for plasmids names and details), all of which were under the control of the constitutive 35S promoter. Preliminary experiments whereby these constructs were expressed in tobacco in the presence of Pst AvrRpt2 before being analyzed by immunoblotting indicated that the proteolytically generated C-terminal fragments of each protein were unstable. Because these new C-terminal fragments bore N-terminal destabilizing residues, we hypothesized that their instability could be due to their targeting for degradation by the N-end rule pathway (see Section 3.1.4). To confirm the instability of the C-terminal fragments and to determine if they were indeed N-end rule substrates, I mutagenized the GFP-NOI-HA constructs mentioned above to change the newly exposed N-terminal destabilizing residue into a stabilizing Ala residue (constructs denoted GFP-NOI^{mt}-HA; see Table 3.3 for a list of NOIs and mutations introduced). To test if the presence of a stabilizing Ala residue resulted in a more stable C-terminal fragment up-

on cleavage by AvrRpt2, these constructs were transiently expressed in tobacco plants before Pst AvrRpt2 was inoculated into the leaves. Ten hours after Pst AvrRpt2 infection, the tissue was collected. Protein extracts were generated by grinding the tissue in 2x SDS loading buffer, and then analyzed using SDS-PAGE and immunoblotting with either a GFP-specific antibody (to follow the N-terminal fragment) or with an antibody raised against the HA tag in order to detect the C-terminal fragment. The expected molecular weight of the full-length proteins and their respective AvrRpt2-cleaved fragments are summarized in Table 3.3, while the results of these experiments are described in Fig. 3.10.

Introduction of active AvrRpt2, but not of AvrRpt2^{C122A}, appeared to result in the disappearance of each of the six full-length protein fusions examined, likely as a result of their AvrRpt2 cleavage. The N-terminal fragment of each protein was detectable with the anti-GFP antibodies, and each N-terminal fragment migrated at the expected size (Table 3.3). Cleavage of the 6 different GFP-NOI-HA proteins appeared to result in C-terminal fragments that were not detected in our experimental conditions, indicating that they might be rapidly degraded. This result was in agreement with at least 2 other independent experiments that had been previously performed in the lab. Notably, though, the AvrRpt2-mediated cleavage of four of GFP-NOI^{mt}-HA proteins (specifically, NOI1, NOI5, NOI6 and NOI11) appeared to generate several fragments that were recognized by the HA-specific antibody and that migrated around the expected molecular weight for the predicted HA-tagged C-terminal fragments of these proteins. This result could hence indicate that NOI1, NOI5, NOI6 and NOI11, but not NOI2 and NOI3, are *bona fide* N-end rule substrates.

It is also worth noting that the introduction of AvrRpt2 into leaves expressing GFP-NOI6-HA results in the appearance of (i) a band that migrates at the predicted size for the GFP-NOI6 N-terminal fragment, and (ii) a faint band slightly higher at ~36kDa (Fig 3.10). This particular protein is also detected with anti-HA antibodies, suggesting that the construct may also be cleaved in a second location by AvrRpt2. Because this protein is recognized by both GFP and HA, we hypothesize that the aspecific cleavage occurs in the GFP moiety, similarly to what had been observed with the control GFP-LUC fusion in Fig. 3.8. This was not observed when GFP-NOI6^{mt}-HA was expressed in the presence of AvrRpt2.

Table 3.3. GFP-NOI-HA full-length molecular weight and predicted fragment size after AvrRpt2 cleavage. Also included is the site of mutation for NOI^{mt} constructs. AGI: Arabidopsis Gene Identifier; MW: molecular weight;

Common name	AGI	MW including GFP and HA tags (kDa)	MW of GFP-tagged N-terminal fragment (kDa)	MW of HA-tagged C-terminal fragment (kDa)	Mutation after AvrRpt2 cleavage site
NOI1	At5g63270	37	28	9	E14A
NOI2	At5g40645	36	29	7	E20A
NOI3	At2g17660	36	28	8	E15A
NOI5	At3g48450	38	28	10	E15A
NOI6	At5g64850	41	29	12	D20A
NOI11	At3G07195	53	28	25	D12A

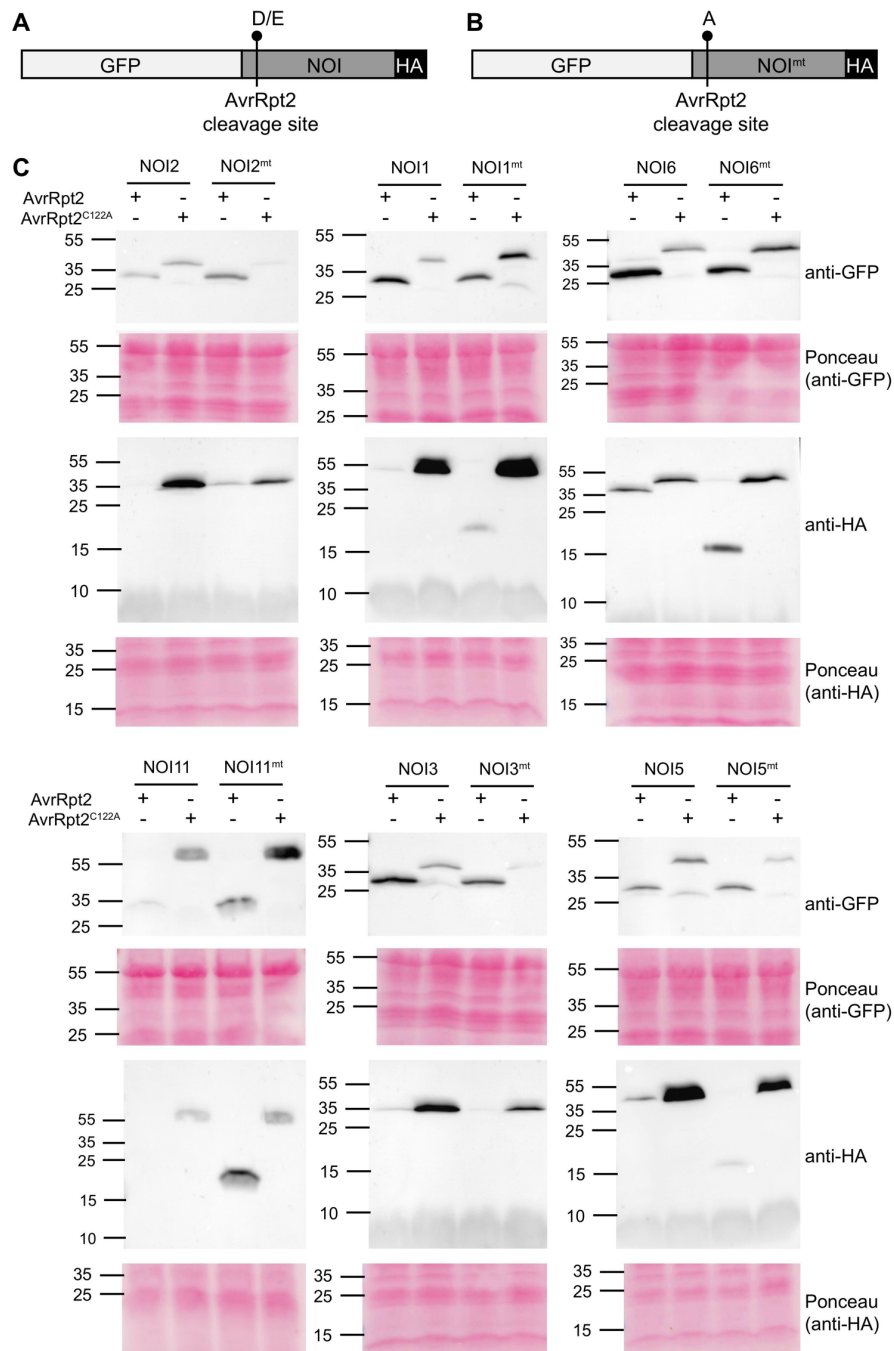


Fig 3.10. AvrRpt2-mediated cleavage of GFP-NOI-HA fusion proteins in tobacco. (A) Schematic representation of the GFP-NOI-HA constructs expressed from the 35S promoter. The predicted AvrRpt2 cleavage site is indicated, as well as the newly exposed Asp or Glu N-terminal residues (D/E). (B) GFP-NOI^{mt}-HA constructs generated to study the stability of the AvrRpt2-released C-terminal fragments in which the newly exposed N-terminal residue was mutated into the stabilizing Ala (A) residue. The resulting mutant NOI is noted NOI^{mt}. (C) Stability of the fragments obtained after AvrRpt2 cleavage. In these experiments, tobacco plants transiently expressing from the 35S promoter the GFP-NOI-HA or GFP-NOI^{mt}-HA fusion proteins were inoculated with Pst AvrRpt2 or Pst AvrRpt2^{C122A}. N-terminal fragments were detected using antibodies directed against the GFP tag,

while C-terminal fragments were detected using anti-HA antibodies. Figure from (Goslin *et al.*, manuscript in press).

3.2.7 Localization of GFP-NOI-HA proteins in tobacco

As mentioned in Section 3.1.4, the RIN4 protein bears three C-terminal Cys residues (Fig. 3.2), which are important for the membrane localization of RIN4 (Takemoto and Jones, 2005). Because the NOI domain proteins also bear these Cys residues, it has been hypothesized that they may also localize to the plasma membrane (Afzal *et al.*, 2013). However, this has not been demonstrated experimentally. I therefore made use of the GFP-NOI-HA constructs to investigate the subcellular localization of the fusion proteins. To this aim, I transiently expressed these constructs in tobacco and analyzed the GFP fluorescence in leaf epidermal cells (abaxial side) using a laser-scanning confocal microscope with the aid of Dr. Ica Dix (Maynooth University). The results of these imaging experiments are summarized in Fig. 3.11. I also imaged tobacco leaves expressing GFP-LUC as a fluorescence signal control, and non-infiltrated tobacco leaves for background control.

The GFP-LUC construct was detected in the cytoplasm and in the nucleus of tobacco epidermal cells (Fig. 3.11B), while the different GFP-NOI-HA fusion proteins appeared to have different subcellular localizations within the cell (Fig 3.11A-H). Fusion proteins with NOI1, NOI3, NOI5 and NOI11 appeared to localize mostly in the periphery of epidermal cells, which likely indicates a membrane localization. The NOI2 fusion protein displayed a strong nuclear signal, with a weaker signal in the cell periphery (Fig 3.11D). Overlay of chlorophyll autofluorescence and GFP fluorescence indicated that the NOI2 fusion protein localized to the membrane of structures that are likely chloroplasts (Fig 3.11D). In addition, the GFP-NOI6-HA fusion protein appeared to localize in small intracellular vesicle-like structures (Fig 3.11J), which could be in agreement with its interaction with the exocyst complex subunit EXO70A1 (Afzal *et al.*, 2013; Sabol *et al.*, 2017).

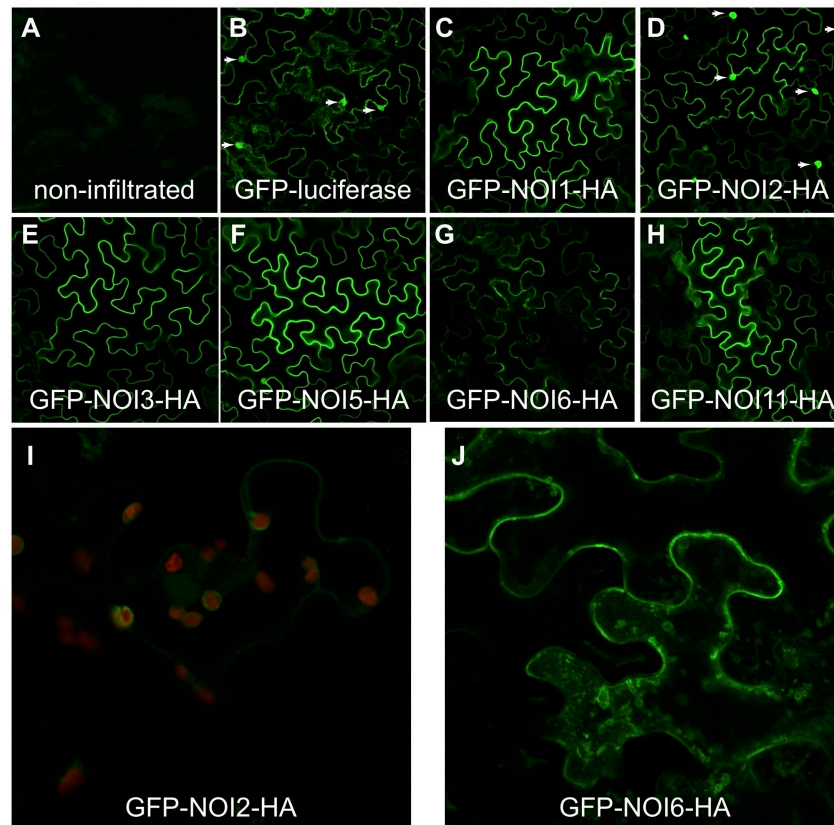


Fig 3.11. Subcellular localization of GFP-NOI-HA proteins. (A-H) Confocal microscopy images of epidermal cells from tobacco leaves (abaxial side) 3 d after infiltration with *Agrobacterium* coding for GFP-NOI-HA constructs. Putative nuclear signal is indicated with white arrowheads (panels B and D). (I) Confocal microscopy image of epidermal peel from tobacco leaf expressing GFP-NOI2-HA. Signal in red corresponds to chlorophyll autofluorescence. (J) Confocal microscope image of epidermal cells from a tobacco leaf expressing GFP-NOI6-HA. Note the presence of intracellular vesicles in the presence of GFP-NOI6-HA. Green signal indicates GFP fluorescence.

3.3 Discussion

3.3.1 Investigating the N-end rule-mediated degradation of RIN4 proteolytic fragments

The instability of the RIN4 proteolytic fragments generated after AvrRpt2 cleavage (Mackey *et al.*, 2003; Axtell and Staskawicz, 2003) and the fact that they bore N-terminal destabilizing residues (Chisholm *et al.*, 2005) led us to test whether the N-end rule pathway was involved in targeting them for degradation. To this aim, I

conducted experiments with different Arabidopsis stable lines, and also using transient expression in tobacco.

Experiments that I have conducted using Arabidopsis AvrRpt2^{DEX} lines show that induction of AvrRpt2 activity results in the rapid disappearance of the full-length RIN4 and of the predicted cleavage products (Fig 3.4 A), as previously published (see Section 3.1.3). Interestingly, in extracts from mock-treated AvrRpt2^{DEX} seedlings, a protein with a molecular weight similar to that of the expected RIN4-II fragment is observed (Fig 3.4C). Although the identity of this protein is not known with confidence, it is possible that it is the result of RIN4 cleavage by low levels of AvrRpt2 activity due to the 'leaky' expression of the inducible AvrRpt2 transgene. As this protein only accumulates to a detectable level in seedlings when AvrRpt2 expression is not induced (i.e. it is no longer detectable after induction of AvrRpt2 expression), it could indicate that RIN4-II fragment degradation is accelerated when full-length RIN4 is cleaved more efficiently or at a higher rate. The efficient cleavage of RIN4 by AvrRpt2 has been shown to disrupt its interaction with the R protein RPS2 (Mackey *et al.*, 2003; Day *et al.*, 2005), thus triggering the onset of ETI (see Section 3.1.2). One could therefore hypothesize that the degradation of the RIN4-II fragment, and possibly also of RIN4-III, might be dependent on the activation of RPS2 and/or the subsequent onset of ETI. This hypothesis would be consistent with previous observations that RIN4 fragments generated after AvrRpt2 cleavage may be more stable in the *rps2 rpm1* double mutant background (Afzal *et al.*, 2011), which lacks RPS2 so that this R protein and ETI may not be triggered despite RIN4 cleavage by AvrRpt2.

DEX-induction of AvrRpt2 activity in seedlings constitutively expressing RIN4^{N11G} did not result in the detection of a fragment that would correspond to stabilized mutant Gly-RIN4-II (Fig 3.4B). Unfortunately, I could not conduct similar experiments with a RIN4^{D153G} lines, as the seeds were no longer viable. I hence complemented the experiments with Arabidopsis AvrRpt2^{DEX} lines by testing the stability of RIN4-II and III, but also of the Gly-RIN4-II and Gly-RIN4-III fragments using transient expression of (i) full-length wild-type RIN4, (ii) RIN4^{N11G} and (iii) RIN4^{D153G} in the presence of AvrRpt2 or of its inactive AvrRpt2^{C122A} variant. In these transient expression experiments, cleavage of wild-type RIN4 by AvrRpt2 generated similar cleavage products to the mutant proteins RIN4^{N11G} or RIN4^{D153G}.

A fragment migrating around the size of RIN4-II seemed to accumulate to slightly higher levels after AvrRpt2 cleavage of the RIN4^{N11G} mutant protein. However, the identity of this fragment is still unclear and any stabilization was not clear (Fig 3.6). Attempts I have made to determine with confidence if this protein corresponds to a slightly stabilized Gly-RIN4-II could not be completed on time. In sum, considering the lack of any clear stabilization of the mutant Gly-RIN4-II or III fragments, these transient expression experiments again suggest that the processing of these fragments is likely not mediated solely by the N-end rule pathway. This does not preclude the possibility that RIN4 fragments may be targeted by more than one pathway, one of which could be dependent on the N-terminal destabilizing residue.

Using different variants of a GFP-RIN4-LUC fusion protein transiently expressed in tobacco, I aimed at using commercial antibodies raised against GFP and LUC to determine more clearly whether the RIN4-II and III fragments could be targeted for degradation by the N-end rule pathway. However, the GFP-RIN4^{FL}-LUC, GFP-RIN4^{FL;D153G}-LUC, GFP-RIN4^{Act}-LUC and GFP-RIN4^{Act;N11G}-LUC did not appear to accumulate to high levels in the absence of AvrRpt2 activity, indicating that these uncleaved fusion proteins might be unstable. Although the full-length fusion proteins were either in low abundance or not-detectable, the cleavage products of these fusion proteins by AvrRpt2 accumulated to detectable levels (Fig 3.8 A). This is in contrast (i) with the accumulation of untagged RIN4, RIN4^{N11G} or RIN4^{D153G} when expressed in the absence of active AvrRpt2; and (ii) with the instability of RIN4-II and III fragments (irrespective of the identity of the N-terminal residue) after AvrRpt2 cleavage (Fig 3.4A). It is therefore likely that the presence of the N- and/or C-terminal tags on these constructs perturbs the stability of the uncleaved fusion proteins, and at the same time, prevents the degradation of the fragments released after AvrRpt2 cleavage. The first effect may be explained by the fact that the tags lead to a mis-folded fusion protein that is targeted for degradation, or that the different fusion proteins no longer interact with partner proteins that would protect them from degradation. The second effect of the tags (i.e. the stabilization of RIN4-II and III) may be explained by the fact that the C-terminal LUC tag could block a degradation signal that is usually involved in RIN4 fragment recognition and destruction, although this data alone is not sufficient to support this conclusion (see Section 3.4.1 below). Importantly, mutations of N-terminal residues of

RIN4-II and III-LUC fusions into stabilizing residues did not appear to significantly change the stability of the fragments. These results are in agreement with the data obtained when expressing untagged RIN4 variants in tobacco and in AvrRpt2^{DEX} Arabidopsis lines.

Altogether, the different experiments I have conducted suggest that the N-terminal destabilizing residues of the RIN4 fragments may not play a significant role in their stability. Hence, RIN4-II and III degradation appears to be either independent of the N-end rule pathway or mediated, at least in some part, by components of the UPS other than the N-end rule pathway. Our conclusion differs from that made from previously published experiments, in which the first 19 residues of RIN4-II (residues 11 – 30) were translationally fused to GFP (noted RIN4¹¹⁻³⁰-GFP). Using such fusion proteins, the authors indicated that the N11G mutation resulted in a slight stabilization of the GFP reporter protein (Takemoto and Jones, 2005; see also Section 3.1.3). However, it is possible that by using only the first 19 amino acid residues of RIN4-II fused to GFP, the N-terminal residue (Asn11) was more accessible to N-end rule recognition components and thus generated an artificial N-end rule substrate. In contrast, several of our experiments were conducted using endogenous RIN4, and were hence within the natural physiological and structural context of the protein.

3.3.2 Investigating the N-end rule-dependent degradation of NOI protein fragments

The introduction of AvrRpt2 into tobacco leaves transiently expressing GFP-NOI-HA or GFP-NOI^{mt}-HA proteins resulted in the cleavage of each of the 12 fusion proteins and resulted in N-terminal fragments that corresponded to the expected molecular weights of these fragments (Fig 3.10 and Table 3.3). For all of the GFP-NOI-HA constructs, cleavage by AvrRpt2 induced the disappearance of the predicted C-terminal HA-tagged fragments, indicating that they may be targeted for degradation. The mutation of the predicted neo N-terminal destabilizing residues for these C-terminal fragments into a stabilizing Ala residue resulted in the detection of HA-tagged protein fragments for the GFP-NOI1^{mt}-HA, GFP-NOI5^{mt}-HA, GFP-NOI6^{mt}-HA and GFP-NOI11^{mt}-HA fusion proteins. This strongly suggests that the presumed N-

terminal destabilizing residue is important for the degradation of these fragments and that they may be genuine N-end rule substrates. Importantly, my results are overall in agreement with observations made by collaborators. Indeed, as part of a collaboration with the group of Dr. Justin Lee (Institute of Plant Biochemistry; Halle; Germany), Dr. Lennart Eschen-Lippold used the same plasmids coding for the GFP-NOI-HA and GFP-NOI^{mt}-HA fusions to test their degradation and stabilization in protoplasts derived from *Arabidopsis* mesophyll cells. In his experiments using protoplasts derived from wild-type Col-0 plants, Dr. Eschen-Lippold found that the C-terminal fragments generated after cleavage of the GFP-NOI-HA fusions were indeed unstable. In addition, he was also able to detect a stabilization of the mutated C-terminal fragments (derived from AvrRpt2 cleavage of GFP-NOI^{mt}-HA proteins) for NOI1, NOI6 and NOI11, but not for NOI5. This was observed consistently across 3 biological replicates. In addition, Dr. Eschen-Lippold tested the stability of the wild-type C-terminal fragments using protoplasts derived from wild-type Col-0 as well as mutant *ate1 ate2* and *prt6-1*. If the C-terminal fragments are indeed N-end rule substrates, we would expect them to accumulate in *ate1 ate2* or *prt6-1* mutant plants, as these enzymatic components are required for the arginylation of the fragments, and their PRT6-mediated ubiquitination. In agreement with the idea that the proteolytic fragments are indeed N-end rule substrates, it was found that after AvrRpt2 cleavage, the C-terminal fragments of GFP-NOI1-HA, GFP-NOI6-HA and GFP-NOI11-HA accumulated in the *ate1 ate2* and *prt6-1* mutant protoplasts, despite some variation between the 3 replicates performed.

The only wild-type HA-tagged fragment detected in these experiments was the NOI6 C-terminal fragment (Fig 3.10). This band does not correspond to the size of an AvrRpt2-cleaved fragment but migrates slightly lower than the full-length fusion protein. As it can be detected weakly by the GFP and strongly by the HA tag it is likely that this fragment is due to a cleavage of the protein around the N-terminus of the GFP tag. There is also a band detected at the molecular weight of the expected N-terminal fragment with anti-GFP, suggesting that NOI6 is also cleaved by AvrRpt2 at the expected position. One possibility for the difference between wild-type and mutant NOI6 constructs could be that the D20A mutation in NOI6 causes the protein to localize to a different subcellular localization, and in that way be exposed to different protease activity or shielded in some way from

certain protease activity. However, the subcellular localization of GFP-NOI-HA and GFP-NOI6^{mt}-HA, as determined by laser-scanning confocal microscopy, does not appear to be markedly different (Dr. Maud Sorel, data not shown). It is also worth noting that this aspecific cleavage of a GFP fusion protein by AvrRpt2 had also been observed using the control GFP-LUC protein, hence suggesting that, in certain conditions, AvrRpt2 may recognize and cleave GFP. This may be due to high expression of AvrRpt2 and remains to be investigated.

In addition to testing the N-end rule-dependent degradation of the NOI-HA fragments generated by AvrRpt2 cleavage, I also examined using laser-scanning confocal microscopy the subcellular localization of the fusion proteins. These experiments allowed me to obtain additional information on these NOI domain proteins which are presumed to be membrane localized, based on the presence of 3 conserved Cys residues that are involved in targeting RIN4 to the membrane. As a control, I used a GFP-LUC fusion protein, which was detected in areas likely to be the cytoplasm and the nucleus. A number of GFP-NOI-HA constructs had different subcellular localizations, indicating that they might have differing functions within the cell (Fig 3.11). For example, NOI1, NOI3, NOI5 and NOI11 were detected strongly around the cell periphery, suggesting a membrane localization. NOI2, however, did not have a strong peripheral signal and instead appeared to accumulate in nuclei (Fig 3.11D). In addition, NOI2 was detected around areas of autofluorescence, indicating that the protein may also localize to chloroplast membranes (Fig 3.11I). Interestingly, the NOI6 fusion protein appeared in small intracellular vesicle-like structures (Fig 3.11). This would be consistent with NOI6 playing some role in protein trafficking and its interaction with subunits of the exocyst complex (Afzal *et al.*, 2013; see section 3.1.4). If NOI6 indeed plays a role in these processes, its targeting by a bacterial effector may be part of the pathogens strategy to enhance virulence through disrupting host protein trafficking.

Altogether, the data I have obtained in tobacco, combined with results obtained by our collaborator, Dr. Eschen-Lippold, using Arabidopsis protoplasts strongly suggest that AvrRpt2-mediated cleavage of NOI1, NOI6 and NOI11 leads to the generation of protein fragments whose degradation is under the control of the N-end rule pathway. Our work has therefore uncovered a novel set of N-end rule substrates. As discussed in more detail below, future work will aim at under-

standing the physiological relevance of their N-end rule-dependent degradation in the context of plant immune responses to pathogen strains coding for the effector protease AvrRpt2 (see Section 3.4.2).

3.4 Future work

3.4.1 Towards characterizing RIN4 fragment degradation

As mentioned in Section 3.2.2, the N-end rule-dependent degradation of the RIN4-II and III fragments would require the activity of the Arg-transferases ATE1 and ATE2 and the activity of the N-recognin PRT6 (see Fig. 1.5 and Section 1.2.4.1). Therefore, the cleavage of RIN4 by AvrRpt2 in *ate1 ate2* double mutant plants or *prt6* single mutant plants should result in the accumulation of these RIN4 fragments if their degradation is dependent on a functional N-end rule pathway. I attempted to examine RIN4 cleavage in the *ate1 ate2* mutant background through the activation of the inducible transgene AvrRpt2^{DEX} but this gene was silenced (discussed in Section 3.2.2). Another approach is to inoculate N-end rule mutant Arabidopsis plants with *P. syringae* encoding AvrRpt2. A member of the lab, Rémi de Marchi, has inoculated 4-week old *ate1 ate2* and *prt6* mutant plants with *P. syringae* strains encoding AvrRpt2 or the inactive AvrRpt2^{C122A}. I aim to carry out protein extraction using this tissue and analyze RIN4 fragment abundance using immunoblotting with RIN4 antibodies as soon as possible.

As discussed in Section 3.2.2 (see Fig 3.5 A) the co-treatment of Col-0 AvrRpt2^{DEX} lines with the proteasomal inhibitor MG132 and DEX resulted in a stabilization of full-length RIN4, likely because MG132 inhibited the cysteine protease activity of AvrRpt2. In order to inhibit the proteasome, while also retaining AvrRpt2 protease activity, I aim to carry out this experiment again using the proteasome inhibitor lactacystin in place of MG132. This chemical inhibits the 20S proteasome complex but does not appear to inhibit the activity of cysteine proteases (reviewed in Lee and Goldberg, 1998; Groll and Huber, 2004).

RIN4 modification by pathogen effectors is monitored by at least two NLR proteins – RPM1 and RPS2 (see Section 3.1.2). In Arabidopsis *rpm1 rps2* double mutant plants, the RIN4-II and RIN4-III fragments appear to be more stable after 6 hrs post-inoculation with a *P. syringae* strain encoding AvrRpt2 (discussed in Section 3.1.3)(Afzal *et al.*, 2011). Immunoblot experiments that I carried out to analyze protein extracts from mock-treated Col-0 AvrRpt2^{DEX} lines indicated that a protein band roughly corresponding to RIN4-II appears (see Section 3.2.2 and Fig 3.4 A). It is possible that the onset of ETI that is triggered by RPM1 or RPS2 activation might accelerate in some way the degradation of RIN4 fragments, which would explain why this band is only visible in mock-treated Col-0 AvrRpt2^{DEX}. To examine this, I aim to inoculate *rpm1 rps2* double mutant plants, as well as *rps2* single mutant and wild-type plants with *P. syringae* encoding AvrRpt2 and compare RIN4 fragment abundance using immunoblotting with anti-RIN4 antibodies. It may also be of interest to test the stability of the RIN4-II and III fragments in a *rps2 prt6* double mutant, to test if in the absence of the ETI, PRT6 could be involved in the targeting of the RIN4 proteolytic fragments for degradation. Interestingly, RIN4 interacts with an uncharacterized NLR protein (AT1G12290) in yeast (Afzal *et al.*, 2013). Mutant Arabidopsis seeds for this locus are available to order from a SALK T-DNA insertion collection. To examine if this NLR protein plays a role in the processing of RIN4 fragments, or the protection of RIN4 from AvrRpt2 cleavage, I would also be interested in inoculating plants carrying mutations in this locus with *P. syringae* encoding AvrRpt2 and analyze RIN4 fragment abundance using immunoblotting with anti-RIN4 antibodies.

3.4.2 Understanding the role of NOI protein degradation by the N-end rule pathway

Experiments that I have conducted in this study using tobacco (see Section 3.2.6) and that have been carried out using Arabidopsis protoplasts by Dr. Lennart Eschen-Lippold (discussed in Section 3.3.2), indicate that a number of Arabidopsis NOI domain-containing proteins are likely to be substrates of the N-end rule pathway after they are cleaved by *P. syringae* AvrRpt2. To confirm that these NOI domain fragments are *bona fide* N-end rule substrates I intend to carry out additional experiments. For example, I will seek to confirm that AvrRpt2-generated C-

terminal fragments of NOI domain proteins are degraded by the proteasome. To this aim, I will express GFP-NOI-HA constructs in tobacco followed by inoculation with *Pst AvrRpt2*. The proteasomal inhibitor lactacystin will be infiltrated at the same time as the *P. syringae* cells, which should allow for the inhibition of the proteasome while not having any effect on *AvrRpt2* protease activity. These protein extracts will then be analyzed using immunoblotting with anti-HA antibodies to test for the stabilization of the C-terminal HA-tagged fragments in the presence of lactacystin. In addition, I will attempt to determine the exact cleavage site of each NOI whose C-terminal fragment is stabilized when the newly exposed N-terminal residue is a stabilizing one. A way in which this could be assessed would be by immunoprecipitating the mutated HA-tagged C-terminal fragments followed by determination of the N-terminal sequence using either MS-MS or N-TAILS (see Section 1.3.1). I will also clone the coding sequences for the C-terminal fragments of NOI1, NOI6 and NOI11 into a fluorescent timer construct with the wild-type destabilizing residue or with a stabilizing Ala residue, as described for the RIN4-II and III fragments in Section 3.2.5. Expressing the fluorescent timers in Arabidopsis tissue and examining the longevity of the fusion proteins in plant cells using confocal microscopy can then be used to determine the effect of these mutations on the half-life of the fragments. Importantly, these experiments can also be conducted in a *prt6* mutant background, and therefore could provide more direct evidence for the PRT6-mediated degradation of the fragments.

Finally, to better understand the role of these NOI domain proteins in plant-pathogen interactions, it would be interesting to generate stable Arabidopsis transformants coding for the NOI and NOI^{mt} constructs described in Section 3.2.6. Introducing these constructs into Col-0 and *prt6-1* plants and then testing the response of these transformants to inoculation with *Pst AvrRpt2* could reveal potential functions of the N-rule-mediated degradation of the fragments.

Chapter 4. Developing a molecular tagging tool to identify N-end rule substrates

4.1 Introduction

The identification of N-end rule substrates using proteomic or bioinformatic methods is challenging (for a detailed discussion see Section 1.3). With the aim of identifying substrates of the Arabidopsis N-recognin PRT6, I aimed at developing a molecular tagging tool, termed a NEDDylator. In this chapter I will introduce the process of NEDDylation, how the NEDDylator molecular tag functions, outline the design of a NEDDylator for PRT6 and describe experiments I conducted to characterize different versions of a PRT6-specific NEDDylator.

4.1.1 NEDD8 conjugation in plants

Besides Ub, eukaryotes encode several other small Ub-like modifiers. Of these, the 76 amino acid protein NEDD8 (neural precursor cell expressed developmentally downregulated gene) is the closest in sequence to Ub (~57% identity). NEDD8 (also called RELATED TO UBIQUITIN (RUB) in plants and yeasts) is highly conserved across eukaryotes and its function is essential for the viability of a number of organisms including Arabidopsis, mouse, *Schizosaccharomyces pombe*, *Caenorhabditis elegans*, and *Drosophila* (Dharmaasiri *et al.*, 2003; Tateishi *et al.*, 2001; Osaka *et al.*, 2000; Jones and Candido, 2000; Ou *et al.*, 2002;), but notably not *Saccharomyces cerevisiae* (Liakopoulos *et al.*, 1998; reviewed in Rabut *et al.*, 2008). The first proteins identified as NEDD8 conjugates were members of the cullin protein family (Lammer *et al.*, 1998; Osaka *et al.*, 1998; Liakopoulos *et al.*, 1998), which function as scaffold proteins for CRL Ub ligases (see Section 1.1.2.4).

NEDD8 conjugation to substrates is biochemically analogous to ubiquitination and it requires the action of a group of conjugating enzymes that function in a stepwise fashion. In Arabidopsis, NEDD8 is encoded by three genes, two of which are expressed as fusion proteins with N-terminal Ub, a feature so far identified only in plants (Rao-Naik *et al.*, 1998). Ub-RUB fusion proteins must first be processed by DUBs (see Section 1.1.1). Hydrolase enzymes must also cleave one or several C-

terminal amino acids off each of the three RUB proteins to generate mature NEDD8. The enzymes that carry out this function in plants have not yet been identified (reviewed in Mergner and Schwechheimer, 2014). Activation of NEDD8 is then carried out by a heterodimeric NEDD8 E1 activating enzyme (NAE) composed of either AUXIN RESISTANT1 (AXR1) or AXR1-LIKE1 (AXL1), and E1 C-terminal RELATED1 (ECR1) (Del Pozo *et al.*, 1998), before NEDD8 is transferred to an E2 NEDD8-conjugating enzyme. In Arabidopsis, RUB-CONJUGATING ENZYME1 (RCE1), an enzyme of the UBC family, carries out this function (Dharmasiri *et al.*, 2003). The NEDD8-E2 complex can interact with a NEDD8 E3 ligase and NEDD8 can be conjugated to a substrate lysine residue *via* its C-terminal glycine (Fig 4.1). Unlike Ub, NEDD8 does not appear to form NEDD8 chains under physiological conditions and the conjugation of NEDD8 does not typically target substrate proteins to the proteasome, although there are some examples of NEDD8-interacting proteins recruiting substrates to the proteasome (reviewed in Enchev *et al.*, 2015). Artificial overexpression of NEDD8 can lead to the formation of mixed NEDD8-Ub chains and ectopic neddylation, which is dependent on E1 Ub-activating enzymes (Singh *et al.*, 2012;Hjerpe *et al.*, 2012;Leidecker *et al.*, 2012). Similarly to ubiquitination, NEDD8 conjugation is a dynamic and reversible process, so that NEDD8 can be deconjugated through the activity of deneddylases. In Arabidopsis, the COP9 signalosome protein complex and the protease DENEDDYLASE1 (DEN1) possess deneddylase activity. In the case of CRLs the deconjugation of NEDD8 causes the CRL complex to become unstable, which allows for the rearrangement of the complex and the exchange of F box proteins (reviewed in Mergner and Schwechheimer, 2014) (Fig. 4.1).

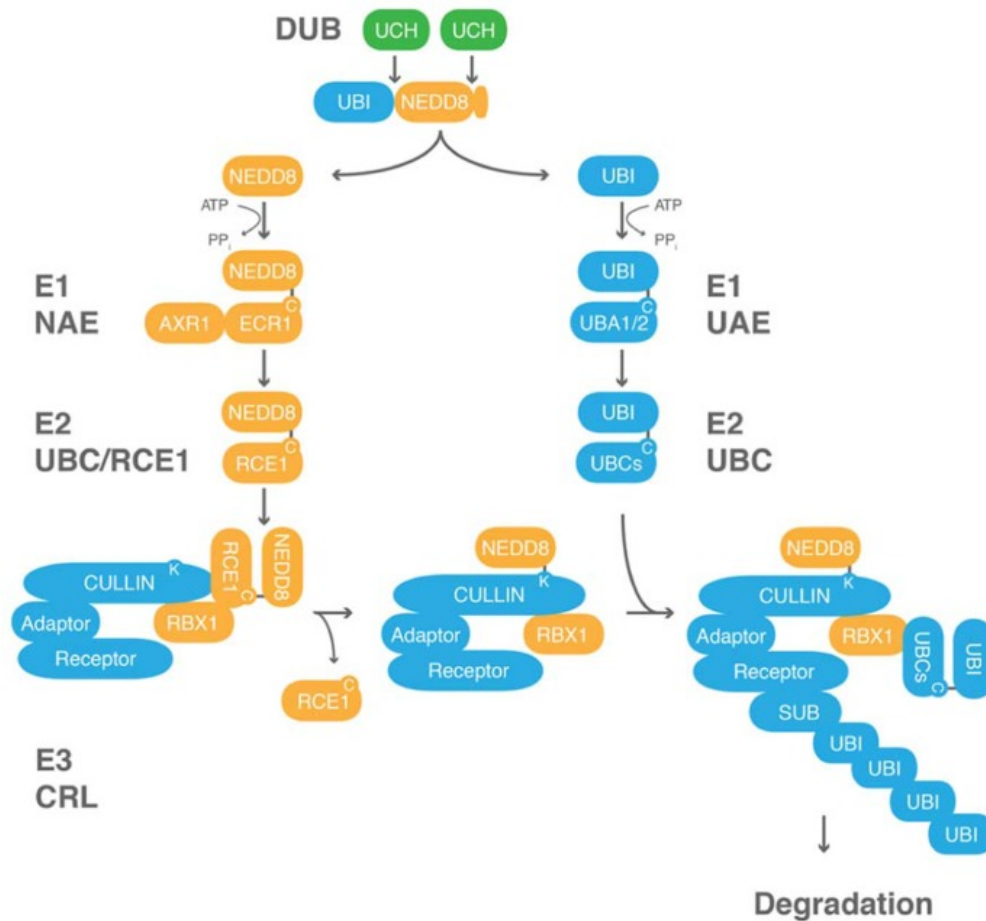


Fig 4.1. Neddylation and ubiquitination are analogous processes. NEDD8 precursor proteins are processed by Ub C-terminal hydrolases before activation by E1 Ub/NAE enzymes. Activated NEDD8 or Ub are transferred *via* an active cysteine (C) residue to an E2 conjugation enzyme (RCE1 for NEDD8 in Arabidopsis). E2-conjugated NEDD8 (or E2-conjugated Ub) is transferred through the action of an E3 ligase to a lysine (K) residue of a substrate protein. RBX1 is one proposed NEDD8 E3 ligase in Arabidopsis. Cullin protein neddylation allows for conformational rearrangement, as well as subunit exchange, of CRL-type Ub E3 ligases that can target substrate proteins for degradation *via* Ub conjugation. Image from (Mergner and Schweichheimer, 2014)

4.1.2 Proximity labeling of E3 Ub ligase substrates by a NEDDylator

Identifying substrates of E3 Ub-ligases can be technically challenging due to the weak and transient nature of the substrate-ligase interaction. Recent strategies for substrate identification make use of enzyme-catalyzed proximity labeling, whereby interaction of a recombinant E3 Ub ligase with its potential substrate results in the conjugation of a molecular tag to the substrate. The modified substrate can then be

isolated using the properties of this molecular tag and identified by downstream proteomics approaches (reviewed in Iconomou and Saunders, 2016). In a study conducted by Zhuang *et al.*, researchers designed a proximity-labeling tool, termed a NEDDylator, to identify substrates of the human RING domain-containing E3 Ub-ligase X chromosome-linked Inhibitor of Apoptosis (XIAP) (Zhuang *et al.*, 2013). To develop a XIAP-specific NEDDylator (noted NEDDylator^{XIAP}), these investigators removed the XIAP E2-Ub-interacting RING domain and replaced it with a flexible linker region translationally fused to an E2 NEDD8-conjugating domain (Ubc12), such that proteins interacting with the XIAP fusion protein would be neddylated and not ubiquitinated (Fig 4.2). NEDDylator^{XIAP} constructs and His-Biotin-tagged NEDD8 were co-expressed in lymphocyte cells before His-Biotin tagged substrates were purified using nickel affinity purification and streptavidin beads. The purified proteins were then analyzed using mass spectrometry, resulting in the identification of ~50 putative substrates of XIAP (Zhuang *et al.*, 2013), several of which were known substrates. In addition, novel substrates identified through the use of the NEDDylator^{XIAP} were confirmed using more classical approaches, such as *in vitro* and *in vivo* ubiquitination assays (Zhuang *et al.*, 2013).

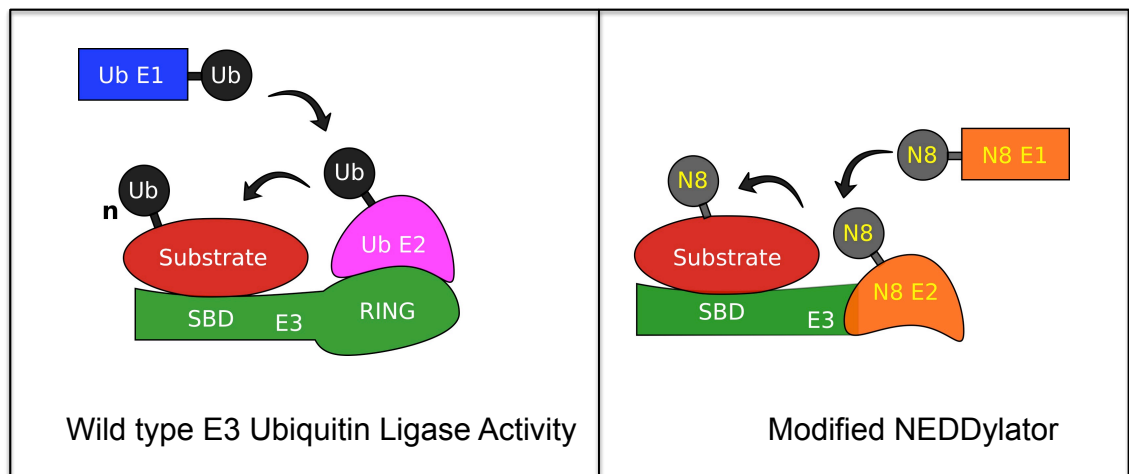


Fig 4.2. Principle of substrate-tagging by a NEDDylator. (Left) Wild-type RING-domain E3 Ub ligase activity. Ub is transferred from the Ub-E1 to Ub-E2. Ub-E2 interacts with the RING domain of the E3 ligase, which facilitates the transfer of Ub to the substrate bound to the substrate binding domain (SBD) of the E3 ligase. (Right) Modified NEDDylator activity. NEDD8 (N8) is transferred from E1 NAE to E2 conjugation enzyme (e.g. Ubc12), which is translationally fused to the SBD of the E3 ligase of interest. Binding of the substrate brings the NEDD8-E2 in close contact with the substrate, resulting in the conjugation of NEDD8. Figure based on an image in (Zhuang *et al.*, 2013).

ator^{PRT6} constructs along with reporter substrates. These constructs were co-expressed in tobacco plants to characterize NEDDylator^{PRT6} activity. As an alternative approach, I also used the yeast *S. cerevisiae* to express different variants of the NEDDylator^{PRT6}.

4.2 Results

4.2.1 Design and generation of a NEDDylator^{PRT6}

The Arabidopsis N-recognin PRT6 contains the well-characterized UBR domain that is involved in the recognition of basic N-terminal destabilizing residues, as well as a RING domain, involved in mediating interaction with the E2 enzyme (see Sections 1.1.2.4, 1.2.4.2 and 4.1.4). To develop a NEDDylator^{PRT6} for expression in plants, I cloned constructs composed of the Arabidopsis PRT6 UBR domain (sequence from Gly119 to Lys188) translationally fused to the Arabidopsis NEDD8 E2-conjugating enzyme RCE1 (see Section 4.1.2) and a Myc epitope tag at either the N or C-terminus of the fusion protein. Short linker sequences (Gly-Gly-Ser-Gly or Ala-Ala-Ala) were added between the different tags and domains. The construct was placed under control of the constitutive 35S promoter and cloned into the pML-BART plant transformation vector (Fig 4.4).

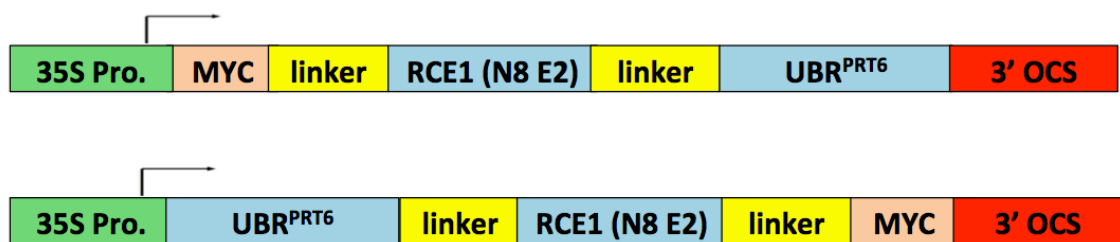


Fig 4.4. Design of different NEDDylator^{PRT6} constructs for expression in plants. The UBR domain of PRT6 is translationally fused to a flexible linker region and the NEDD8 E2 conjugation enzyme RCE1. Another flexible linker region links either an N-terminal or C-terminal Myc-tag. Each construct is expressed under the control of a 35S promoter and contains the 3' transcriptional terminator sequence from the *Agrobacterium* octopine synthase gene (OCS). The full-length fusion protein is ~30 kDa.

4.2.2 Testing *in vivo* transient neddylation in tobacco

Before characterizing the activity of the two above-mentioned NEDDylator^{PRT6} constructs in tobacco plants, I carried out preliminary *in vivo* transient neddylation

assays to ensure that I could detect neddylation of proteins in tobacco using reagents available in the lab. To this end, I used plasmids that were kindly provided by Prof. Judy Callis (UC Davis). A first set of plasmids encoded the known neddylation substrates Arabidopsis CULLIN1 (CUL1) or the neddylation site mutant CUL1^{K682R} fused to the Myc epitope tag (these constructs are noted Myc-CUL1 and Myc-CUL1^{K682R}, respectively) under the control of the 35S promoter (Hotton *et al.*, 2012). A second set of plasmids I used in these transient expression experiments coded for a 6xHis-3xhemagglutinin (HA)-tagged Arabidopsis NEDD8 (noted 6His-3HA-NEDD8) under the control of the 35S promoter (Hotton *et al.*, 2012). As described by Hotton *et al.*, following *Agrobacterium*-mediated co-expression of either Myc-CUL1 variants in tobacco with 6His-3HA-NEDD8, the tagged cullins were immunoprecipitated using agarose beads conjugated to anti-Myc antibodies (Hotton *et al.*, 2012). The neddylation status of the Myc-CUL1 or Myc-CUL1^{K682R} proteins was then determined by immunoblotting using antibodies raised against the HA epitope tag to detect 6His-3HA-NEDD8. The results for this experiment are described in Fig. 4.5.

Anti-HA and anti-Myc immunoblotting confirmed that Myc-tagged cullin variants, as well as 6His-3HA-NEDD8, were expressed in tobacco leaves (Input panel in Fig 4.5). Using proteins recovered after the immunoprecipitation procedure, immunoblotting using a Myc-specific antibody revealed that both Myc-tagged cullins were successfully immunoprecipitated. The use of an anti-HA antibody to detect the potential conjugation of 6His-3HA-NEDD8 to the two CUL1 proteins further indicated that the Myc-CUL1 protein, but not Myc-CUL1^{K682R}, had detectable anti-HA signal, indicative of 6His-3HA-NEDD8 conjugation to Myc-CUL1 specifically (Fig 4.5). This signal appeared as multiple bands increasing in size, suggesting that Myc-CUL1 may have been neddylated multiple times or conjugated to a NEDD8 chain. Although this experiment was only conducted once, the results obtained suggest that *in vivo* transient neddylation using transient co-expression in tobacco leaves can be detected.

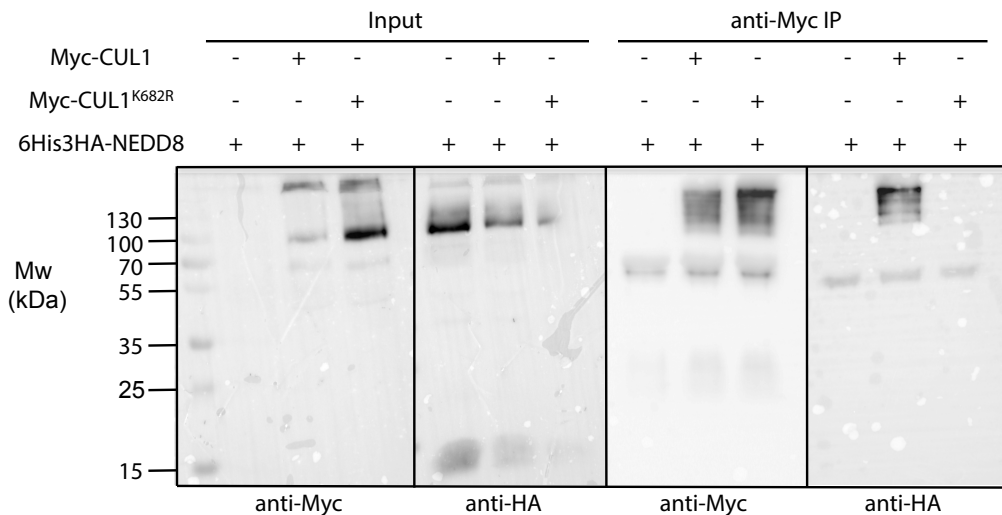


Fig 4.5 Transient neddylation assay in tobacco. Myc-tagged Arabidopsis CUL1 or the neddylation site mutant CUL1^{K682R} (both ~88 kDa) were co-expressed with 6His-3HA-NEDD8 (~15 kDa) in tobacco leaves using *Agrobacterium*-mediated transformation. Three days after agroinfiltration, tissue was collected and ground in liquid nitrogen before protein extracts were prepared in IP buffer (see Appendix 1). A fraction of this protein extract was saved and used for the 'Input' sample. Anti-Myc agarose beads were added to the other fraction and incubated with rotation in order to carry out immunoprecipitation under non-denaturing conditions of Myc-tagged cullins. To elute bound proteins, the beads were incubated at 95°C with 1X SDS loading dye (Appendix 1). Samples were separated using SDS-PAGE and then analyzed using immunoblotting. Anti-Myc antibodies were used to check for the presence of Myc-tagged cullins and anti-HA was used to detect 6His-3HA-NEDD8 conjugated proteins. Please note that this experiment was conducted once.

4.2.3 Testing self-neddylation of NEDDylator^{PRT6} in tobacco

The previously described NEDDylator^{XIAP} was composed of the XIAP protein lacking the RING domain translationally fused to the mammalian NEDD8 E2 conjugating enzyme Ubc12 (Zhuang *et al.*, 2013). Ubc12 displays auto-neddylation activity *in vitro* as well as in mammalian cells (Coleman *et al.*, 2017). In addition, it was shown that the NEDDylator^{XIAP} displayed the ability to self-neddylate (Zhuang *et al.*, 2013). The Arabidopsis NEDD8 E2 conjugating enzyme RCE1 used for NEDDylator^{PRT6} was identified by its homology to Ubc12 (del Pozo and Estelle, 1999). RCE1 has also been shown to self-neddylate *in vitro* and is likely to self-neddylate *in vivo* (Mergner *et al.*, 2015; Mergner *et al.*, 2017). To determine if the NEDDylator^{PRT6} displays auto-neddylation activity *in planta*, I transiently co-expressed the

N- and C-terminally tagged NEDDylator^{PRT6} constructs (Fig. 4.4) with 6His-3HA-NEDD8 in tobacco leaves. The Myc-tagged NEDDylators could then be immunoprecipitated using anti-Myc agarose beads and checked for 6His-3HA-NEDD8 conjugation using immunoblotting with anti-HA antibodies. The results for this experiment are depicted in Fig. 4.6.

Analysis of the 'input' fractions with an antibody raised against the Myc tag indicates that the N-terminally Myc-tagged NEDDylator^{PRT6} (labeled Myc-NEDDylator^{PRT6}) was expressed and accumulated to detectable levels whether 6His-3HA-NEDD8 was co-expressed or not (Fig. 4.6). In contrast, the C-terminally tagged NEDDylator^{PRT6} (noted NEDDylator^{PRT6}-Myc) was not easily detected in this experiment. This difference in NEDDylator^{PRT6} abundance was reproducible across several independent experiments (data not shown), and may be due to lower transcription, reduced translation efficiency, or instability of the NEDDylator^{PRT6}-Myc fusion protein in tobacco. Immunoblot of the 'input' fractions with an HA-specific antibody revealed that in all samples derived from leaves in which 6His-3HA-NEDD8 was (co-)expressed, the tagged NEDD8 could be detected (see lower band near 15 kDa). In addition, a signal corresponding to high molecular weight proteins (~45 kDa and ~100 kDa) was detected with the anti-HA antibody. Interestingly, the signal around 100 kDa could correspond to the neddylated form of the endogenous tobacco cullin(s).

I also analyzed the immunopurified proteins using Myc-specific antibodies (Fig 4.6). In agreement with the analysis of the 'input' fractions, the C-terminally tagged NEDDylator^{PRT6}-Myc fusion could not be detected after immunoprecipitation. In contrast, a strong signal could be detected for the N-terminally tagged Myc-NEDDylator^{PRT6} after immunoblot with the anti-Myc antibody. Surprisingly though, the ~35 kDa protein corresponding to an unmodified Myc-NEDDylator^{PRT6} was not detected after purification on anti-Myc beads, although it accumulated to high levels in the input fractions. Instead, high molecular weight proteins appeared as smears between 70 and 130 kDa and around 45 kDa. This signal was only present when the Myc-NEDDylator^{PRT6} was expressed but was independent of 6His-3HA-NEDD8 expression, suggesting that these proteins do not correspond to neddylated forms of the Myc-NEDDylator^{PRT6}.

Immunoblots carried out on the immunoprecipitated fractions using an HA-specific antibody showed the presence of HA-tagged proteins in the immunoprecipitated protein fraction obtained when Myc-NEDDylator^{PRT6} and 6His-3HA-NEDD8 were co-expressed. Importantly, these HA-tagged proteins were not present when Myc-NEDDylator^{PRT6} was expressed in the absence of 6His-3HA-NEDD8, or when 6His-3HA-NEDD8 was expressed in the absence of the Myc-NEDDylator^{PRT6}. These results suggest that the neddylated proteins do not correspond to either cross-reacting proteins or to neddylated cullins. In particular, the protein migrating around 40 kDa could correspond to a Myc-NEDDylator^{PRT6} conjugated to a single 6His-3HA-NEDD8, while the higher molecular weight smear could potentially correspond to a poly-neddylated or multi-neddylated Myc-NEDDylator^{PRT6}. Immunoblot analysis with an anti-HA antibody of the immunoprecipitated proteins obtained upon expression of the C-terminally tagged NEDDylator^{PRT6}-Myc indicated the presence of an HA-tagged proteins around 40 kDa, again possibly corresponding to a self-neddylated version of NEDDylator^{PRT6}-Myc.

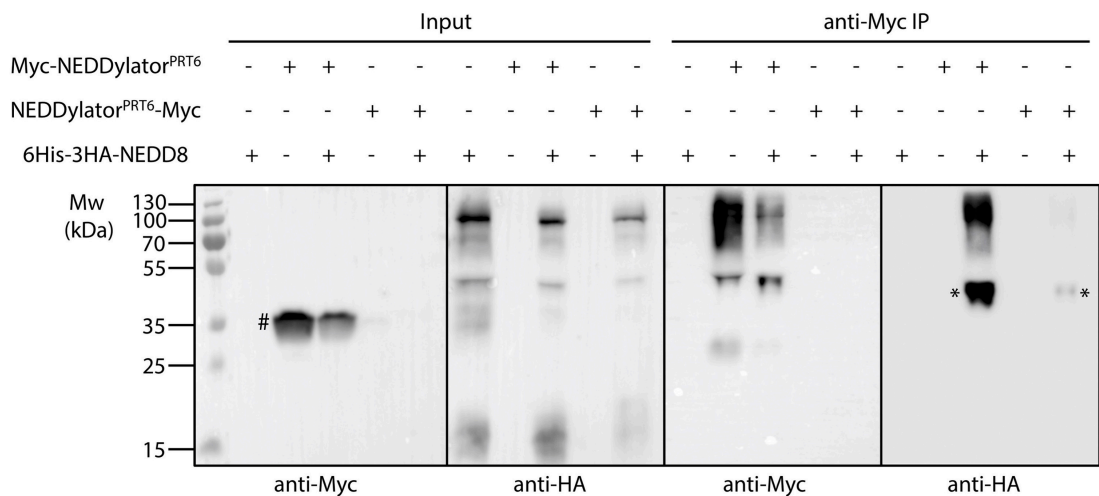


Fig 4.6. Self-neddylation of NEDDylator^{PRT6} in tobacco. NEDDylator^{PRT6} constructs with an N- or C-terminal Myc tag (~30 kDa) were co-expressed with 6His-3HA-NEDD8 (~15 kDa) in tobacco leaves. Three days after agroinfiltration, leaf tissue was collected and ground in liquid nitrogen. A small amount of tissue powder was taken at this stage and resuspended in 2x SDS loading dye (Appendix 1) and used as an 'input' sample. Protein extracts in the remaining powder were solubilized in IP buffer (see Appendix 1). Anti-Myc agarose beads were added to this fraction and incubated with rotation in order to carry out immunoprecipitation of Myc-tagged NEDDylator^{PRT6} under non-denaturing conditions. To elute immunoprecipitated proteins beads were incubated at 95°C with 1X SDS loading dye (Appendix 1). Samples were separated using SDS-PAGE and then analyzed by

immunoblotting. Anti-Myc antibodies were used to check for the presence of Myc-tagged NEDDylator^{PRT6} constructs, while HA tag-specific antibodies were used to check for the presence of 6His-3HA-NEDD8 conjugation. This experiment was conducted once again using only N-terminally tagged NEDDylator^{PRT6} with similar results. # indicates the unmodified Myc-tagged NEDDylator^{PRT6}; * denotes the putative self-neddylated Myc-tagged NEDDylator^{PRT6}.

In summary, the results of these experiments show that both Myc-NEDDylator^{PRT6} and NEDDylator^{PRT6}-Myc are expressed in the transient expression system in tobacco, although Myc-NEDDylator^{PRT6} appears to accumulate at much higher levels. In addition, these experiments suggest that both versions of the NEDDylator^{PRT6} may self-neddylate, indicating that RCE1 is active in this context and that it can utilize the 6His-3HA-NEDD8 fusion protein. In order to verify these results using independent reagents, I attempted to optimize an immunoprecipitation protocol with beads coupled to an anti-HA antibody (data not shown). Unfortunately, the immunoprecipitation with anti-HA antibodies did not work despite several attempts made at optimizing the protocol using the previously mentioned Myc-tagged CUL1 neddylation assay. Furthermore, the identity or origin of the high molecular weight proteins detected by the Myc-specific antibody following immunoprecipitation on anti-Myc beads also remains to be uncovered. One possibility is that they may correspond to neddylated versions of the Myc-NEDDylator^{PRT6} to which endogenous tobacco NEDD8 was conjugated in the absence of the 6His-3HA-NEDD8 variant. This would explain the similar migration pattern for the Myc-NEDDylator^{PRT6} in the presence or absence of tagged-NEDD8, and would also be in agreement with the fact that these proteins are only recognized by the anti-HA antibody when 6His-3HA-NEDD8 is co-expressed. Another observation that remains unexplained is the absence of the ~35 kDa (unmodified) Myc-NEDDylator^{PRT6} after immunoprecipitation, even though it accumulated to high levels in the input. One possible explanation for this result is that the self-neddylation activity of the Myc-NEDDylator^{PRT6} may occur during the immunoprecipitation on anti-Myc beads, so that in the course of the experiment, the abundance of the self-NEDDylated forms of the Myc-NEDDylator^{PRT6} increase, at the expense of the unmodified 35 kDa form.

The N-terminal acetylation of the yeast and mammalian NEDD8-E2 Ubc12 increases the affinity for Ubc12 with an E3 NEDD8 ligase involved in the specific

neddylation of cullins (Scott *et al.*, 2011). In order to reduce background neddylation of cullins in NEDDylator^{XIAP} experiments Zhuang *et al.* translationally fused the XIAP sequence to the N-terminus of Ubc12, blocking the N-terminal acetylation site (Zhuang *et al.*, 2013). To reduce background neddylation of cullins in downstream experiments and because the N-terminally Myc-tagged NEDDylator^{PRT6} appeared to accumulate to higher levels in tobacco cells, I carried out further experiments to characterize the activity of the N-terminally Myc-tagged NEDDylator^{PRT6} (denoted NEDDylator^{PRT6} hereafter) towards physiological and artificial substrates of PRT6.

4.2.4 Testing for the NEDDylator^{PRT6}-mediated neddylation of physiological PRT6 substrates

In order to determine if the NEDDylator^{PRT6} could neddylate proteins that interacted with the PRT6 UBR domain, I aimed to transiently co-express in tobacco known substrates of PRT6 as epitope-tagged fusion proteins with the NEDDylator^{PRT6} and 6His-3HA-NEDD8. The substrates could then be immunoprecipitated using antibodies raised against their epitope tag and checked for 6His-3HA-NEDD8-conjugation using anti-HA antibodies, as described in the experiments above.

Proteins so far identified as likely PRT6 targets are those encoding Met-Cys N-terminal residues such as members of the ERF VII family of TFs in Arabidopsis, including hypoxia responsive factors HRE1 and HRE2 (discussed in Section 1.2.5). I generated constructs made up of HRE1 or HRE2 translationally fused to a C-terminal FLAG epitope tag (~1 kDa) and placed under the control of the Ub (UBQ3) or 35S promoter to allow for their constitutive expression. I conducted preliminary experiments with HRE1 first. However, I subsequently found that HRE2-FLAG could accumulate to detectable levels, which made the work easier, so I focused on HRE2-FLAG fusion proteins more in detail. In the two sub-sections below, I will present some of the experiments I have conducted with HRE1-FLAG and HRE2-FLAG fusion proteins in order to illustrate some of the problems encountered and experimental strategies tested to overcome them.

For the experiments described below, the HRE1/2-FLAG fusion was generated with an N-terminal Met-Cys (i.e. the endogenous form of the protein with a C-terminal FLAG tag) and as a Ub-R-HRE1/2-FLAG fusion to examine if expression of either form of the substrate had any effect on the detection of the substrate or

its interaction with the NEDDylator^{PRT6}. Indeed, expression of HRE1/2-FLAG starting with Met-Cys should be first cleaved by a MetAP to expose the Cys residue at the N-terminus. This residue would then be expected to be oxidized under the conditions used, arginylated by the Arg-transferases and finally bound and neddylated by NEDDylator^{PRT6}. In contrast, expression of the Ub-R-HRE1/2-FLAG fusion protein should lead to its co-translational deubiquitination, resulting in the release of the R-HRE1/2-FLAG protein (which starts with an Arg), and hence could be recognized and modified by the NEDDylator^{PRT6}. Importantly, it is expected that neddylation of HRE1/2-FLAG would lead to its stabilization, thus facilitating its detection in the subsequent immunoblot analyses.

4.2.4.1 Experiments conducted with an HRE1-FLAG fusion protein

- **Transient expression of the Ub-R-HRE1-FLAG fusion protein**

The Ub-R-HRE1-FLAG fusion protein was expressed under the control of the Ub UBQ3 promoter, to allow for its constitutive expression. I first attempted to transiently co-express Ub-R-HRE1-FLAG, NEDDylator^{PRT6} and 6His-3HA-NEDD8 and monitored the results of this experiment using immunoblot on protein extracts from leaf tissue with anti-HA (to detect neddylation), anti-Myc (to detect NEDDylator^{PRT6}) and anti-FLAG (to check for the presence and deubiquitylation of HRE1-FLAG) antibodies (Fig. 4.7).

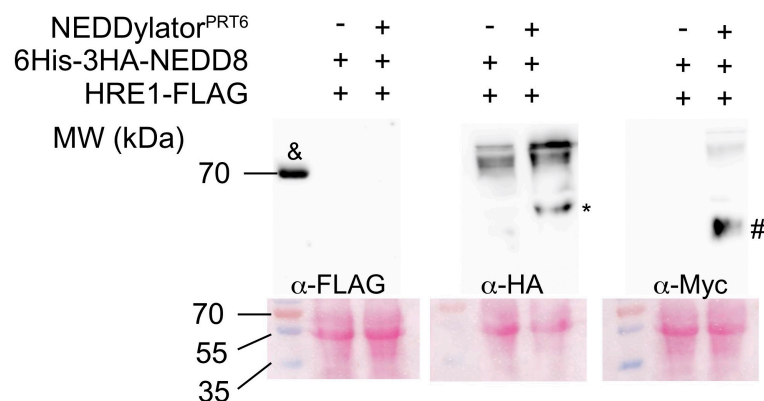


Fig. 4.7. Immunoblot analysis to determine transient co-expression of the 3 proteins of interest. NEDDylator^{PRT6} with an N-terminal Myc tag (~30 kDa) was co-expressed with 6His-3HA-NEDD8 (~15 kDa) and HRE1-FLAG (~30 kDa) in tobacco leaves. Three days after agroinfiltration, leaf tissue was collected and ground in liquid nitrogen. Proteins were extracted in 2x SDS loading

buffer, separated by SDS-PAGE and analyzed using immunoblotting with anti-Myc, HA or FLAG antibodies. # indicates the unmodified Myc-tagged NEDDylator^{PRT6} fusion; * denotes the putative self-neddylated Myc-tagged NEDDylator^{PRT6}; & indicates the 70 kDa marker which cross-reacts with the FLAG-specific antibodies.

Immunoblot with the anti-Myc antibody indicated that NEDDylator^{PRT6} was expressed and accumulated in the cells. Protein detection with the antibody raised against the HA tag revealed the presence of high molecular weight proteins conjugated to 6His-3HA-NEDD8, including the presumed self-neddylated NEDDylator^{PRT6} (indicated with an asterisk). Unfortunately, use of an anti-FLAG antibody to detect the HRE1-FLAG protein failed. This could be due to either a lack of expression or to instability of the protein, presumably because it can be targeted for degradation by the tobacco N-end rule pathway, even in the presence of the NEDDylator^{PRT6}, which would stabilize the protein if it could neddylate it efficiently. To distinguish between these two possibilities and test that the Ub-R-HRE1-FLAG construct could indeed be transcribed in the transient expression experiments, I agroinfiltrated tobacco leaves with a strain coding for the Ub-R-HRE1-FLAG fusion. I collected tobacco leaves before inoculation, as well as one day and 3 days after agroinfiltration. I then extracted total RNA and carried out reverse transcription coupled to PCR (RT-PCR) using primers specific for the fusion (Fig. 4.8). The result of this control RT-PCR experiment indicates that the construct is indeed transcribed in tobacco leaves.

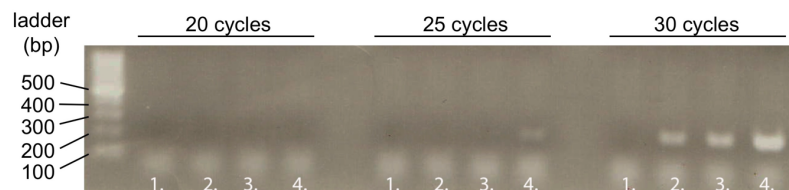


Fig. 4.8. RT-PCR analysis to determine expression of the Ub-R-HRE1-FLAG fusion. Tobacco leaves were infiltrated with agrobacterium encoding the Ub-R-HRE1-FLAG construct and leaves were subsequently collected and frozen in liquid nitrogen. Total RNA was extracted and cDNA was prepared using oligo(dT18) primers and 1 µg total RNA. cDNA was used for PCR reactions at a concentration of 8 ng/µL. Lane 1: RNA from non-infiltrated leaves; Lane 2: RNA from infiltrated leaves immediately after infiltration; Lane 3: RNA from infiltrated leaves that were collected 1 day after infiltration; Lane 4: RNA from infiltrated leaves that were collected 3 days after agroinfiltration.

Number of PCR amplification cycles is indicated above the gel. PCR primer At93 and KG21 were used (expected amplicon is 225 bp).

Finally, to ensure that the FLAG tag-specific antibodies I used were indeed functional, I performed an immunoblot with protein samples kindly donated by Drs. Darren Martin and Conor Breen (Maynooth University) and which contained a FLAG-tagged protein with a molecular weight of 63 kDa. This control experiment showed that the anti-FLAG antibodies were functional in the conditions of the experiments (data not shown).

- **Transient expression of the Met-Cys-HRE1-FLAG fusion protein**

To ensure that the expression of a Ub-R-HRE1-FLAG fusion protein was not targeting HRE1-FLAG for degradation because of the presence of the N-terminal Ub moiety, I cloned the cDNA of HRE1 with a C-terminal FLAG tag. In this case, the HRE1-FLAG protein produced should start with the Met-Cys dipeptide, with the initial Met being removed by MetAPs and with the newly exposed Cys being oxidized, arginylated and recognized by PRT6 or NEDDylator^{PRT6}. To ensure constitutive expression, the FLAG-tagged HRE1 construct was placed under the control of the 35S promoter. I then agroinfiltrated tobacco leaves with *Agrobacterium* containing the plasmid of interest and collected tissue at 3 days after infiltration. Proteins were extracted in 2x SDS loading buffer, separated by SDS-PAGE and FLAG-tagged proteins were detected using the anti-FLAG antibody. I also repeated these experiments in the presence of 100 μ M MG132 (treatment made at ~2.5 days after agroinfiltration and tissue collected 6 hrs after MG132 infiltration (i.e. ~3 days after agroinfiltration)) in order to inhibit proteasomal degradation. Neither of the conditions tested resulted in detectable levels of HRE1-FLAG (Fig. 4.9).

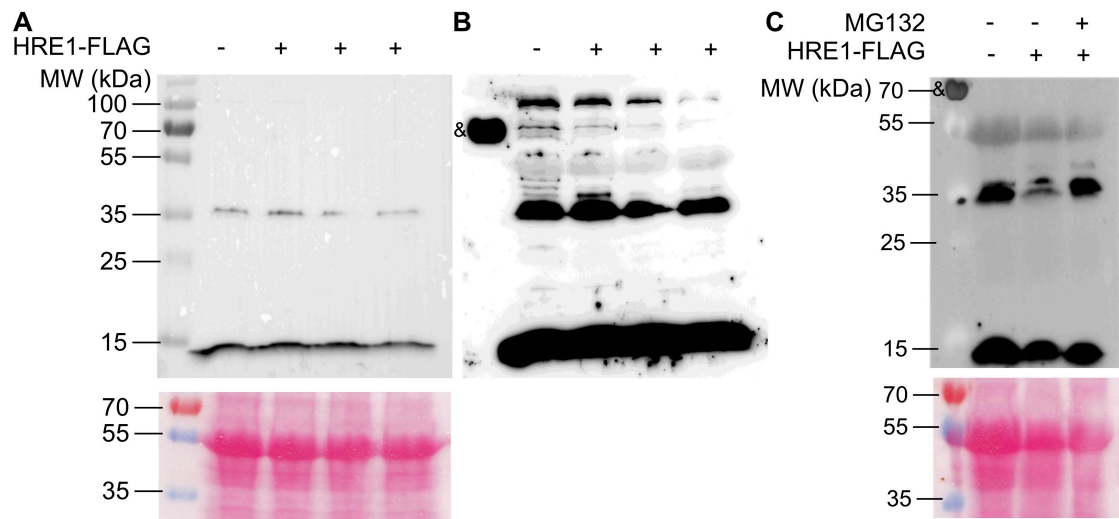


Fig. 4.9. Immunoblot analyses to detect HRE1-FLAG. (A) Tissue from tobacco leaves transiently expressing HRE1-FLAG constructs was collected 3 d after agroinfiltration and ground in liquid nitrogen before protein was solubilized using 2x SDS loading buffer. Protein extracts were separated by SDS-PAGE and FLAG-tagged proteins were detected using the anti-FLAG antibody. (B) Longer exposure of the immunoblot presented in panel A. ‘&’ indicates one of the ladder proteins (70 kDa) that is recognized by the FLAG-specific antibodies. (C) 2.5 d after agroinfiltration, tobacco leaves transiently expressing HRE1-FLAG constructs were infiltrated with 100 μ M MG132. After 6 hrs tissue was collected and ground in liquid nitrogen before protein was solubilized using 2x SDS loading buffer. Protein extracts were separated by SDS-PAGE and FLAG-tagged proteins were detected using the anti-FLAG antibody. The expected molecular weight of HRE1-FLAG is \sim 30 kDa.

4.2.4.2 Experiments conducted with HRE2-FLAG fusion proteins

In parallel to the work conducted with HRE1-FLAG, I generated a plasmid to allow for the expression of FLAG-tagged HRE2 under the control of the 35S promoter. This fusion protein, noted HRE2-FLAG, starts with the initial Met-Cys residues of HRE2, and is expected to be modified by MetAPs (removal of Met), followed by oxidation of Cys, arginylation and finally recognition by PRT6 or the NEDDylator^{PRT6}. Similarly to the work I carried out with the HRE1-FLAG fusion protein, I first sought to determine if I could detect HRE2-FLAG in immunoblots with an anti-FLAG antibody. To this aim, I transiently expressed HRE2-FLAG in transient expression experiments in tobacco, with infiltrated leaf tissue being collected 3 days after agroinfiltration. Proteins were then extracted in 1x SDS loading buffer, separated by SDS-PAGE and subjected to immunoblotting with an anti-FLAG antibody (Fig. 4.10). HRE2-FLAG expression was carried out in the presence or absence of

MG132 in order to test if proteasome inhibition could allow for accumulation of HRE2-FLAG (Fig. 4.10).

In contrast with HRE1-FLAG, HRE2 fused to the FLAG tag accumulated to levels that could be detected in immunoblot experiments with an anti-FLAG antibody (Fig. 4.10A). However, the levels of HRE2-FLAG varied greatly from one experiment to another (data not shown), so that it was not always detected in the total protein extract. I therefore tested if the addition of MG132 could further stabilize the HRE2-FLAG protein. This was indeed the case in some experiments, but the results were again very variable from one experiment to another (data not shown), making it very difficult to draw a conclusion.

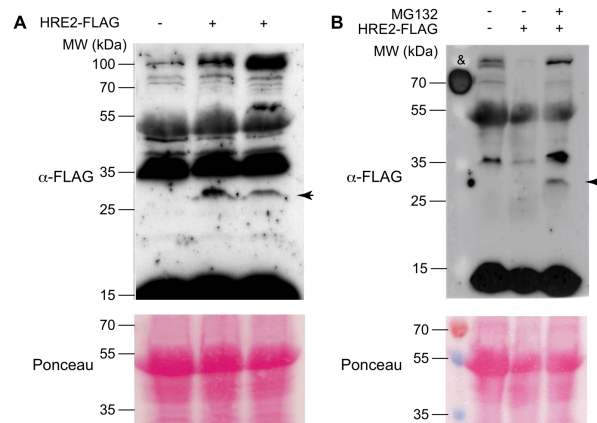


Fig. 4.10. Expression of HRE2-FLAG in transient expression experiments in tobacco. (A) Three days after agroinfiltration of tobacco plants, leaf tissue was collected. Total protein extracts were generated by grinding the tissue in 1x SDS loading buffer. Proteins were then separated by SDS-PAGE and FLAG-tagged proteins were identified using immunoblot with a FLAG-specific antibody. Leaf tissue that had not been agroinfiltrated was used as a control for background. (B) Tobacco leaves were agroinfiltrated with an *Agrobacterium* strain containing the HRE2-FLAG-coding transgene. Three days after agroinfiltration, the same leaves were infiltrated with a 100 μ M solution of MG132 or using a mock solution. Six hours after this second infiltration, leaf tissue was collected. Total protein extracts were generated by grinding the tissue in 1x SDS loading buffer. Proteins were then separated by SDS-PAGE and FLAG-tagged proteins were identified using immunoblot with a FLAG-specific antibody. Leaf tissue that had not been agroinfiltrated was used as a control for background. HRE2-FLAG has an expected molecular weight \sim 21 kDa and is indicated by a black arrowhead.

Despite these difficulties, I used HRE2-FLAG transient expression to optimize the immunoprecipitation procedure for the HRE2-FLAG fusion protein before proceeding with transient expression experiments in the presence of the NEDDylator^{PRT6} and 6His-3HA-NEDD8. As shown in Fig. 4.11 below, even when HRE2-FLAG did not accumulate to detectable levels in the input fraction the protein could be immunoprecipitated using anti-FLAG beads and elution with 100 µg/mL of the FLAG peptide.

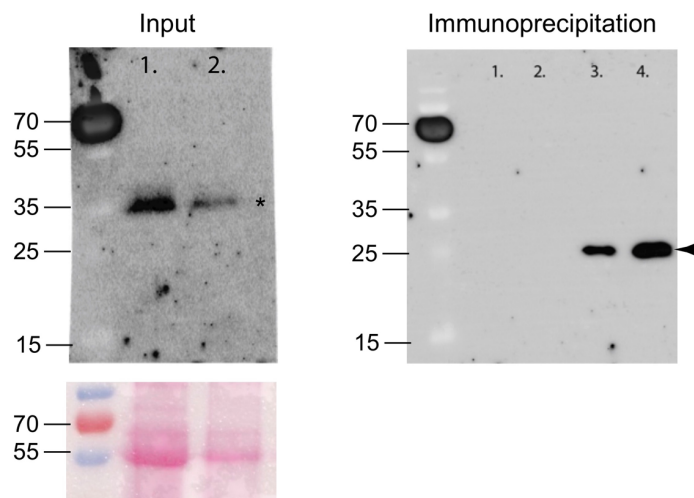


Fig. 4.11. Representative result of HRE2-FLAG immunoprecipitation using anti-FLAG beads. Left: immunoblot on the 'input' fraction, which corresponds to total protein extracts solubilized in 2x SDS loading dye. The asterisk indicates a cross-reaction protein that is not HRE2-FLAG. Lane 1: protein extract from non-infiltrated leaves to determine background; Lane 2: protein extract from leaves transiently expressing HRE2-FLAG. Right: detection of FLAG-tagged proteins in the elution fractions obtained after immunoprecipitation. Proteins were eluted using 100 µg/mL of the FLAG peptide to compete for binding to the anti-FLAG beads. Lanes 1 and 2 correspond to the first and second elution fractions obtained with non-infiltrated leaves (i.e. background control); Lanes 3 and 4 correspond to the first and second elutions obtained with protein extracts prepared from leaves transiently expression HRE2-FLAG. The arrowhead indicates the HRE2-FLAG fusion protein.

Since HRE2-FLAG could be efficiently immunoprecipitated, I attempted to transiently co-express HRE2-FLAG, NEDDylator^{PRT6} and 6His-3HA-NEDD8 in order to determine if the NEDDylator^{PRT6} was able to neddylate HRE2-FLAG. In order to test this possibility, I co-infiltrated tobacco leaves with three different *Agrobacterium* strains each bearing one of the three plasmids. Three days after agroinfiltration, I also infiltrated a solution of 100 µM MG132 and collected the leaf tissue 6

hrs after the MG132 treatment. The latter was added to the experiment in order to further accumulate HRE2-FLAG and increase the likelihood of detecting its neddylation by the NEDDylator^{PRT6}. The leaf tissue was then frozen in liquid nitrogen and ground into a fine powder. A small aliquot of this powder was resuspended in 2x SDS loading buffer to serve as 'input' fraction, while the rest of the powder was resuspended in IP buffer (see Appendix 1). Soluble proteins were obtained after centrifugation and subjected to immunoprecipitation with anti-FLAG beads, using the same procedure as the one used for the immunoprecipitation experiment presented in Fig. 4.11.

Analysis of the input fractions with a FLAG-specific antibody results in the detection of a cross-reacting protein only. However, based on previous experiments, this does not preclude an efficient immunoprecipitation of the potentially expressed HRE2-FLAG protein. Analysis of the same input fractions with the HA-specific antibody revealed the presence of 6His-3HA-NEDD8 (migrating close to ~15 kDa) and of higher molecular weight proteins that were specific to the protein extracts prepared from leaves that transiently expressed the tagged NEDD8. These HA-tagged proteins probably correspond to neddylated cullins. Immunoblot using a Myc-specific antibody finally indicated that the NEDDylator^{PRT6} was expressed. After elution of the proteins bound to the anti-FLAG beads through competition with a FLAG peptide, I carried out an immunoblot analysis to detect HRE2-FLAG, as well as its potential neddylation. If the NEDDylator^{PRT6} could indeed bind and neddylate HRE2-FLAG, I would have expected a common signal with the anti-FLAG and the anti-HA antibodies in elution fractions originating from leaves that co-expressed the 3 proteins. While the results of the anti-FLAG immunoblot confirmed the presence of HRE2-FLAG in immunoprecipitated proteins when the 3 constructs were co-expressed, I could not detect HRE2-FLAG in the elution fractions of leaves that co-expressed HRE2-FLAG and 6His-3HA-NEDD8 only. This is likely due to the fact that HRE2-FLAG levels could vary greatly from one experiment to another. Immunoblot analysis of the eluted proteins with a HA-specific antibody revealed the presence of 2 proteins. However, the proteins detected by the anti-HA antibody following affinity purification were unlikely to correspond to neddylated HRE2-FLAG, because the same proteins could be detected in the elu-

tion fractions from protein extracts that did not express the NEDDylator^{PRT6}. The identity of these proteins is unknown at this stage.

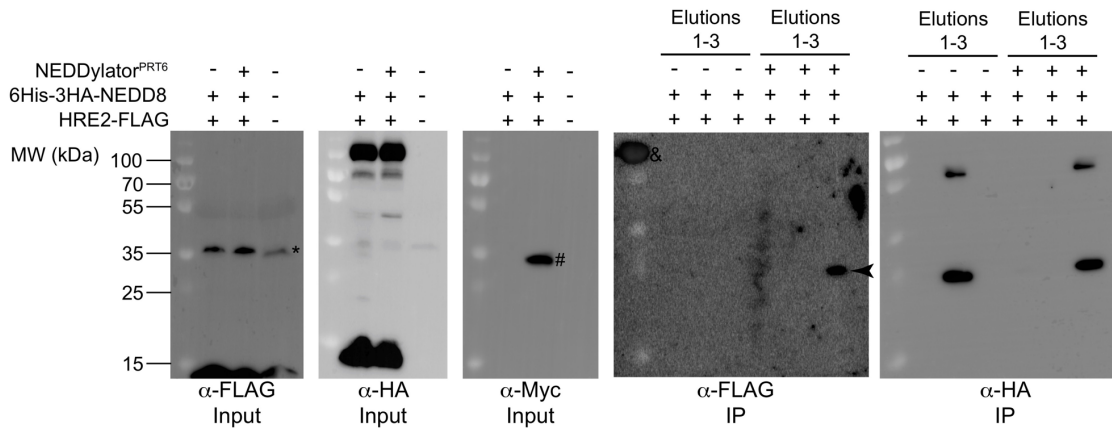


Fig. 4.12. Testing the NEDDylator^{PRT6} in the presence of HRE2-FLAG and 6His-3HA-NEDD8.

The ‘input’ fractions were analyzed with three different epitope-specific antibodies to determine if each of the components was indeed expressed in tobacco. Anti-FLAG was used to detect HRE2-FLAG, anti-HA was used to detect 6His-3HA-NEDD8, while the NEDDylator^{PRT6} was detected using an anti-myc antibody. Proteins bound to the anti-FLAG beads were eluted using 100 µg/mL of the FLAG peptide. Three consecutive elution fractions were obtained (noted ‘Elutions 1-3’), separated by SDS-PAGE and subjected to immunoblot analysis with FLAG-specific and HA-tag-specific antibodies. * indicates a cross-reacting protein recognized by the anti-FLAG antibody; # denotes the NEDDylator^{PRT6}; the arrowhead indicates HRE2-FLAG.

In summary, despite the fact that I could co-express an endogenous substrate of PRT6, an epitope tagged form of NEDD8 and the NEDDylator^{PRT6}, I could not detect neddylation of the HRE2-FLAG or HRE1-FLAG substrates. Because HRE1 and HRE2 remained overall difficult to detect in tobacco, I tested the activity of the NEDDylator^{PRT6} towards artificial N-end rule substrates that accumulated at higher levels in tobacco.

4.2.5 NEDDylation assays in tobacco using an artificial N-end rule reporter substrate

Experiments carried out in the lab previously made use of artificial N-end rule substrates encoding firefly luciferase (LUC) with different N-termini translationally fused to an N-terminal Ub (fusion noted Ub-X-LUC, where X denotes any amino ac-

id residue) (Graciet *et al.*, 2010; Worley *et al.*, 1998). As described in Section 1.2, this Ub fusion protein is co-translationally cleaved after the last residue of Ub, thus releasing a LUC reporter with a defined N-terminal residue X. The Ub fusion protein encoding an N-terminal Arg after co-translational deubiquitination is predicted to be a substrate of PRT6 and is likely to interact with its UBR domain. In fact, unpublished data obtained in the lab show that expression of the Ub-R-LUC fusion in a *prt6-5* mutant of *Arabidopsis* leads to its stabilization compared to the wild type (Alexandra Miricescu; unpublished), thus indicating that this Ub-R-LUC may be used to generate an artificial substrate of PRT6.

To ensure that Ub-R-LUC was detectable in tobacco transient expression experiments, I agroinfiltrated tobacco leaves with an *Agrobacterium* strain coding for the Ub-R-LUC reporter. In addition, to verify that the Ub-R-LUC fusion was being deubiquitinated as expected, I expressed another variant of the construct (Ub-T-LUC) that was available in the lab in *E. coli* cells and used these *E. coli* cell extracts to check for the deubiquitination of Ub-R-LUC *in planta*. Indeed, as *E. coli* does not possess deubiquitinase activity, the Ub-T-LUC would be expected to migrate at a higher molecular weight (~+8 kDa) than the expected R-LUC reporter obtained after deubiquitination of the Ub-R-LUC fusion. When Ub-R-LUC that had been expressed in tobacco was analyzed with Ub-T-LUC expressed in *E. coli* using SDS PAGE and immunoblotting with a LUC-specific antibody, Ub-R-LUC migrated at a lower molecular weight than Ub-T-LUC, indicating that it was deubiquitinated in tobacco leaves, likely exposing its N-terminal Arg (Fig 4.13B).

I next conducted immunoprecipitation experiments in order to determine if the commercial LUC antibodies that were available in the lab could be used to efficiently immunoprecipitate R-LUC. Unfortunately, while R-LUC was detectable in tobacco leaves (Fig 4.13B), immunoprecipitation of the artificial substrate using anti-LUC antibodies resulted high background, making it difficult to distinguish the R-LUC protein from other cross-reacting proteins (data not shown). To address this technical problem and to facilitate the immunoprecipitation of this reporter protein, I generated a Ub-R-LUC-FLAG construct (Fig 4.13A). The addition of the C-terminal FLAG to the artificial PRT6 substrate meant that this protein could be immunoprecipitated using anti-FLAG agarose beads and then eluted from the beads using the FLAG peptide, similarly to the protocol I had optimized for HRE2-

FLAG (Section 4.2.4.2). To ensure that I could detect the resulting R-LUC-FLAG construct in tobacco neddylation assays, I first transiently expressed it in tobacco leaves and analyzed it alongside the R-LUC reporter. The protein extracts from these tobacco leaves were separated using SDS PAGE and analyzed using immunoblotting with either anti-LUC or anti-FLAG antibodies. The results for these experiments are described in Fig. 4.13C.

Immunoblot with the anti-LUC antibody indicated a small shift in molecular weight when Ub-R-LUC-FLAG was expressed compared to Ub-R-LUC, suggesting that the fusion is deubiquitinated as expected (i.e. the shift would be consistent with the presence of a FLAG tag, but not with the absence of deubiquitination). Furthermore, immunoblot using a FLAG-specific antibody confirmed that the R-LUC-FLAG protein could be readily detected. I therefore carried out subsequent neddylation assays using this reporter substrate.

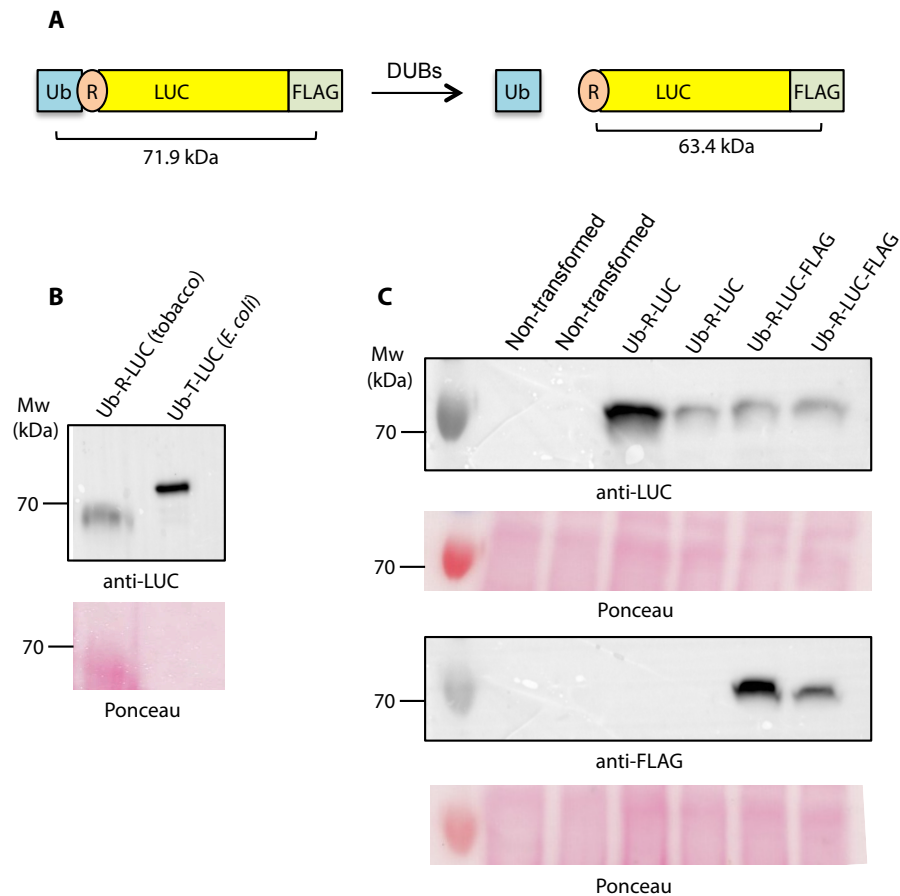


Fig 4.13 Detection of Ub-R-LUC and Ub-R-LUC-FLAG in tobacco leaves. (A) Design of an artificial PRT6 substrate for plant NEDDylator^{PRT6} assays. Ub is co-translationally cleaved, leaving N-terminal Arg. The R-LUC-FLAG protein can be immunoprecipitated using the C-terminal FLAG tag. (B) Ub-R-LUC expression in tobacco results in a lower molecular weight product than Ub-T-LUC expressed in *E. coli*, indicating that it is deubiquitinated as expected. Ub-R-LUC was transiently expressed in tobacco using *Agrobacterium*-mediated transformation and 3 days after agroinfiltration tissue was frozen and ground in liquid nitrogen. Ub-T-LUC was expressed in *E. coli* using the Ub-T-LUC construct under the control of an IPTG inducible promoter. 2X SDS loading dye was used to extract total protein from both samples followed by separation with SDS PAGE and analysis using immunoblotting with anti-LUC antibodies. (C) R-LUC and R-LUC-FLAG are both detectable after transient expression in tobacco using *Agrobacterium*-mediated transformation. Three days after agroinfiltration, leaf tissue was frozen and ground in liquid nitrogen. Proteins were extracted in 2X SDS loading buffer, followed by analysis using SDS PAGE and western blotting with either anti-LUC or anti-FLAG antibodies. Western blots described in B and C were conducted once.

To determine if the NEDDylator^{PRT6} could potentially neddylate the R-LUC-FLAG reporter, I co-expressed the NEDDylator^{PRT6} in tobacco with the Ub-R-LUC-FLAG fusion and 6His-3HA-NEDD8 using *Agrobacterium*-mediated transfection.

Following protein extraction in IP buffer (Appendix 1), I carried out an immunoprecipitation using anti-FLAG agarose beads to pull down the artificial substrate followed by elution of bound proteins with a FLAG peptide. These eluted proteins were then separated by SDS PAGE and analyzed by immunoblotting using (i) anti-LUC antibodies to determine if the immunoprecipitation of R-LUC-FLAG was successful; and (ii) anti-HA antibodies to check for 6His-3HA-NEDD8 conjugation to R-LUC-FLAG, which would indicate that the artificial substrate had been neddylation by the NEDDylator^{PRT6}. These results are described in Fig. 4.14.

Western blot analysis confirmed that R-LUC-FLAG, 6His-3HA-NEDD8 and the Myc-NEDDylator^{PRT6} proteins were expressed in tobacco plants (Fig 4.14 'Input'). The immunoprecipitation of R-LUC-FLAG appeared to be successful as a clear band corresponding to the size of this protein was detected using anti-LUC antibodies in the eluate from the anti-FLAG agarose beads (Fig 4.14 'anti-FLAG IP'). However, neither of the immunoprecipitated protein samples from tobacco leaves, with or without NEDDylator^{PRT6} expression, gave a strong signal when probed with anti-HA antibodies. After a long exposure, some signal could be detected in the presence of the NEDDylator^{PRT6}, but this is likely not due to 6His-3HA-NEDD8 conjugation as the protein migrates at the same molecular weight as R-LUC-FLAG and the 15-kDa (or larger) size shift that would be expected after neddylation is not observed. This signal is more likely background signal due to the abundance of the immunoprecipitated protein. Indeed, the total protein ponceau stain indicates that there is more protein present on the membrane in the samples containing the NEDDylator^{PRT6} (Fig 4.14 'anti-FLAG IP'). In this experiment, I also tested for co-immunoprecipitation of the NEDDylator^{PRT6} using anti-Myc antibodies on the eluted fractions. However, no signal corresponding to the NEDDylator^{PRT6} could be identified, suggesting that it may not bind efficiently to the R-LUC-FLAG substrate.

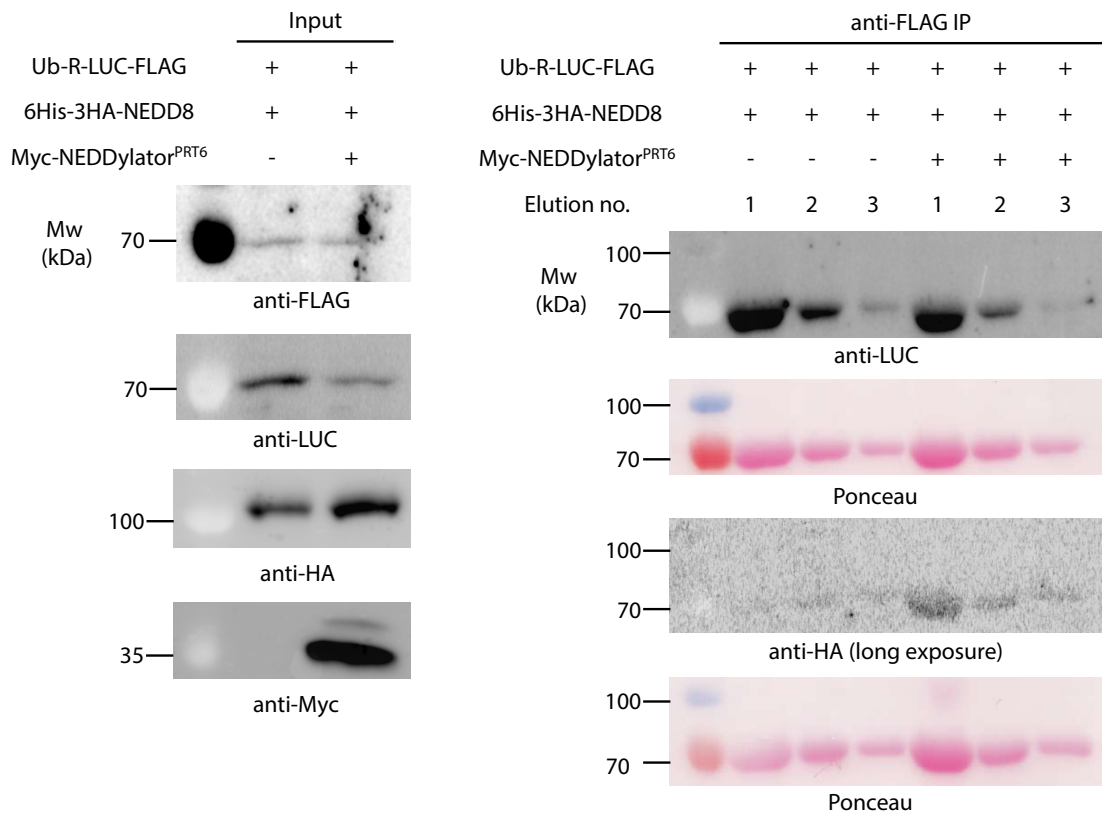


Fig 4.14. Neddylaton assay using artificial PRT6 substrate in tobacco. R-LUC-FLAG and 6His-3HA-NEDD8 were co-expressed in tobacco leaves with or without co-expression of Myc-NEDDylator^{PRT6} using *Agrobacterium*-mediated transformation. Three days after agroinfiltration, tissue was collected and ground in liquid nitrogen before proteins were solubilized in IP buffer (see Appendix 1). A fraction of this protein extract was saved and used for the 'Input' sample. Anti-FLAG agarose beads were added to the other fraction and incubated with rotation in order to carry out immunoprecipitation under non-denaturing conditions of the artificial substrate Ub-R-LUC-FLAG. To elute immunoprecipitated proteins beads were incubated with FLAG peptide with shaking for 10 mins at 4°C. Elution of beads was carried out three times sequentially (elution n°. indicated). Samples were separated using SDS PAGE and then analyzed using immunoblotting. Anti-LUC or anti-FLAG antibodies were used to check for the presence of R-LUC-FLAG, anti-Myc antibodies were used to test for the presence of Myc-NEDDylator^{PRT6} and anti-HA antibodies were used to check for the presence of 6His-3HA-NEDD8 conjugated proteins. This experiment was conducted once.

In sum, the experiments I have carried out to test the recognition and neddylation of endogenous PRT6 substrates (HRE1-FLAG and HRE2-FLAG) and of artificial substrates such as R-LUC-FLAG indicate that the NEDDylator^{PRT6} containing the UBR domain of PRT6 alone is not sufficient to either bind efficiently and/or neddylate known PRT6 substrates.

4.2.6 Additional strategies to design and test different versions of a NEDDylator^{PRT6}

The initial version of the NEDDylator^{PRT6} tested so far relied on the fact that the UBR domain of mammalian UBR1, which the ortholog of plant PRT6, had been shown to be sufficient to bind efficiently N-end rule substrates *in vitro*. However, both mammalian UBR1 and plant PRT6 are large proteins. Hence, it was possible that other domains of PRT6 could be important to (i) increase the affinity of the UBR domain for its substrates; and/or (ii) allow for the neddylation of the substrate once it was bound to the UBR domain. As the UBR domain of PRT6 and its RING domain are separated by 990 amino acid residues. We hypothesized that the sequence between the UBR and the RING domains of PRT6 may be essential for the correct folding of the substrate recognition domain and/or to allow contact between the PRT6-bound substrate and the E2 conjugating enzyme (see also Discussion in Section 4.3.1). In order to address these two possibilities, I designed a novel strategy to test different versions of the NEDDylator^{PRT6}, which differed by the length of the linker region between the UBR domain and RCE1. The resulting NEDDylators would then be tested *in planta* for their ability to neddylate known PRT6 substrates, but also *in vitro* for their ability to bind efficiently purified N-end rule substrates. The latter could be done using NEDDylator expression in *E. coli*, followed by purification and pulldown assays or more quantitative protein-protein interactions assays.

4.2.6.1. Designing longer versions of NEDDylator^{PRT6}

I first aimed at cloning different versions of the NEDDylator in *E. coli* (Fig. 4.15). These different NEDDylators encompassed increasing PRT6 sequences located between the UBR and RING domains. The last NEDDylator depicted in Fig.4.15 corresponded to the full-length sequence of PRT6, from the initial methionine residue to the last residue located just upstream of the RING domain, so that most domains of the protein were present, with the exception of the RING domain and the downstream C-terminal sequences. In addition, I aimed at expressing these different NEDDylators as fusion proteins with the Myc epitope tag and a poly-histidine (6xHis) tag in order to facilitate purification of the recombinant proteins, as well as their detection using immunoblot analyses.

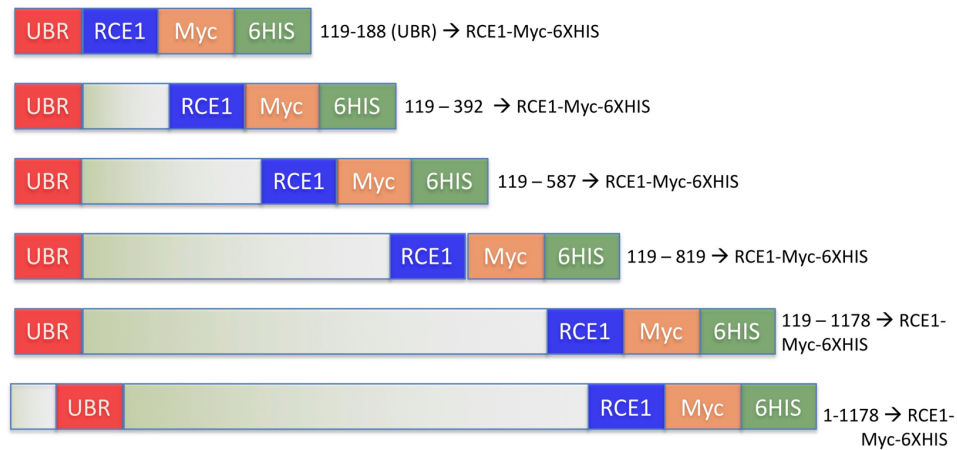


Fig. 4.15. Schematic representation of the different versions of the NEDDylator. The first NEDDylator depicted encompasses residues 119 to 188 of PRT6, which corresponds to the UBR domain alone, and therefore is similar to the NEDDylator^{PRT6} tested in tobacco, except for the presence of a poly-histidine tag (6xHis). The next 3 NEDDylators represented have longer fragments encompassing the intermediate region of PRT6 located between the UBR and RING domains. Finally, the NEDDylator presented at the bottom also contains the N-terminal region of PRT6 up to the RING domain.

Unfortunately, despite repeated attempts at cloning these constructs, they were unstable in *E. coli*, so that the plasmids could not be successfully generated (data not shown).

4.2.6.2. Generation of a NEDDylator^{PRT6} in yeast

Considering the problems encountered in *E. coli*, I aimed at generating the different versions of the NEDDylator^{PRT6} described in Fig. 4.15 in *S. cerevisiae* cells. Previous experience in the lab had indicated that *PRT6*-coding constructs were stable in yeast, so that they could be generated using homologous recombination. In addition, the expression of NEDDylator^{PRT6} constructs in yeast could facilitate three different approaches for studying the fusion protein's function:

- (i) NEDDylator constructs could be expressed and purified from yeast cells using the 6xHis tag and then used for *in vitro* neddylation assays, as well as to test binding of the NEDDylators to purified PRT6 substrates *in vitro*.
- (ii) the most promising NEDDylator could be expressed in yeast, purified and incubated with protein extracts from Arabidopsis plants expressing a tagged

NEDD8 fusion protein. This would allow to establish an in vitro neddylation assay to affinity purify neddylated substrates

(iii) if the Arabidopsis RCE1 NEDD8 E2 conjugating domain is also active in yeast, then NEDDylator^{PRT6} constructs could be co-expressed in yeast with tagged-NEDD8 and a PRT6 reporter substrate. Carrying out the neddylation assays entirely in yeast would facilitate the rapid characterization and screening of the NEDDylators in order to select the most efficient construct.

In order to generate different NEDDylator^{PRT6} constructs in yeast, I first constructed a yeast expression vector in *E. coli* containing the Arabidopsis NEDD8 E2 conjugating enzyme RCE1 translationally fused to a C-terminal Myc tag and 6xHis tag separated by linker regions under the control of the yeast constitutive alcohol dehydrogenase 1 promoter (ADH1). This plasmid could then be digested into a linear form and PCR-amplified *PRT6* cDNA fragments containing homologous regions flanking the desired insertion site could be inserted using homologous recombination in yeast. This method should result in the generation of different NEDDylator^{PRT6} made up of a *PRT6* cDNA sequence of varying length with C-terminal RCE1-Myc-6His (Fig 4.16).

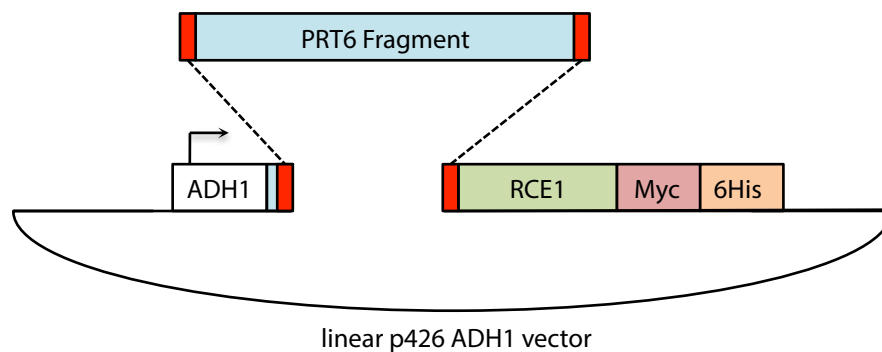


Fig 4.16. Design and cloning strategy for NEDDylator^{PRT6} in yeast cells. RCE1-Myc-6His was cloned into the yeast expression vector p426 ADH1 under the control of the ADH1 promoter. Following linearization of this vector using restriction enzymes, PCR fragments bearing homologous sequences to the linear vector could be inserted by homologous recombination upon co-transformation of the PCR fragment and the linear vector into yeast cells. Red rectangles indicate the 30 bp homologous regions between vector and PCR product.

In order to check if the ADH1 promoter was sufficient for expression of RCE1-Myc-6His at high levels in yeast cells, I transformed the protease deficient

yeast strain Sc295 (Hovland *et al.*, 1989; Sikorski and Hieter, 1989; Joshua-Tor *et al.*, 1995) with the p426 ADH1_p:RCE1-Myc-6His construct. After overnight growth in selective medium, proteins were extracted in 2x SDS loading buffer and separated using SDS-PAGE, followed by immunoblotting with anti-Myc antibodies (Fig 4.17A). The results of this experiment indicated that the RCE1-Myc-6His protein accumulated to detectable levels and that the ADH1 promoter was suitable for the expression of the different versions of the NEDDylator^{PRT6}.

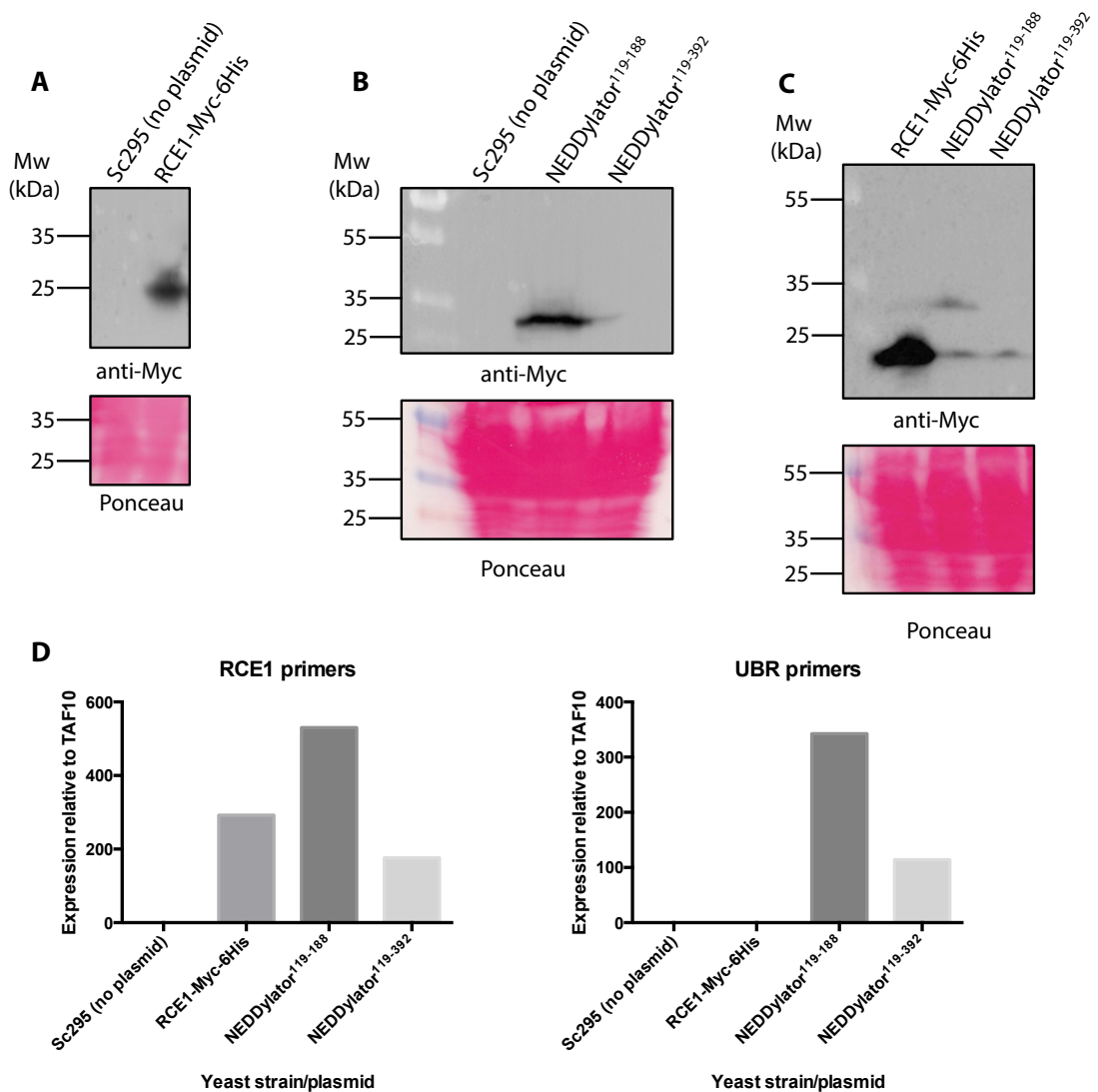


Fig 4.17. Detection of RCE1-Myc-6His and NEDDylator constructs in yeast cells. (A-C) Plasmids encoding RCE1-Myc-6His (23.2 kDa), NEDDylator¹¹⁹⁻¹⁸⁸ (31.4 kDa) or NEDDylator¹¹⁹⁻³⁹² (53.9 kDa) under the control of the ADH1 promoter were transformed in to yeast Sc295 cells. Cells were grown overnight in selective media. Cells were pelleted by centrifugation and total protein was extracted using 2x SDS loading dye (Appendix 1). Proteins were separated using SDS PAGE and analyzed using western blotting with anti-Myc antibodies. (D) qPCR analysis of the expression of plasmid constructs in transformed Sc295 cells. Cells containing plasmids described above were grown

overnight in selective media. The following day cells were pelleted with centrifugation. Total RNA was extracted and cDNA was prepared using oligo(dT18) primers. qPCR was carried out using primer pairs specific to either the RCE1 sequence or the UBR sequence. Western blots and qPCR experiments were conducted once.

Next, I cloned two PRT6 fragments into this vector using homologous recombination in yeast. The first insert contained only the PRT6 UBR domain (Gly119 – Lys188) and the second fragment contained a slightly longer section of PRT6 (Gly119 – Thr392). The two resulting NEDDylators are noted NEDDylator¹¹⁹⁻¹⁸⁸ and NEDDylator¹¹⁹⁻³⁹², respectively. Please note that NEDDylator¹¹⁹⁻¹⁸⁸ is identical to the NEDDylator^{PRT6} characterized in tobacco, except for the presence of a poly-histidine tag at the C-terminus of the Myc tag. These two NEDDylator constructs were then transformed into yeast Sc295 cells. The resulting cells were grown overnight in selective medium, before the total protein was extracted and analyzed using immunoblotting with anti-Myc antibodies (Fig 4.17B). While the NEDDylator¹¹⁹⁻¹⁸⁸ accumulated to detectable levels, the NEDDylator¹¹⁹⁻³⁹² was not detected (Fig 4.17B). In order to compare the protein levels of RCE1-Myc-6His, NEDDylator¹¹⁹⁻¹⁸⁸ and NEDDylator¹¹⁹⁻³⁹² and examine if there was a transcriptional difference, I grew Sc295 cells containing the respective vectors overnight in selective medium. The cultures were then split in two, so that one fraction was used for total protein extraction (Fig. 4.17C), while the other fraction was used for total RNA preparation followed by reverse transcription coupled to quantitative PCR (RT-qPCR) (Fig. 4.17D).

Expression of RCE1-Myc-6His and of NEDDylator¹¹⁹⁻¹⁸⁸ resulted in the accumulation of detectable proteins in Sc295 cells (Fig 4.17 A-C). The NEDDylator¹¹⁹⁻³⁹², however, was not detected by the Myc-specific antibodies (Fig 4.17 B and C). RT-qPCR analysis using primers for the RCE1 or for the UBR domain sequence of PRT6 indicated that all of the constructs were expressed in Sc295 cells (Fig 4.17 D). Although the NEDDylator¹¹⁹⁻¹⁸⁸ appeared to be transcribed at higher levels than RCE1-Myc-His6 in Sc295, the NEDDylator¹¹⁹⁻¹⁸⁸ protein accumulated to lower levels (Fig 4.17 C). This could suggest that the PRT6 sequences included in the NEDDylator might reduce the stability of the fusion protein. The NEDDylator¹¹⁹⁻³⁹² transcript levels were lower than either of the other 2 constructs (Fig 4.17 D) and the protein also accumulated to lower levels. Although the RT-qPCR experiments

were only conducted once and more replicates are needed to draw any significant conclusions, it appears that addition of the two PRT6 sequences to RCE1 might affect the stability of the resulting NEDDylators in yeast.

Before considering cloning longer versions of the NEDDylator, I decided to test if self-neddylation of NEDDylator¹¹⁹⁻¹⁸⁸ could be observed in yeast. The idea is that an *in vivo* yeast system could then be used to characterize and screen the different NEDDylators before performing large-scale expression and purification to obtain sufficient protein for neddylation assays in plant extracts. To test self-neddylation of the NEDDylator¹¹⁹⁻¹⁸⁸, I co-expressed the NEDDylator¹¹⁹⁻¹⁸⁸ with a 9xMyc-tagged NEDD8 (under the control of the constitutive TEF1 promoter) received from the lab of Dr. Gwenaël Rabut (Rabut *et al.*, 2011) in *ubr1Δ* yeast cells. After co-expression, the NEDDylator¹¹⁹⁻¹⁸⁸ was affinity-purified using a nickel column that binds to the 6His tag of the NEDDylator. This protein was then eluted using imidazole, and elution fractions were checked for the presence of both the NEDDylator¹¹⁹⁻¹⁸⁸ and any 9xMyc-NEDD8 conjugation using immunoblotting with anti-Myc antibodies (Fig. 4.18).

These immunoblots indicated that the NEDDylator¹¹⁹⁻¹⁸⁸ was expressed in yeast, and that the 9xMyc-NEDD8 was also likely expressed in the *ubr1Δ* yeast cells as a long-range molecular weight pattern was observed which might be caused by neddylation patterns (Fig 4.18 'Input'). The affinity purification of the NEDDylator¹¹⁹⁻¹⁸⁸ constructs was successful (Fig 4.18 'nickel column eluate'), but no size shift that could be attributed to neddylation of the NEDDylator¹¹⁹⁻¹⁸⁸ was observed when it was co-expressed with 9xMyc-NEDD8 (Fig 4.18 'nickel column eluate'). The results of this preliminary experiment therefore suggest that the Arabidopsis RCE1 NEDD8 E2 conjugating enzyme incorporated into the NEDDylator does not self-neddylate in yeast. Unfortunately, due to time constraints, I was not able to repeat this experiment and determine more clearly if the NEDDylator tool could be studied *in vivo* in yeast.

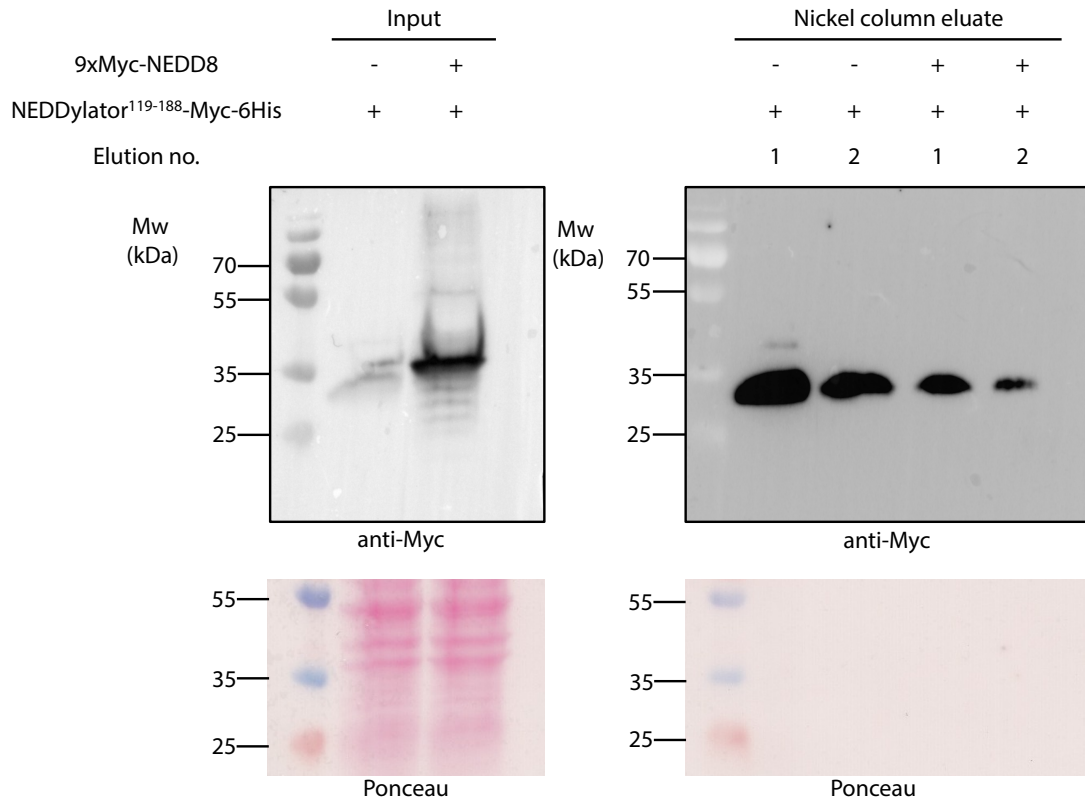


Fig 4.18. Self-neddylation assay in yeast cells. 9xMyc-NEDD8 (~24 kDa) expressed in *ubr1Δ* cells with or without co-expression of NEDDylator¹¹⁹⁻¹⁸⁸-Myc-6His (~31 kDa). Cells were grown in selective medium overnight. The morning after cells were pelleted using centrifugation and lysed using glass beads and 10% (v/v) trichloroacetic acid. A fraction of the solubilized proteins was used for the 'Input' sample. The remaining protein extract was incubated with His-Select nickel affinity column for 2 hrs. Bound proteins were eluted using 500 mM imidazole. Proteins from the Input or nickel column eluate were separated using SDS PAGE and analyzed by immunoblotting with anti-Myc antibodies. This experiment was conducted once.

4.2.7 Generation of an Arabidopsis N-end rule mutant line expressing tagged NEDD8

The initial idea behind the development of a NEDDylator^{PRT6} is that the construct could be used to generate stable transformants of a *prt6* mutant expressing an inducible epitope-tagged NEDD8. The use of a *prt6* mutant background was essential to ensure accumulation of the PRT6 substrates. An inducible version of NEDD8 was also important so that its expression could be induced, thus reducing any side effects of NEDD8 overexpression in plants (reviewed in; Enchev *et al.*, 2015). The epitope tags on NEDD8 were required to immunoprecipitate or affinity purify

PRT6 substrates that were neddylylated by the NEDDylator^{PRT6}. Considering the problems encountered in generating the longer NEDDylator^{PRT6}, an alternative considered was to add purified NEDDylator^{PRT6} to protein extracts from Arabidopsis plants expressing an epitope-tagged NEDD8. Hence, irrespective of the strategy used, a pre-requisite for this project was to generate *prt6* mutant plants that stably expressed epitope tagged NEDD8. To this aim, Dr. Emmanuelle Graciet crossed the N-end rule mutant *prt6-5* with a previously published Arabidopsis line (kindly shared by Prof. Claus Schwechheimer) that expresses HA-STREPII-tagged NEDD8 (HSN) under the control of a DEX inducible promoter (Hakenjos *et al.*, 2011). I isolated F4 lines that were homozygous for the *prt6-5* and HSN T-DNA insertions (see Section 2.2.3.8). I then grew seedlings of the F4 generation in liquid culture. When these lines were tested for the presence of HSN in immunoblot experiments, the presence of HSN or of neddylylated cullins could not be detected using an anti-HA antibody (data not shown). One possibility to explain the lack of HSN in these lines is that (i) the treatment conditions with the DEX-containing solution would need to be optimized; or (ii) the transgene expressing the DEX-inducible transcription factor was silenced in the *prt6-5* HSN plants I isolated. To test these two possibilities, I repeated the experiment in the same conditions as above, but instead of extracting proteins, I used the tissue to purify total RNA, followed by RT-qPCR reactions to determine the expression of HSN. The expression of endogenous NEDD8 in mock compared to DEX-treated HSN lines was compared in the parental line, as well as in *prt6-5* HSN lines of the F2 and F4 generations (Fig 4.19).

The preliminary results I obtained suggest that while the HSN construct is expressed at high levels following treatment of the parental line with a DEX-containing solution (line noted Col-0 HSN), expression of the transgene was reduced after crossing with the *prt6-5* mutant allele. Reduced expression, presumably due to silencing of the transgene, was exacerbated in the F4 population compared to plants of the F2 generation. Although additional replicates are needed to draw conclusion, this preliminary RT-qPCR experiment strongly suggests that in the *prt6-5* mutant background the *HSN* transgene may be silenced (Fig 4.19), so that alternative methods are likely to be needed to generate *prt6* mutant lines that could be combined with a functional NEDDylator^{PRT6} (see Section 4.3.1 below for additional details).

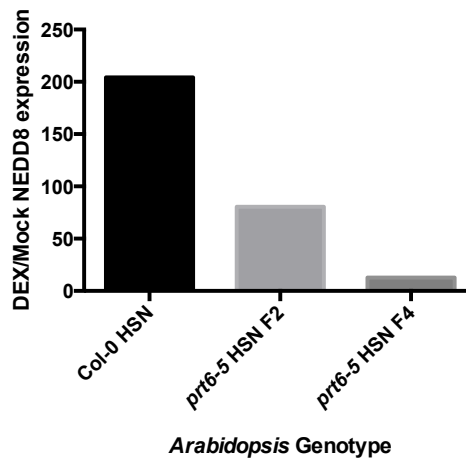


Fig 4.19. Expression of NEDD8 in HSN Arabidopsis lines. Arabidopsis seedlings with indicated genotypes were grown for 7 days in liquid MS medium with shaking. To induce expression of the HSN transgene, a solution containing 100 μ M DEX was added to the growth medium together with vacuum infiltration. After 10 hrs of induction, seedlings were dried and ground in liquid nitrogen. Total RNA was extracted and cDNA was generated using Oligo(dt18) primers. qPCR was carried out using primers specific for endogenous NEDD8 and the reference gene REF1 (see Table 2.3 and Section 2.2.3.7). Relative expression values of DEX/Mock treated samples was calculated and plotted above. This experiment was conducted once.

4.3 Discussion

4.3.1 Developing a functional NEDDylator^{PRT6} in plants

In the experiments described above, I generated a NEDDylator^{PRT6} containing the PRT6 substrate-binding UBR domain translationally fused to the Arabidopsis NEDD8 E2 conjugation enzyme RCE1. Preliminary results indicate that this NEDDylator^{PRT6} can accumulate to detectable levels and self-neddylate in tobacco plants (Section 4.2.2). These results were very promising and indicated that it may be possible to generate a functional NEDDylator *in planta*. However, the co-expression of this NEDDylator^{PRT6} with tagged-NEDD8 and known substrates of PRT6 (i.e. HRE1/2 and R-LUC-FLAG) did not result in the detectable conjugation of NEDD8 to these substrates (Section 4.2.5). Additional attempts at testing if the

NEDDylator^{PRT6} protein co-immunoprecipitated with the R-LUC-FLAG substrates also suggested that this was not the case.

The XIAP Ub ligase that was used in a previous study to generate a NEDDylator^{XIAP} (see Section 4.1.3) is a relatively small protein compared to PRT6. In addition, its RING domain is relatively close to the substrate-binding domain of the E3 ligase compared to PRT6 (Fig 4.20).

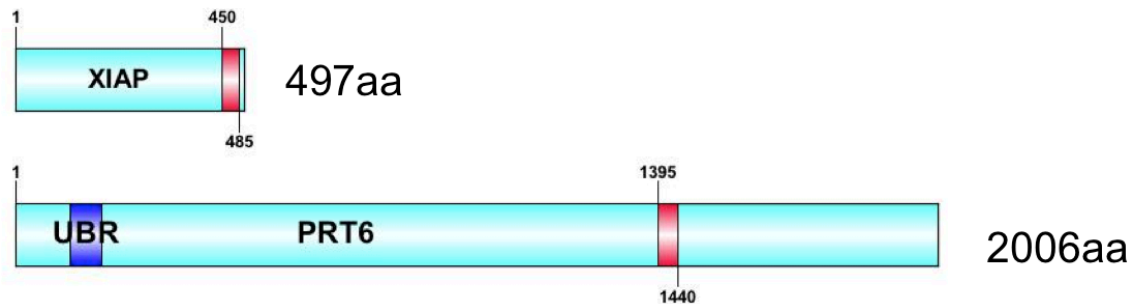


Fig 4.20. Comparison of the E3 Ub ligases human XIAP and Arabidopsis PRT6. Human *XIAP* encodes an E3 Ub ligase of 497 amino acids ('aa') in length, while Arabidopsis *PRT6* encodes a 2006-amino acid long protein. RING domains are indicated in red.

Notably, it has been previously shown that a conserved C-terminal region of yeast UBR1 interacts with the N-terminal region of the protein, where the UBR domain is located (Du *et al.*, 2002). Considering the strong sequence similarities between yeast UBR1 and PRT6, one could hypothesize that, in PRT6, the C-terminal half of the protein, which encompasses the RING domain, also folds back on the UBR domain, which is located towards the N-terminus of the protein, and thus facilitates the transfer of Ub to the substrate by bringing the E2 enzyme closer to the substrate. In this case, efficient neddylation of a substrate would require more of the PRT6 sequence that lies downstream of the UBR domain in order to engage a transfer of NEDD8 to the substrate. Another, not mutually exclusive possibility, is that the UBR domain of PRT6 is not sufficient to bind N-end rule substrates with high affinity. This would be in contrast with the fact that the UBR domain of mammalian UBR1, which shows strong sequence similarities with that of PRT6, has repeatedly been shown to be necessary and sufficient to bind substrates starting with positively charged N-terminal residues such as Arg.

In order to address the possible requirement for the intermediate region between the UBR and the RING domains, I attempted to clone different versions of the NEDDylator (Fig. 4.15), that encompassed different sections of this intermediate region. Unfortunately, the constructs could not be generated due to instability of the resulting plasmids in *E. coli*, even when strains with reduced recombination activity were used. Based on these attempts, as well as previous experience with *PRT6*-encoding plasmids in the lab (and in other groups working with *PRT6* sequences), it was very likely that the new NEDDylator constructs I tried to generate would not be stable in *Agrobacterium* cells either, and hence could not be transferred into plants. These difficulties prevented me from any further testing of different versions of the NEDDylator *in planta* using transient expression assays. They also limited the approaches that could be taken to generate and study other versions of the NEDDylator, since *E. coli* could not be used (i) to clone the constructs; or (ii) to express them for purification and use in *in vitro* neddylation assays using plant extracts.

Another problem encountered for the development of a functional NEDDylator tool to identify *PRT6* substrates was the generation *prt6* mutant plants that expressed an epitope-tagged form of NEDD8. Indeed, preliminary experiments conducted with *prt6-5* HSN plants suggest that the inducible expression of HSN may be compromised by silencing problems, perhaps due to the presence of several transgenes under the control of the 35S promoter.

Strategies and future work aimed at overcoming these problems are discussed in Section 4.3.3.

4.3.2 Using a yeast-based system to develop a functional NEDDylator^{PRT6}

Considering the limitations described above, I attempted to develop a novel approach to generate and characterize different NEDDylator^{PRT6} constructs that could be (i) purified from yeast cells and characterized for their ability to bind *PRT6* substrates *in vitro*; (ii) added to plant protein extracts for *in vitro* neddylation assays; or (iii) used to carry out neddylation assays directly in yeast cells. These approaches would have facilitated the full characterization of the different

versions of the NEDDylator in order to select the most efficient one for substrate identification.

Using homologous recombination in yeast, I was able to clone two versions of the NEDDylator, one of which was similar to the NEDDylator^{PRT6} characterized in tobacco (NEDDylator¹¹⁹⁻¹⁸⁸). However, preliminary experiments I performed suggest that the larger NEDDylator may not be very stable in yeast cells (Section 4.2.6.2). Instead of optimizing this further, I tested if the NEDDylator¹¹⁹⁻¹⁸⁸ could self-neddylate *in vivo* in yeast. This was a pre-requisite to screen the different NEDDylator constructs in yeast and it was hoped that this would also allow to test if the Arabidopsis NEDD8 E2 RCE1 is active in yeast. Due to time constraints, only one experiment could be performed. The preliminary data obtained suggest that the NEDDylator¹¹⁹⁻¹⁸⁸ may not be able to self-neddylate in yeast. This is in contrast with the self-neddylation observed in tobacco transient expression assays using a construct that was nearly identical. Although additional experiments are necessary to confirm the absence of self-neddylation, one could hypothesize that Arabidopsis RCE1 may not be active in yeast, or that the C-terminal tags are inhibiting RCE1 function in yeast. Although RCE1 is homologous to the yeast Ubc12 and contains the conserved UBC NEDD8 conjugation domain and the active cysteine in this site (del Pozo and Estelle, 1999), it is not clear if RCE1 can interact with yeast NEDD8 E1 enzymes. Before additional neddylation assays are tested in yeast experiments, the activity of RCE1 in yeast would first need to be thoroughly tested (see next section).

4.3.3 Future Work

4.3.3.1 Identification of necessary PRT6 domains for neddylation

Although PRT6 contains the highly conserved substrate-binding UBR domain, the binding of PRT6 to substrates has not been biochemically dissected. Similarly, it is unknown if other domains of the protein have functions that would be important either for a more efficient binding of substrates, or to allow for efficient ubiquitination once the RING domain interacts with an E2 enzyme. Experiments investigating

the PRT6 fragments necessary for substrate binding and for substrate ubiquitination (besides the role of the RING domain) would greatly facilitate the design and optimization of a NEDDylator^{PRT6}.

In order to identify the minimum PRT6 domain that is required for the efficient binding of N-end rule substrates, I propose to conduct experiments in yeast, whereby different fragments of PRT6 fused to a poly-histidine tag would be expressed in the presence of a known Ub-R-βgal substrate of PRT6. I would then test for their interaction using co-immunoprecipitation. In parallel, it would be interesting to express these poly-histidine-tagged PRT6 fragments in yeast, followed by their purification. I could then test their interaction with peptides bearing Arg at their N-terminus. Such peptides, identical to those used in Tasaki *et al.* (Tasaki *et al.*, 2005) are available in the lab and can be efficiently coupled to agarose beads (E. Graciet; unpublished) to test for interaction with different fragments of PRT6.

In addition, the N-terminal domain of yeast UBR1 has been shown to bind a conserved C-terminal domain in yeast (Du *et al.*, 2002). This was shown by expressing tagged N-terminal and C-terminal UBR1 fragments in yeast and carrying out co-immunoprecipitation assays followed by immunoblotting (Du *et al.*, 2002). In order to investigate if the PRT6 N-terminal domain interacts with the C-terminal PRT6 sequence, I aim to carry out a similar experiment by expressing a tagged N-terminal domain of PRT6 with a tagged C-terminal domain and carrying out co-immunoprecipitation assays to determine if they interact. These experiments would provide novel information on the conformation of PRT6 and on the mechanisms that lead to ubiquitination, while also providing sufficient evidence for the need to include longer PRT6 fragments for the design of a functional NEDDylator^{PRT6}.

Another problem that would need to be overcome is the generation of a *prt6* mutant line expressing an inducible epitope-tagged version of NEDD8. The problems encountered are likely linked to the number of 35S promoters present in the line isolated. Approaches taken to reduce silencing problems include the isolation of novel *prt6* mutant alleles generated using the CRISPR/Cas9 system (collaboration with the group of Prof. Frank Wellmer). These novel alleles could then be used in conjunction with the current HSN transgene.

4.3.3.2 Considerations for novel approaches to design a functional PRT6-specific NEDDylator

One potential new approach that could overcome cloning problems in *E. coli* would be to add artificial linker sequences of different lengths between the UBR domain and RCE1 in the NEDDylator^{PRT6}. These artificial sequences could be specifically designed to allow for flexibility between the UBR domain and RCE1, while minimizing problems with the stability of the constructs in *E. coli* and in *Agrobacterium*. Finally, the artificial sequences could also be designed so that they do not affect the protein stability of the new NEDDylator^{PRT6} *in planta*.

Finally, another approach that could be tested would involve using the UBR domain of mammalian UBR1 fused to RCE1. Indeed, this particular UBR has been repeatedly shown to be sufficient for the binding of N-end rule substrates and allows for the recognition of positively charged N-terminal destabilizing residues, similarly to PRT6

4.3.3.3 Future experiments to develop a yeast-based assay to test PRT6-specific NEDDylators

As mentioned above, in order to carry out NEDDylator^{PRT6} assays in yeast using the current construct design, it would have to be determined if Arabidopsis RCE1 is active in yeast. To this aim, I will transform wild type and *ubc12Δ* mutant yeast strains with tagged NEDD8 and RCE1-Myc-6His. Cullin neddylation status will be determined using western blotting with antibodies against the tagged-NEDD8, as cullin neddylation can be observed in total protein extracts (Liakopoulos *et al.*, 1999). If RCE1-Myc-6His cannot rescue the *ubc12Δ* mutant the NEDDylator^{PRT6}, an alternative strategy that could be used would involve the replacement of RCE1 by yeast UBC12 in the longer NEDDylator versions that would be characterized in yeast.

Chapter 5. Characterization of Arabidopsis PRT6 in yeast

5.1 Introduction

The Arabidopsis N-recognin PRT6 is homologous to the yeast N-recognin UBR1 (see Section 1.2.4.2). Previous experiments carried out in the lab indicated that expression of Arabidopsis PRT6 in yeast cells resulted in a functional N-recognin that could rescue a *ubr1* Δ mutant yeast for the degradation of reporter substrates with basic (or type I) N-terminal residues (Francesca Mesiti, unpublished results; Fig. 5.1).

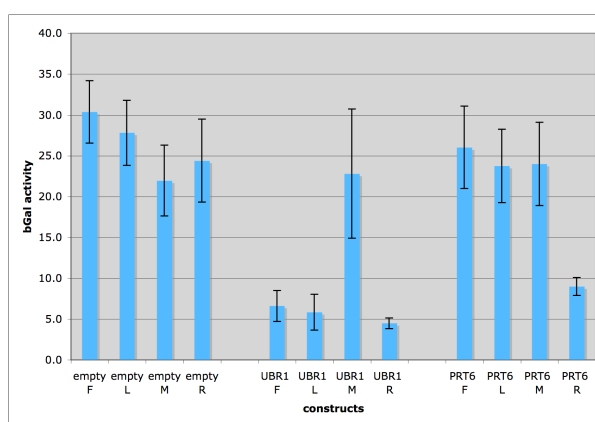


Fig. 5.1. Expression of Arabidopsis PRT6 is sufficient to rescue a yeast *ubr1* Δ mutant for the degradation of substrates with basic N-terminal residues. Enzymatic activities of β -gal in a *ubr1* Δ mutant of *S. cerevisiae* transformed with plasmids expressing Ub-X- β -gal test proteins (X being Phe, Leu, Met or Arg) together with a plasmid encoding yeast UBR1, or Arabidopsis PRT6, or an empty plasmid. Results shown are the average of four independent measurements and error bars refer to standard errors. Amino acid residues are represented by single letter abbreviations. Figure from Francesca Mesiti's MSc thesis (Trinity College Dublin).

Expression of mutant PRT6 in yeast cells can therefore be used to biochemically dissect domains or residues important for PRT6 function by analyzing the effect of the mutations on the ability of PRT6 to rescue a yeast *ubr1* Δ mutant strain. In this chapter, I will discuss biochemical properties of UBR1, describe preliminary bioinformatic analysis of the WTH domain of PRT6 (see Section 1.2.4.2), as well as experiments carried out to characterize the function of this domain in *S. cerevisiae*.

5.1.1 CUP9 is recognized by yeast UBR1 through an internal degradation signal

As mentioned in Section 1.2.1, the *S. cerevisiae* N-recognin UBR1 has been shown to recognize substrates through internal degrons. One well-characterized substrate that is recognized by UBR1 in this manner is the TF CUP9. CUP9 acts as a transcriptional repressor of the transmembrane peptide transporter gene *PEPTIDE TRANSPORT2* (*PTR2*) (Byrd *et al.*, 1998; Turner *et al.*, 2000). The CUP9 binding site in UBR1 is regulated by a C-terminal autoinhibitory domain that binds to the N-terminus of UBR1 and blocks CUP9 recognition. This is mediated by the interaction between the N-terminal half of UBR1 with a C-terminal UBR/Leu/Cys (UBL) domain (UBL) domain (Du *et al.*, 2002). When pairs of di or tri-peptides are introduced to yeast cells, they can bind to the N-terminal type-I or type-II UBR1 binding pockets, probably resulting in a conformational rearrangement of the autoinhibitory domain and ‘activation’ of the CUP9 binding site (Fig 5.2). This allows for UBR1 recognition of a C-terminal proximal domain of CUP9 and its degradation (Du *et al.*, 2002). The removal of CUP9 results in the transcriptional activation of *PTR2* and the accelerated uptake of extracellular peptides (Byrd *et al.*, 1998; Turner *et al.*, 2000; Du *et al.*, 2002).

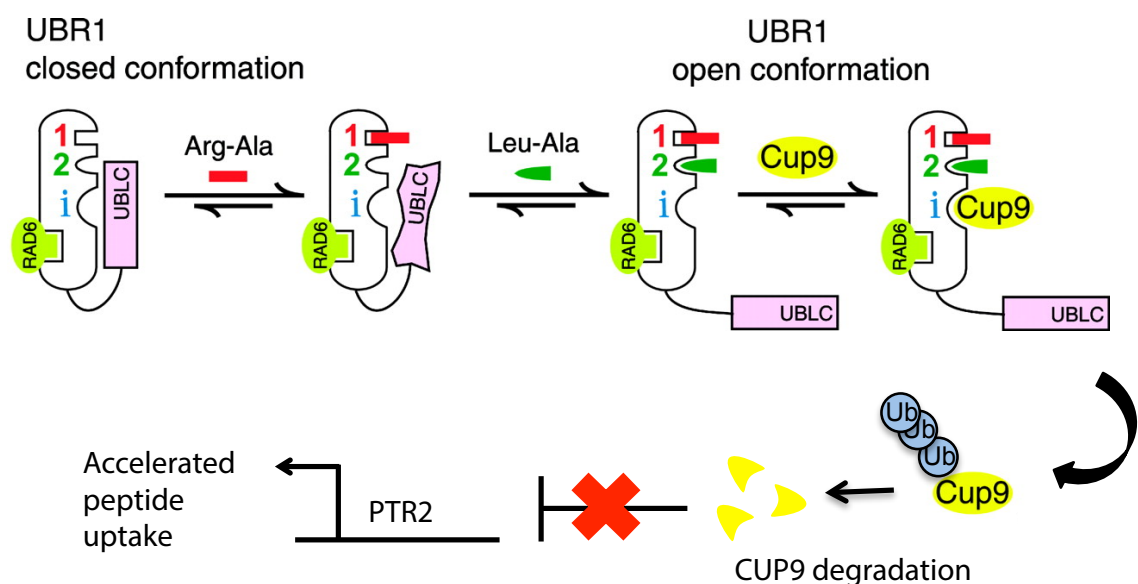


Fig 5.2. *S. cerevisiae* UBR1 recognition of CUP9 is regulated by an autoinhibitory domain. The C-terminal UBL domain of UBR1 interacts with the N-terminal half of yeast UBR1, resulting in the autoinhibition of the CUP9 binding site (denoted i). The binding of dipeptides Arg-Ala or Leu-Ala to

type-I or type-II UBR1 binding pockets, respectively, results in the allosteric ‘activation’ of the CUP9 binding site by disrupting UBLC interaction with the N-terminal half of UBR1. CUP9 interaction with UBR1 results in its polyubiquitination and degradation. This allows for the activation of *PTR2* transcription and an acceleration in peptide uptake. The E2 Ub-conjugating enzyme RAD6 interacts constitutively with UBR1 in these conditions. Image adapted from (Du *et al.*, 2002).

Like yeast UBR1, Arabidopsis PRT6 appears to recognize basic N-terminal destabilizing residues (also known as type I destabilizing residues) through the UBR domain. It is not clear, though, if PRT6 shares other binding specificities with UBR1, such as being able to recognize substrates through an internal degron like that of CUP9. In wild-type yeast cells, the addition of the dipeptide Arg-Ala is sufficient to induce UBR1-mediated CUP9 degradation and activation of *PTR2* expression. This *PTR2* activation does not occur in *ubr1Δ* mutant cells (Byrd *et al.*, 1998; Turner *et al.*, 2000). I sought to determine if PRT6 could also target proteins through an internal degron, by using CUP9 as a model substrate. To this aim, *ubr1Δ* cells could be transformed with a plasmid coding for PRT6. If treatment of *ubr1Δ* cells expressing PRT6 with the Arg-Ala dipeptide resulted in the activation of *PTR2* expression, this would indicate that PRT6 also encompasses the domain that is responsible for the recognition of CUP9, and possibly other proteins with internal degrons.

5.1.2 PRT6 contains a conserved wHTH domain of unknown function

As discussed in Section 1.2.4.2, Arabidopsis PRT6 encodes a substrate-binding UBR domain and an uncharacterized wHTH domain followed by the RING E2 Ub-conjugating enzyme interaction domain (Fig 1.6). The wHTH domain is a subtype of the helix-turn-helix family (Fig 5.3A) that classically comprises two small beta-sheets or ‘wings’ (W1 and W2), three alpha helix motifs (H1, H2, H3) and three beta-sheets (S1, S2, S3). These secondary structures are arranged in the order H1-S1-H2-H3-S2-W1-S3-W2 (reviewed in Gajiwala and Burley, 2000; Teichmann *et al.*, 2012). wHTH domains that lack the W2 motif or contain additional structural elements have also been described (reviewed in Harami *et al.*, 2013). This type of protein fold appears to have diverse functions and has been characterized in enzymes that make up the prokaryotic and eukaryotic transcription machinery such as RNA

polymerase II and III subunits and DNA-binding TFs (Teichmann *et al.*, 2012), as well as mediating RNA-binding and protein-protein interactions (Schuetz *et al.*, 2014; Harami *et al.*, 2013). One example of a well-characterized protein that contains a wHTH domain is the bifunctional transcriptional repressor/biotin-protein ligase BirA encoded by *E. coli*. Mutation of residues in the wing of the wHTH domain of BirA abolishes DNA binding of the repressor and results in lowered ligase activity (Chakravartty and Cronan, 2013). A search for structural homologues of the PRT6 wHTH using a database of known structures (Phyre2, www.sbg.bio.ic.ac.uk/phyre2/)(Kelley *et al.*, 2015) resulted in the identification of the human RNA polymerase-II elongation factor ELL2 (ELL2) as a top-scoring alignment sequence. ELL2 is a component of the super elongation complex that increases the catalytic rate of RNA polymerase II transcription (Shilatifard *et al.*, 1997; Park *et al.*, 2014). An alignment of the predicted secondary structure of the wHTH domain of BirA, ELL2 and PRT6 is described in Fig. 5.3B.

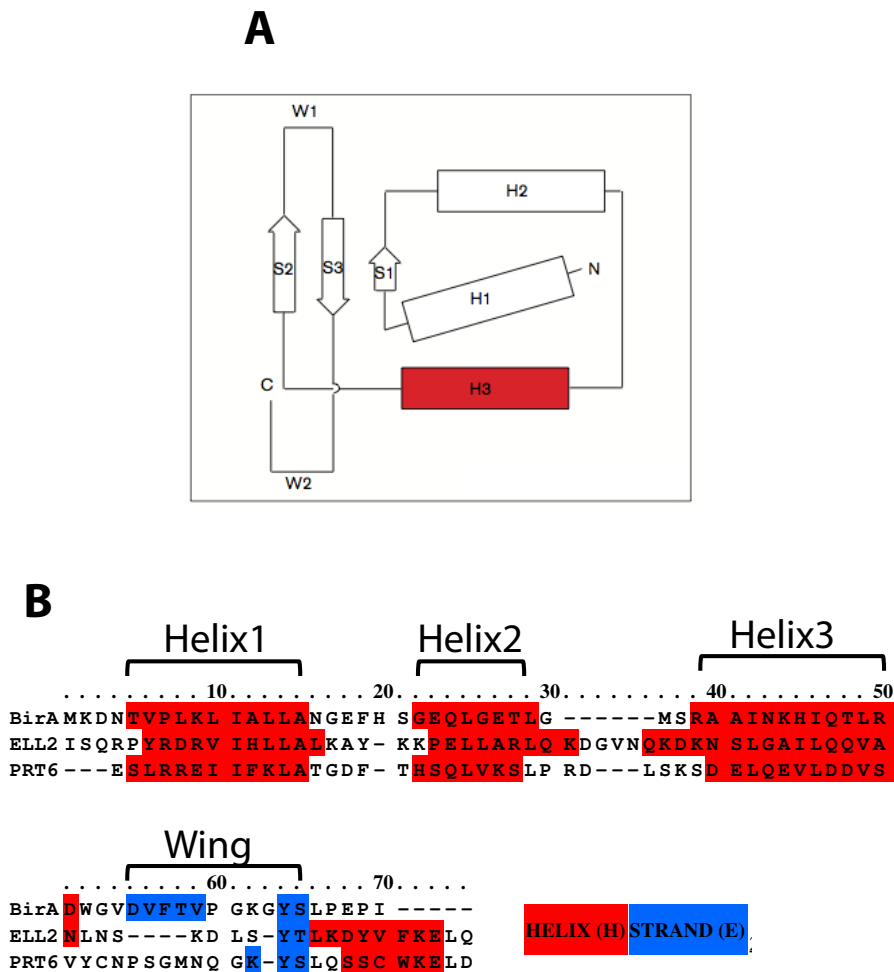


Fig 5.3. Overview of typical wHTH domain and alignment of predicted secondary structures of the wHTH domain of BirA (*E. coli*), ELL2 (human) and PRT6 (*Arabidopsis*). (A) Overview of typical wHTH fold. H denotes alpha helix, S denotes beta strand and W denotes wing. The DNA binding site of multiple wHTH domain proteins is H3, which is shaded in red. Image adapted from (Gajiwala and Burley, 2000). (B) The wHTH domain of *E. coli* BirA, human ELL2 and Arabidopsis PRT6 was obtained from the UniProt database (<https://www.uniprot.org/>). Multiple sequence alignment was carried out using PRALINE (<http://www.ibi.vu.nl/programs/pralinewww/>) with secondary structure prediction generated using the PSIPRED server (<http://bioinf.cs.ucl.ac.uk/psipred/>). The helix and wing domains are annotated according to previously published results (Wilson *et al.*, 1992; Chakravarty and Cronan, 2013).

The wHTH domain of PRT6 is conserved across PRT6-like sequences in multiple plant lineages (Fig 5.4). This domain is also present in mammalian UBR-domain containing RING domain E3 ligases, such as the mouse N-recogin UBR2, when the protein sequence is queried using the online domain prediction tool InterPro (<https://www.ebi.ac.uk/interpro/>) (Fig 5.4). In these enzymes the wHTH is

dues. Alignment was carried out using Clustal 2.1 software and then annotated using EXPASY BOXSHADE (https://embnet.vital-it.ch/software/BOX_form.html).

5.1.3 Experimental aims

The aim of the following experiments is to characterize Arabidopsis PRT6 using the yeast *S. cerevisiae*. The first set of experiments is designed to determine if PRT6 can target the yeast UBR1 substrate CUP9 for degradation. In *ubr1Δ* mutant yeast cells, CUP9 is stabilized (see Section 5.1.1). As mentioned above, PRT6 activity towards CUP9 can be examined by transforming *ubr1Δ* cells with a PRT6 construct and testing for the induction of *PTR2* expression upon addition of the Arg-Ala dipeptide to the medium. The second set of experiments is aimed at characterizing the wHTH domain of PRT6. To this end, mutants of PRT6 that either lack or contain a mutant wHTH domain were generated to examine if this domain is important for the N-recognin activity of PRT6 in a yeast *ubr1Δ* mutant.

5.2 Results

5.2.1 Assaying CUP9 stability using *PTR2* expression

As discussed in Section 5.1.1, the addition of dipeptide Arg-Ala to *S. cerevisiae* cells results in the UBR1-mediated degradation of CUP9 and the transcriptional activation of the peptide uptake receptor gene *PTR2*. The activation of *PTR2* can therefore be used as an indirect estimation for CUP9 degradation upon Arg-Ala dipeptide treatment. In order to establish a *PTR2* activation assay, I compared *PTR2* expression after mock or dipeptide treatment in either JD52 (denoted 'wild-type' hereafter) or *ubr1Δ* mutant yeast cells. Cells were grown for 3 days on selective SD medium agar plates, using glucose (2%) as a carbon source, before being grown overnight in liquid SD medium. The next day, 10 mM Arg-Ala dipeptide or a mock treatment (H₂O) was added to the growing cells. The cultures were incubated with shaking at 30°C for another 2 hrs. This initial time point was chosen as previous studies by Turner *et al.* saw an increase in *PTR2* expression after incubating yeast

cells for 30 min with dipeptides and this upregulation of expression lasted for at least 2.5 hrs (Turner *et al.*, 2000). *PTR2* expression in both wild-type and *ubr1Δ* strains was then analyzed using RT-qPCR with primers specific for the *PTR2* gene and a reference (housekeeping) gene. These results indicated that *PTR2* expression was activated by dipeptide addition in wild-type cells, while *ubr1Δ* cells did not display any change in *PTR2* expression, as expected. These results are described in Fig. 5.5A as the log₂ fold-change of *PTR2* expression in dipeptide-treated cells compared to mock-treated cells. The differences between the wild-type and the *ubr1Δ* strain were reproducible across different experiments, despite slight variations in the growth medium used (see for example Fig. 5.5B and Fig. 5.6A).

A former student in the lab, Francesca Mesiti, had previously generated *Arabidopsis* PRT6 and *S. cerevisiae* UBR1 each tagged at the C-terminus with a 6xHA epitope tag under the control of the galactose-inducible GALL promoter (pGALL) in the p416 yeast expression vector. I first aimed to establish a control experiment whereby *PTR2* activation by dipeptide treatment could be rescued with the galactose-inducible expression of UBR1-6HA in a *ubr1Δ* mutant strain. To this end, I transformed wild-type and *ubr1Δ* cells with the plasmid encoding pGALL:UBR1-6HA. In order to repress expression of the UBR1-6HA transgene until treatment with dipeptides, these cells were initially grown on SD agar plates with raffinose as a carbon source. I then used the same protocol that had been successfully used to test the rescue of the *ubr1Δ* strain for the degradation of the Ub-R-βgal reporter substrate (Fig. 5.1). More specifically, cells were grown overnight in liquid SD medium with raffinose. The following day, cells were brought to an OD₆₀₀ of 1 before galactose was introduced to a final concentration of 1% (w/v) to induce UBR1-6HA expression. At the same time, the dipeptide Arg-Ala was added to a concentration of 10 mM. In order to ensure that UBR1-HA6 expression was induced, cells were incubated for 5 hrs with shaking at 30°C before being pelleted by centrifugation. Total RNA was extracted from these cells and used to prepare cDNA for RT-qPCR analysis using primers specific to *PTR2* and a reference gene. As indicated by the results of this preliminary experiments in Fig. 5.5B (blue columns), wild-type cells that carried either an empty vector or pGALL:UBR1-HA6 displayed activation of *PTR2* expression in these conditions, while in *ubr1Δ* cells carrying either of these two constructs no activation of *PTR2* expression was observed, sug-

gesting that (i) expression of inducible UBR1-6HA in these conditions did not rescue CUP9 degradation; or that (ii) UBR1-6HA expression was not induced in the experimental conditions used (Fig 5.5B).

To try to optimize the experimental conditions for these assays, I conducted another exploratory experiment in which I increased the galactose concentration used to induce the expression of the GALL promoter. I also increased the time of induction to allow for a more robust induction of the UBR1-6HA fusion. Hence, in this experiment, *ubr1Δ* pGALL:UBR1-HA6 cells were grown on SD medium agar plates with raffinose, before being grown overnight in liquid SD medium containing raffinose. The following day, cells were brought to an OD₆₀₀ of 1, galactose was introduced to a final concentration of 2% (instead of 1% in the previous experiment), and dipeptide Arg-Ala was added to a concentration of 5 mM (instead of 10 mM in the first exploratory experiment). A lower concentration of the Arg-Ala dipeptide was tried because various dipeptide concentrations have been previously shown to induce CUP9 degradation (Turner *et al.*, 2000). The cells were then incubated for 20 hrs (instead of 5 hrs) at 30°C with shaking. *PTR2* expression was then analyzed using RT-qPCR, as described above (Fig. 5.5B; green column). This preliminary experiment suggested that a longer induction and a higher concentration of galactose could potentially improve the rescue of *PTR2* expression upon UBR1-6HA expression.

I therefore tested whether a prolonged galactose treatment would result in a rescue of *PTR2* activation. In the experimental set-up described below, the cells are grown continuously with galactose, which should result in the constitutive expression of UBR1-6HA. More specifically, I grew *ubr1Δ* pGALL:UBR1-6HA cells on SD medium plates containing 4% galactose (instead of raffinose in the previous experiments) as carbon source for 3 days. Cells were then grown overnight in SD liquid medium containing 4% galactose. The next day, cells were incubated with 10 mM Arg-Ala for 5.5 hrs before being pelleted and used for total RNA extraction and RT-qPCR analysis. However, in these conditions the activation of *PTR2* appeared to be highly variable, as indicated by the large error bar from 2 independent experiments (Fig 5.5B; red column).

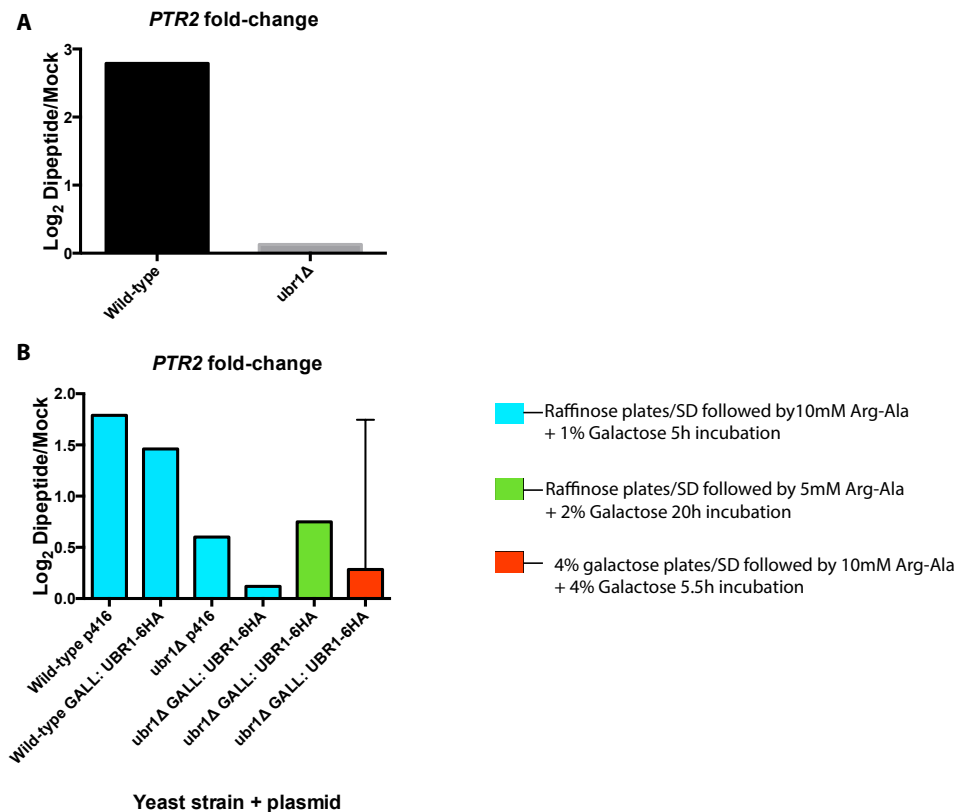


Fig 5.5. Activation of *PTR2* expression following dipeptide Arg-Ala treatment in yeast. (A) Fold-change of *PTR2* expression in wild-type and *ubr1Δ* cells. Cells were grown on glucose-containing SD agar plates prior to overnight growth in liquid SD medium. The cells were then incubated with 10 mM Arg-Ala for 2 hrs before RT-qPCR analysis using primers specific for *PTR2* and the reference gene *TAF10*. *PTR2* expression relative to *TAF10* expression was plotted as the log₂ fold-change of *PTR2* expression in dipeptide treated cells/mock treated cells. (B) Fold-change of *PTR2* expression in wild-type or *ubr1Δ* cells transformed with empty vector (p416) or with p416 pGALL: UBR1-6HA (which is cloned into the p416 vector). Cells were grown in different conditions: (blue bars) cells were grown on raffinose containing SD medium plates for 3 d prior to overnight growth in liquid SD medium supplemented with raffinose. The following day, cells were treated with 1% galactose and 10 mM Arg-Ala, and were incubated with shaking at 30°C for 5 hrs; (green bar) cells were grown on raffinose-containing SD medium plates for 3 d prior to overnight growth in raffinose-containing liquid SD medium. The following day, cells were treated with galactose to a final concentration of 2% and 5 mM Arg-Ala, and were incubated with shaking at 30°C for 20 hrs; (red bar) cells were grown on SD plates with 4% galactose for 3 d and then grown overnight in liquid SD medium containing 4% galactose. The following day, cells were incubated in liquid SD medium containing 4% galactose with 10 mM Arg-Ala for 5.5 hrs. Cells grown under these different conditions were collected by centrifugation. Pellets were then used for RNA extraction and this total RNA was used to prepare cDNA for RT-qPCR analysis using primers specific to *PTR2* and the *TAF10* reference gene. *PTR2* expression relative expression to *TAF10* was plotted as the log₂ fold-change of *PTR2* expression in dipeptide-treated cells versus mock -treated cells. The experiment described in

B (red legend) was conducted twice. Error bars denote standard deviation between these two experiments.

In order to reduce the complexity of the experiment, I generated yeast expression constructs expressing UBR1-6HA or PRT6-6HA under the control of the constitutive ADH1 promoter. This removed the need to induce UBR1-6HA or PRT6-6HA expression with the addition of galactose, and cells could instead be grown with glucose as the sole carbon source. UBR1-6HA was cloned using restriction enzymes and transformed into *E. coli* to propagate the plasmid, while PRT6-6HA was cloned into the yeast expression vector using homologous recombination in yeast in order to avoid potential construct instability in *E. coli* (see Chapter 4 and Section 2.2.1.7). *ubr1Δ* cells were transformed with constructs encoding pADH1:UBR1-6HA or pADH1:PRT6-6HA and were grown on SD medium agar plates with glucose as the carbon source. These cells were then grown overnight in liquid SD medium also containing glucose. The following day, cells were treated with 10 mM Arg-Ala dipeptide for 2 hrs. Cells were then pelleted by centrifugation and were used for either total RNA extraction or for protein extraction. Total RNA was used for RT-qPCR analysis using primers specific for *PTR2*, *UBR1*, *PRT6* and a reference gene. Protein extracts were used to examine UBR1-6HA and PRT6-6HA protein abundance by immunoblotting with an HA-specific antibody (Fig. 5.6).

The results from these preliminary RT-qPCR experiments indicate that constitutively expressed UBR1-6HA can rescue *PTR2* activation upon dipeptide treatment, although the fold-change of expression may be somewhat lower than in wild-type cells (Fig 5.6A). In contrast, PRT6-6HA expression did not appear to rescue *PTR2* activation upon dipeptide treatment (Fig 5.6A). RT-qPCR analysis using primers specific for *UBR1* or *PRT6* indicated that both genes were successfully expressed in yeast (Fig 5.6B) and immunoblots using anti-HA antibodies confirmed that both UBR1-6HA and PRT6-6HA accumulated to a detectable and comparable level in the *ubr1Δ* cells (Fig 5.6C). Although additional replicates are necessary to draw a conclusion, these preliminary results suggest that PRT6 may not be able to target CUP9 for degradation.

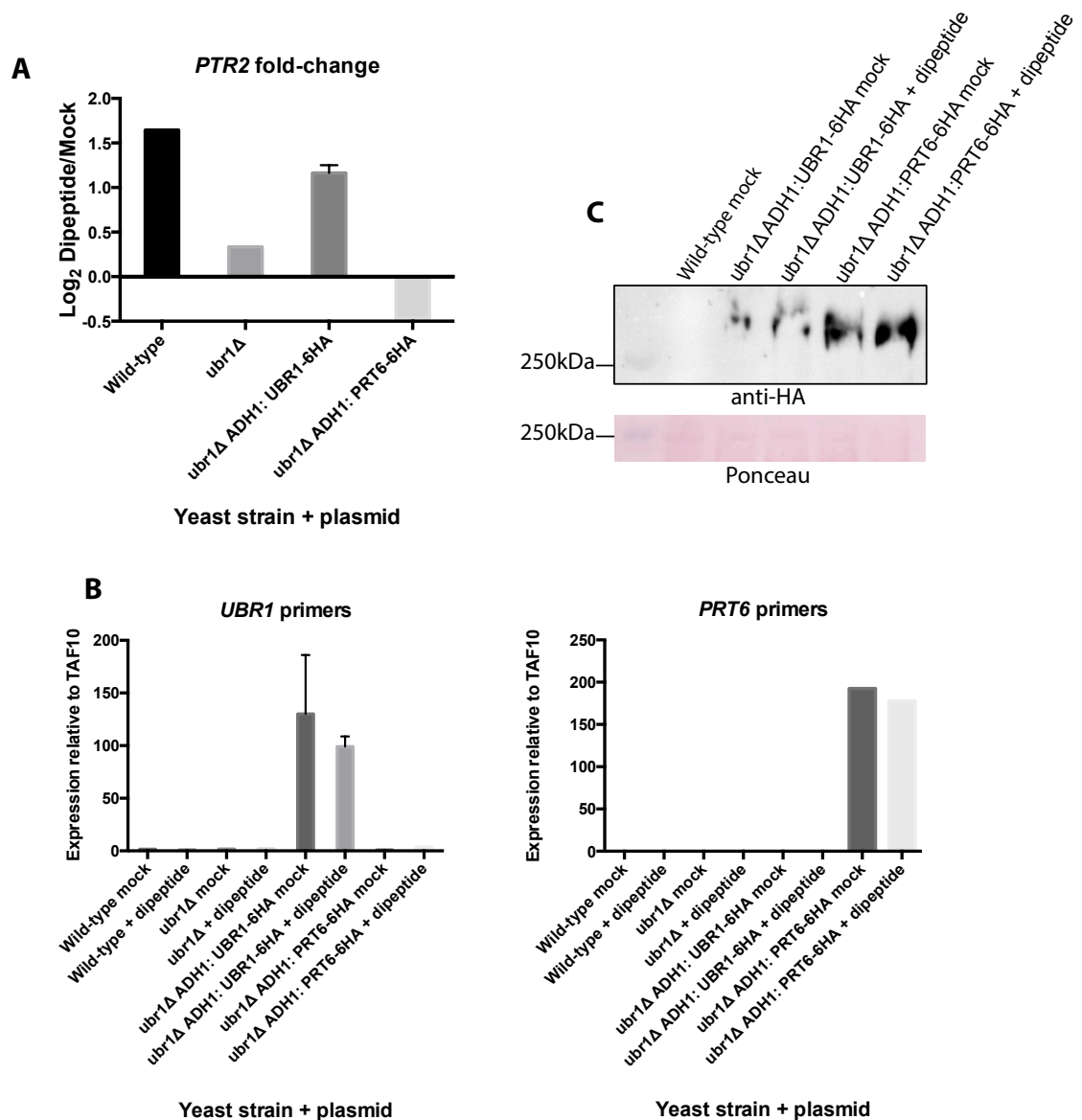


Fig 5.6. *PTR2* activation in dipeptide-treated yeast cells upon *UBR1-6HA* or *PRT6-6HA* expression. (A) Fold-change of *PTR2* expression in wild-type or *ubr1Δ* cells containing plasmids encoding pADH1:*UBR1-6HA* or pADH1:*PRT6-6HA*. Cells were grown on glucose-containing SD agar plates prior to overnight growth in liquid SD medium with glucose. The following day, cells were incubated with 10 mM Arg-Ala for 2 hrs before being pelleted by centrifugation. RNA was extracted and used to prepare cDNA for RT-qPCR analysis using primers specific for *PTR2* and the *TAF10* reference gene. *PTR2* expression relative to *TAF10* expression was plotted as the log₂ fold-change of *PTR2* expression in dipeptide treated cells versus mock treated cells. (B) cDNA prepared as described in (A) was analyzed by qPCR using primers specific to *UBR1* or *PRT6*. Expression relative to the reference gene *TAF10* is plotted. (C) Cells were prepared as described in (A). Cell pellets were incubated with 0.1M NaOH before pelleting and resuspending cells in 1X SDS loading dye, followed by a 5 min treatment at 95°C. Protein extracts were separated using SDS-PAGE and analyzed using immunoblotting with anti-HA antibodies. Two biological replicates using *ubr1Δ* pADH1:*UBR1-6HA*

were conducted. For qPCR analysis, error bars represent standard deviation between these two experiments.

5.2.2 Generation of a PRT6 Δ wHTH yeast expression construct

Previous experiments carried out in the lab demonstrated that PRT6 can target reporter substrates with basic N-termini for degradation in *ubr1* Δ cells (Fig. 5.1). These experiments involved the co-transformation of yeast cells with plasmids encoding the galactose-inducible pGALL:PRT6-6HA fusion protein, as well as galactose inducible reporter substrates. Reporter substrates that were used encode N-terminal Ub translationally fused to the yeast enzyme β -galactosidase (β -gal) bearing different N-terminal residues (X) such that expression in yeast results in a β -gal enzyme with different N-terminal residues X (discussed in Section 1.2). When PRT6-6HA was co-expressed in *ubr1* Δ cells that lack endogenous β -gal activity with various Ub-X- β gal constructs, the constructs bearing N-terminal Arg, Lys and His displayed significantly less β -gal enzymatic activity, compared to a construct containing N-terminal Met, indicating that they were being targeted for degradation by PRT6 (Fig. 5.1).

As discussed in Section 5.1.2, the plant N-recognin PRT6 contains an uncharacterized wHTH domain that is conserved in UBR and RING-domain containing protein sequences in eukaryotes (Fig 5.4). To examine if the wHTH domain might have a role in the recognition or ubiquitination of N-end rule substrates by PRT6, I aimed to carry out mutagenesis of this domain and examine if these mutations affect PRT6's ability to target N-end rule reporter substrates for degradation in yeast using the same Ub-X- β gal N-end rule reporter assays described above.

Before mutating any conserved residues of the wHTH, I first sought to characterize a PRT6 mutant enzyme with a deletion of the domain. As the *PRT6* sequence appears to be unstable in *E. coli* I carried out this cloning using homologous recombination in yeast. The plasmid encoding pGALL: PRT6-6HA was linearized with restriction enzymes that cut the cDNA sequence upstream and downstream of the wHTH coding sequence. A PCR-amplified mutant *PRT6* sequence lacking the wHTH sequence and containing homology to the plasmid was then co-transformed

into *ubr1Δ* cells with the linearized plasmid and inserted into this plasmid by homologous recombination (Fig 5.7). This resulted in a *PRT6* sequence that encodes a protein lacking residues 867 to 953 (construct noted pGALL: PRT6ΔwHTH-6HA) (see Table 2.4).

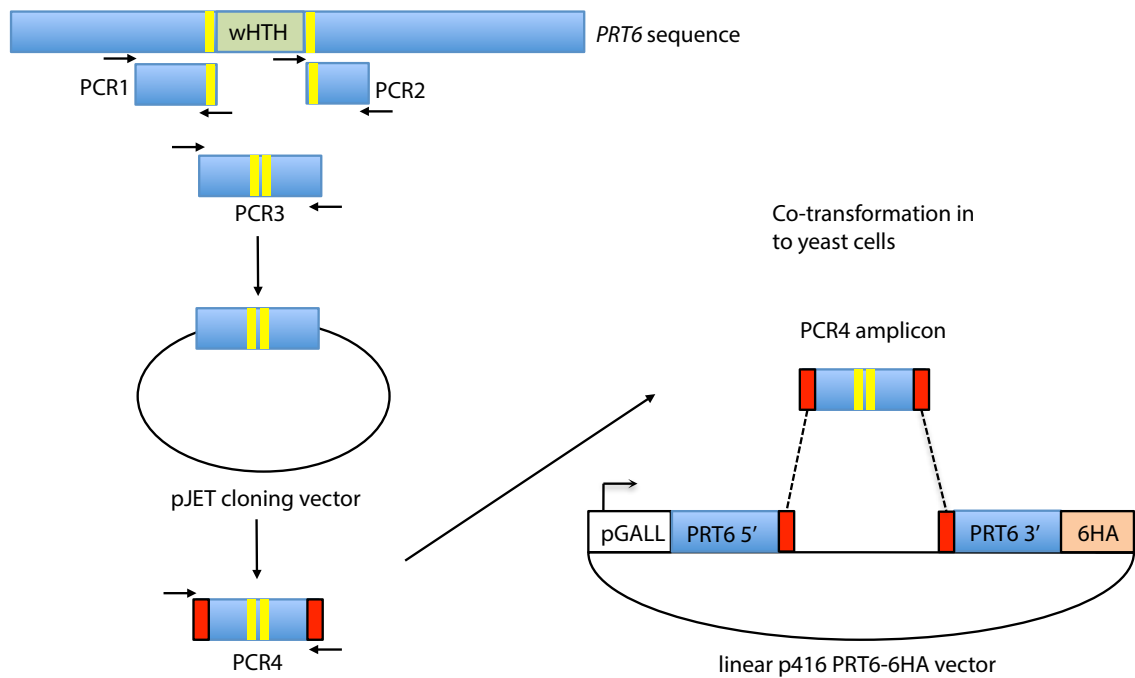


Fig 5.8. Generation of pGALL: PRT6ΔwHTH-6HA. In order to generate a *PRT6* sequence lacking the wHTH domain *PRT6* sequence was amplified before (PCR1) and after (PCR2) the wHTH encoding sequence. These PCR products were then fused (PCR3) and ligated in to a pJET cloning vector and this vector was propagated in *E. coli*. This vector was used as a DNA template which was amplified using primers that added 30 bp of homology (PCR4) (indicated by red rectangles) to the template towards the sequence of restriction enzyme digested linear p416 pGALL: PRT6-6HA. The purified PCR product of PCR4 and linearized p416 pGALL: PRT6-6HA were co-transformed in to *S. cerevisiae* cells and the pGALL: PRT6ΔwHTH-6HA plasmid was generated by homologous recombination. For specific primers used and plasmids generated see Table 2.2 and Table 2.4.

Yeast colonies that grew as a result of this transformation were screened using primers that amplified regions flanking the wHTH coding DNA in order to ensure that this domain had been deleted (Fig 5.8A). Following this, these PCR products were also analyzed by Sanger sequencing to confirm deletion of the wHTH domain. To ensure that the protein was being expressed in *ubr1Δ* cells, I grew *ubr1Δ* pGALL:PRT6ΔwHTH-6HA cells overnight in SD medium containing 2%

galactose. The following day, cells were collected by centrifugation and total protein was extracted in 2x SDS buffer. This protein extract was separated by SDS PAGE and analyzed using immunoblotting with anti-HA antibodies. The PRT6 Δ wHTH-6HA protein accumulated to detectable levels (Fig 5.8B).

To examine if the wHTH is necessary for PRT6 to function as an N-recognin, I carried out a preliminary colony lift assay for β -gal activity of different Ub-X- β gal reporter constructs. To this aim, *ubr1* Δ cells were transformed with plasmids encoding pGALL:PRT6-6HA or pGALL:PRT6 Δ wHTH-6HA along with reporter substrates encoding pGALL:Ub-Met- β gal, pGALL:Ub-Arg- β gal or an empty vector. These cells were grown on SD medium agar plates containing 2% galactose, so that all inducible constructs were expressed. The cells were then lysed and soaked in a buffer containing the β -gal substrate 5-bromo-4-chloro-3-indolyl- β -D-galactopyranoside (X-GAL), which forms a blue colour when cleaved by β -gal enzymes (Fig. 5.8C). With yeast cells coding for PRT6-6HA, the blue signal was stronger when Ub-Met- β gal was expressed compared to Ub-Arg- β gal. This indicates that, as expected, Met- β gal appears to be more stable than Arg- β gal in the presence of PRT6-6HA. A similar result was obtained with cells expressing PRT6 Δ wHTH-6HA, suggesting that PRT6 lacking the wHTH domain may still have functional N-recognin activity. Cells co-expressing an empty vector did not exhibit any β -gal activity.

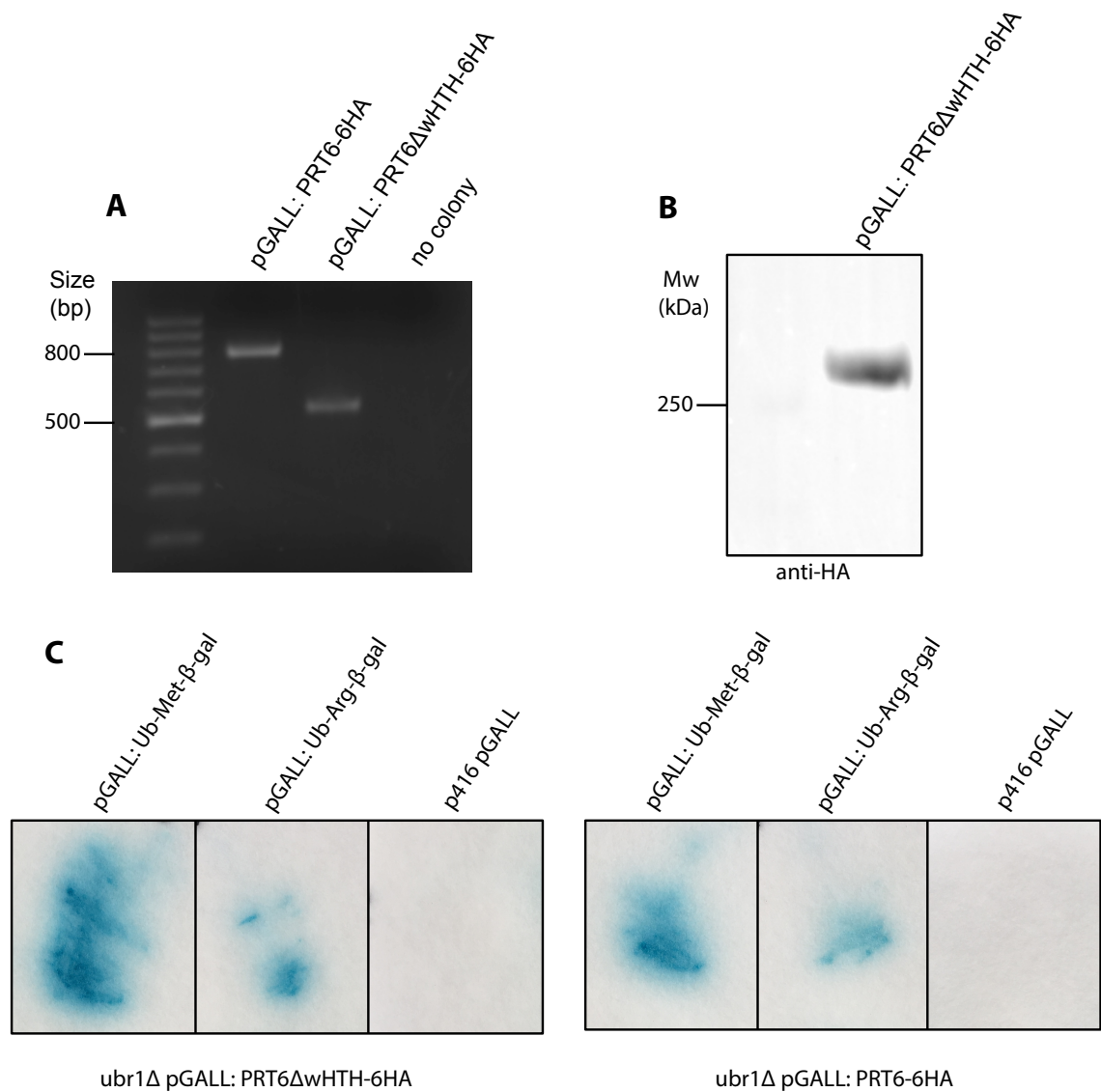


Fig 5.8. Preliminary characterization of PRT6 Δ wHTH-6HA. (A) Control PCR carried out on yeast colonies containing either the vectors coding for pGALL:PRT6-6HA or pGALL:PRT6 Δ wHTH-6HA. As a control, a PCR without yeast was also included. Primers amplifying the PRT6 wHTH sequence were used that would produce a 792 bp fragment for full length wHTH and a 531 bp fragment for the wHTH sequence. (B) Detection of PRT6 Δ wHTH-6HA expressed in *ubr1 Δ* cells. *ubr1 Δ* pGALL: PRT6 Δ wHTH-6HA cells were grown on SD medium containing 2% galactose overnight before being collected by centrifugation. Total protein extracts were prepared by incubating cells in 0.1M NaOH before pelleting and resuspending cells in 1X SDS loading dye with 5 min at 95°C. Protein extracts were separated using SDS-PAGE and analyzed using immunoblotting with anti-HA antibodies. (C) Colony lift assay using cells co-expressing galactose inducible PRT6-6HA or PRT6 Δ wHTH-6HA with reporter substrates Ub-Met- β gal, Ub-Arg- β gal or an empty vector (p416 pGALL). Cells were grown on SD medium plates supplemented with 2% galactose. A filter was laid over the plates to lift the cells, which were equivalent. The filters were then soaked in liquid nitrogen and then in Z buffer (Appendix 1) containing X-GAL. The appearance of a blue colour indicates cleavage of X-GAL by β gal activity, and should be roughly proportional to the amount of X- β gal reporter in the cells.

5.3 Discussion and future work

5.3.1 PRT6 may not target CUP9 for degradation

The Arabidopsis N-recognin PRT6 is homologous to yeast UBR1 and they both contain a conserved substrate-binding domain that targets substrates with basic N-termini for degradation. However, the substrate binding domain for type II destabilizing residues (also known as hydrophobic destabilizing residues) is absent in PRT6 compared to yeast and mammalian UBR1 orthologs. Yeast UBR1 has been relatively well characterized in terms of biochemical function, whereas little is known about how PRT6 interacts with its substrates or potential cofactor proteins, possibly because of difficulties associated with cloning or expressing PRT6 in bacterial systems. It has been shown that UBR1 contains a substrate-binding site that targets proteins *via* an internal degron, including the yeast transcriptional repressor CUP9 (see Section 5.1.1). As PRT6 shares other similar substrates to UBR1, and the sequence similarities extend beyond the UBR domain, I aimed to determine if PRT6 could also bind substrates through an internal degron by testing the possible degradation of CUP9 in a yeast *ubr1* Δ mutant strain.

UBR1-mediated degradation of CUP9 is induced in the presence of dipeptide Arg-Ala, with *PTR2* being transcriptionally activated following CUP9 degradation. I first aimed to establish reproducible conditions whereby *PTR2* activation in *ubr1* Δ cells is rescued by yeast UBR1 expression. The use of galactose-inducible UBR1-6HA did not result in a reproducible change in *PTR2* activity, although wild-type cells grown in the same conditions did have a higher level of *PTR2* transcript compared to *ubr1* Δ cells. This suggests that the galactose inducible promoter system may not be suitable for such experiments.

As an alternative, a plasmid encoding UBR1-6HA under the control of the constitutive ADH1 promoter did rescue *PTR2* activation when cells were grown on medium containing glucose, although *PTR2* activation appeared to be slightly lower than in wild-type cells. This could possibly be due to a difference in the level of UBR1-6HA compared to endogenous yeast UBR1, or to a negative effect of the 6HA tag on the activity of the yeast enzyme. The latter effect would be mild, as it is known that expression of UBR1-6HA is sufficient to rescue the *ubr1* Δ phenotype

for the degradation of substrates with type I or type II N-terminal destabilizing residues (Fig. 5.1). Preliminary experiments presented in Fig. 5.6 suggest that despite constitutive expression of PRT6, the PRT6-6HA fusion protein is unlikely to be able to target CUP9 for degradation. Unfortunately, due to time constraints, I could not carry out sufficient independent replicates to be able to confirm this preliminary result. I aim at completing these experiments in order to confirm that PRT6-6HA does not target CUP9 for degradation.

Previous studies have shown that the N-terminal half of UBR1 (residues 1-1140) are involved in CUP9 binding, although the specific residues involved have not yet been described (Xia *et al.*, 2008). The degradation of CUP9 by UBR1 involves other UBR1 cofactors including the HECT domain E3 Ub ligase Ubiquitin fusion degradation4 (Ufd4). In wild-type yeast cells, the half-life of CUP9 was ~5 min whereas in *ufd4Δ* mutant yeast cells the half-life of CUP9 was ~14 min (Xia *et al.*, 2008). The site of UBR1 that interacts with Ufd4 was reduced to UBR1 residues 454-795 in a study conducted by Hwang *et al.* (Hwang *et al.*, 2010a). Preliminary analysis of PRT6 using this sequence as an alignment template does not indicate that PRT6 bears significant homology to the UBR1 Ufd4 interaction site, which might suggest that PRT6 would not be able to interact with this cofactor in yeast. This could potentially hinder our ability to test the potential binding of CUP9 using the methods I applied.

5.3.2 Characterizing the PRT6 wHTH domain

In order to characterize a potential role of the wHTH domain of PRT6, I have generated a mutant PRT6 construct lacking this domain. A preliminary experiment using a colony lift assay indicates that the PRT6 reporter substrate Arg-βgal accumulates to lower levels than the Met-βgal enzyme in *ubr1Δ* cells expressing either full length PRT6-6HA or PRT6ΔwHTH-6HA. This suggests that PRT6ΔwHTH retains some function as an N-recognin towards substrates bearing N-terminal Arg (Fig 5.8). However, colony lift assays are not quantitative and thus have limited power to determine a potential role of the wHTH domain in either substrate recognition or ubiquitination.

In the future, I aim to quantify the N-recognin activity of full-length PRT6-6HA *versus* that of PRT6ΔwHTH-6HA using the constructs generated in this study.

To this end, I will grow yeast strains encoding galactose inducible PRT6-6HA or PRT6 Δ wHTH-6HA with galactose inducible Ub-X- β gal reporter substrates as described in this study. Instead of using a colony lift assay to measure the activity of reporter substrates, I will carry out a quantitative β gal enzyme assay, similarly to the experiments shown in Fig. 5.1. If the deletion of the wHTH domain has an effect on the ability of PRT6 to target reporter substrates for degradation, I will conduct a more thorough characterization of the PRT6 Δ wHTH-6HA mutant. This will be done by mutagenizing individual conserved amino acids of the domain and determining which residues are critical for its function. Preliminary bioinformatic analysis of the PRT6 wHTH structure using the Phyre2 server (www.sbg.bio.ic.ac.uk/phyre2/; Kelley *et al.*, 2015) coupled with the SuSpect server (<http://www.sbg.bio.ic.ac.uk/suspect/>; Yates *et al.*, 2014) has identified a number of residues that are predicted to be critical for correct folding of the wHTH domain (Fig 5.9)

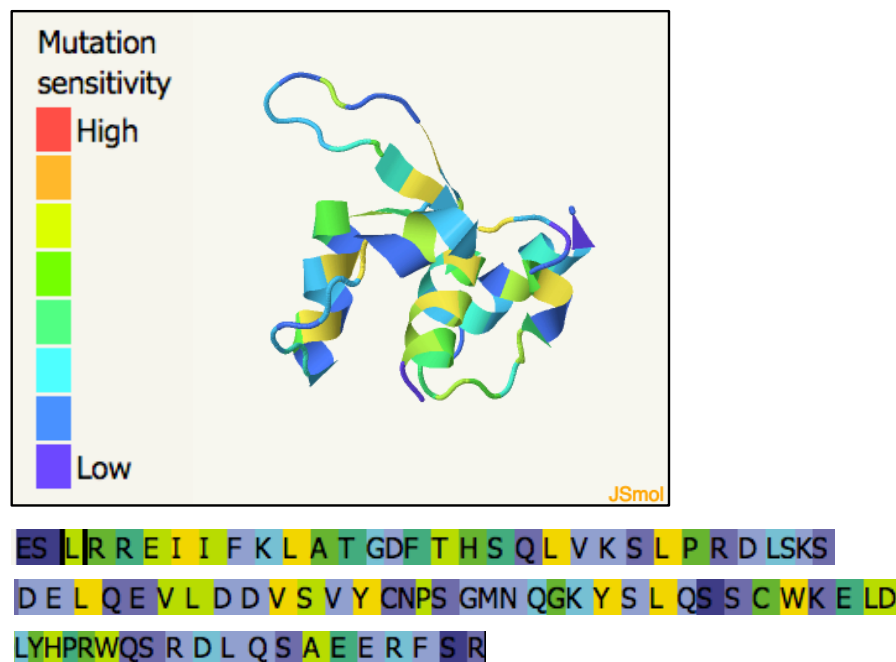


Fig 5.9. Predicted mutational sensitivity of wHTH domain residues. The tertiary structure of the wHTH domain of PRT6 (aa867 - 953) was predicted using the Phyre2 server, found online at www.sbg.bio.ic.ac.uk/phyre2/ (Kelley *et al.*, 2015). The predicted mutational sensitivity of these residues was predicted using the SuSpect server, found at <http://www.sbg.bio.ic.ac.uk/suspect/> (Yates *et al.*, 2014).

Considering the proximity of the wHTH domain to the RING domain, one possible role of this domain may be to strengthen the interaction between PRT6 and the E2 conjugating enzyme. If the above-mentioned tests with the PRT6 Δ wHTH-6HA fusion protein suggest a role of the wHTH for the activity of PRT6 as an N-recogin, I will seek to determine if this is linked to differences in E2 binding using again yeast as a model system. One possible limitation though, is that the yeast E2 that interacts with PRT6 is unknown. Therefore, to test this hypothesis, I will first determine if the yeast E2 Rad6, which interacts with yeast UBR1, is also required for the activity of PRT6 in a yeast *ubr1* Δ strain. If this is indeed the case, then I will study a potential role of the wHTH domain of PRT6 in mediating the interaction with Rad6 together with PRT6's RING domain.

Chapter 6. References

- Abbas, M., Berckhan, S., Rooney, D. J., Gibbs, D. J., Vicente Conde, J., Sousa Correia, C., Bassel, G. W., Marin-de la Rosa, N., Leon, J., Alabadi, D., Blazquez, M. A. & Holdsworth, M. J. 2015. Oxygen sensing coordinates photomorphogenesis to facilitate seedling survival. *Curr Biol*, 25(11), pp 1483-8.
- Afzal, A. J., da Cunha, L. & Mackey, D. 2011. Separable fragments and membrane tethering of Arabidopsis RIN4 regulate its suppression of PAMP-triggered immunity. *Plant Cell*, 23(10), pp 3798-811.
- Afzal, A. J., Kim, J. H. & Mackey, D. 2013. The role of NOI-domain containing proteins in plant immune signaling. *BMC Genomics*, 14(327).
- Aksnes, H., Drazic, A., Marie, M. & Arnesen, T. 2016. First Things First: Vital Protein Marks by N-Terminal Acetyltransferases. *Trends Biochem Sci*, 41(9), pp 746-760.
- Arc, E., Galland, M., Godin, B., Cueff, G. & Rajjou, L. 2013. Nitric oxide implication in the control of seed dormancy and germination. *Front Plant Sci*, 4(346).
- Axtell, M. J., Chisholm, S. T., Dahlbeck, D. & Staskawicz, B. J. 2003. Genetic and molecular evidence that the *Pseudomonas syringae* type III effector protein AvrRpt2 is a cysteine protease. *Mol Microbiol*, 49(6), pp 1537-46.
- Axtell, M. J. & Staskawicz, B. J. 2003. Initiation of RPS2-specified disease resistance in Arabidopsis is coupled to the AvrRpt2-directed elimination of RIN4. *Cell*, 112(3), pp 369-77.
- Azevedo, C., Santos-Rosa, M. J. & Shirasu, K. 2001. The U-box protein family in plants. *Trends Plant Sci*, 6(8), pp 354-8.
- Bachmair, A., Finley, D. & Varshavsky, A. 1986. In vivo half-life of a protein is a function of its amino-terminal residue. *Science*, 234(4773), pp 179-86.
- Balzi, E., Choder, M., Chen, W. N., Varshavsky, A. & Goffeau, A. 1990. Cloning and functional analysis of the arginyl-tRNA-protein transferase gene ATE1 of *Saccharomyces cerevisiae*. *J Biol Chem*, 265(13), pp 7464-71.
- Bartel, B., Wüning, I. & Varshavsky, A. 1990. The recognition component of the N-end rule pathway. *Embo j*, 9(10), pp 3179-89.
- Bedford, L., Paine, S., Sheppard, P. W., Mayer, R. J. & Roelofs, J. 2010. Assembly, structure, and function of the 26S proteasome. *Trends Cell Biol*, 20(7), pp 391-401.

- Bigeard, J., Colcombet, J. & Hirt, H. 2015. Signaling mechanisms in pattern-triggered immunity (PTI). *Mol Plant*, 8(4), pp 521-39.
- Brower, C. S., Piatkov, K. I. & Varshavsky, A. 2013. Neurodegeneration-associated protein fragments as short-lived substrates of the N-end rule pathway. *Mol Cell*, 50(2), pp 161-71.
- Bui, L. T., Giuntoli, B., Kosmacz, M., Parlanti, S. & Licausi, F. 2015. Constitutively expressed ERF-VII transcription factors redundantly activate the core anaerobic response in *Arabidopsis thaliana*. *Plant Sci*, 236(37-43).
- Byrd, C., Turner, G. C. & Varshavsky, A. 1998. The N-end rule pathway controls the import of peptides through degradation of a transcriptional repressor. *Embo j*, 17(1), pp 269-77.
- Callis, J. 2014. The ubiquitination machinery of the ubiquitin system. *Arabidopsis Book*, 12(e0174).
- Callis, J., Carpenter, T., Sun, C. W. & Vierstra, R. D. 1995. Structure and evolution of genes encoding polyubiquitin and ubiquitin-like proteins in *Arabidopsis thaliana* ecotype Columbia. *Genetics*, 139(2), pp 921-39.
- Carlson, M. & Botstein, D. 1982. Two differentially regulated mRNAs with different 5' ends encode secreted with intracellular forms of yeast invertase. *Cell*, 28(1), pp 145-54.
- Cha-Molstad, H., Sung, K. S., Hwang, J., Kim, K. A., Yu, J. E., Yoo, Y. D., Jang, J. M., Han, D. H., Molstad, M., Kim, J. G., Lee, Y. J., Zakrzewska, A., Kim, S. H., Kim, S. T., Kim, S. Y., Lee, H. G., Soung, N. K., Ahn, J. S., Ciechanover, A., Kim, B. Y. & Kwon, Y. T. 2015. Amino-terminal arginylation targets endoplasmic reticulum chaperone BiP for autophagy through p62 binding. *Nat Cell Biol*, 17(7), pp 917-29.
- Cha-Molstad, H., Yu, J. E., Feng, Z., Lee, S. H., Kim, J. G., Yang, P., Han, B., Sung, K. W., Yoo, Y. D., Hwang, J., McGuire, T., Shim, S. M., Song, H. D., Ganipisetti, S., Wang, N., Jang, J. M., Lee, M. J., Kim, S. J., Lee, K. H., Hong, J. T., Ciechanover, A., Mook-Jung, I., Kim, K. P., Xie, X. Q., Kwon, Y. T. & Kim, B. Y. 2017. p62/SQSTM1/Sequestosome-1 is an N-recognin of the N-end rule pathway which modulates autophagosome biogenesis. *Nat Commun*, 8(1), pp 102.
- Chakravartty, V. & Cronan, J. E. 2013. The wing of a winged helix-turn-helix transcription factor organizes the active site of BirA, a bifunctional repressor/ligase. *J Biol Chem*, 288(50), pp 36029-39.
- Chen, L. & Hellmann, H. 2013. Plant E3 ligases: flexible enzymes in a sessile world. *Mol Plant*, 6(5), pp 1388-404.

- Chen, S. J., Wu, X., Wadas, B., Oh, J. H. & Varshavsky, A. 2017. An N-end rule pathway that recognizes proline and destroys gluconeogenic enzymes. *Science*, 355(6323), pp.
- Chen, Z., Agnew, J. L., Cohen, J. D., He, P., Shan, L., Sheen, J. & Kunkel, B. N. 2007. Pseudomonas syringae type III effector AvrRpt2 alters Arabidopsis thaliana auxin physiology. *Proc Natl Acad Sci U S A*, 104(50), pp 20131-6.
- Chisholm, S. T., Dahlbeck, D., Krishnamurthy, N., Day, B., Sjolander, K. & Staskawicz, B. J. 2005. Molecular characterization of proteolytic cleavage sites of the Pseudomonas syringae effector AvrRpt2. *Proc Natl Acad Sci U S A*, 102(6), pp 2087-92.
- Ciechanover, A., Elias, S., Heller, H. & Hershko, A. 1982. "Covalent affinity" purification of ubiquitin-activating enzyme. *J Biol Chem*, 257(5), pp 2537-42.
- Ciechanover, A., Hod, Y. & Hershko, A. 1978. A heat-stable polypeptide component of an ATP-dependent proteolytic system from reticulocytes. *Biochem Biophys Res Commun*, 81(4), pp 1100-5.
- Coaker, G., Falick, A. & Staskawicz, B. 2005. Activation of a phytopathogenic bacterial effector protein by a eukaryotic cyclophilin. *Science*, 308(5721), pp 548-50.
- Coleman, K. E., Bekes, M., Chapman, J. R., Crist, S. B., Jones, M. J., Ueberheide, B. M. & Huang, T. T. 2017. SENP8 limits aberrant neddylation of NEDD8 pathway components to promote cullin-RING ubiquitin ligase function. *Elife*, 6(
- Cui, F., Wu, S., Sun, W., Coaker, G., Kunkel, B., He, P. & Shan, L. 2013. The Pseudomonas syringae type III effector AvrRpt2 promotes pathogen virulence via stimulating Arabidopsis auxin/indole acetic acid protein turnover. *Plant Physiol*, 162(2), pp 1018-29.
- Cui, H., Tsuda, K. & Parker, J. E. 2015. Effector-triggered immunity: from pathogen perception to robust defense. *Annu Rev Plant Biol*, 66(487-511).
- Dangl, J. L., Horvath, D. M. & Staskawicz, B. J. 2013. Pivoting the plant immune system from dissection to deployment. *Science*, 341(6147), pp 746-51.
- Day, B., Dahlbeck, D., Huang, J., Chisholm, S. T., Li, D. & Staskawicz, B. J. 2005. Molecular basis for the RIN4 negative regulation of RPS2 disease resistance. *Plant Cell*, 17(4), pp 1292-305.
- DE DUVE, C., PRESSMAN, B. C., GIANETTO, R., WATTIAUX, R. & APPELMANS, F. 1955. Tissue fractionation studies. 6. Intracellular distribution patterns of enzymes in rat-liver tissue. *Biochem J*, 60(4), pp 604-17.
- de Marchi, R., Sorel, M., Mooney, B., Fudal, I., Goslin, K., Kwasniewska, K., Ryan, P. T., Pfalz, M., Kroymann, J., Pollmann, S., Feechan, A., Wellmer, F., Rivas, S. &

- Graciet, E. 2016. The N-end rule pathway regulates pathogen responses in plants. *Sci Rep*, 6(26020).
- del Pozo, J. C. & Estelle, M. 1999. The Arabidopsis cullin AtCUL1 is modified by the ubiquitin-related protein RUB1. *Proc Natl Acad Sci U S A*, 96(26), pp 15342-7.
- Deshaies, R. J. & Joazeiro, C. A. 2009. RING domain E3 ubiquitin ligases. *Annu Rev Biochem*, 78(399-434).
- Dey, S., Wenig, M., Langen, G., Sharma, S., Kugler, K. G., Knappe, C., Hause, B., Bichlmeier, M., Babaeizad, V., Imani, J., Janzik, I., Stempf, T., Huckelhoven, R., Kogel, K. H., Mayer, K. F. & Vlot, A. C. 2014. Bacteria-triggered systemic immunity in barley is associated with WRKY and ETHYLENE RESPONSIVE FACTORS but not with salicylic acid. *Plant Physiol*, 166(4), pp 2133-51.
- Dharmasiri, S., Dharmasiri, N., Hellmann, H. & Estelle, M. 2003. The RUB/Nedd8 conjugation pathway is required for early development in Arabidopsis. *Embo j*, 22(8), pp 1762-70.
- Dinh, T. V., Bienvenut, W. V., Linster, E., Feldman-Salit, A., Jung, V. A., Meinnel, T., Hell, R., Giglione, C. & Wirtz, M. 2015. Molecular identification and functional characterization of the first N α -acetyltransferase in plastids by global acetylome profiling. *Proteomics*, 15(14), pp 2426-35.
- Dissmeyer, N., Rivas, S. & Graciet, E. 2018. Life and death of proteins after protease cleavage: protein degradation by the N-end rule pathway. *New Phytol*, 218(3), pp 929-935.
- Ditzel, M., Wilson, R., Tenev, T., Zachariou, A., Paul, A., Deas, E. & Meier, P. 2003. Degradation of DIAP1 by the N-end rule pathway is essential for regulating apoptosis. *Nat Cell Biol*, 5(5), pp 467-73.
- Dong, H., Dumenil, J., Lu, F. H., Na, L., Vanhaeren, H., Naumann, C., Klecker, M., Prior, R., Smith, C., McKenzie, N., Saalbach, G., Chen, L., Xia, T., Gonzalez, N., Seguela, M., Inze, D., Dissmeyer, N., Li, Y. & Bevan, M. W. 2017. Ubiquitylation activates a peptidase that promotes cleavage and destabilization of its activating E3 ligases and diverse growth regulatory proteins to limit cell proliferation in Arabidopsis. *Genes Dev*, 31(2), pp 197-208.
- Downes, B. P., Stupar, R. M., Gingerich, D. J. & Vierstra, R. D. 2003. The HECT ubiquitin-protein ligase (UPL) family in Arabidopsis: UPL3 has a specific role in trichome development. *Plant J*, 35(6), pp 729-42.
- Du, F., Navarro-Garcia, F., Xia, Z., Tasaki, T. & Varshavsky, A. 2002. Pairs of dipeptides synergistically activate the binding of substrate by ubiquitin ligase through dissociation of its autoinhibitory domain. *Proc Natl Acad Sci U S A*, 99(22), pp 14110-5.

- Edwards, K., Johnstone, C. & Thompson, C. 1991. A simple and rapid method for the preparation of plant genomic DNA for PCR analysis. *Nucleic Acids Res*, 19(6), pp 1349.
- Elmore, J. M., Liu, J., Smith, B., Phinney, B. & Coaker, G. 2012. Quantitative proteomics reveals dynamic changes in the plasma membrane during Arabidopsis immune signaling. *Mol Cell Proteomics*, 11(4), pp M111.014555.
- Enchev, R. I., Schulman, B. A. & Peter, M. 2015. Protein neddylation: beyond cullin-RING ligases. *Nat Rev Mol Cell Biol*, 16(1), pp 30-44.
- Eschen-Lippold, L., Jiang, X., Elmore, J. M., Mackey, D., Shan, L., Coaker, G., Scheel, D. & Lee, J. 2016. Bacterial AvrRpt2-Like Cysteine Proteases Block Activation of the Arabidopsis Mitogen-Activated Protein Kinases, MPK4 and MPK11. *Plant Physiol*, 171(3), pp 2223-38.
- Etlinger, J. D. & Goldberg, A. L. 1977. A soluble ATP-dependent proteolytic system responsible for the degradation of abnormal proteins in reticulocytes. *Proc Natl Acad Sci U S A*, 74(1), pp 54-8.
- Ferrari, S., Plotnikova, J. M., De Lorenzo, G. & Ausubel, F. M. 2003. Arabidopsis local resistance to *Botrytis cinerea* involves salicylic acid and camalexin and requires EDS4 and PAD2, but not SID2, EDS5 or PAD4. *Plant J*, 35(2), pp 193-205.
- Finley, D. 2009. Recognition and processing of ubiquitin-protein conjugates by the proteasome. *Annu Rev Biochem*, 78(477-513).
- Finley, D., Bartel, B. & Varshavsky, A. 1989. The tails of ubiquitin precursors are ribosomal proteins whose fusion to ubiquitin facilitates ribosome biogenesis. *Nature*, 338(6214), pp 394-401.
- Finley, D., Ulrich, H. D., Sommer, T. & Kaiser, P. 2012. The ubiquitin-proteasome system of *Saccharomyces cerevisiae*. *Genetics*, 192(2), pp 319-60.
- Freemont, P. S., Hanson, I. M. & Trowsdale, J. 1991. A novel cysteine-rich sequence motif. *Cell*. United States.
- Fu, H., Doelling, J. H., Arendt, C. S., Hochstrasser, M. & Vierstra, R. D. 1998. Molecular organization of the 20S proteasome gene family from *Arabidopsis thaliana*. *Genetics*, 149(2), pp 677-92.
- Gajiwala, K. S. & Burley, S. K. 2000. Winged helix proteins. *Curr Opin Struct Biol*, 10(1), pp 110-6.
- Gamsjaeger, R., Liew, C. K., Loughlin, F. E., Crossley, M. & Mackay, J. P. 2007. Sticky fingers: zinc-fingers as protein-recognition motifs. *Trends Biochem Sci*, 32(2), pp 63-70.

- Garzon, M., Eifler, K., Faust, A., Scheel, H., Hofmann, K., Koncz, C., Yephremov, A. & Bachmair, A. 2007. PRT6/At5g02310 encodes an Arabidopsis ubiquitin ligase of the N-end rule pathway with arginine specificity and is not the CER3 locus. *FEBS Lett*, 581(17), pp 3189-96.
- Gasch, P., Fundinger, M., Muller, J. T., Lee, T., Bailey-Serres, J. & Mustroph, A. 2016. Redundant ERF-VII Transcription Factors Bind to an Evolutionarily Conserved cis-Motif to Regulate Hypoxia-Responsive Gene Expression in Arabidopsis. *Plant Cell*, 28(1), pp 160-80.
- Gevaert, K., Van Damme, J., Goethals, M., Thomas, G. R., Hoorelbeke, B., Demol, H., Martens, L., Puype, M., Staes, A. & Vandekerckhove, J. 2002. Chromatographic isolation of methionine-containing peptides for gel-free proteome analysis: identification of more than 800 Escherichia coli proteins. *Mol Cell Proteomics*, 1(11), pp 896-903.
- Gibbs, D. J., Bacardit, J., Bachmair, A. & Holdsworth, M. J. 2014a. The eukaryotic N-end rule pathway: conserved mechanisms and diverse functions. *Trends Cell Biol*, 24(10), pp 603-11.
- Gibbs, D. J., Lee, S. C., Isa, N. M., Gramuglia, S., Fukao, T., Bassel, G. W., Correia, C. S., Corbineau, F., Theodoulou, F. L., Bailey-Serres, J. & Holdsworth, M. J. 2011. Homeostatic response to hypoxia is regulated by the N-end rule pathway in plants. *Nature*, 479(7373), pp 415-8.
- Gibbs, D. J., Md Isa, N., Movahedi, M., Lozano-Juste, J., Mendiondo, G. M., Berckhan, S., Marin-de la Rosa, N., Vicente Conde, J., Sousa Correia, C., Pearce, S. P., Bassel, G. W., Hamali, B., Talloji, P., Tome, D. F., Coego, A., Beynon, J., Alabadi, D., Bachmair, A., Leon, J., Gray, J. E., Theodoulou, F. L. & Holdsworth, M. J. 2014b. Nitric oxide sensing in plants is mediated by proteolytic control of group VII ERF transcription factors. *Mol Cell*, 53(3), pp 369-79.
- Gonda, D. K., Bachmair, A., Wunning, I., Tobias, J. W., Lane, W. S. & Varshavsky, A. 1989. Universality and structure of the N-end rule. *J Biol Chem*, 264(28), pp 16700-12.
- Goritschnig, S., Zhang, Y. & Li, X. 2007. The ubiquitin pathway is required for innate immunity in Arabidopsis. *Plant J*, 49(3), pp 540-51.
- Graciet, E., Mesiti, F. & Wellmer, F. 2010. Structure and evolutionary conservation of the plant N-end rule pathway. *Plant J*, 61(5), pp 741-51.
- Graciet, E., Walter, F., O'Maoileidigh, D. S., Pollmann, S., Meyerowitz, E. M., Varshavsky, A. & Wellmer, F. 2009. The N-end rule pathway controls multiple functions during Arabidopsis shoot and leaf development. *Proc Natl Acad Sci U S A*, 106(32), pp 13618-23.
- Graciet, E. & Wellmer, F. 2010. The plant N-end rule pathway: structure and functions. *Trends Plant Sci*, 15(8), pp 447-53.

- Gravot, A., Richard, G., Lime, T., Lemarie, S., Jubault, M., Lariagon, C., Lemoine, J., Vicente, J., Robert-Seilaniantz, A., Holdsworth, M. J. & Manzanares-Dauleux, M. J. 2016. Hypoxia response in Arabidopsis roots infected by *Plasmodiophora brassicae* supports the development of clubroot. *BMC Plant Biol*, 16(1), pp 251.
- Groll, M. & Huber, R. 2004. Inhibitors of the eukaryotic 20S proteasome core particle: a structural approach. *Biochim Biophys Acta*, 1695(1-3), pp 33-44.
- Haas, A. L., Warme, J. V., Hershko, A. & Rose, I. A. 1982. Ubiquitin-activating enzyme. Mechanism and role in protein-ubiquitin conjugation. *J Biol Chem*, 257(5), pp 2543-8.
- Hakenjos, J. P., Richter, R., Dohmann, E. M., Katsiarimpa, A., Isono, E. & Schwechheimer, C. 2011. MLN4924 is an efficient inhibitor of NEDD8 conjugation in plants. *Plant Physiol*, 156(2), pp 527-36.
- Hanna, M. & Xiao, W. 2006. Isolation of nucleic acids. *Methods Mol Biol*, 313(15-20).
- Harami, G. M., Gyimesi, M. & Kovacs, M. 2013. From keys to bulldozers: expanding roles for winged helix domains in nucleic-acid-binding proteins. *Trends Biochem Sci*, 38(7), pp 364-71.
- Hatfield, P. M., Gosink, M. M., Carpenter, T. B. & Vierstra, R. D. 1997. The ubiquitin-activating enzyme (E1) gene family in Arabidopsis thaliana. *Plant J*, 11(2), pp 213-26.
- Hershko, A., Ciechanover, A., Heller, H., Haas, A. L. & Rose, I. A. 1980. Proposed role of ATP in protein breakdown: conjugation of protein with multiple chains of the polypeptide of ATP-dependent proteolysis. *Proc Natl Acad Sci U S A*, 77(4), pp 1783-6.
- Hershko, A., Heller, H., Elias, S. & Ciechanover, A. 1983. Components of ubiquitin-protein ligase system. Resolution, affinity purification, and role in protein breakdown. *J Biol Chem*, 258(13), pp 8206-14.
- Hinz, M., Wilson, I. W., Yang, J., Buerstenbinder, K., Llewellyn, D., Dennis, E. S., Sauter, M. & Dolferus, R. 2010. Arabidopsis RAP2.2: an ethylene response transcription factor that is important for hypoxia survival. *Plant Physiol*, 153(2), pp 757-72.
- Hjerpe, R., Thomas, Y., Chen, J., Zemla, A., Curran, S., Shpiro, N., Dick, L. R. & Kurz, T. 2012. Changes in the ratio of free NEDD8 to ubiquitin triggers NEDDylation by ubiquitin enzymes. *Biochem J*, 441(3), pp 927-36.
- Hoernstein, S. N., Mueller, S. J., Fiedler, K., Schuelke, M., Vanselow, J. T., Schuessele, C., Lang, D., Nitschke, R., Igloi, G. L., Schlosser, A. & Reski, R. 2016. Identification of Targets and Interaction Partners of Arginyl-tRNA Protein Transfer-

- ase in the Moss *Physcomitrella patens*. *Mol Cell Proteomics*, 15(6), pp 1808-22.
- Holman, T. J., Jones, P. D., Russell, L., Medhurst, A., Ubeda Tomas, S., Talloji, P., Marquez, J., Schmuths, H., Tung, S. A., Taylor, I., Footitt, S., Bachmair, A., Theodoulou, F. L. & Holdsworth, M. J. 2009. The N-end rule pathway promotes seed germination and establishment through removal of ABA sensitivity in *Arabidopsis*. *Proc Natl Acad Sci U S A*, 106(11), pp 4549-54.
- Hoppe, T. 2005. Multiubiquitylation by E4 enzymes: 'one size' doesn't fit all. *Trends Biochem Sci*, 30(4), pp 183-7.
- Hotton, S. K., Castro, M. F., Eigenheer, R. A. & Callis, J. 2012. Recovery of DDB1a (damaged DNA binding protein1a) in a screen to identify novel RUB-modified proteins in *Arabidopsis thaliana*. *Mol Plant*. England.
- Hovland, P., Flick, J., Johnston, M. & Sclafani, R. A. 1989. Galactose as a gratuitous inducer of GAL gene expression in yeasts growing on glucose. *Gene*, 83(1), pp 57-64.
- Hovsepian, J., Becuwe, M., Kleifeld, O., Glickman, M. H. & Leon, S. 2016. Studying Protein Ubiquitylation in Yeast. *Methods Mol Biol*, 1449(117-42).
- Hu, R. G., Sheng, J., Qi, X., Xu, Z., Takahashi, T. T. & Varshavsky, A. 2005. The N-end rule pathway as a nitric oxide sensor controlling the levels of multiple regulators. *Nature*, 437(7061), pp 981-6.
- Hua, Z. & Vierstra, R. D. 2011. The cullin-RING ubiquitin-protein ligases. *Annu Rev Plant Biol*, 62(299-334).
- Huang, Y., Minaker, S., Roth, C., Huang, S., Hieter, P., Lipka, V., Wiermer, M. & Li, X. 2014. An E4 Ligase Facilitates Polyubiquitination of Plant Immune Receptor Resistance Proteins in *Arabidopsis*. *Plant Cell*.
- Huesgen, P. F. & Overall, C. M. 2012. N- and C-terminal degradomics: new approaches to reveal biological roles for plant proteases from substrate identification. *Physiol Plant*, 145(1), pp 5-17.
- Hurley, B., Lee, D., Mott, A., Wilton, M., Liu, J., Liu, Y. C., Angers, S., Coaker, G., Guttman, D. S. & Desveaux, D. 2014. The *Pseudomonas syringae* type III effector HopF2 suppresses *Arabidopsis* stomatal immunity. *PLoS One*, 9(12), pp e114921.
- Hwang, C. S., Shemorry, A., Auerbach, D. & Varshavsky, A. 2010a. The N-end rule pathway is mediated by a complex of the RING-type Ubr1 and HECT-type Ufd4 ubiquitin ligases. *Nat Cell Biol*, 12(12), pp 1177-85.

- Hwang, C. S., Shemorry, A. & Varshavsky, A. 2010b. N-terminal acetylation of cellular proteins creates specific degradation signals. *Science*, 327(5968), pp 973-7.
- Iconomou, M. & Saunders, D. N. 2016. Systematic approaches to identify E3 ligase substrates. *Biochem J*, 473(22), pp 4083-4101.
- Inoue, H., Nojima, H. & Okayama, H. 1990. High efficiency transformation of *Escherichia coli* with plasmids. *Gene*, 96(1), pp 23-8.
- Isono, E. & Nagel, M. K. 2014. Deubiquitylating enzymes and their emerging role in plant biology. *Front Plant Sci*, 5(
- Ito, H., Fukuda, Y., Murata, K. & Kimura, A. 1983. Transformation of intact yeast cells treated with alkali cations. *J Bacteriol*, 153(1), pp 163-8.
- Jones, D. & Candido, E. P. 2000. The NED-8 conjugating system in *Caenorhabditis elegans* is required for embryogenesis and terminal differentiation of the hypodermis. *Dev Biol*, 226(1), pp 152-65.
- Jones, J. D. & Dangl, J. L. 2006. The plant immune system. *Nature*, 444(7117), pp 323-9.
- Joshua-Tor, L., Xu, H. E., Johnston, S. A. & Rees, D. C. 1995. Crystal structure of a conserved protease that binds DNA: the bleomycin hydrolase, Gal6. *Science*, 269(5226), pp 945-50.
- Kelley, L. A., Mezulis, S., Yates, C. M., Wass, M. N. & Sternberg, M. J. 2015. The Phyre2 web portal for protein modeling, prediction and analysis. *Nat Protoc*, 10(6), pp 845-58.
- Khmelniskii, A., Keller, P. J., Bartosik, A., Meurer, M., Barry, J. D., Mardin, B. R., Kaufmann, A., Trautmann, S., Wachsmuth, M., Pereira, G., Huber, W., Schiebel, E. & Knop, M. 2012. Tandem fluorescent protein timers for in vivo analysis of protein dynamics. *Nat Biotechnol*, 30(7), pp 708-14.
- Kim, H. K., Kim, R. R., Oh, J. H., Cho, H., Varshavsky, A. & Hwang, C. S. 2014. The N-terminal methionine of cellular proteins as a degradation signal. *Cell*, 156(1-2), pp 158-69.
- Kim, H. S., Desveaux, D., Singer, A. U., Patel, P., Sondek, J. & Dangl, J. L. 2005a. The *Pseudomonas syringae* effector AvrRpt2 cleaves its C-terminally acylated target, RIN4, from *Arabidopsis* membranes to block RPM1 activation. *Proc Natl Acad Sci U S A*, 102(18), pp 6496-501.
- Kim, M. G., da Cunha, L., McFall, A. J., Belkhadir, Y., DebRoy, S., Dangl, J. L. & Mackey, D. 2005b. Two *Pseudomonas syringae* type III effectors inhibit RIN4-regulated basal defense in *Arabidopsis*. *Cell*, 121(5), pp 749-59.

- Kleifeld, O., Doucet, A., Prudova, A., auf dem Keller, U., Gioia, M., Kizhakkedathu, J. N. & Overall, C. M. 2011. Identifying and quantifying proteolytic events and the natural N terminome by terminal amine isotopic labeling of substrates. *Nat Protoc*, 6(10), pp 1578-611.
- Koegl, M., Hoppe, T., Schlenker, S., Ulrich, H. D., Mayer, T. U. & Jentsch, S. 1999. A novel ubiquitination factor, E4, is involved in multiubiquitin chain assembly. *Cell*, 96(5), pp 635-44.
- Komander, D. & Rape, M. 2012. The ubiquitin code. *Annu Rev Biochem*, 81(203-29).
- Kraft, E., Stone, S. L., Ma, L., Su, N., Gao, Y., Lau, O. S., Deng, X. W. & Callis, J. 2005. Genome analysis and functional characterization of the E2 and RING-type E3 ligase ubiquitination enzymes of Arabidopsis. *Plant Physiol*, 139(4), pp 1597-611.
- Kushnirov, V. V. 2000. Rapid and reliable protein extraction from yeast. *Yeast*, 16(9), pp 857-60.
- Lammer, D., Mathias, N., Laplaza, J. M., Jiang, W., Liu, Y., Callis, J., Goebel, M. & Estelle, M. 1998. Modification of yeast Cdc53p by the ubiquitin-related protein rub1p affects function of the SCFCdc4 complex. *Genes Dev*, 12(7), pp 914-26.
- Lampl, N., Alkan, N., Davydov, O. & Fluhr, R. 2013. Set-point control of RD21 protease activity by AtSerp1 controls cell death in Arabidopsis. *Plant J*, 74(3), pp 498-510.
- Lee, D. H. & Goldberg, A. L. 1998. Proteasome inhibitors: valuable new tools for cell biologists. *Trends Cell Biol*, 8(10), pp 397-403.
- Lee, J. H. & Kim, W. T. 2011. Regulation of abiotic stress signal transduction by E3 ubiquitin ligases in Arabidopsis. *Mol Cells*, 31(3), pp 201-8.
- Leidecker, O., Matic, I., Mahata, B., Pion, E. & Xirodimas, D. P. 2012. The ubiquitin E1 enzyme Ube1 mediates NEDD8 activation under diverse stress conditions. *Cell Cycle*, 11(6), pp 1142-50.
- Li, W., Bengtson, M. H., Ulbrich, A., Matsuda, A., Reddy, V. A., Orth, A., Chanda, S. K., Batalov, S. & Joazeiro, C. A. P. 2008a. Genome-Wide and Functional Annotation of Human E3 Ubiquitin Ligases Identifies MULAN, a Mitochondrial E3 that Regulates the Organelle's Dynamics and Signaling. *PLOS ONE*, 3(1), pp e1487.
- Li, Y., Zheng, L., Corke, F., Smith, C. & Bevan, M. W. 2008b. Control of final seed and organ size by the DA1 gene family in Arabidopsis thaliana. *Genes Dev*, 22(10), pp 1331-6.

- Liakopoulos, D., Busgen, T., Brychzy, A., Jentsch, S. & Pause, A. 1999. Conjugation of the ubiquitin-like protein NEDD8 to cullin-2 is linked to von Hippel-Lindau tumor suppressor function. *Proc Natl Acad Sci U S A*, 96(10), pp 5510-5.
- Liakopoulos, D., Doenges, G., Matuschewski, K. & Jentsch, S. 1998. A novel protein modification pathway related to the ubiquitin system. *Embo j*, 17(8), pp 2208-14.
- Licausi, F., Kosmacz, M., Weits, D. A., Giuntoli, B., Giorgi, F. M., Voeselek, L. A., Perata, P. & van Dongen, J. T. 2011. Oxygen sensing in plants is mediated by an N-end rule pathway for protein destabilization. *Nature*, 479(7373), pp 419-22.
- Licausi, F., van Dongen, J. T., Giuntoli, B., Novi, G., Santaniello, A., Geigenberger, P. & Perata, P. 2010. HRE1 and HRE2, two hypoxia-inducible ethylene response factors, affect anaerobic responses in *Arabidopsis thaliana*. *Plant J*, 62(2), pp 302-15.
- Liu, J., Elmore, J. M., Fuglsang, A. T., Palmgren, M. G., Staskawicz, B. J. & Coaker, G. 2009. RIN4 functions with plasma membrane H⁺-ATPases to regulate stomatal apertures during pathogen attack. *PLoS Biol*, 7(6), pp e1000139.
- Liu, J., Elmore, J. M., Lin, Z. J. & Coaker, G. 2011. A receptor-like cytoplasmic kinase phosphorylates the host target RIN4, leading to the activation of a plant innate immune receptor. *Cell Host Microbe*, 9(2), pp 137-46.
- Lorick, K. L., Jensen, J. P., Fang, S., Ong, A. M., Hatakeyama, S. & Weissman, A. M. 1999. RING fingers mediate ubiquitin-conjugating enzyme (E2)-dependent ubiquitination. *Proc Natl Acad Sci U S A*, 96(20), pp 11364-9.
- Luehrsen, K. R., de Wet, J. R. & Walbot, V. 1992. Transient expression analysis in plants using firefly luciferase reporter gene. *Methods Enzymol*, 216(397-414).
- Mackey, D., Belkhadir, Y., Alonso, J. M., Ecker, J. R. & Dangl, J. L. 2003. *Arabidopsis* RIN4 is a target of the type III virulence effector AvrRpt2 and modulates RPS2-mediated resistance. *Cell*, 112(3), pp 379-89.
- Mackey, D., Holt, B. F., 3rd, Wiig, A. & Dangl, J. L. 2002. RIN4 interacts with *Pseudomonas syringae* type III effector molecules and is required for RPM1-mediated resistance in *Arabidopsis*. *Cell*, 108(6), pp 743-54.
- Majovsky, P., Naumann, C., Lee, C. W., Lassowskat, I., Trujillo, M., Dissmeyer, N. & Hoehenwarter, W. 2014. Targeted proteomics analysis of protein degradation in plant signaling on an LTQ-Orbitrap mass spectrometer. *J Proteome Res*, 13(10), pp 4246-58.
- Marín, I. 2013. Evolution of Plant HECT Ubiquitin Ligases. In: Zhang, Z. (ed.) *PLoS One*. San Francisco, USA.

- McBride, K. E. & Summerfelt, K. R. 1990. Improved binary vectors for *Agrobacterium*-mediated plant transformation. *Plant Mol Biol*, 14(2), pp 269-76.
- McNellis, T. W., Mudgett, M. B., Li, K., Aoyama, T., Horvath, D., Chua, N. H. & Staskawicz, B. J. 1998. Glucocorticoid-inducible expression of a bacterial avirulence gene in transgenic *Arabidopsis* induces hypersensitive cell death. *Plant J*, 14(2), pp 247-57.
- Mendiondo, G. M., Gibbs, D. J., Szurman-Zubrzycka, M., Korn, A., Marquez, J., Szarejko, I., Maluszynski, M., King, J., Axcell, B., Smart, K., Corbineau, F. & Holdsworth, M. J. 2016. Enhanced waterlogging tolerance in barley by manipulation of expression of the N-end rule pathway E3 ligase PROTEOLYSIS6. *Plant Biotechnol J*, 14(1), pp 40-50.
- Mergner, J., Heinzlmeir, S., Kuster, B. & Schwechheimer, C. 2015. DENEDDYLASE1 deconjugates NEDD8 from non-cullin protein substrates in *Arabidopsis thaliana*. *Plant Cell*, 27(3), pp 741-53.
- Mergner, J., Kuster, B. & Schwechheimer, C. 2017. DENEDDYLASE1 Protein Counters Automodification of Neddylating Enzymes to Maintain NEDD8 Protein Homeostasis in *Arabidopsis*. *J Biol Chem*, 292(9), pp 3854-3865.
- Mergner, J. & Schwechheimer, C. 2014. The NEDD8 modification pathway in plants. *Front Plant Sci*, 5(103).
- Mesiti & Francesca. 2011. *The N-end rule pathway in Arabidopsis: characterization of N-recognins*. MSc.
- Miricescu, A., Goslin, K. & Graciet, E. 2018. Ubiquitylation in plants: signaling hub for the integration of environmental signals. *J Exp Bot*, 69(19), pp 4511-4527.
- Moerschell, R. P., Hosokawa, Y., Tsunasawa, S. & Sherman, F. 1990. The specificities of yeast methionine aminopeptidase and acetylation of amino-terminal methionine in vivo. Processing of altered iso-1-cytochromes c created by oligonucleotide transformation. *J Biol Chem*, 265(32), pp 19638-43.
- Mot, A. C., Prell, E., Klecker, M., Naumann, C., Faden, F., Westermann, B. & Dissmeyer, N. 2018. Real-time detection of N-end rule-mediated ubiquitination via fluorescently labeled substrate probes. *New Phytol*, 217(2), pp 613-624.
- Nguyen, K. T., Mun, S. H., Lee, C. S. & Hwang, C. S. 2018. Control of protein degradation by N-terminal acetylation and the N-end rule pathway. *Exp Mol Med*.
- Nishimura, K., Asakura, Y., Friso, G., Kim, J., Oh, S. H., Rutschow, H., Ponnala, L. & van Wijk, K. J. 2013. ClpS1 is a conserved substrate selector for the chloroplast Clp protease system in *Arabidopsis*. *Plant Cell*, 25(6), pp 2276-301.

- NOVIKOFF, A. B., BEAUFAY, H. & DE DUVE, C. 1956. Electron microscopy of lysosomeric fractions from rat liver. *J Biophys Biochem Cytol*, 2(4 Suppl), pp 179-84.
- Ohi, M. D., Vander Kooi, C. W., Rosenberg, J. A., Chazin, W. J. & Gould, K. L. 2003. Structural insights into the U-box, a domain associated with multi-ubiquitination. *Nat Struct Biol*, 10(4), pp 250-5.
- Osaka, F., Kawasaki, H., Aida, N., Saeki, M., Chiba, T., Kawashima, S., Tanaka, K. & Kato, S. 1998. A new NEDD8-ligating system for cullin-4A. *Genes Dev*, 12(15), pp 2263-8.
- Osaka, F., Saeki, M., Katayama, S., Aida, N., Toh, E. A., Kominami, K., Toda, T., Suzuki, T., Chiba, T., Tanaka, K. & Kato, S. 2000. Covalent modifier NEDD8 is essential for SCF ubiquitin-ligase in fission yeast. *Embo j*, 19(13), pp 3475-84.
- Ou, C. Y., Lin, Y. F., Chen, Y. J. & Chien, C. T. 2002. Distinct protein degradation mechanisms mediated by Cul1 and Cul3 controlling Ci stability in *Drosophila* eye development. *Genes Dev*, 16(18), pp 2403-14.
- Ozkaynak, E., Finley, D. & Varshavsky, A. 1984. The yeast ubiquitin gene: head-to-tail repeats encoding a polyubiquitin precursor protein. *Nature*, 312(5995), pp 663-6.
- Papdi, C., Abraham, E., Joseph, M. P., Popescu, C., Koncz, C. & Szabados, L. 2008. Functional identification of Arabidopsis stress regulatory genes using the controlled cDNA overexpression system. *Plant Physiol*, 147(2), pp 528-42.
- Park, K. S., Bayles, I., Szlachta-McGinn, A., Paul, J., Boiko, J., Santos, P., Liu, J., Wang, Z., Borghesi, L. & Milcarek, C. 2014. Transcription elongation factor ELL2 drives Ig secretory-specific mRNA production and the unfolded protein response. *J Immunol*, 193(9), pp 4663-74.
- Piatkov, K. I., Brower, C. S. & Varshavsky, A. 2012. The N-end rule pathway counteracts cell death by destroying proapoptotic protein fragments. *Proc Natl Acad Sci U S A*, 109(27), pp E1839-47.
- Polevoda, B., Arnesen, T. & Sherman, F. 2009. A synopsis of eukaryotic N(α)-terminal acetyltransferases: nomenclature, subunits and substrates. *BMC Proc*.
- Poole, B., Ohkuma, S. & Warburton, M. J. 1977. The accumulation of weakly basic substances in lysosomes and the inhibition of intracellular protein degradation. *Acta Biol Med Ger*, 36(11-12), pp 1777-88.
- Potuschak, T., Stary, S., Schlogelhofer, P., Becker, F., Nejinskaia, V. & Bachmair, A. 1998. PRT1 of Arabidopsis thaliana encodes a component of the plant N-end rule pathway. *Proc Natl Acad Sci U S A*, 95(14), pp 7904-8.

- Pozo, J. C., Timpte, C., Tan, S., Callis, J. & Estelle, M. 1998. The ubiquitin-related protein RUB1 and auxin response in Arabidopsis. *Science*, 280(5370), pp 1760-3.
- Rabut, G., Le Dez, G., Verma, R., Makhnevych, T., Knebel, A., Kurz, T., Boone, C., Deshaies, R. J. & Peter, M. 2011. The TFIID subunit Tfb3 regulates cullin neddylation. *Mol Cell*, 43(3), pp 488-95.
- Rabut, G. & Peter, M. 2008. Function and regulation of protein neddylation. 'Protein modifications: beyond the usual suspects' review series. *EMBO Rep*, 9(10), pp 969-76.
- Rao, H., Uhlmann, F., Nasmyth, K. & Varshavsky, A. 2001. Degradation of a cohesin subunit by the N-end rule pathway is essential for chromosome stability. *Nature*, 410(6831), pp 955-9.
- Rao-Naik, C., delaCruz, W., Laplaza, J. M., Tan, S., Callis, J. & Fisher, A. J. 1998. The rub family of ubiquitin-like proteins. Crystal structure of Arabidopsis rub1 and expression of multiple rubs in Arabidopsis. *J Biol Chem*, 273(52), pp 34976-82.
- Rauniyar, N. 2015. Parallel Reaction Monitoring: A Targeted Experiment Performed Using High Resolution and High Mass Accuracy Mass Spectrometry. *Int J Mol Sci*, 16(12), pp 28566-81.
- Richter, S. & Lamppa, G. K. 1998. A chloroplast processing enzyme functions as the general stromal processing peptidase. *Proc Natl Acad Sci U S A*, 95(13), pp 7463-8.
- Rowland, E., Kim, J., Bhuiyan, N. H. & van Wijk, K. J. 2015. The Arabidopsis Chloroplast Stromal N-Terminome: Complexities of Amino-Terminal Protein Maturation and Stability. *Plant Physiol*, 169(3), pp 1881-96.
- Rustgi, S., Boex-Fontvieille, E., Reinbothe, C., von Wettstein, D. & Reinbothe, S. 2017. Serpin1 and WSCP differentially regulate the activity of the cysteine protease RD21 during plant development in Arabidopsis thaliana. *Proc Natl Acad Sci U S A*, 114(9), pp 2212-2217.
- Sabol, P., Kulich, I. & Zarsky, V. 2017. RIN4 recruits the exocyst subunit EXO70B1 to the plasma membrane. *J Exp Bot*, 68(12), pp 3253-3265.
- Santt, O., Pfirrmann, T., Braun, B., Juretschke, J., Kimmig, P., Scheel, H., Hofmann, K., Thumm, M. & Wolf, D. H. 2008. The Yeast GID Complex, a Novel Ubiquitin Ligase (E3) Involved in the Regulation of Carbohydrate Metabolism. In: Sommer, T. (ed.) *Mol Biol Cell*.
- Scheffner, M., Nuber, U. & Huibregtse, J. M. 1995. Protein ubiquitination involving an E1-E2-E3 enzyme ubiquitin thioester cascade. *Nature*, 373(6509), pp 81-3.

- Schoenheimer, R. 1942. *The Dynamic State of Body Constituents*, reprint: Harvard University Press.
- Schuessele, C., Hoernstein, S. N., Mueller, S. J., Rodriguez-Franco, M., Lorenz, T., Lang, D., Igloi, G. L. & Reski, R. 2016. Spatio-temporal patterning of arginyl-tRNA protein transferase (ATE) contributes to gametophytic development in a moss. *New Phytol*, 209(3), pp 1014-27.
- Schuetz, A., Murakawa, Y., Rosenbaum, E., Landthaler, M. & Heinemann, U. 2014. Roquin binding to target mRNAs involves a winged helix-turn-helix motif. *Nat Commun*, 5(5701).
- Schwarz, S. E., Rosa, J. L. & Scheffner, M. 1998. Characterization of human hect domain family members and their interaction with Ubch5 and Ubch7. *J Biol Chem*, 273(20), pp 12148-54.
- Scott, D. C., Monda, J. K., Bennett, E. J., Harper, J. W. & Schulman, B. A. 2011. N-terminal acetylation acts as an avidity enhancer within an interconnected multiprotein complex. *Science*, 334(6056), pp 674-8.
- Sharp, P. M. & Li, W. H. 1987. Molecular evolution of ubiquitin genes. *Trends Ecol Evol*, 2(11), pp 328-32.
- Shemorry, A., Hwang, C. S. & Varshavsky, A. 2013. Control of protein quality and stoichiometries by N-terminal acetylation and the N-end rule pathway. *Mol Cell*, 50(4), pp 540-51.
- Shilatifard, A., Duan, D. R., Haque, D., Florence, C., Schubach, W. H., Conaway, J. W. & Conaway, R. C. 1997. ELL2, a new member of an ELL family of RNA polymerase II elongation factors. *Proc Natl Acad Sci U S A*, 94(8), pp 3639-43.
- Shindo, T., Misas-Villamil, J. C., Horger, A. C., Song, J. & van der Hoorn, R. A. 2012. A role in immunity for Arabidopsis cysteine protease RD21, the ortholog of the tomato immune protease C14. *PLoS One*, 7(1), pp e29317.
- Sikorski, R. S. & Hieter, P. 1989. A system of shuttle vectors and yeast host strains designed for efficient manipulation of DNA in *Saccharomyces cerevisiae*. *Genetics*, 122(1), pp 19-27.
- Singh, R. K., Zerath, S., Kleifeld, O., Scheffner, M., Glickman, M. H. & Fushman, D. 2012. Recognition and cleavage of related to ubiquitin 1 (Rub1) and Rub1-ubiquitin chains by components of the ubiquitin-proteasome system. *Mol Cell Proteomics*, 11(12), pp 1595-611.
- Soffer, R. L. & Horinishi, H. 1969. Enzymic modification of proteins. I. General characteristics of the arginine-transfer reaction in rabbit liver cytoplasm. *J Mol Biol*, 43(1), pp 163-75.

- Stary, S., Yin, X. J., Potuschak, T., Schlogelhofer, P., Nizhynska, V. & Bachmair, A. 2003. PRT1 of Arabidopsis is a ubiquitin protein ligase of the plant N-end rule pathway with specificity for aromatic amino-terminal residues. *Plant Physiol*, 133(3), pp 1360-6.
- Stewart, M. D., Ritterhoff, T., Klevit, R. E. & Brzovic, P. S. 2016. E2 enzymes: more than just middle men. *Cell Res*, 26(4), pp 423-40.
- Stone, S. L., Hauksdóttir, H., Troy, A., Herschleb, J., Kraft, E. & Callis, J. 2005. Functional analysis of the RING-type ubiquitin ligase family of Arabidopsis. *Plant Physiol*, 137(1), pp 13-30.
- Streich, F. C. & Lima, C. D. 2014. Structural and Functional Insights to Ubiquitin-Like Protein Conjugation. *Annu Rev Biophys*, 43(357-79).
- Takemoto, D. & Jones, D. A. 2005. Membrane release and destabilization of Arabidopsis RIN4 following cleavage by Pseudomonas syringae AvrRpt2. *Mol Plant Microbe Interact*, 18(12), pp 1258-68.
- Tanaka, K. 2009. The proteasome: Overview of structure and functions. *Proc Jpn Acad Ser B Phys Biol Sci*.
- Tasaki, T., Mulder, L. C., Iwamatsu, A., Lee, M. J., Davydov, I. V., Varshavsky, A., Muesing, M. & Kwon, Y. T. 2005. A family of mammalian E3 ubiquitin ligases that contain the UBR box motif and recognize N-degrons. *Mol Cell Biol*, 25(16), pp 7120-36.
- Tasaki, T., Sriram, S. M., Park, K. S. & Kwon, Y. T. 2012. The N-end rule pathway. *Annu Rev Biochem*, 81(261-89).
- Tasaki, T., Zakrzewska, A., Dudgeon, D. D., Jiang, Y., Lazo, J. S. & Kwon, Y. T. 2009. The substrate recognition domains of the N-end rule pathway. *J Biol Chem*, 284(3), pp 1884-95.
- Tateishi, K., Omata, M., Tanaka, K. & Chiba, T. 2001. The NEDD8 system is essential for cell cycle progression and morphogenetic pathway in mice. *J Cell Biol*, 155(4), pp 571-9.
- Teichmann, M., Dumay-Odelot, H. & Fribourg, S. 2012. Structural and functional aspects of winged-helix domains at the core of transcription initiation complexes. *Transcription*, 3(1), pp 2-7.
- Teste, M. A., Duquenne, M., Francois, J. M. & Parrou, J. L. 2009. Validation of reference genes for quantitative expression analysis by real-time RT-PCR in *Saccharomyces cerevisiae*. *BMC Mol Biol*, 10(99).
- Thrower, J. S., Hoffman, L., Rechsteiner, M. & Pickart, C. M. 2000. Recognition of the polyubiquitin proteolytic signal. *Embo j*, 19(1), pp 94-102.

- Trujillo, M. 2018. News from the PUB: plant U-box type E3 ubiquitin ligases. *J Exp Bot*, 69(3), pp 371-384.
- Turner, G. C., Du, F. & Varshavsky, A. 2000. Peptides accelerate their uptake by activating a ubiquitin-dependent proteolytic pathway. *Nature*, 405(6786), pp 579-83.
- Van Damme, P., Hole, K., Pimenta-Marques, A., Helsens, K., Vandekerckhove, J., Martinho, R. G., Gevaert, K. & Arnesen, T. 2011. NatF contributes to an evolutionary shift in protein N-terminal acetylation and is important for normal chromosome segregation. *PLoS Genet*, 7(7), pp e1002169.
- Varshavsky, A. 1991. Naming a targeting signal. *Cell*. United States.
- Varshavsky, A. 1996. The N-end rule: functions, mysteries, uses. *Proc Natl Acad Sci USA*, 93(22), pp 12142-9.
- Varshavsky, A. 2011. The N-end rule pathway and regulation by proteolysis. *Protein Sci*, 20(8), pp 1298-345.
- Venne, A. S., Solari, F. A., Faden, F., Paretto, T., Dissmeyer, N. & Zahedi, R. P. 2015. An improved workflow for quantitative N-terminal charge-based fractional diagonal chromatography (ChaFRADIC) to study proteolytic events in *Arabidopsis thaliana*. *Proteomics*, 15(14), pp 2458-69.
- Venne, A. S., Vogtle, F. N., Meisinger, C., Sickmann, A. & Zahedi, R. P. 2013. Novel highly sensitive, specific, and straightforward strategy for comprehensive N-terminal proteomics reveals unknown substrates of the mitochondrial peptidase Icp55. *J Proteome Res*, 12(9), pp 3823-30.
- Verma, R., Aravind, L., Oania, R., McDonald, W. H., Yates, J. R., 3rd, Koonin, E. V. & Deshaies, R. J. 2002. Role of Rpn11 metalloprotease in deubiquitination and degradation by the 26S proteasome. *Science*, 298(5593), pp 611-5.
- Vicente, J., Mendiondo, G. M., Movahedi, M., Peirats-Llobet, M., Juan, Y. T., Shen, Y. Y., Dambire, C., Smart, K., Rodriguez, P. L., Charng, Y. Y., Gray, J. E. & Holdsworth, M. J. 2017. The Cys-Arg/N-End Rule Pathway Is a General Sensor of Abiotic Stress in Flowering Plants. *Curr Biol*, 27(20), pp 3183-3190.e4.
- Vicente, J., Mendiondo, G. M., Pauwels, J., Pastor, V., Izquierdo, Y., Naumann, C., Movahedi, M., Rooney, D., Gibbs, D. J., Smart, K., Bachmair, A., Gray, J. E., Dissmeyer, N., Castresana, C., Ray, R. V., Gevaert, K. & Holdsworth, M. J. 2018. Distinct branches of the N-end rule pathway modulate the plant immune response. *New Phytol*.
- Vierstra, R. D. 2003. The ubiquitin/26S proteasome pathway, the complex last chapter in the life of many plant proteins. *Trends Plant Sci*, 8(3), pp 135-42.

- Wang, H., Wang, J., Jiang, J., Chen, S., Guan, Z., Liao, Y. & Chen, F. 2014. Reference genes for normalizing transcription in diploid and tetraploid Arabidopsis. *Sci Rep*, 4(6781).
- Wang, Y., Li, J., Hou, S., Wang, X., Li, Y., Ren, D., Chen, S., Tang, X. & Zhou, J. M. 2010. A *Pseudomonas syringae* ADP-ribosyltransferase inhibits Arabidopsis mitogen-activated protein kinase kinases. *Plant Cell*, 22(6), pp 2033-44.
- Weits, D. A., Giuntoli, B., Kosmacz, M., Parlanti, S., Hubberten, H. M., Riegler, H., Hoefgen, R., Perata, P., van Dongen, J. T. & Licausi, F. 2014. Plant cysteine oxidases control the oxygen-dependent branch of the N-end-rule pathway. *Nat Commun*, 5(3425).
- Welchman, R. L., Gordon, C. & Mayer, R. J. 2005. Ubiquitin and ubiquitin-like proteins as multifunctional signals. *Nat Rev Mol Cell Biol*, 6(8), pp 599-609.
- White, M. D., Klecker, M., Hopkinson, R. J., Weits, D. A., Mueller, C., Naumann, C., O'Neill, R., Wickens, J., Yang, J., Brooks-Bartlett, J. C., Garman, E. F., Grossmann, T. N., Dissmeyer, N. & Flashman, E. 2017. Plant cysteine oxidases are dioxygenases that directly enable arginyl transferase-catalysed arginylation of N-end rule targets. *Nat Commun*, 8(14690).
- Wilson, K. P., Shewchuk, L. M., Brennan, R. G., Otsuka, A. J. & Matthews, B. W. 1992. Escherichia coli biotin holoenzyme synthetase/bio repressor crystal structure delineates the biotin- and DNA-binding domains. *Proc Natl Acad Sci U S A*, 89(19), pp 9257-61.
- Wong, C. C., Xu, T., Rai, R., Bailey, A. O., Yates, J. R., 3rd, Wolf, Y. I., Zebroski, H. & Kashina, A. 2007. Global analysis of posttranslational protein arginylation. *PLoS Biol*, 5(10), pp e258.
- Worley, C. K., Ling, R. & Callis, J. 1998. Engineering in vivo instability of firefly luciferase and Escherichia coli beta-glucuronidase in higher plants using recognition elements from the ubiquitin pathway. *Plant Mol Biol*, 37(2), pp 337-47.
- Xia, Z., Webster, A., Du, F., Piatkov, K., Ghislain, M. & Varshavsky, A. 2008. Substrate-binding sites of UBR1, the ubiquitin ligase of the N-end rule pathway. *J Biol Chem*, 283(35), pp 24011-28.
- Xu, H. & Ren, D. 2015. Lysosomal physiology. *Annu Rev Physiol*, 77(57-80).
- Yang, P., Fu, H., Walker, J., Papa, C. M., Smalle, J., Ju, Y. M. & Vierstra, R. D. 2004. Purification of the Arabidopsis 26 S proteasome: biochemical and molecular analyses revealed the presence of multiple isoforms. *J Biol Chem*, 279(8), pp 6401-13.
- Yao, T. & Cohen, R. E. 2002. A cryptic protease couples deubiquitination and degradation by the proteasome. *Nature*, 419(6905), pp 403-7.

- Yates, C. M., Filippis, I., Kelley, L. A. & Sternberg, M. J. 2014. SuSPect: enhanced prediction of single amino acid variant (SAV) phenotype using network features. *J Mol Biol*, 426(14), pp 2692-701.
- Yoshida, S., Ito, M., Callis, J., Nishida, I. & Watanabe, A. 2002. A delayed leaf senescence mutant is defective in arginyl-tRNA:protein arginyltransferase, a component of the N-end rule pathway in Arabidopsis. *Plant J*, 32(1), pp 129-37.
- Zhang, H., Deery, M. J., Gannon, L., Powers, S. J., Lilley, K. S. & Theodoulou, F. L. 2015. Quantitative proteomics analysis of the Arg/N-end rule pathway of targeted degradation in Arabidopsis roots. *Proteomics*, 15(14), pp 2447-57.
- Zhang, H., Gannon, L., Hassall, K. L., Deery, M. J., Gibbs, D. J., Holdsworth, M. J., van der Hoorn, R. A. L., Lilley, K. S. & Theodoulou, F. L. 2018. N-terminomics reveals control of Arabidopsis seed storage proteins and proteases by the Arg/N-end rule pathway. *New Phytol*, 218(3), pp 1106-1126.
- Zhuang, M., Guan, S., Wang, H., Burlingame, A. L. & Wells, J. A. 2013. Substrates of IAP ubiquitin ligases identified with a designed orthogonal E3 ligase, the NEDDylator. *Mol Cell*, 49(2), pp 273-82.
- Zuin, A., Isasa, M. & Crosas, B. 2014. Ubiquitin Signaling: Extreme Conservation as a Source of Diversity. *Cells*.

Appendix 1

The composition of buffers used in this work are described below in alphabetical order.

Name	Composition
2X SDS loading dye	25% (v/v) 4x stacking buffer, 20% (v/v) glycerol, 4% (v/v) SDS, 2% (v/v) β -mercaptoethanol, 1% (w/v) bromophenol blue
Amido black staining solution	10% (v/v) acetic acid, 90% (v/v) methanol, amido black 10B
Amido black wash solution	10% (v/v) acetic acid, 90% (v/v) methanol
5x CCLR buffer (Promega)	25 mM Tris-phosphate pH7.8, 2 mM DTT, 2 mM 1,2-diaminocyclohexane-N,N,N',N'-tetraacetic acid, 10% (v/v) glycerol, 1% (v/v) Triton X-100
EB buffer	10 mM Tris-Cl, pH 8.5
Edward's extraction buffer	200 mM Tris-HCl pH7.5-8.0, 250 mM NaCl, 25 mM EDTA, 0.5% (w/v) SDS
HisA buffer	8 M urea, 20 mM Tris pH8.0, 100 mM K_2HPO_4 , 10 mM imidazole, 100 mM NaCl, 0.1% (v/v) Triton X-100
His Elution buffer	20 mM Tris pH8.0, 100 mM K_2HPO_4 , 500 mM imidazole, 100 mM NaCl
HisWB1 buffer	20 mM Tris pH8.0, 100 mM K_2HPO_4 , 20 mM imidazole, 100 mM NaCl, 0.1% (v/v) Triton X-100
HisWB2 buffer	20 mM Tris pH8.0, 100 mM K_2HPO_4 , 10 mM imidazole, 100 mM NaCl, 0.1% (v/v) Triton X-100
Infiltration Medium	10 mM MES pH5.6, 10 mM $MgCl_2$, 150 μ M acetosyringone
IP buffer	50 mM Tris pH8.0, 150 mM NaCl, 20 mM EDTA, 0.15% (v/v) NP-40, 1 mg/mL BSA, 1:100 plant protease inhibitor cocktail (Sigma)
LAR buffer	20 mM tricine pH7.8, 1.07 mM $(MgCO_3)_4Mg(OH)_2 \cdot 5H_2O$, 2.67 mM

	MgSO ₄ , 0.1 mM EDTA, 33.3 mM DTT, 270 μM coenzyme A, 470 μM luciferin, 530 μM ATP
LiAc buffer	100 mM LiAc, 10 mM TE
Luciferase Ex- traction buffer	1x CCLR buffer, 1 mM PMSF, 1:100 plant protease inhibitor cock- tail (Sigma)
N3 buffer	3 M potassium acetate, pH 5.5
P1 buffer	50 mM Tris-HCl, pH8.0, 10 mM EDTA, 100 μg/mL RNase A
P2 buffer	200 mM NaOH, 1% SDS
PBS	8 g/L NaCl, 0.2 g/L KCl, 1.15 g/L Na ₂ HPO ₄ , 0.2 g/L KH ₂ PO ₄
PEG/LiAc buff- er	10 mM TE, 100 mM LiAc, 33% PEG3350
Ponceau solu- tion	0.2% (w/v) Ponceau, 10% (v/v) acetic acid
Separating buffer	1.5 M Tris pH8.8, 0.4% (w/v) SDS
SOB medium	2% (w/v) tryptone, 0.5% (w/v) yeast extract, 0.05% (w/v) NaCl, 10 mM MgSO ₄ , 10 mM MgCl ₂
Stacking buffer	0.5 M Tris pH6.8, 0.4% (w/v) SDS
TB buffer	10 mM PIPES/KOH pH6.7, 15 mM CaCl ₂ , 250 mM KCl, 55 mM MnCl ₂
TBS buffer	10 mM Tris HCl, 150 mM NaCl, pH 7.4
TE	0.1 M Tris-HCl pH7.5, 0.01 M NaEDTA pH8.0
TfbI buffer	30 mM KOAc, 50 mM MnCl ₂ ·4H ₂ O, 100 mM KCl, 10 mM CaCl ₂ , 15% glycerol
TfbII buffer	10 mM NaMOPS pH7.0, 75 mM CaCl ₂ , 10 mM KCl, 15% glycerol
Transfer buffer	10 mM Tris base, 0.1 M glycine, 10% ethanol
Tris-Glycine buffer	0.025 M Tris pH8.3, 0.192 M glycine, 0.1% SDS

Yeast RNA Lysis buffer	0.5 M NaCl, 10 mM EDTA, 1% SDS, 0.2 M Tris-HCL, pH7.6
Z buffer	60 mM Na ₂ HPO ₄ · 7H ₂ O, 40 mM NaH ₂ PO ₄ · H ₂ O, 10 mM KCl, 1 mM MgSO ₄ · 7H ₂ O, 50 mM β-mercaptoethanol, 0.5 mg/mL X-Gal